IN-VITRO VASCULARIZED TISSUE EQUIVALENTS FROM HUMAN EMBRYONIC STEM CELL-DERIVED ENDOTHELIAL AND VASCULAR SMOOTH MUSCLE CELLS

SRIRAM GOPU

(BDS, MDS (Oral Pathology))

A THESIS SUBMITTED

FOR THE DEGREE OF DOCTOR OF PHILOSOPHY

DISCIPLINE OF ORAL SCIENCES

FACULTY OF DENTISTRY

NATIONAL UNIVERSITY OF SINGAPORE

2014

DECLARATION

I hereby declare that this thesis is my original work and it has been written by me in its entirety. I have duly acknowledged all the sources of information which have been used in the thesis.

This thesis has also not been submitted for any degree in any university previously.

[SRIRAM GOPU]

Date:

ACKNOWLEDGEMENTS

This doctoral thesis is the result of my research journey for the past four years of my life which would not have been possible without the aid, support and contribution of several friends, teachers, mentors, colleagues, and sales personnel to whom I wish to express my thanks here. To begin with, I would like to thank all those persons who came across in my PhD journey and their contribution was very important, however insignificant it may be. I am extremely thankful to National University of Singapore for providing me with this wonderful opportunity and supporting me with not just one but two scholarships (President's Graduate Fellowship and NUS Research Scholarship).

I owe my deepest and sincere gratitude to my primary supervisor, A/P. Cao Tong for his patience, advice, scientific support, financial support and persistent faith in me and my project. I am extremely thankful to him for providing me a free-hand to venture different avenues in my research. Further, I am grateful for the academic and administrative experiences I gained under his guidance and supervision. Overall, it was a pleasure and I am fortunate to be able to work with him.

I would like to express my thanks to co-supervisor, Dr. Rufaihah Abdul Jalil for her academic support, constructive criticism and also allowing me to use various reagents and equipments in her lab which contributed greatly towards the smooth progress of my research experiments.

Special thanks go to Dr. Evelyn Yim for being part of my thesis advisory committee and refereeing my research. Besides my supervisors, I am grateful to Dr. Gan Shu Uin, who helped me fluorescently label the cells with DsRed2; and Mr. Zou Yu for fluorescent labeling of hESCs with eGFP which formed an important part of my work. My special thanks to Dr. Tan Jiayong in establishing the initial stages of the differentiation protocol. Of course, I cannot forget Dr. Lu Kai who taught me the basics of embryonic stem cell culture and molecular techniques that laid the foundation and provided me the confidence.

I also owe my thanks to Dr. Intekhab Islam for providing me with the opportunity to work under him. I am also indebted to all the mentors I had come across in the course of various modules and training programs.

I am extremely thankful to Dr. Paul Hutchinson and Mr. Guo Hui Teo for their invaluable support and troubleshooting in flow cytometry. My sincere thanks to Ms. Lee Shu Ying and Mr. Zhang Weian for their support in confocal microscopy. My sincere thanks to Dr. Kothandharaman Subramaniam for his help in processing angioarrays. I also thank Mr. Chan

Swee Heng, Ms. Nurazareen Zaid, Ms. Zarina Zainol, Ms. Angeline Han, Mr. Bufford Ang, Mdm. Lina and Ms. Cynthia Sing for their training and administrative support.

Of course I owe my special thanks to all my colleagues in DSO (a long list) for their help, discussions, chats and support. But I need to mention a few names that include Dr. Liu Hua, Dr. Toh Wei Seong, Dr. Vinoth Kumar, Dr. Aarthi Saminathan, Dr. Fu Xin, Dr. Fahad Kidwai, Dr. Li Mingming, Dr. Lu Qiqi, Mr. Mehdi Movahednia, Ms. Li Lulu, Mr. Harish Handral, Dr. Zhu Qian, Dr. Tong Hui Jinn, and Dr. Tan Kai Soo. I am also grateful to all the other friends and colleagues who have helped and contributed, in one way or another, to my research project.

Lastly, I owe my deepest thanks to the Almighty, classical musicians and my family, especially my parents Mr. Gopu and Mrs. Harini; my siblings Mr. Srihari and Ms. Subhasri; my in-laws Dr. Prakash and Mrs. Seema; and most importantly my wife, Dr. Vaishali and my son Mast. Anirudha for their moral support, encouragement, and sacrifices throughout my PhD career. Their unconditional love and their invaluable trust, support and loyalty are the most beautiful gift that I will always keep in my heart. I owe you all a lot more than what I can write.

_____

[SRIRAM GOPU]

Date:

Table of Contents

List of Tables

List of Figures

List of Abbreviations

Abbreviation	Description
3D	Three dimensional
AP	Alkaline phosphatase
APC	Allophycocyanin
Art-ECs	Arterial endothelial cells
bFGF	basic fibroblast growth factor
BMP4	Bone morphogenetic factor
BSA	Bovine serum albumin
cAMP	Cyclic adenosine monophosphate
CD	Cluster of differentiation
CD105	Cluster of differentiation 105; Endoglin
CD31	Platelet endothelial cell adhesion molecule (PECAM-1)
CD73	Cluster of differentiation 73; ecto-5'-nucleotidase
CD90	Cluster of differentiation 90; THYmocyte differentiation antigen 1 (Thy-1)
cDNA	complementary DNA (Deoxyribonucleic acid)
CNN1	Calponin
COUP-TFII	Chicken ovalbumin upstream promoter-transcription factor-11
CXCR4	C-X-C chemokine receptor type 4
DAPI	4',6-diamidino-2-phenylindole
Dil-Ac-LDL	Dil-acetylated-low density lipoprotein
DLL4	Delta-like ligand 4
DMEM	Dulbecco’s modified Eagle's minimal essential medium
DMSO	Dimethyl sulfoxide
ECM	Extracellular matrix proteins
ECs	Endothelial cells
EGF	Epidermal growth factor
eGFP	Enhanced green fluorescent protein
eGFP	Enhanced green fluorescent protein
EMT	Epithelial-mesenchymal transition
EndMT	Endothelial-mesenchymal transition
eNOS	Endothelial nitric oxide synthase
EPH-B4	Ephrin type-B receptor 4
EPHRIN-B2	Ephrin type-B
ESCs	Embryonic stem cells
ESFM	Endothelial serum free medium
FACS	Fluorescence-activated cell sorting
FBS	Fetal bovine serum
FGF	Fibroblast growth factor
FITC	Fluorescein isothiocyanate
FOXA2	Forkhead box protein a2
GSK-3	Glycogen synthase kinase-3
GSKi	Inhibition of gsk-3
hESCs	Human embryonic stem cells

Abbreviation	Description
ICM	Inner cell mass
iPSCs	Induced pluripotent stem cells
MACS	Magnetic assisted cell sorting
Mixl1	Mix1 homeobox-like 1
mRNA	Messenger RNA (ribonucleic acid)
NANOG	Nanog homeobox
NO	Nitric oxide
NOTCH1	Notch homolog 1, translocation-associated
NRP1	Neuropilin-1
NRP2	Neuropilin-2
OCT4	Octamer-binding transcription factor 4
PAX6	Paired box protein-6
PBS	Phosphate buffered saline
$PDGF_{bb}$	Platelet derived growth factor-BB
PDGFRα	Platelet-derived growth factor receptors α
PDGFRβ	Platelet-derived growth factor receptors β
PE	Phycoerythrin
PEG	Polyethylene glycol
PS	Primitive streak
PSCs	Pluripotent stem cells
RT-PCR	Reverse transcriptase polymerase chain reaction
SFM	Serum free medium
Shh	Sonic hedgehog
SM-MHCII	Smooth muscle-myosin heavy chain II
SNAI1	Snail family zinc finger 1
SOX1	SRY (sex determining region y)-box 1
SOX2	SRY (sex determining region y)-box 2
SSEA3/4	Stage-specific embryonic antigens 3/4
TGF- β1	Transforming growth factor-β1
TNFα	Tumor necrosis factor-α
TRA-1-60	Tumor rejection antigen-1-60
TRA-1-81	Tumor rejection antigen-1-81
VE-CAD	Vascular endothelial-cadherin
VEGF	Vascular endothelial growth factor
VEGFR2	Vascular endothelial growth factor receptor-2; kinase-domain receptor (KDR); fetal liver kinase-1 (Flk-1)
Ven-ECs	Venous endothelial cells
vSMCs	Vascular smooth muscle cells
vWF	Von willebrand factor
Wnt	Wingless
αSMA	alpha-smooth muscle actin

List of Publications & Awards

Journal Publications

1. ***Sriram G***, Tan JY, Zou Y, Gan SU, Islam I, Rufaihah AJ, Cao T. *In-vitro* vascularized tissue equivalents from self-assembly of hESC-derived vascular cells. *[Under preparation]*
2. ***Sriram G***, Tan JY, Islam I, Rufaihah AJ, Cao T. Efficient differentiation of human embryonic stem cells to arterial and venous endothelial cells under feeder-free and serum-free conditions. *[under review]*
3. Saminathan A, ***Sriram G***, Vinoth JK, Cao T, Meikle MC. Engineering the periodontal ligament in hyaluronan–gelatin–type I collagen constructs: upregulation of apoptosis and alterations in gene expression by cyclic compressive strain. *[under review]*
4. Tan JY, ***Sriram G***, Rufaihah AJ, Neoh KG, Cao T. (2013). Efficient derivation of lateral plate and paraxial mesoderm subtypes from human embryonic stem cells through GSKi-mediated differentiation. Stem Cells Dev 22, 1893-1906.

Conference Abstracts and Presentations

1. ***Sriram G***, Tan JY, Zou Y, Islam I, Rufaihah AJ, Cao T. *In-vitro* vascularized tissue equivalents from human embryonic stem cell derived endothelial and smooth muscle cells. University Surgical Cluster Undergraduate Research Week, Singapore: 14-19 Oct 2013. *(Poster)*
2. ***Sriram G***, Tan JY, Rufaihah AJ, Zou Y, Islam I, Cao T. Clinically competent human embryonic stem cell derived vascular cells form vascular networks. TERMIS-EU 2013, Istanbul, Turkey: 17-20 Jun 2013. *(Poster)*
3. ***Sriram G***, Tan JY, Islam I, Rufaihah AJ, Cao T. Towards defined and xeno-free differentiation of human embryonic stem cells to endothelial lineage. EMBO|EMBL Symposium 2013: Cardiac Biology, Hiedelberg, Germany: 7-10 Jun 2013. *(Poster)*
4. ***Sriram G***, Tan JY, Rufaihah AJ, Islam I, Cao T. hESC-derived vascular cells as an alternative source of cells for fabrication of i*n-vitro* prevascularized tissue construct. YLL-SoM 3rd Annual Graduate Scientific Congress 2013, Singapore: 30 Jan 2013 *(Oral; Faculty Nomination)*
5. ***Sriram G***, Rufaihah AJ, Islam I, Cao T. In-vitro vascularized tissue constructs from hESC derived vascular cells. 26th Annual Meeting of the IADR Southeast Asian Division, Hong

Kong: November 3-4, 2012. (*Oral; IADR/Unilever Divisional Competition and Awards - Senior category*)

6. ***Sriram G***, Tan JY, Rufaihah AJ, Intekhab I, Neoh KG, Cao T (2012). Differentiation of hESCs to vascular lineage in an autologous feeder-free system. YLL School of Medicine 2nd Annual Graduate Student Congress, Singapore. *(Poster)*

Awards

1. Lee Foundation Travel Award (for attendance to TERMIS-EU 2013), (2013)
2. EMBL Corporate Partnership Registration Fee Fellowship (for attending EMBO|EMBL Symposium 2013), (2013)
3. President's Graduate Fellowship (2012-2014).
4. NUS Research Scholarship (2010-2011).

Patent Applications

1. Cao T, Sriram G. Efficient Differentiation of human embryonic stem cells to arterial and venous endothelial cells under feeder-free and serum-free conditions (Patent application submitted to Industry Liason Office, NUS)

Summary

Vascularization is one of the key components required to engineer three-dimensional (3D) tissues and organs. To realize the potential of cell-based approach for vascularizing tissue requires scalable production of homogeneous populations of vascular cells that include endothelial cells (ECs) and vascular smooth muscle cells (vSMCs). Human embryonic stem cells (hESCs) are virtually an unlimited source of differentiated cells including ECs and vSMCs. However, current differentiation strategies need improvisation in terms of efficiency, reproducibility, and use of xenogeneic (animal-derived) products. To obtain scalable amounts of clinically competent vascular cells, we aimed to develop differentiation protocols with minimal use of xenogeneic products. Further, we investigated the functionality of hESC-derived vascular cells to engineer *in-vitro* vascularized tissue equivalents.

Under feeder-free and chemically-defined conditions, we demonstrate efficient differentiation of hESCs into progenitor populations expressing markers related to endothelial lineage (lateral plate mesoderm; $VEGFR2^{+}CD34^{+}PDGFR\beta^{-}$) and paraxial mesoderm ($PDGFR\beta^{+}CD34^{-}CD31^{-}VEGFR2^{-}$) using sequential modulation of Wnt, FGF, BMP and VEGF signaling pathways. Further, we demonstrate the differentiation of hESC-derived $CD34^{+}CD31^{+}$ endothelial progenitor cells into homogeneous populations of arterial and venous ECs under serum-free conditions by modulating the concentration of VEGF. Similarly, the $PDGFR\beta^{+}CD34^{-}CD31^{-}$ paraxial mesoderm intermediates were differentiated to vSMCs under smooth muscle differentiation conditions. Further, the hESC-derived ECs (arterial and venous phenotypes) and vSMCs were extensively characterized for expression of corresponding cell surface and intracellular markers, and for their *in-vitro* functionality. Additionally, various angiocrines secreted by all the three vascular progenies were surveyed.

A prerequisite to realize the full potential of these ECs and vSMCs is their ability to form blood vessels. We analyzed this potential by *in-vitro* 3D co-culture of the hESC-derived arterial ECs and vSMCs in a polyethylene-glycol-fibrin gel under serum-free conditions. To enable visualization of the ECs and vSMCs in 3D cultures, they were fluorescently labeled with eGFP and DsRed2 respectively. Upon 3D co-culture, the arterial ECs formed anastomosing endothelial cords; however, they regressed within 6 days of culture. In contrast, in the presence of vSMCs, the ECs organized and matured into a microvascular network of endothelial tubes (with patent lumen) and the vascular network was stable in culture for 3 weeks. Further, the microvessels were mature in terms of their barrier function, and also were capable of regulating the permeability in responsive to physiological stimulus like histamine.

In summary, we demonstrate the efficient differentiation of hESCs to ECs (arterial and venous) and vSMCs in relatively xenogeneic-free microenvironment; and the utility of these cells in the fabrication of *in-vitro* vascularized tissue equivalent. From a future perspective, we believe that these hESC-derived ECs, vSMCs and vascularized tissue equivalents could provide a potential human model to study vascular tissues for various clinical, research and pharmaceutical applications.

Chapter 1

Introduction

1. Introduction

Endothelial cells (ECs) and vascular smooth muscle cells (vSMCs) constitute the principal cells of all the small and large, arterial and venous blood vessels in the body. Deficiency of ECs and vSMCs in terms of their presence and/or function plays a major role in development and progression of various diseases, including cardiovascular diseases (Carmeliet, 2005; Carmeliet and Jain, 2000). Further, the development, maintenance and function of all the organs in the human body depends on adequate supply of nutrients and removal of waste by-products, which in turn is depend on adequate blood supply to the organs. Various efforts have been reported to construct tissue-engineered blood vessels *in-vitro* and *in-vivo* using mature ECs and vSMCs (Lokmic and Mitchell, 2008; Novosel et al., 2011; Rivron et al., 2008).

Human embryonic stem cells (hESCs) and induced pluripotent stem cells (iPSCs) have shown a great promise as a tool to early human development, develop *in-vitro* testing platforms and as a therapeutic cell source. Owing to the capacity to self-renew almost indefinitely and the potential to differentiate into lineage-specific cells, hESCs could be used as an unlimited source of lineage-committed cells including ECs and vSMCs. Various protocols have been reported to differentiate hESCs into vascular cells that include ECs and vSMCs (Cheung and Sinha, 2011; Kane et al., 2011). However, one of the major challenges for the use of these hESC-derived vascular cells for engineering functional vascular tissues is the heterogeneous population of differentiated cells, which may lead to inferior tissue organization, ectopic formation of unintended tissue and teratoma formation. Hence, strategies need to be developed to efficiently differentiate hESCs towards vascular lineage and to enrich ECs and vSMCs prior to their use for vascular tissue engineering. Secondly, most of the current protocols to differentiate PSCs to vascular cells utilize various xenogeneic (animal-derived) products like serum, feeder cells, matrices that limit the clinical translation potential of these cells, and also limit the ability to tune the culture milieu due to the presence of undefined components (Kaupisch et al., 2012). Another challenge is the heterogeneous nature of ECs at molecular, morphological and functional levels (Aird, 2007a). ECs that form the arteries and veins differ in terms of molecular and functional levels, and further, the ECs in different tissues display different characteristics (Torres-Vazquez et al., 2003). Similarly, the vSMCs also display different characteristics with phenotypes ranging from synthetic to contractile types. Additionally, vSMCs arise from diverse developmental origin and display differences in their function (Majesky, 2007). Current hESC and iPSC differentiation protocols are limited in terms of generating a heterogeneous pool of ECs and vSMCs. Hence protocols need

to be developed that address the specific developmental origins and associated heterogeneity among ECs and vSMCs.

Vascularization is a key component required to engineer three-dimensional (3D) tissues and organs which requires the establishment of vascular networks within the tissue construct (Novosel et al., 2011). Engineering vascularized 3D tissue constructs requires the use of an appropriate scaffold that would encourage the formation of vascular networks, angiogenic cells that include ECs or their progenitors and supporting cells, and/or provision of appropriate angiogenic signals (Lokmic and Mitchell, 2008).

Hence, in this doctoral work we aimed to efficiently differentiate hESCs to ECs and vSMCs with attention to developmental origins and heterogeneity among these cells in a feeder- and serum-free microenvironment. Further we utilize these hESC-derived ECs and vSMCs to engineer vascularized tissue equivalents in a serum-free microenvironment.

Chapter 2

Review of Literature

2. Review of Literature

Successful isolation and culture of hESCs (Thomson et al., 1998), and the generation of iPSCs (Takahashi et al., 2007; Yu et al., 2007), has initiated a new field of research for studying human development, cell therapy, tissue engineering, drug screening and disease modeling (Daley and Scadden, 2008). hESCs are derived from the inner cell mass (ICM) of the developing blastocyst that can proliferate almost indefinitely upon culture (Thomson et al., 1998). iPSCs on the other hand are derived from nuclear reprogramming and induction of pluripotency in somatic cells (Park et al., 2008). Both the types of pluripotent stem cells (PSCs), hESCs and iPSCs have the potential to differentiate *in-vitro* into derivatives of the three primary germ layers (***Figure 1***). PSCs could differentiate spontaneously to all the three germ layers, however to differentiate to the cell types of interest, reproducible and efficient differentiation protocols are needed.

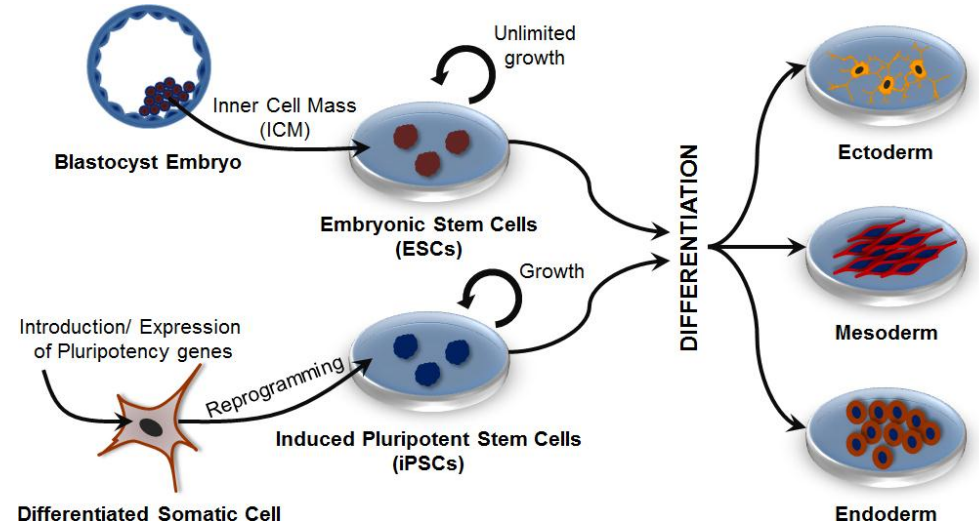

Figure 1. Derivation and differentiation of pluripotent stem cells

The illustration depicts the derivation of ESCs from the ICM of the blastocyst embryo and iPSCs from introduction or expression of pluripotency genes in differentiated somatic cells. The ESCs and iPSCs have the ability to self-renew and differentiate to cell types of the three germ layers.

In the present context of engineering vascularized tissue equivalents, the cell types of interest that fall the umbrella of vascular lineage includes, ECs, vSMCs or pericytes, hematopoietic cells and cardiomyocytes. Differentiation of PSCs into ECs and vSMCs is of growing interest for various applications as it provides an access to study vascular development in both physiological and diseased states, which otherwise is not possible due to ethical issues. Secondly, the PSC-derived ECs and vSMCs serve as a human vascular model to study various

cellular and molecular aspects. These cells also provide access to abundant population of cells for the pharmaceutical industry to screen and develop novel cardiovascular compounds (Rubin, 2008). Finally, in the long term these cells can lend for cellular therapy to repair ischemic tissues and develop tissue engineered vascular grafts (***Figure 2***).

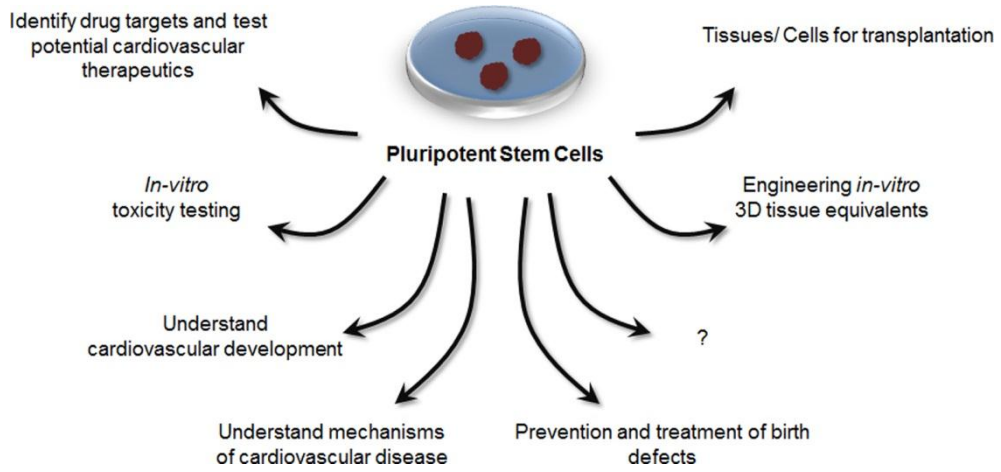

Figure 2. Promise of PSCs in cardiovascular research

The illustration highlights the potential scope of pluripotent stem cells in cardiovascular research ranging from understanding normal physiology, disease mechanisms, developing therapeutics to cellular therapy.

Several protocols to differentiate hESCs towards vascular lineage have been reported till date (Descamps and Emanueli, 2012; Kane et al., 2011). These protocols involve: (1) embryoid body-based differentiation, (2) co-culture of hPSCs over murine stromal cells, (3) culture of hESCs or iPSCs as monolayers over extracellular matrix proteins like Matrigel, and collagen IV, and/or (4) growth factor, cytokines or small molecule mediated differentiation in serum containing/ serum-free conditions. Despite the enormous amount of progress made in directing hESCs towards functional cells of the vascular lineage, there remain certain major challenges in the hESC differentiation paradigm. These include low differentiation efficiency, reproducibility, animal product contamination, tumorigenicity and immunocompatibility (Kaupisch et al., 2012).

Use of xenogeneic (animal-derived) products like serum, Matrigel, feeder cells within the culture milieu is associated with two concerns. Xenogeneic products would affect the differentiation efficiency and limit the precise control over the differentiation system due to the presence of undefined factors and batch variability. Secondly, hESCs cultured or differentiated in the presence of xenogeneic products are not compatible with clinical applications due to the risk of graft rejection and potential transfer of xenogeneic pathogens (Kaupisch et al., 2012). Recent advances in culture media, extracellular matrices and small

molecules are believed to assist in achieving PSC-derived progenies differentiated under xenogeneic-free conditions.

A thorough understanding of the progression of lineage commitment and differentiation *in-vivo* would aid us in achieving improved differentiation efficiency of PSCs. ECs and vSMCs predominantly develop from mesodermal progenitors. To be specific, ECs arise from lateral plate mesoderm while vSMCs are known to arise from diverse origins including lateral plate mesoderm, paraxial mesoderm and neural crest (Majesky, 2007). To reproduce these complex developmental processes *in-vitro*, requires the dissection of the process into simple steps marked by specific biological markers.

The first few sections of this chapter would focus on understanding the commitment of cells in the embryo and PSCs towards mesodermal lineage, followed by their commitment to progenitors related to vascular lineage cells (ECs and vSMCs). The next few sections would focus on the isolation of these progenitors, terminal differentiation of isolated vascular progenitor cells and characterization of the terminally differentiated ECs and vSMCs. Since the vascular system is broadly divided into arterial and venous systems, a section is included on commitment of ECs towards arterial and venous phenotypes. The final section reviews the relevant approaches and biomaterials for co-culture of ECs and vSMCs to engineer vascularized tissue equivalents.

2.1. Mesodermal induction and associated markers

The *in-vitro* differentiation of hESCs in most cases recapitulates the sequential stages of development observed in embryological studies. In the developing embryo, the cells of the hematopoietic and cardio-vascular lineage arise from subpopulations of mesoderm in a defined temporal sequence. An understanding of the embryonic development would facilitate their differentiation form hESCs. Mesodermal induction starts with formation of primitive streak (PS) from the epiblast which gives rise to the progenitors related to cells of the mesoderm and endoderm germ layers.

2.1.1. Primitive streak and germ layer specification in mammalian embryos

In mammalian embryogenesis, the generation of the three germ layers (ectoderm, mesoderm and endoderm) occurs during the process of gastrulation. The beginning of gastrulation is marked by the epithelial-mesenchymal transition (EMT) of certain epiblast cells to from a transient structure known as primitive streak (PS) that forms on the posterior midline of the embryo. As the epiblast cells undergo EMT, they ingress into the PS (between the epiblast and hypoblast) which results in the formation of mesoderm and definitive endoderm germ layers (Ciruna and Rossant, 2001). Hence the formation of PS results in transformation of a bilayered germ disc (epiblasts and hypoblasts) to a trilayered germ disc consisting of ectoderm, mesoderm and endoderm (***Figure 3***). Due to their ability to contribute to mesoderm or endoderm, PS is also referred to as mesendoderm.

Molecular and lineage tracking studies have divided the PS into anterior, mid and posterior regions that exhibit distinct gene expression patterns (Tam and Loebel, 2007). Genes like Brachyury (Kispert and Herrmann, 1994) and *Mixl1* (Hart et al., 2002) characterize the PS in general, while anterior PS preferentially express *Foxa2* and *Goosecoid* (GSC) (Kinder et al., 2001b); and the posterior PS expresses *HoxB1* (Forlani et al., 2003) and *Evx1* (Dush and Martin, 1992). The cells of the anterior PS form the anterior mesendoderm that gives rise to endoderm and axial mesoderm. With progression of gastrulation, the cells migrate through the posterior PS and give rise to paraxial, intermediate and lateral mesoderm (Tam and Behringer, 1997) (***Figure 4***). The axial mesoderm gives rise to prechordal plate and notochord; paraxial mesoderm to somites that further develop to muscles, bone and cartilage; intermediate mesoderm to renal and gonadal systems; and the lateral plate mesoderm gives rise to heart, blood vessels and hematopoietic cells (Kitagawa and Era, 2010) (***Figure 5***). This segregation of cell fates during gastrulation occurs in a temporal and spatially controlled manner that are regulated by coordinated activation of various signaling pathways that include BMP, Nodal, Wnt, and FGF pathways(Tam and Loebel, 2007).

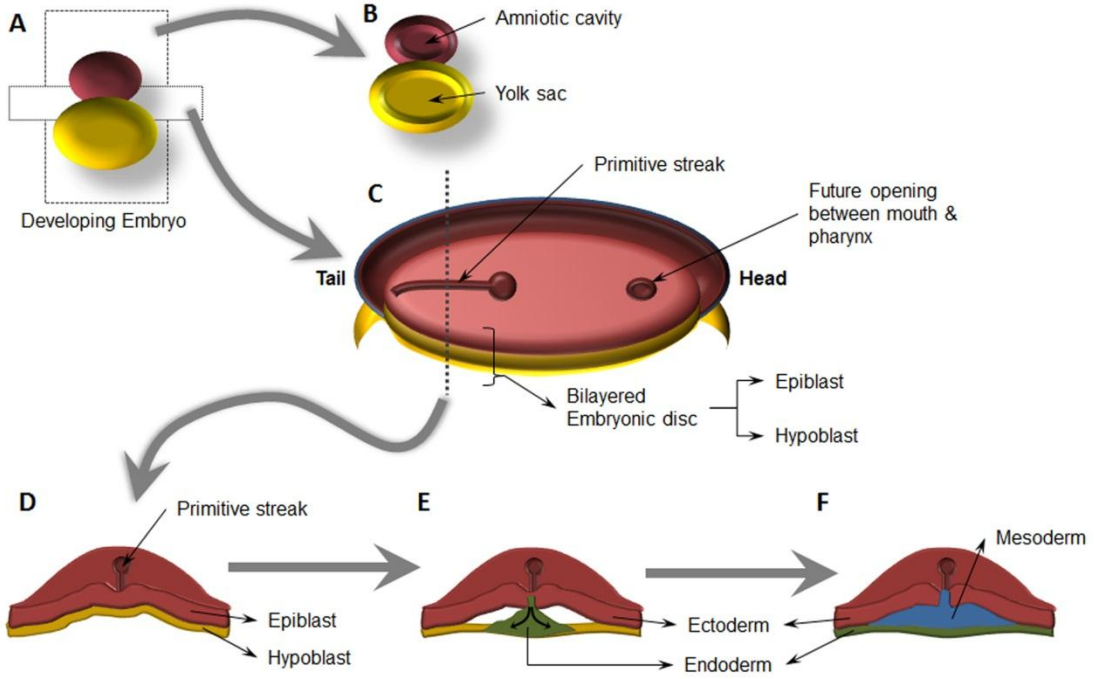

Figure 3. Formation of primitive streak, mesoderm and endoderm.

Cells of the inner cell mass of the embryo forms the bilayered embryonic disc that separates the amniotic cavity from the yolk sac **(A-B)**. The bilaminar embryonic disc consists of a layer of epiblast (forms the floor of amniotic cavity) and hypoblast (forms the roof of yolk sac) **(C)**. Certain cells within the epiblasts in the posterior midline ingress between the epiblasts and hypoblast to form the primitive streak (PS) **(C-D)**. A cross-section through the PS shows the ingression of PS cells in between epiblast and hypoblast that forms the endoderm €. The epiblast cells are now referred to as ectoderm. Later, the mesoderm is formed by additional cells that migrate in between the ectoderm and endoderm resulting in the formation of a trilayered embryonic disc **(F)**. *Source: Drawn based on an illustration from Human Anatomy and Physiology, 7e, Marieb EN, Marieb KH.*

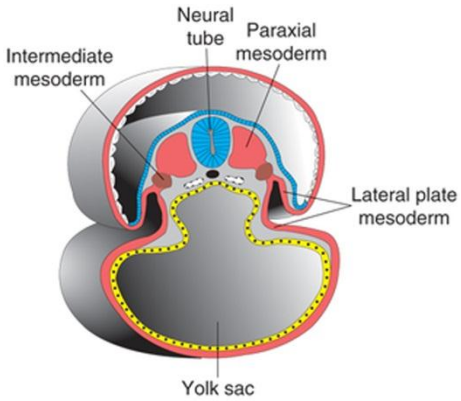

Figure 4. Segregation of mesoderm during embryogenesis.

Migration of PS and the mesodermal cells gives rise to different parts of the mesoderm, namely paraxial, intermediate and lateral plate mesoderm.
Source: http://renalsystem.weebly.com/embryological-source-of-urinary-system.html

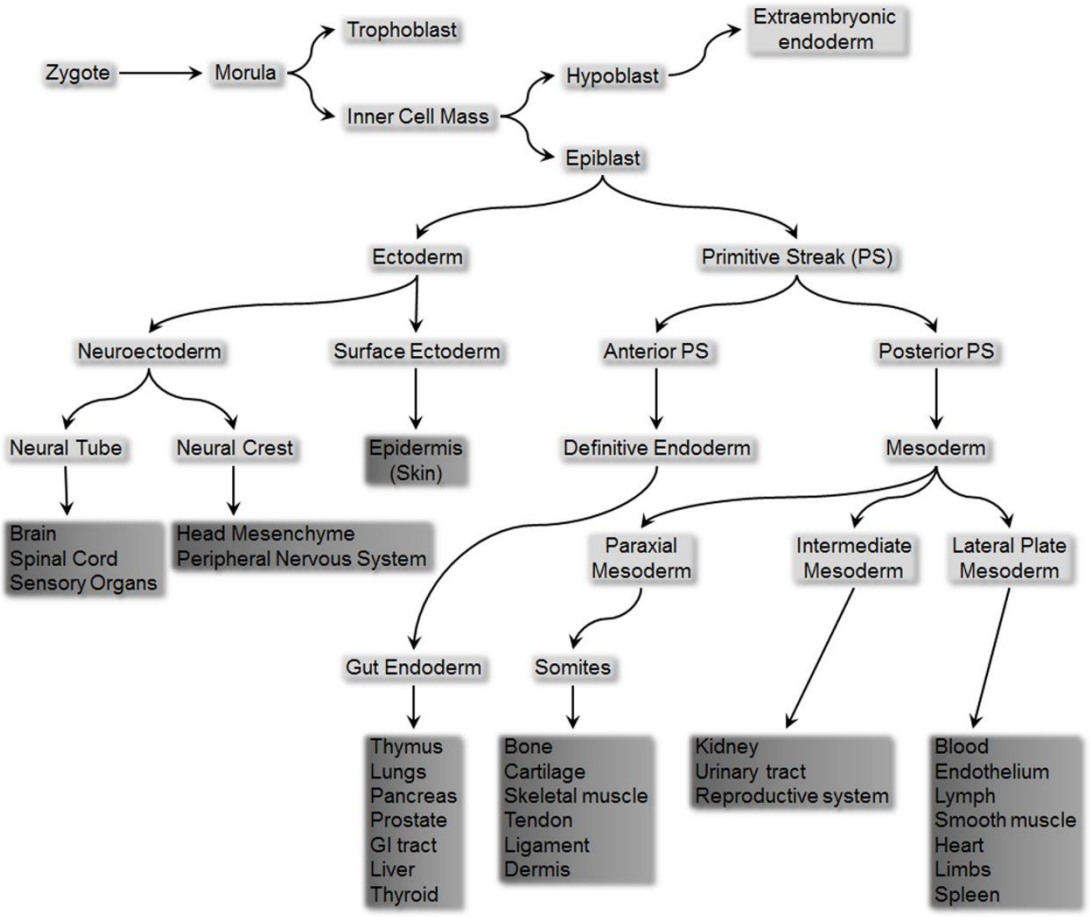

Figure 5. Germ layer derivatives

The schematic flow chart illustrates the embryonic development of various derivatives of the germ layers of the embryo. *Source: Drawn based on an illustration from http://discovery.lifemapsc.com.*

2.1.2. Markers associated with the early stages of mesoderm and endoderm development

The markers expressed in the early stages of embryonic development are extensive. The important markers used in the literature to identify/ track the development of PS, early mesodermal subsets and endoderm would be discussed below.

Brachyury (*T*) is a transcription factor required for PS development and hence, is expressed in the mesendoderm (Wilkinson et al., 1990). Mouse embryos lacking *Brachyury* exhibit severe abnormalities and die by day 10 of gestation (Yanagisawa et al., 1981). The abnormalities include lack of migration of cells through PS, and a reduced mesoderm formation. Hence, it is commonly used as a marker along with other markers to monitor the development of PS and induction of mesoderm. *Brachyury* is a transient marker that upregualtes with the induction of PS and downregulates when the cells undergo specification towards specific mesodermal tissues (Beddington et al., 1992). Other markers used along with *Brachyury* are *Wnt3* and

Mixl1 which are expressed in PS and mesoderm; *GSC* and *Foxa2* which are expressed in PS and endoderm.

Mixl1 is a homeobox gene expressed in the PS of gastrulating embryo, and visceral endoderm of pre-gastrulation embryo (Pearce and Evans, 1999; Robb et al., 2000). *Mixl1* is predominantly expressed in the mesoderm/endoderm boundary, and marks the cells fated to differentiate to mesoderm and endoderm (Grapin-Botton, 2008; Ng et al., 2005a). *Mixl1*-null mutants die at embryonic day 8.5 and show an enlarged PS and abnormalities in the formation of definitive endoderm (Hart et al., 2002).

In addition to *Brachyury* and *Mixl1*, the PS also expresses *SNAI1* and *SNAI2* as the epiblast cells undergo EMT. *SNAI* belongs to a family of zinc-finger transcription factors that is involved in processes required to induce EMT through which the epithelial cells loose contacts with adjacent cells and become migratory and invasive (Blanco et al., 2007). In addition, to expression of *SNAI* other markers used to identify cells undergoing EMT include loss of E-cadherin and upregulation of CD56 (neuronal cell adhesion molecule, NCAM) (Evseenko et al., 2010).

VEGFR2 (vascular endothelial growth factor receptor-2) is also known as *KDR* (kinase-insert domain containing receptor) in humans and *Flk-1* (fetal liver kinase-1) in mice. *VEGFR2* is well established marker for mesoderm (in particular lateral plate mesoderm) and hemato-endothelial progenitors in mouse embryos, and differentiated mouse and human ESCs (Evseenko et al., 2010; Kataoka et al., 1997; Park et al., 2004; Sakurai et al., 2006; Tan et al., 2013a; Yamaguchi et al., 1993; Yamashita et al., 2000). Other markers associated with commitment to lateral plate mesoderm especially cardiovascular lineage include CD34, Mesp1, Nkx2.5, and Isl1 (Mummery et al., 2012).

FoxA2 and *GATA* factors are among the various transcription factors expressed in mesendoderm and endoderm. *FoxA2* is expressed at the onset of gastrulation and is essential for the specification of foregut and midgut structures (Grapin-Botton, 2008). Among the various *Gata* genes, *Gata4* and *Gata6* are expressed in the mesendoderm and endoderm; and are involved in the commitment of mesendoderm cells towards endoderm (Grapin-Botton, 2008). Other markers associated with endoderm specification include *Goosecoid (GSC)*, *CXCR4*, *Sox17* and *alpha fetoprotein (AFP)* (Grapin-Botton, 2008). In early stages of mouse embryogenesis, *CXCR4* (chemokine receptor 4) is associated with primitive and definitive endoderm (Drukker et al., 2012; McGrath et al., 1999). *CXCR4* has been used as one of the markers of endodermal commitment in early hESC differentiation cultures (Drukker et al., 2012; Tan et al., 2013a).

PDGFRs are tyrosine kinase receptors that are expressed in the paraxial mesoderm, somites, and neural tube (Kataoka et al., 1997; Schatteman et al., 1992). Expression of *PDGFRα* in combination with lack of expression of *VEGFR2* is used as a marker for paraxial mesoderm progenitors (Sakurai et al., 2006; Sakurai et al., 2012; Tan et al., 2013a). Further, embryos lacking *PDGFRβ* expression show significant lack of pericytes in the brain, lung, and gastrointestinal tract (Hellstrom et al., 1999).

The list of markers that mark the PS, mesoderm and endoderm subtypes are numerous. Hence, various markers have been used in the literature to track the above set of populations.

2.1.3. Role of BMP pathway in primitive streak and germ layer specification

Genetic studies in mice have demonstrated the critical role of BMP signaling in mesoderm formation and dorso-ventral patterning (Winnier et al., 1995). Mouse embryos lacking *Bmp4* or its receptors (*Bmpr1*, *Bmpr2*) function fail to gastrulate and form mesoderm (Mishina et al., 1995; Winnier et al., 1995). BMP antagonists Chordin and Noggin modulate BMP signaling and hence influence the cell fate decision during early embryogenesis (Loebel et al., 2003). Both Chordin and Noggin antagonize BMP signaling and drives the commitment of neuroectoderm towards neural fate. Similarly, the BMP antagonists counteract the mesoderm inducing effects of BMP4.

In contrast to in-vivo studies, observations using ESCs have yielded conflicting results. Induction of ESCs with BMP4 inhibits neural differentiation and upregulates *Brachyury* in a dose-dependent manner (Johansson and Wiles, 1995). Under serum-free conditions, BMP4 has been reported to efficiently induce mouse (Ng et al., 2005a; Nostro et al., 2008; Park et al., 2004; Wiles and Johansson, 1999) and human (Davis et al., 2008; Kennedy et al., 2007; Ng et al., 2005b; Pick et al., 2007) ESCs to *Brachyury* expressing PS population capable of differentiation to *VEGFR2*+ (Flk-1+) mesodermal cells. Similarly, BMP4 alone or in combination with Activin, rapidly induces *BRACHYURY* in hESCs (Vallier et al., 2009; Yang et al., 2008a; Zhang et al., 2008c). However, Nostro et al., (Nostro et al., 2008) and Tan et al., (Tan et al., 2013a) proposed that BMP4 alone is not sufficient in inducing PS. Zhang et al., (Zhang et al., 2008c) demonstrated the need for concomitant activation of FGF and TGFβ/Nodal/Activin signaling in addition to BMP4 for PS induction of hESCs. Similarly, Yu et al., (Yu et al., 2011) have demonstrated the mesoendodermal induction potential of BMP4 depends on FGF signaling. Under serum containing conditions Xu et al., reported that BMP4 induces differentiation to homogenous population of trophoectoderm cells (Xu et al., 2002). While under chemically defined conditions, Vallier et al., found that BMP4 drives differentiation to a heterogenous population of primitive endoderm and trophoectoderm (Vallier et al., 2009). Complimentary to these findings, Bernado et al., reported expression of

mesodermal genes by BMP4 in the presence of FGF, while BMP4 alone induces expression of trophoblast-associated genes (Bernardo et al., 2011). Hence, the outcome of BMP signaling in *in-vitro* systems seems to be dependent on the culture milieu and influence of other signaling molecules. The integrated role of BMP, Wnt, Nodal and FGF signaling in mesendoderm induction of mouse ESCs is highlighted in ***Figures 6-8***.

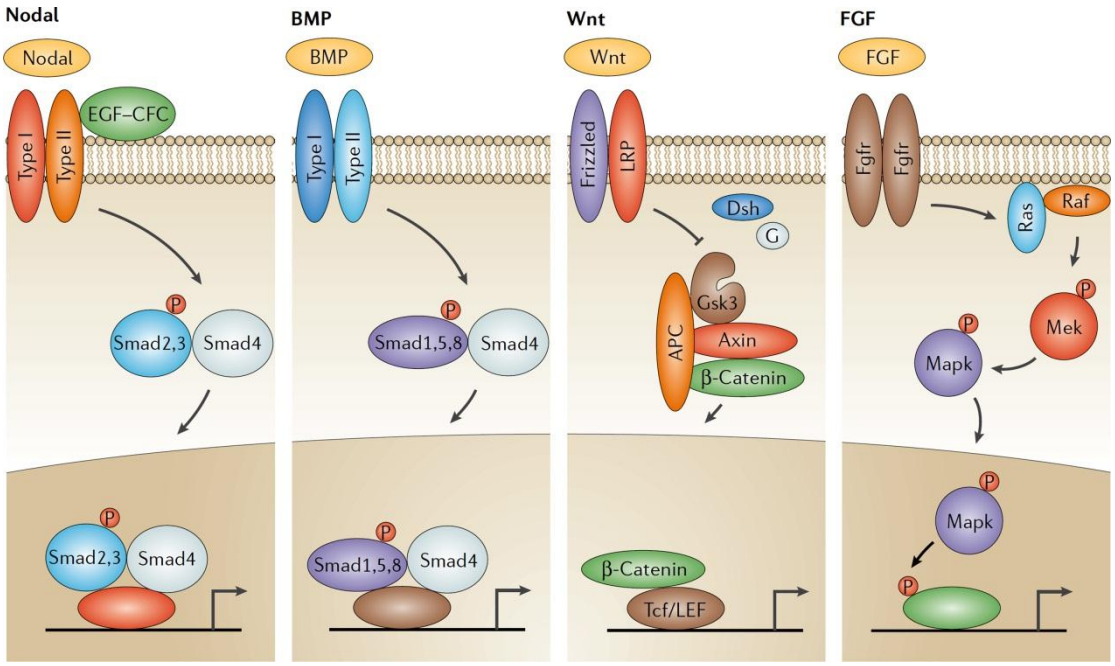

Figure 6. Intracellular signaling pathways.

The schematic represents the receptors and intracellular events involved in Nodal, BMP, Wnt and FGF signaling pathways. *Source: Adapted with permission from (Kimelman, 2006)*

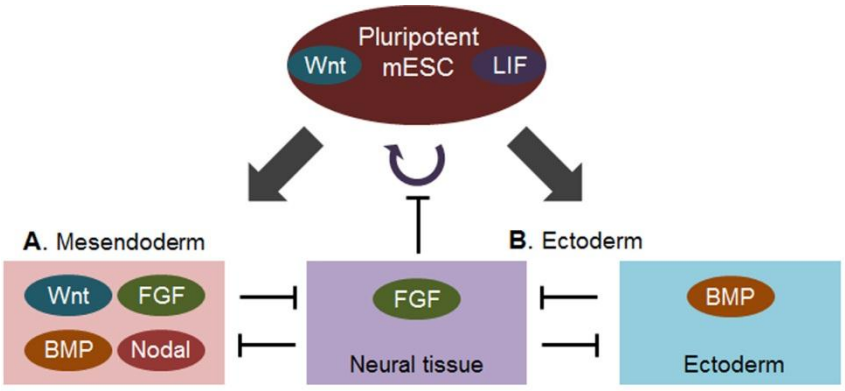

Figure 7. Signaling pathways controlling lineage choice and differentiation.

The schematic represents the choice of lineage decision based on studies in mouse ESCs. (A) Nodal, Wnt, BMP and FGF signaling pathways co-ordinate to induce mesendoderm induction and inhibit neural differentiation. (B) On the other hand, FGF alone inhibits pluripotency and induces commitment towards neural lineage. *Source: Redrawn based on an illustration in (Sokol, 2011a)*

2.1.4. Role of Nodal pathway in primitive streak and germ layer specification

Mouse studies have demonstrated that blockade of TGFβ/Nodal/Activin signaling pathway abrogates the formation of PS and mesoderm (Conlon et al., 1994). Nodal a member of TGFβ family is known to be required for anterior-posterior axis during gastrulation. Mouse embryos deficient for *Nodal* fail to form both mesoderm and definitive endoderm (Brennan et al., 2001). Intracellular events following activation of TGFβ, Activin, and Nodal operate through Smad2 and *Smad3* intracellular mediators (***Figure 6***). Mouse embryos lacking one allele of *Smad2* and *Smad3* display defects in definitive endoderm (Liu et al., 2004). Further, loss of *Smad3* and one allele of *Smad2* results in impaired formation of anterior axial PS; while selective deletion of *Smad2* and *Smad3* from epiblast cells interferes with commitment of axial and paraxial mesoderm (Dunn et al., 2004). Additionally, *Smad2-Smad3* double homozygous mutants lack mesoderm in entirety and fail to gastrulate (Dunn et al., 2004). Collectively, these observations suggest the role of TGFβ/Nodal/Activin signaling in early stages of mesoderm and endoderm specification.

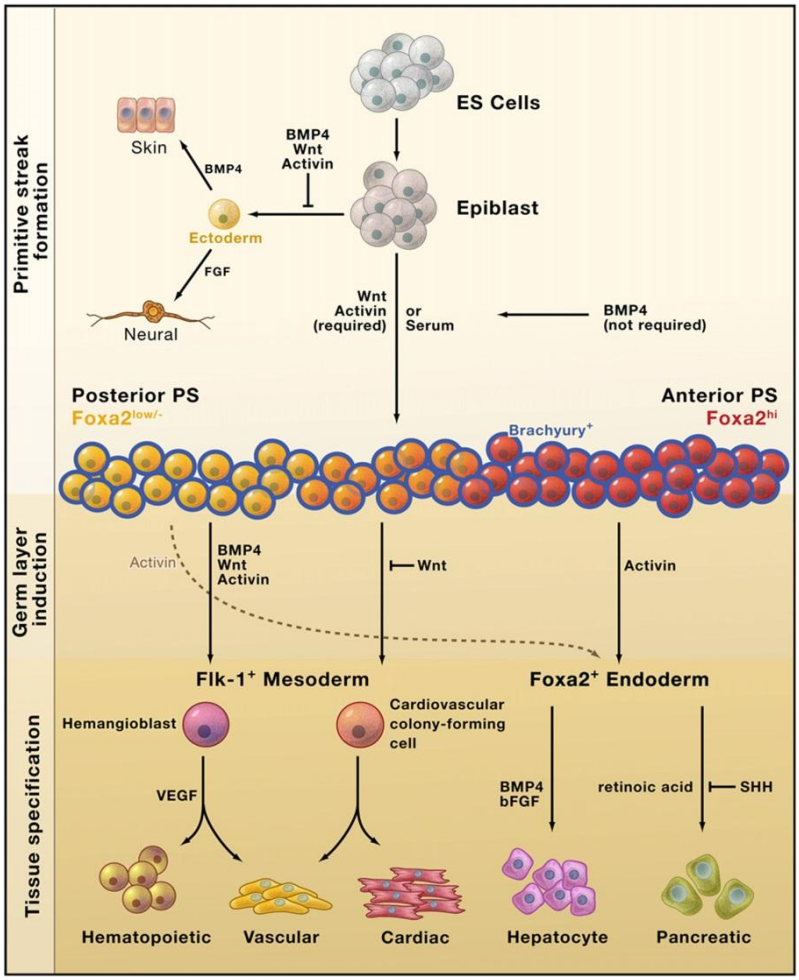

Figure 8. Role of intracellular signaling pathways in differentiation towards the three germ layers.

The schematic represents the regulation of induction of mouse ESCs to PS, primary germ layers and further tissue specification. Induction of mouse ESCs with Wnt, Activin, BMP4 and/or serum induces induction of PS-like cells (row of cells outlined in blue) while inhibits the induction towards ectoderm lineage. In contrast, inhibition or lack of activation of these pathways results in differentiation towards ectoderm lineage. The posterior PS cells (yellow) express Brachyury and low levels of Foxa2; and these cells commit towards Flk1^{+} mesodermal progenitors that differentiates further towards cardiovascular and hematopoietic lineages. While the anterior PS cells (dark orange) express Brachyury and high levels of Foxa2; and these cells commit towards Foxa2^{+} definitive endoderm cells. *Source: Adapted with permission from (Murry and Keller, 2008)*

Activation of Nodal pathway using Activin A in mouse and human ESCs induces specification of PS which further differentiates to mesoderm or endoderm depending on the concentration of activin with higher concentrations favoring endoderm (D'Amour et al., 2005; D'Amour et al., 2006; Kubo et al., 2004; Vallier et al., 2009) (***Figure 8***). Based on studies in mouse ESCs, it has been suggested that the *Brachyury*$^{+}$ PS cells exist as two subpopulations (Kubo et al., 2004). The *Brachyury*$^{+}$ PS cells committing to mesoderm lineage had low levels of *Foxa2* expression suggesting a posterior PS-like subpopulation. While the *Brachyury*$^{+}$ cells

that committed to endoderm had higher levels of *Foxa2* indicating an anterior PS-like subpopulation. Similarly, in hESC-embryoid bodies low doses of Activin A in combination with BMP4 and hematopoietic growth factors promotes the development of hematopoietic fated mesoderm through induction of *Brachyury* (Cerdan et al., 2012). However, under chemically defined conditions, Activin A is reported to be insufficient in driving mesendoderm differentiation (Nakanishi et al., 2009b; Vallier et al., 2009), while a cross talk between Activin, FGF and BMP4 signaling efficiently induced mesendoderm differentiation (Vallier et al., 2009). Further, the intensity of Activin signaling influences the choice between mesoderm or endoderm differentiation of mesendeodermal cells.

2.1.5. Role of Wnt pathway in primitive streak and germ layer specification

The formation of PS is considered as the central structural marker for mesodermal and endodermal precursors (Tam and Beddington, 1987). Among the various signaling pathways, the canonical Wnt signaling has been established as playing a pivotal role in the induction of PS and the formation of mesoderm and endoderm. Wnt/β-catenin pathway is mediated via a post-translational control over the stability of β-catenin (Sokol, 2011a). Lack of Wnt signal leads to a rapid degradation of β-catenin by β-catenin degradation complex. The β-catenin degradation complex consists of Axin, adenomatous polyposis coli (APC) and glycogen synthase kinase-3 (GSK3) (***Figures 6 & 9***). Activation of Wnt pathway through either frizzled receptors, or Lrp5/6 co-receptors leads to inhibition of GSK3 resulting in inactivation of the β-catenin degradation complex. When β-catenin is not degraded, it leads to accumulation and translocation of β-catenin from cytoplasmic membrane to the nucleus. In the nucleus, the β-catenin binds to members of T-cell factors (TCF) family of transcription factors and activates the target genes (Kimelman, 2006; Sokol, 2011b).

Previous studies have established the essential role of Wnt/β-catenin pathway in mammalian germ layer specification. It is well established that Wnt activation leads to stabilization of β-catenin; in transgenic mouse models constitutive expression of stabilized β-catenin induces premature EMT of epiblasts to mesodermal progenitors (Kemler et al., 2004). Lack of *Wnt3a* (Liu et al., 1999) or β-catenin (Huelsken et al., 2000) in mouse embryos result in the diversion of ingressing epiblast cells towards neuroectodermal fate rather than mesendoderm which in turn results in improper formation of body axis and excessive development of anterior neuroectoderm. Similarly, in double-homozygous mutants of *Wnt3* co-receptors *Lrp5/6,* PS and mesoderm fail to form (Kelly et al., 2004). In contrast, genetic inactivation of negative regulators of Wnt pathway like the *Axin1, Tcf3,* and *dickkopf1* (*Dkk1*) results in absence of head and formation of ectopic axial structures (Sokol, 2011b). These *in-vivo* studies highlight the role of Wnt/β-catenin pathway in PS and germ layer specification.

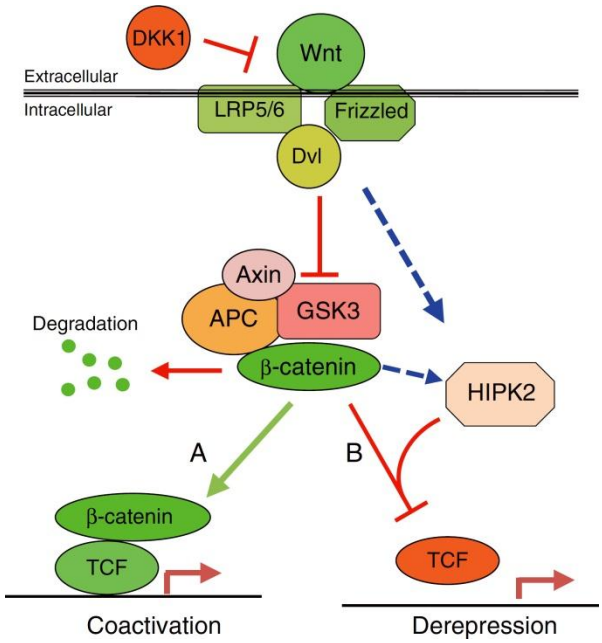

Figure 9. Canonical Wnt signaling pathway.

The schematic represents the activation of Wnt through frizzled receptors or Lrp5/6 co-receptors result in inactivation of β-catenin degradation complex. Inhibition of Wnt results in degradation of β-catenin. Inhibition of GSK-3 activity results in stabilization of β-catenin and activation of target genes by the β-catenin-TCF complex. *Source: Adapted from open source article (Sokol, 2011b).*

In contrast to *in-vivo* findings, the role of Wnt/β-catenin signaling in mouse and human ESCs has been controversial due to contradictory findings. Studies have reported the activation of Wnt/β-catenin signaling maintains pluripotency of both mouse and human ESCs (Hao et al., 2006; Miyabayashi et al., 2007; Ogawa et al., 2006; Sato et al., 2004; Singla et al., 2006; Takao et al., 2007; ten Berge et al., 2011; Wagner et al., 2010). Further, Wnt pathway has been implicated in promoting the reprogramming of somatic cells to iPSCs (Lluis et al., 2008; Marson et al., 2008). On the other hand, activation using either Wnt3a or GSK3 inhibitors has been demonstrated to induce differentiation of ESCs towards PS, mesoderm and endoderm (Bone et al., 2011b; Davidson et al., 2012; Nakanishi et al., 2009a; Tan et al., 2013a). These controversial observations may be due to differences in dose and duration of Wnt activation, differences in differentiation methods and presence of serum or other factors like bFGF in the differentiation medium. In hESCs, Wnt signaling and Activin/ Nodal has been reported to synergistically induce specification towards anterior PS/ endoderm; while in association with BMP signaling induces a posterior PS/ mesoderm fate (Sumi et al., 2008). Similarly, in mouse ESCs, Wnt or low levels of Activin induce differentiation to posterior PS; while high levels of Activin favor anterior PS fate (Gadue et al., 2006). Murry and colleagues using transgenic zebrafish embryos, mouse ESCs and hESCs reported that activation of Wnt/β-catenin signaling in early stages enhances mesoderm commitment, while at later stages inhibits

cardiac induction (Paige et al., 2010; Ueno et al., 2007). Additionally, addition of Wnt3a or inhibition of GSK3 markedly reduces the differentiation to ectodermal lineages (Nakanishi et al., 2009a; Tan et al., 2013a). Hence, the role of Wnt signaling in mesodermal induction of ESCs is dependent on the culture conditions and may be integrated with other signaling pathways.

2.1.6. Role of FGF signaling in mesoderm induction

Basic fibroblast growth factor (bFGF) is the first identified mesoderm inducer (Bottcher and Niehrs, 2005; Slack et al., 1987). Studies in mouse embryos (Ciruna and Rossant, 2001), have implicated the role of FGFs in controlling the specification and maintenance of mesoderm by regulating the *T* box transcription factors (*Brachyury*). Gain-of-function of FGF induces mesodermal markers while, inhibtion of FGF blocks mesoderm formation (Bottcher and Niehrs, 2005). Studies in mouse embryos (Deng et al., 1994; Yamaguchi et al., 1994) lacking FGF receptor 1 (*fgfr1*), show death of the embryos during late-gastrulation stage with defects in cell migration, specification and patterning. Observations of the embryos reveal accumulation of cells at the primitive streak, few cells that contribute to the formation of mesoderm and endoderm lineages, and failure of EMT. Additionally, the cells that gather at the primitive streak form ectopic neural tubes. Similarly, mouse embryos lacking *fgf8* display sever gastrulation defects that include lack of mesodermal and endodermal tissues (Sun et al., 1999). These studies indicate the role of FGF signaling in specification, migration, and patterning of mesoderm (Ciruna and Rossant, 2001).

2.2. Endothelial development and associated markers

An understanding of the embryonic development of ECs and its precursors could aid in their differentiation from hESCs. The embryo develops into three germ layers ectoderm, mesoderm and endoderm. The mesoderm further differentiates into axial, paraxial, intermediate and lateral mesodermal subtypes. The endothelium is the first tissue to develop during the process of vertebrate embryogenesis, as all other organ systems depend on supply of oxygen, nutrients and signals. The vascular progenitor cells (termed as hemangioblasts/ angioblasts) arise within the lateral plate mesoderm and give rise to the cardiovascular system (heart, blood vessels and hematopoietic cells) (Atkins et al., 2011). The progenitors within the lateral plate mesoderm migrate as cell clusters known as blood islands or hemangioblastic aggregates or hemogenic endothelial aggregates (Eichmann et al., 1998; Jaffredo et al., 1998). The cells at the periphery of these aggregates flatten and differentiate into ECs; while the cells in the center develop into primitive hematopoietic cells. Formation of such blood islands are seen both in the embryo proper (intra-embryonic vasculogenesis) and the yolk sac (extra-embryonic vasculogenesis). The aggregates of ECs connect with those in neighboring aggregates to form a primitive vascular network. This process of *de novo* formation of primitive plexus of vessels from the endothelial progenitors is known as vasculogenesis (Coultas et al., 2005; Flamme et al., 1997). The interconnected cords of vessels undergo a series of morphogenetic changes involving sprouting, proliferation and migration of the ECs and remodeling of the vascular channels. This process of branching and reorganization of existing vessels is termed as angiogenesis. Ultimately, the intra-embryonic and extra-embryonic vascular networks coalesce to form a vascular plexus that connects the embryo to the uterine wall. As the endothelial vessels remodel and mature, they recruit mural cells (pericytes and vSMCs) resulting in a complex network of arteries, arterioles, capillaries, venules and veins (Carmeliet, 2000; Carmeliet, 2005; Coultas et al., 2005; Flamme et al., 1997) (***Figures 10 & 11***). While in the adult life, most of the neovascularization occurs through angiogenesis (i.e., through endothelial sprouting, intussusception and bridging of existing blood vessels). Few evidences point to occurrence of vasculogenesis (i.e., *de novo* blood vessel formation) in the adult life. The endothelial progenitors in the bone marrow and circulating angiogenic cells seem to play a role in vasculogenesis and angiogenesis in the adult life (***Figure 11***).

The early events in the endothelial differentiation and the formation of blood vessels involve various signaling and regulatory cues that are not yet fully understood. The earliest marker expressed by the endothelial progenitor cells of avian and murine embryos is the VEGF receptor, Vegfr2 (Eichmann et al., 1998). VEGF is the pivotal mediator of endothelial differentiation, and VEGFR2 is the major receptor in endothelial progenitors and ECs for

VEGF-induced responses (Millauer et al., 1993; Shalaby et al., 1997). The Vegfr2+ cells in the posterior mesoderm segment generate hemangioblasts that differentiate further to hematopoietic cells and ECs; while the Vegfr2+ cells in the anterior mesoderm (angioblasts) are committed to endothelial lineage and give rise to ECs only (Eichmann et al., 1998). The primitive endothelial progenitors that emerge from the lateral plate mesoderm express markers such as CD34, CD31, VE-Cadherin, endoglin and Tie-2 in addition to VEGFR2 (Cleaver and Melton, 2003; Ema et al., 2006).

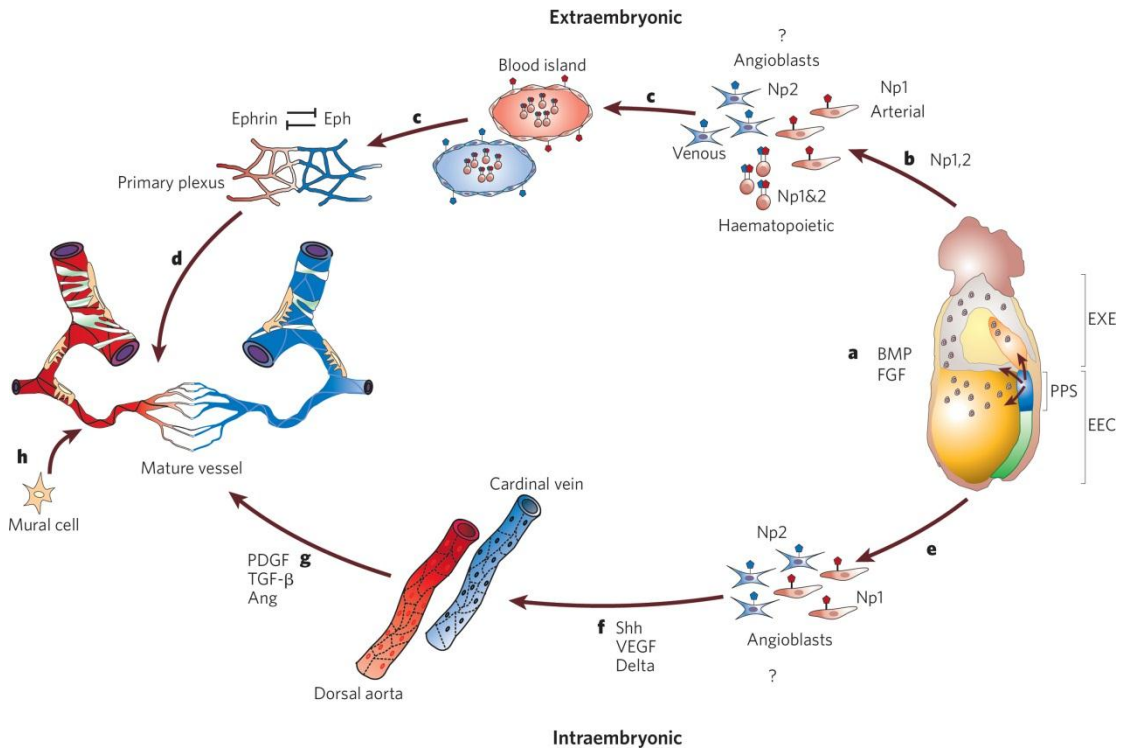

Figure 10. Embryonic vascular development.

Formation of the first vascular channels in the embryo begins with differentiation of mesodermal cells in posterior primitive streak (PPS) to hemangioblasts or angioblasts under the influence of BMP4, bFGF and VEGF. The VEGFR2+ cells in the PS gives rise to aggregates of hemangioblasts or angioblasts that undergo a series of morphogenesis forming vascular cords. The peripheral cells of the vascular cords form ECs and the central cells hematopietic cells resulting nascent endothelial tubes called primary plexus (primitive vacular plexus). These nascent endothelial vessels mature to form a primary capillary plexus. The capillary plexus undergoes a series of morphogenetic process under the influence of Ephrin/Eph signaling, PDGF, TGFβ and angiopoietins (Ang) and recruits mural cells to form a mature circulatory system. *Source: Adapted with permission from (Coultas et al., 2005)*

The differentiation of ESC-derived VEGFR2$^+$ cells into hematopoietic and ECs *in-vitro* provide proof for the existence of a common progenitor for a common progenitor for both the lineages (Park et al., 2004). Further, certain other studies have shown the ability of VEGFR2$^+$ progenitors to differentiate to vSMCs, cardiomyocytes and ECs under appropriate conditions (Yang et al., 2008a). These results indicate a broad differentiation potential of VEGFR2$^+$

progenitors. However certain cell-lineage tracing studies *in-vivo* has failed to reveal the existence of such common progenitors, which might be due to issues related to timing of the lineage commitment from the primitive streak (Kinder et al., 2001a). Recent advancements in imaging technologies might provide more light on the fate of Vegfr2+ cells.

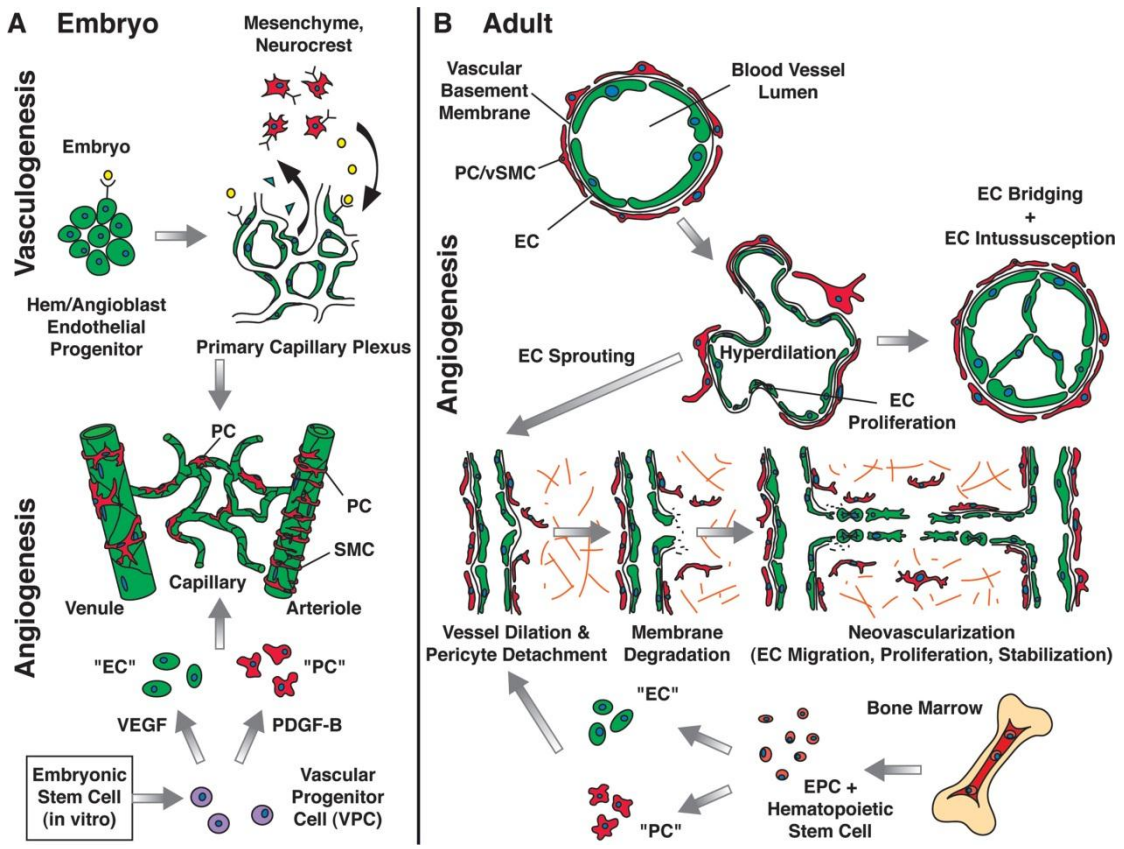

Figure 11. Vasculogenesis and angiogenesis in embryo and adult life.

(A) ECs from angioblasts/ hemangioblasts in the embryo, while the mural cells (vSMC/PC) arise from progenitors in the mesenchyme and neural crest. The ECs assemble to form a simple capillary network known as primary capillary plexus, which matures into a network of arteries, veins and capillaries through recruitment of mural cells and angiogenesis. However, *in-vitro* data from ESCs point to a common precursor for ECs and mural cells that assemble to form vascular network. (B) In the adult life, new vessels form from existing blood vessels through endothelial cell bridging, intussusception, and/or sprouting. The morphogenetic process involved during sprouting angiogenesis is also highlighted. *Source: Adapted with permission from (Bergers and Song, 2005)*

2.2.1. Role of VEGF and VEGFR2 in early vascular development

Mouse embryos lacking *Vegf*$^{-/-}$, display severe defects in vascular development and die early at mid-gestation (Carmeliet et al., 1996). Similarly, mouse embryos lacking *Vegfr1* (*Vegfr1*$^{-/-}$) die at E8.5 to E9.5 due to impaired vascular development; and mice lacking *Vegfr2* (*Vegfr2*$^{-/-}$) are embryonic lethal at the same stage with defects in vasculogenesis and hematopoiesis (Ferrara et al., 1996; Shalaby et al., 1995). In Vegfr2-null embryos, the yolk sac is pale and

completely lacks vasculature (Shalaby et al., 1995). Similarly, the mice lacking *Vegfr3* (*Vegfr3*$^{-/-}$) are lethal at the same stage but display unorganized and poorly lumenized large vessels indicating its early role in vascular development (Dumont et al., 1998). Neuropilins are co-receptors for VEGF, and mice lacking neuropilin 1 (*Nrp1*$^{-/-}$) display defects in yolk sac and vasculogenesis. But, mice lacking neuropilin 2 (*Nrp2*$^{-/-}$) exhibit only minor defects in development of lymphatic system. However, mice with *Nrp1/Nrp2* double knockouts die due to totally avascular yolk sac similar to mice lacking *Vegfr2* (Takashima et al., 2002). The similarity in the phenotype of *Vegfr2*$^{-/-}$ and *Nrp2*$^{-/-}$ mice indicate the obligate relationship between the two receptors and their role in early vascular development. On the other hand, overexpression of Vegf by two-three folds results in embryonic lethality at E12.5-E14 due to aberrant heart development(Miquerol et al., 2000).

Hence, a balanced function of VEGF and its receptors play an extremely important role in early vascular development. In addition to VEGF, other signaling pathways like Wnt, Notch, Shh, cAMP, TGFβ, FGF and BMP4 are also implicated in early to late vascular development (Kane et al., 2011).

2.3. *In-vitro* differentiation to endothelial/ vascular progenitors

The potential use of PSCs depends on efficient differentiation protocols to derive tissue-specific progenitor cells. Various approaches have been reported to induce *in-vitro* differentiation of PSCs towards endothelial or vascular lineage. However, currently, there is no standardized protocol available that could be used reproducibly and efficiently across different cell lines. The different approaches to differentiate PSCs towards endothelial lineage could be categorized as: (1) embryoid body-mediated differentiation, (2) co-culture of hPSCs over murine stromal cells, and (3) culture as monolayers over extracellular matrix proteins like Matrigel and collagen IV with defined chemical conditions (***Figure 12, Tables 1-3***).

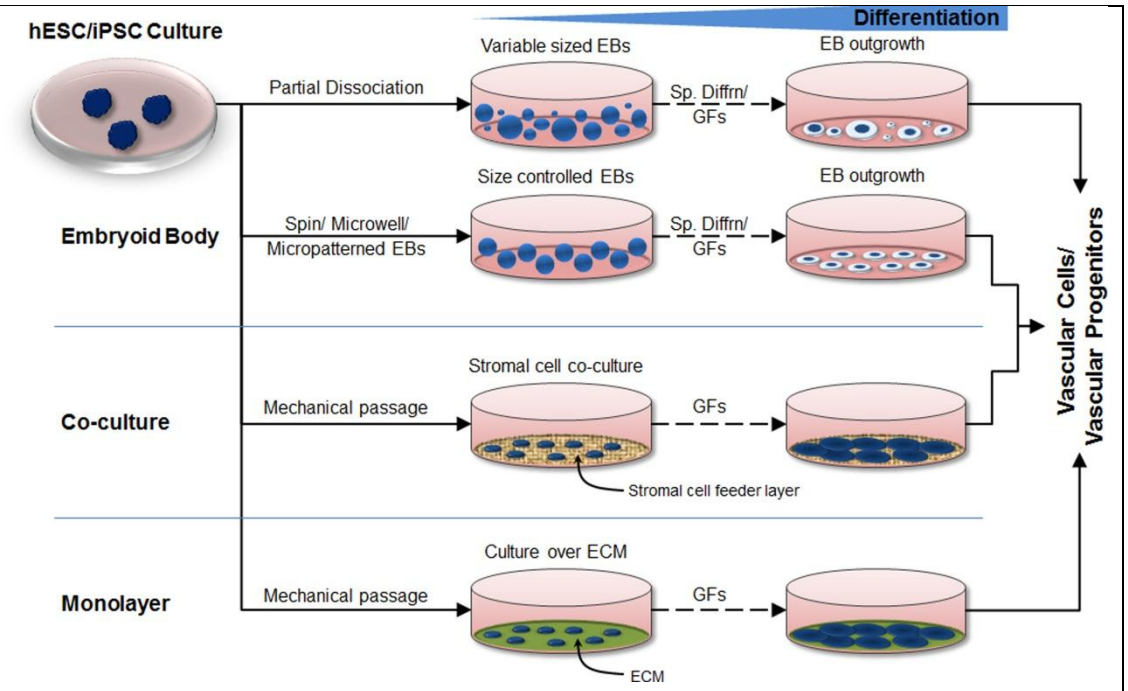

Figure 12. Current methods for differentiation of pluripotent stem cells towards vascular lineage.

The schematic illustrates the three major approaches for directing the differentiation of PSCs towards vascular lineage: Embryoid body (EB), co-culture and monolayer-based methods. EB-based approach range from a simple partial dissociation of PSC colonies followed by suspension culture that yields EBs of varying sizes to methods that could precisely control the size of the EBs (Spin-, microwell- and micropatterned-EBs). The EBs could be spontaneous differentiated (Sp. Diffrn.) or differentiated under the influence of various growth factor combinations (GFs) to yield vascular cells or vascular progenitors. Alternatively the PSCs could be differentiated over stromal cell feeder layers like OP9 or ECMs like Matrigel, collagen IV to direct the differentiation towards vascular lineage. *Source: Modified from (Mummery et al., 2012)*

Table 1. Differentiation of human PSCs to endothelial progenitors and ECs using embryoid body-based approach.

Cell type	Culture Condition	Supplemental Factors	Marker Profile of Progenitors (Other markers)	Progenitor Isolation (day of isolation)	Progenitor yield	Inducers for EC differentiation from Progenitors	*In-vitro* characterization	Other Differentiation Potential	Reference
hESCs (H1)	Spontaneous EB differentiation	Serum	CD31+	FACS (13-15d)	~2%	Gelatin; EM (+ Serum)	Expression of CD31, CD34, VEGFR2, VE-Cad, N-Cad, vWF; Ac-LDL uptake; MTF.	-	(Levenberg et al., 2002)
hESCs (H1, H9)	EB + Cytokines	Hematopoietic cytokines+ Serum	CD31+, VEGFR2+, VE-Cad+, CD45-	FACS (10d)	?	Fibronectin; Serum + BPE + VEGF	Expression of CD31, CD34, VE-Cad, vWF, eNOS, endothelin, Tie2; Ac-LDL uptake.	Hematopoietic lineage	(Chadwick et al., 2003; Wang et al., 2004)
hESCs (CHA3)	EB outgrowth	EM (+Serum)	-	Mechanical isolation and FACS: vWF+	-	Gelatin; EM (+ Serum)	Expression of CD31, VE-Cad, vWF, Tie2, VEGFR2; Ac-LDL uptake, MTF.	-	(Cho et al., 2007; Kim et al., 2007)
hESCs (H1, HuES2)	EB + Cytokines	SFM; BMP4 + bFGF	VEGFR2+ CD31+ (CD177+)	FACS (d8)	?	EM (+Serum); + VEGF+bFGF + Hematopoietic cytokines	Expression of CD31, VE-Cad, Ac-LDL uptake.	Hematopoietic lineage	(Kennedy et al., 2007)
hESCs (many cell lines)	EB + Cytokines	SFM; BMP4 + VEGF + SCF + thrompbopoietin + Flt3	Blast colonies (Oct4+, Brachyury+, VEGFR2+, Isl1+, Nkx2.5+, Mesp+)	-	-	Fibronectin; EM (+Serum)	Expression of CD31, VE-Cad, vWF; Ac-LDL uptake, MTF.	Hematopoietic lineage, Cardiomyocytes, SMCs	(Lu et al., 2007; Lu et al., 2009)
hESCs (H1)	Spontaneous EB differentiation	hESCs transduced with VEGF gene (+Serum)	CD133+	FACS (7-21d)	~35-50%	Gelatin; EM (+ Serum)	Expression of CD31, VE-Cad, vWF	-	(Rufaihah et al., 2010; Rufaihah et al., 2007)
hESCs (H1, hES2)	EB + Cytokines	SFM; BMP4 + bFGF + VEGF + DKK1 + Activin-A	VEGFR2+ c-kit- (ISL+ TBX5+ NKX2.5+)	FACS (6d)	?	Matrigel; SFM + VEGF + bFGF + DKK1	Expression of CD31, VE-Cad; Ac-LDL uptake; MTF.	SMCs, Cardiomyocytes	(Yang et al., 2008a)

Table 1. Differentiation of human PSCs to endothelial progenitors and ECs using embryoid body-based approach. (Continued-1)

Cell type	Culture Condition	Supplemental Factors	Marker Profile of Progenitors (Other markers)	Progenitor Isolation (day of isolation)	Progenitor yield	Inducers for EC differentiation from Progenitors	*In-vitro* characterization	Other Differentiation Potential	Reference
hESCs (H9) hiPSCs	EB + Cytokines	Serum/ SFM medium + BMP4 + VEGF + bFGF + Hypoxia	CD34+ CD31+ CD146+ CD143+	FACS (8-10d)	~15-40%	Fibronectin; EM (+Serum)	Expression of CD31; Ac-LDL uptake.	Hematopoietic lineage	(Park et al., 2013; Zambidis et al., 2008)
hESCs (H9)	EB + Cytokines	Hematopoietic cytokines + BMP4 + Serum	CD133+, VEGFR2+ (CD31-, CD133-, CD14-, CD45-, vWF+)	FACS (12d)	~10%	Fibronectin; Serum + BPE + VEGF	Expression of CD31, CD34, VE-Cad; Ac-LDL uptake, MTF, wound healing, migration assay, activation by TNFα.	-	(Goldman et al., 2009)
hESCs (H9, HUES3)	Spontaneous EB differentiation	Serum; *ISL1-cre* knock-in	ISL+ (NKX2.5+, VEGFR2-)	FACS (8d)	?	MEF feeders; B27 medium	Expression of CD31	Cardiomyocytes, SMCs	(Bu et al., 2009)
hESCs (H9); hiPSCs	EBs suspended in Collagen I gel	EM with KO serum + VEGF + bFGF	CD31+ (VE-Cad+, VEGFR2+)	FACS (12d)	~3-7%	Fibronectin; EM + VEGF (+ Serum)	Expression of CD31, VE-Cad, vWF; Ac-LDL uptake, MTF.	-	(Li et al., 2011; Li et al., 2009)
hESCs (khES-1,3)	EB outgrowth + Cytokines	Hematopoietic cytokines + Serum	-	No sorting	-	Gelatin; EM (+ Serum)	Expression of CD31, VE-Cad, vWF, eNOS; Ac-LDL uptake, MTF	-	(Nakahara et al., 2009)
hESCs (H9)	EB outgrowth + Cytokines	EM (+ Serum)	CD31+	FACS (12d)	~10%	Gelatin; EM (+ Serum)	Expression of CD31, VE-Cad, vWF; Ac-LDL uptake, MTF	-	(Yu et al., 2009)
hESCs (many cell lines)	EB + Cytokines	SFM; Cytokines (BMP4, bFGF, Activin A, Noggin)	NRP1+VEGFR2+ (CD31- CD34-)	FACS (5d)	30-40%	Gelatin; EM (+ Serum) + VEGF	Expression of CD34, CD31, VE-Cad, Endoglin, NRP1; Ac-LDL uptake, MTF	-	(Cimato et al., 2009)

Table 1. Differentiation of human PSCs to endothelial progenitors and ECs using embryoid body-based approach. (Continued-2)

Cell type	Culture Condition	Supplemental Factors	Marker Profile of Progenitors (Other markers)	Progenitor Isolation (day of isolation)	Progenitor yield	Inducers for EC differentiation from Progenitors	*In-vitro* characterization	Other Differentiation Potential	Reference
hESCs (H1, H9, H13)	Spontaneous EB differentiation	Serum	CD34+ (CD31+, αSMA+, VEGFR2+/-, SSEA4+, CD45-)	MACS (10d)	~10%	Gelatin; EM + VEGF (+ Serum)	Expression of CD31, CD34, VE-Cad, vWF; Ac-LDL uptake, MTF.	SMCs	(Chen et al., 2007b; Ferreira et al., 2007; Levenberg et al., 2010)
hESCs (H1, H7)	EB + Cytokines	VEGF (+ Serum)	CD31+ (VE-Cad+, c-kit+, CD45-)	FACS (10-14d)	~8%	Gelatin; EM (+ Serum)	Expression of CD31, CD34, VE-Cad, VEGFR2, vWF, Ulex, eNOS; Ac-LDL uptake; activation by TNFα, MTF.	-	(Nourse et al., 2010)
hiPSCs	EB outgrowth + Cytokines + Feeders	MEF feeders; B27+ BMP2 + FGFR inhibitor	Nkx2.5+ VEGFR2+	FACS (6d)	~6%	B27+ VEGF + Ascorbic acid	Expression of CD31	Cardiomyocytes, SMCs	(Moretti et al., 2010)
hESCs [RUES1, WMC (-2,-7,-8), H9] iPSCs	EB + Cytokines	Matrigel; Cytokines (BMP4, Activin A, bFGF, VEGF) + Inhibition of TGFβ (+ Serum)	GFP+ VE-Cad+ (CD31+, VEGFR2)	FACS/ MACS (14d)	~2%	Gelatin; EM (+ Serum)	Expression of CD31, VE-Cad	-	(James et al., 2010)
hiPSCs	EB outgrowth + Cytokines	Gelatin; Cytokines (BMP4, VEGF) (+ Serum)	CD31+	FACS (14d)	5-20%	Gelatin; EM (+ Serum)	Expression of CD31, VE-Cad, eNOS, vWF; Ac-LDL uptake; chemotaxis, MTF.	-	(Huang et al., 2013; Rufaihah et al., 2011)
hESCs (CHA3)	EB outgrowth + Cytokines	Matrigel; BMP4 + Serum	CD31+	FACS (12d)	~20%	Gelatin; EM (+ Serum)	Expression of CD31, Ac-LDL uptake; MTF; Angiocrine secretion (Ang1, VEGF)	-	(Moon et al., 2011)

Table 1. Differentiation of human PSCs to endothelial progenitors and ECs using embryoid body-based approach. (Continued-3)

Cell type	Culture Condition	Supplemental Factors	Marker Profile of Progenitors (Other markers)	Progenitor Isolation (day of isolation)	Progenitor yield	Inducers for EC differentiation from Progenitors	*In-vitro* characterization	Other Differentiation Potential	Reference
hESCs (chESC-1, -3, -8, -20, -22)	Spontaneous EB differentiation	Serum	VEGFR2+/ CD31+	MACS (9d)	12%/ 2%	Gelatin; EM (+ Serum)	Expression of CD31, CD34, VE-Cad, VEGFR2, vWF, Ulex; Ac-LDL uptake; MTF.	-	(Sun et al., 2012)
hESCs hiPSCs	Spontaneous EB differentiation	Serum	CD31+ CD105+ CD146+	FACS (14d)	~3-8%	Gelatin; EM (+ Serum)	Expression of CD31; Ac-LDL uptake.	Pericytes	(Dar et al., 2012)
hESCs (H1, H7, H9) iPSCs	EB outgrowth + Cytokines	Gelatin; Cytokines (BMP4, VEGF) (+ Serum)	VEGFR2+ CD31+	MACS (6d) FACS (14d)	6-70%	Gelatin; EM (+ Serum)	Expression of CD31, VE-Cad, eNOS, vWF; Ac-LDL uptake; MTF.	-	(White et al., 2013)
hiPSCs	EB outgrowth + Cytokines	Gelatin; Cytokines (BMP4, VEGF ± cAMP ± VEGF-C ± Ang-1) (+ Serum)	CD31+	FACS (14d)	5-20%	Gelatin; EM (+ Serum)	Expression of CD31, VE-Cad, eNOS, vWF; Ac-LDL uptake; MTF. Expression of arterial/ venous/ lymphatic markers	-	(Rufaihah et al., 2013a)
hESCs (H9)	EB outgrowth + Cytokines	Gelatin; Hypoxia; Cytokines (BMP4, VEGF, Activin-A) (+ Serum)	CD34+ (CD31+/-)	FACS (15d)	~3-7%	EM+VEGF (+ Serum)	Expression of VE-Cad, vWF	SMCs	(Song et al., 2013)

Table 1. Differentiation of human PSCs to endothelial progenitors and ECs using embryoid body-based approach. (Continued-4)

Cell type	Culture Condition	Supplemental Factors	Marker Profile of Progenitors (Other markers)	Progenitor Isolation (day of isolation)	Progenitor yield	Inducers for EC differentiation from Progenitors	*In-vitro* characterization	Other Differentiation Potential	Reference
hiPSCs	Spontaneous EB differentiation	Serum	VE-Cad+ (CD31+, VEGFR2+)	MACS (10d)	~5-20%	Fibronectin; EM (+Serum)	Expression of CD31, VE-Cad, VEGFR2, thrombomodulin, eNOS; Ac-LDL uptake, activation by TNFα; chemokine secretion; migration assays; permeability assays; biomechanical stimulation assays.	-	(Adams et al., 2013)
hESCs (HES3, H9, MEL1) hiPSCs	EB + Cytokines	CDM; VEGF, SCF, FGF2, FGF8, $LiCl_2$	CD34+ VEGFR2+ (CD105, Tie2, VE-Cad; E-Cad)	FACS (6d)	~45%	Fibronectin; CDM + VEGF	Expression of CD31, VE-Cad, eNOS, Tie2, CD133, E-Cad, CD105, vWF; Ac-LDL uptake; activation by TNFα; MTF	Hematopoietic cells	(Costa et al., 2013)

Notes: BPE: Bovine pituitary extract. CDM: animal component-free, chemically defined medium. DM: minimum essential medium + FBS. EM: standard endothelial media containing serum (2-5%), VEGF, bFGF and EGF. FACS: flow cytometry assisted cell sorting. KO serum: Knockout serum. MACS: magnetic assisted cell sorting. MTF: tube formation over Matrigel. SFM: Serum-free medium

Table 2. Differentiation of human PSCs to endothelial progenitors and ECs using co-culture-based approach.

Cell type	Feeder co-culture	Supplemental Factors	Marker Profile of Progenitors (Other markers)	Progenitor Isolation (day of isolation)	Progenitor yield	Inducers for EC differentiation from Progenitors	*In-vitro* characterization	Other Differentiation Potential	Reference
hESCs (H1,H9)	MEF	Serum/ SFM media+VEGF+ bFGF+BMP4	CD34+ (CD31+, CD45-)	MACS (10d)	~10-20%	Gelatin; EM (+ Serum)	Expression of CD31, VE-Cad; Ac-LDL uptake; MTF	Hematopoietic cells	(Wang et al., 2007)
hESCs (HES3, khES-1) hiPSCs	OP9	Serum	VEGF-R2+/ TRA1-60-/ VE-Cad+ (Flt1+, cKit-PDGFRα/β+, CD133+, CD34+)	FACS (8d)	~10-15%	Collagen IV, EM+VEGF (+ Serum)	Expression of CD31, VE-Cad, CD34, eNOS; angiocrine secretion	SMCs	(Oyamada et al., 2008; Sone et al., 2007; Taura et al., 2009; Yamahara et al., 2008)
hESCs (H1,H9, H13, H14, SNUhES#3) hiPSCs	OP9	Serum	CD34+ (CD31+, CD43-) (APLNR+)	FACS (7-8d) (3-4d)	~10-20% (~60%)	Fibronectin; EM (+ Serum)	Expression of CD31, VE-Cad; Ac-LDL uptake; MTF	Hematopoietic cells Mesenchymal cells with trilineage commitment	(Choi et al., 2009a; Choi et al., 2009b; Vodyanik and Slukvin, 2007; Vodyanik et al., 2010)
hESCs (H1,H9)	S17 and M210	Serum	CD34+/ CD31+/ VEGFR2+	MACS +FACS (10d)	15-20%	Fibronectin; EM (+ Serum)	Expression of CD31, VE-Cad; Ac-LDL uptake; MTF	Hematopoietic cells	(Woll et al., 2008)
hESCs (H9)	S17 and M210	Serum	CD34+ (CD31+, VEGFR2+)	MACS (13-15d)	~10%	Fibronectin; EM (+ Serum)	Expression of CD31, CD34, VE-Cad, CD146, VEGFR2, eNOS, Tie2, Lectins; Ac-LDL uptake; MTF; response to calcium signaling agonists	SMCs	(Hill et al., 2010; Xiong et al., 2011)
hESCs (H1, H9)	Hs27	SFM; Cytokines (BMP4, VEGF, bFGF, TGFβ1)	CD34+, CD31+	MACS/ FACS (d10-12)	~15-20%	Collagen-I; SFM + VEGF	Expression of CD31, VE-cad, vWF, VEGF, VEGFR2, EphB4, ephrinB2	SMCs	(Bai et al., 2010)

Table 2. Differentiation of human PSCs to endothelial progenitors and ECs using co-culture-based approach. (Continued-1)

Cell type	Feeder co-culture	Supplemental Factors	Marker Profile of Progenitors (Other markers)	Progenitor Isolation (day of isolation)	Progenitor yield	Inducers for EC differentiation from Progenitors	*In-vitro* characterization	Other Differentiation Potential	Reference
hESCs hiPSCs	OP9	Serum + Cytokines (BMPs, VEGF, bFGF)	CD34+ CD31+ (VE-Cad+, VEGFR2+)	FACS (8d)	~10-15%	Fibronectin/ Collagen IV; EM + VEGF (+Serum)	Expression of CD31, CD34, VE-Cad, CD105, VEGFR2; Ac-LDL uptake; MTF	SMCs	(Marchand et al., 2013)

Notes: EM: standard endothelial media containing serum (2-5%), VEGF, bFGF and EGF. FACS: flow cytometry assisted cell sorting. MACS: magnetic assisted cell sorting. MTF: tube formation over Matrigel.

Table 3. Differentiation of human PSCs to endothelial progenitors and ECs using 2D ECM-based approach.

Cell type	ECM Substrate	Supplemental Factors	Marker Profile of Progenitors (Other markers)	Progenitor Isolation (day of isolation)	Progenitor yield	Inducers for EC differentiation from Progenitors	*In-vitro* characterization	Other Differentiation Potential	Reference
hESCs (H9.2)	Collagen IV	Serum	-	Mechanical-40µm strainer (6d)	-	Collagen IV; DM+VEGF (+Serum)	Expression of CD31, CD34, Tie2, GATA2, AC133, vWF; Ac-LDL uptake; Matrigel sprouting	SMCs	(Gerecht-Nir et al., 2003)
hESCs (hESM01 hESM03)	Collagen IV	Serum + VEGF + bFGF + TGFβ1	CD31+ (VE-Cad+, VEGFR2+, CD34+)	MACS (6d)	~45%	Collagen IV; EM (+Serum)	Expression of CD31, GATA2, eNOS, Flk1; Ac-LDL uptake; MTF.	-	(Lagarkova et al., 2008)
hESCs (SA461, SA121)	Fibronectin	EM	CD31+ CD105+ (CD34+, VEGFR2+)	No isolation (21d)	~60%	-	Expression of CD31, VE-Cad; Ac-LDL uptake; MTF, wound healing, angiocrine secretion.	-	(Howard et al., 2013; Kane et al., 2010)
hESCs (CHA4) hiPSCs	Matrigel	KO serum + PD98059 + BMP4 + VEGF + BMPF	CD34+ (CD31+, CD73+, CD90+, CD105+, CD45-)	MACS (10-15d)	~10-25%	EM + VEGF + bFGF (+Serum)	Expression of CD31, VE-Cad, Ang2, VEGFR2, vWF; Ac-LDL uptake; MTF.	SMCs, Hematopoietic cells	(Park et al., 2010)
hESCs (KhES-1,2,3)	Collagen I	N2/B27+GSKi; SFM+VEGF	VE-Cad+ (VEGFR2+, CD34+, CD31+)	MACS (5d)	~20%	Collagen I; SFM+VEGF	Expression of VE-Cad; Ac-LDL uptake; MTF.	-	(Tatsumi et al., 2011)
hESCs (RC-6, 9, 10,13)	Fibronectin	EM (+ Serum; GMP grade)/ SFM + VEGF + EGF + bFGF	CD56+ CD133+ (CD34+, VEGFR2+, VE-Cad+, CD105+)	FACS (21d)	~35-70%	Matrigel; EM (GMP grade)	Expression of CD31; MTF.	-	(Kaupisch et al., 2012)
hESCs (H1, H9)	Matrigel	CDM + GSKi + BMP4 +VEGF	CD34+ VEGFR2+ PDGFRα-	FACS (4d)	~50%	Collagen IV; EM+VEGF (+Serum)	Expression of CD31, CD34, VE-Cad, vWF; Ac-LDL uptake; MTF.	SMCs	(Tan et al., 2013a)
hiPSCs	Matrigel	Serum + BMP4 + VEG(Huang et al., 2006)F+bFGF	CD34+, VEGFR2+, NRP1+	FACS (7d)	~3%	Collagen I; EM+VEGF + bFGF (+Serum)	Expression of CD31, VE-Cad, vWF; Ac-LDL uptake; MTF.	-	(Samuel et al., 2013)

2.3.1. Embryoid body-mediated differentiation to endothelial/ vascular lineage

When colonies of PSCs are suspended in hanging drop cultures or in ultra-low attachment plates, they form cell aggregates/ spheroids with mesodermal cells sandwiched between ectoderm-like cells in the core, and endodermal cells on the outer layer of the spheroids (Mummery et al., 2012). As these cell spheroids exhibit similarity to early postimplantation embryos and hence are termed as embryoid bodies (EBs). The cells in the EBs generally differentiate to progenies of all the three germ layers (Trounson, 2006). The pioneering study of EB differentiation of hESCs to endothelial cells reported isolation of $CD31^+$ cells after 13 days of differentiation; and demonstrated the expression of EC markers (*CD34, CD31, VE-CAD, VEGFR2*) and formation of tube-like structures over Matrigel (Levenberg et al., 2002). Following this report, Wang et al., reported isolation of endothelial progenitors characterized by $CD31^+/VEGFR2^+/VE\text{-}CAD^+/CD45^-$ expression after differentiating EBs for 10 days (Wang et al., 2004). These endothelial progenitors were demonstrated to differentiate to mature endothelial phenotype after 7 days of culture under endothelial conditions. After these initial reports, several studies have demonstrated the spontaneous differentiation of hESCs through EB formation towards endothelial progenitors and ECs (Chen et al., 2007a; Cho et al., 2007; Ferreira et al., 2007; Levenberg et al., 2010; Li et al., 2008; Lu et al., 2007). However, these protocols suffer from low differentiation efficiency (ranging from 1-3% for ECs and ~10% for progenitors) and reproducibility. Low efficiency and reproducibility of these early differentiation protocols could be due to various reasons, that include heterogeneous sizes of EBs, presence of undefined components like serum, and differences in the conditions used for hESC culture. Hence, subsequent studies focused on improving the efficiency by inclusion of specific growth factors, transduction with angiogenic factors, elimination of serum in the differentiation milieu and/or generation of EBs of uniform and defined sizes.

2.3.2. Optimization of media and growth factor conditions for EB-based differentiation

Though spontaneous differentiation occurs within EBs, the culture conditions also play an important role in directing differentiation. To address the role of culture conditions, and to address the issues related with efficiency and reproducibility of EB-based differentiation protocols the use of serum-free media and mesodermal and/or vascular lineage inducing factors like bFGF, BMP4 and VEGF were investigated (James et al., 2010; Nakahara et al., 2009; Rufaihah et al., 2007; Saeki et al., 2008). Culture of EBs in the presence of VEGF for 2 weeks, was reported to express higher levels of endothelial markers compared to conditions lacking VEGF (Nourse et al., 2010). Goldman et al., demonstrated boost of BMP4 in early stages of differentiation aids the induction of vascular progenitors (Goldman et al., 2009).

Similarly, inhibition of TGFβ was shown to increase the yield of endothelial cells (James et al., 2010).

Protocols were developed using a variety of serum-free media that includes commercially available media like Stemdiff APEL (Stem Cell Technologies), Aggrewell media (Stem Cell Technologies), and StemPro-34 (Invitrogen). Stemdiff APEL medium requires a special mention as it is a chemically-defined media that is free of animal or human-derived products. APEL is an acronym for Albumin, Polyvinyl alcohol, Essential Lipids (Ng et al., 2008). This medium replaces animal and human derived proteins with synthetic chemicals and recombinant human proteins (albumin, insulin and transferrin). Because of the absence of undefined factors, this media could be used to assess the role of exogenously added growth factors and aid in the precise control of the differentiation microenvironment. Hence, using serum-free EB differentiation conditions and sequential application of specific growth factors and small molecules seem to aid in improved yield of vascular progenitors and ECs.

2.3.3. Controlling the size of EBs

To control the heterogeneity in the size of EBs, various methods were developed that includes the generation of spin-EBs, microwell EBs and micropatterned EBs. To generate spin-EBs of uniform and defined sizes, defined numbers of dissociated hESCs were seeded onto ultra-low attachment multiwell plates (e.g., Aggrewell Plates, Stem Cell Technologies) and centrifuged to aid the aggregation of dissociated hESCs into aggregates of uniform size (Burridge et al., 2007; Ng et al., 2005b; Ungrin et al., 2008). The size of the EBs could be precisely controlled by varying the number of input cells in each well. Using the spin-EB approach, it was demonstrated that human EBs of 250-300μm in size are optimal for cardiogenic differentiation (Ungrin et al., 2008). While using mouse EBs, it has been demonstrated that smaller EBs (~150μm) favored endothelial lineage and larger EBs (~450μm) promoted cardiac differentiation (Hwang et al., 2009). Similarly, methods were developed to culture ESC colonies of defined sizes by using microwells/ micropatterns of defined size (Bauwens et al., 2008; Khademhosseini et al., 2006; Mohr et al., 2006; Mohr et al., 2010). These microwell/ micropattern cultured hESCs generated EBs of uniform and defined size depending on the size of the microwell.

2.3.4. Co-culture mediated differentiation to endothelial/ vascular lineage

Though various strategies to address the differentiation efficiency and variability of EB-based protocols have been reported, EB formation results in differentiation to all three germ layers. To circumvent the use of EB-based differentiation protocols, alternative models were developed. These models employed the use of murine feeder cell-based co-culture method to

promote vascular development. The murine feeder cells used for vascular induction include stromal cells (OP9, S17, MS-5, and M2-10B4) (Choi et al., 2009b; Hill et al., 2010; Oyamada et al., 2008; Sone et al., 2007; Vodyanik et al., 2005; Vodyanik and Slukvin, 2007; Yamahara et al., 2008), mouse embryonic fibroblasts (MEFs) (Wang et al., 2007) or mouse ECs (Kaufman et al., 2001). Among the various murine feeders, OP9 bone marrow stromal cells have been utilized most commonly. The use of OP9 stromal cell co-cultures for hematopoietic and endothelial cells from hESCs and hPSCs have been extensively characterized by Vodyanik and Slukvin (Choi et al., 2009b; Vodyanik et al., 2005; Vodyanik and Slukvin, 2007). OP9 feeder layer system results in ~20% cells with $CD34^+$ expression (Choi et al., 2009b; Vodyanik et al., 2005; Vodyanik and Slukvin, 2007), or ~15% cells with $VEGFR2^+$/TRA-1-60^- expression (Sone et al., 2007) capable of differentiation to ECs and vSMCs . Other studies using S17, M2-10B4 stromal cells, or MEFs as feeders have reported a yield of 5-10% $CD34^+$ cells after 10-15 days of differentiation (Hill et al., 2010; Wang et al., 2007). Towards avoiding the use of murine feeders and serum, Bai et al., used human foreskin derived fibroblasts (Hs27) as feeders in a serum-free medium and demonstrated the role of BMP4 in induction of vascular progenitors ($CD34^+CD31^+$ cells) from hESCs(Bai et al., 2010). They demonstrated that BMP4 supplementation at early stages promotes the induction of vascular progenitors, while TGFβ suppressed the induction potential of BMP4. Using Hs27 feeders in the presence of BMP4, VEGF and bFGF they demonstrate a yield of 10-20% $CD34^+CD31^+$ cells.

Though the co-culture method eliminates the need for EB-based differentiation, it only enables production of not more than 20% vascular progenitors ($CD34^+$ cells). Additionally, the presence of murine feeders is associated with the inclusion of undefined, animal-derived products and limits the ability to tune the culture milieu.

2.3.5. Monolayer differentiation (feeder-free) to endothelial/ vascular lineage

Differentiation protocols involving EB- and co-culture-based methods have aided in understanding the early stages of vascular commitment of hPSCs and the role of various growth factor combinations. However, significant scientific obstacles need to be resolved in terms of developing efficient differentiation strategies and removal animal-derived products in the culture milieu. Feeder-free differentiation of hPSCs is an attractive alternative to other differentiation strategies. In the monolayer differentiation strategy, the monolayer of hPSCs lacks the complex diffusion barriers present in EBs and the feeder cells present in co-culture model. Hence, theoretically it provides a platform to readily control the application of growth factors and other interventions. Furthermore, hPSCs grown over feeder-free culture systems

could be directly differentiated without the necessity for additional steps like replating and EB formation.

Monolayer differentiation over collagen IV has been extensively studied using mouse ESCs (Blancas et al., 2008; Xiao et al., 2006; Yamashita et al., 2000; Zeng et al., 2006). A differentiation protocol using collagen IV as substrate was reported, wherein the hESCs were differentiated to ECs in the presence of VEGF and to vSMCs in the presence of $PDGF_{bb}$ (Gerecht-Nir et al., 2003). Similarly, Lagarkowa et al., developed a serum-free monolayer differentiation system using collagen IV and a cocktail of growth factors to direct hESC to $CD31^+VECadherin^+$ cells with an efficiency of 50% after 6 days of differentiation (Lagarkova et al., 2008).

Using Matrigel as substrate in serum-free conditions, a recent report indicates the differentiation of hESCs and iPSCs to $CD34^+$ cells (~13-20%) by combined regulation of MEK/ERK and BMP4 signaling pathways (Park et al., 2010). Further the study demonstrates the role of MEK/ERK and BMP4 signaling in mesodermal induction; and bFGF and VEGF in induction of mesodermal cells to $CD34^+$ cells capable of tri-lineage differentiation to ECs, vSMCs, and hematopoietic cells. Similarly, another study by Tan et al., reported the differentiation of hESCs to endothelial progenitors ($VEGFR2^+CD34^+$ cells) using Matrigel as substrate, chemically defined medium (Stemdiff APEL) and sequential modulation of Wnt/β-catenin, BMP4 and VEGF signaling pathways (Tan et al., 2013a). Under chemically defined conditions, they reported almost 50% of the cells being positive for $VEGFR2^+$ and $CD34^+$ within a differentiation span of 4 days.

A study using fibronectin as substrate reported the differentiation of hESCs to $VE\text{-}Cadherin^+CD31^+$ ECs (~80%) after 21 days of differentiation under serum-free conditions (Kane et al., 2010). Further they explored the role of microRNAs (miRs) in vascular differentiation. The same group also modified their protocol with the use of good manufacturing practice (GMP)-grade components in the differentiation system to obtain vascular cells under GMP-compliant conditions (Kaupisch et al., 2012). A recent report using mESCs, verified the role of various ECM substrates including gelatin, fibronectin, laminin, collagen I and collagen IV in endothelial differentiation using serum-free conditions (Blancas et al., 2011). Their results indicate the endothelial induction was maximum on fibronectin, while culture over gelatin, laminin and collagen I favored induction towards vSMCs. Further, collagen IV was found to be the optimal substrate for co-differentiation of ECs and vSMCs.

Using monolayer differentiation over various ECM substrates, many studies have indicated the ability to improve the endothelial differentiation ability, and the potential towards eliminating the use of animal-derived products in the culture milieu.

2.4. Vascular smooth muscle development and associated markers

Formation of mature and functional microvascular network relies on the interaction between ECs and mural cells (Carmeliet and Conway, 2001; Jain, 2003). Mural cells are contractile and supportive cells that are associated with all vascular channels that play a role in vascular maturation, vascular remodeling and maintaining the vessel tone (Armulik et al., 2011). These mural cells found in the larger vessels (arteries and veins) are known as vascular smooth muscle cells (vSMCs) and those in association with the smaller channels (arterioles, capillaries, venules) are known as pericytes (Shepro and Morel, 1993). These vSMCs and/or pericytes share many morphological, molecular, and functional features and hence would be commonly referred to as vSMCs unless specified.

In early embryogenesis and in adult life, newly formed endothelial vessels recruit mural cells resulting in a complex network of arteries, arterioles, capillaries, venules and veins (Coultas et al., 2005; Flamme et al., 1997) (***Figure 11***). Without the mural cells, the endothelial vessels undergo regression, and hence, the vSMCs play a crucial role in providing structural and functional support to the nascent endothelial vessels (Carmeliet, 2003; Jain, 2003) (***Figure 13***).

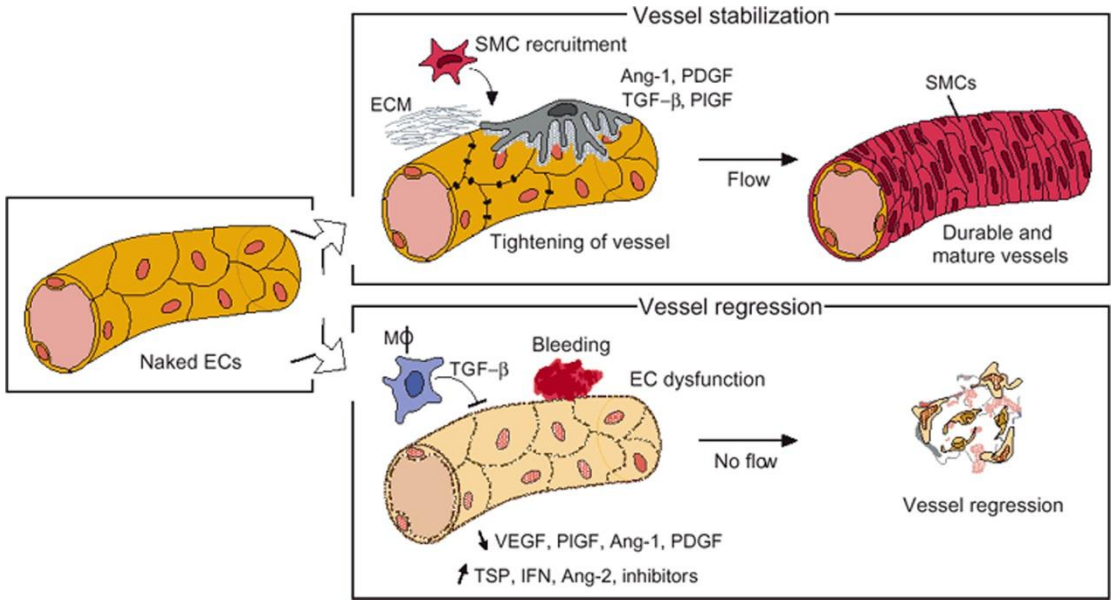

Figure 13. Blood vessel stabilization and regression.

The nascent vessels formed either through vasculogenesis or angiogenesis is composed of ECs only. Under the influence of various factors secreted by ECs, mural cells (vSMCs/ pericytes) are recruited that cover the nascent endothelial tubes. The recruitment of mural cells and secretion of ECM stabilizes the endothelial tubes and also reduces the permeability of these vessels. On the other hand, without mural cell recruitment, the endothelial tubes remain nascent, fragile and leaky leading to rupture and bleeding which leads to reduced blood flow and vessel regression. *Source: Adapted with permission from (Carmeliet, 2003).*

vSMCs are heterogeneous group of cells derived from diverse embryological origins that include lateral plate mesoderm (secondary heart field, splanchnic mesoderm), paraxial mesoderm (somites) and neural crest (Majesky, 2007) (***Figure 14, 15***). Different vessels or different segments of the same vessel have been found to contain vSMCs of diverse embryonic origin (Majesky, 2007). More interestingly, the demarcation between the vSMCs of diverse origin is often sharp with little or no intermixing (Majesky, 2003). Additionally, the vSMCs from different origins exhibit lineage-specific response to the same stimulus. For instance, SMCs derived from neural crest and mesoderm display different growth and transcriptional responses to the stimulation with morphogenetic factors such as TGFβ1 (Topouzis and Majesky, 1996). Hence, an understanding of the embryonic development of vSMCs and its precursors could aid in their differentiation from hESCs.

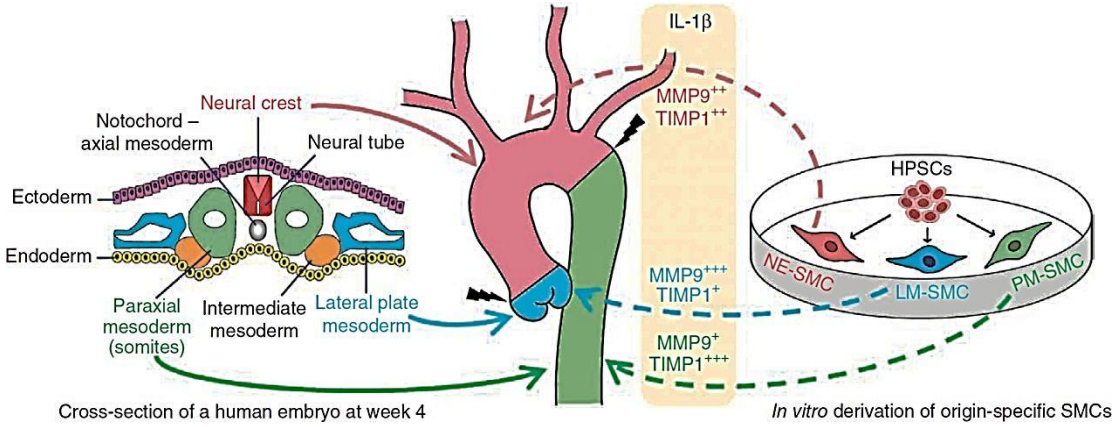

Figure 14. Diverse developmental origin of vSMCs.

The schematic illustrates the diverse origin of vSMCs. The vSMCs that line the aorta develop from three distinct embryonic lineages. The root of aorta (blue) develops from secondary heart field (derivative of lateral plate mesoderm). While the ascending aorta and the arch of aorta (red) develops from neural crest and the descending aorta (green) from paraxial mesoderm. The illustration also demonstrates the differentiation of human PSCs towards vSMCs of neuroectoderm (NE-SMC), lateral plate mesoderm (LM-SMC) and paraxial mesoderm (PM-SMC) origin and the associated differences in expression of MMP and TIMP. *Source: Adapted with permission from (Cheung et al., 2012)*

2.4.1. Origin from lateral plate mesoderm

Soon after gastrulation, the mesodermal cells segregate into paraxial, intermediate and lateral plate mesodermal subtypes. The lateral plate mesoderm gives rise to various derivatives that include somatic mesoderm and splanchnic mesoderm. The splanchnic mesoderm further gives rise to derivatives that include heart fields, endocardium, procardium and epicardium.

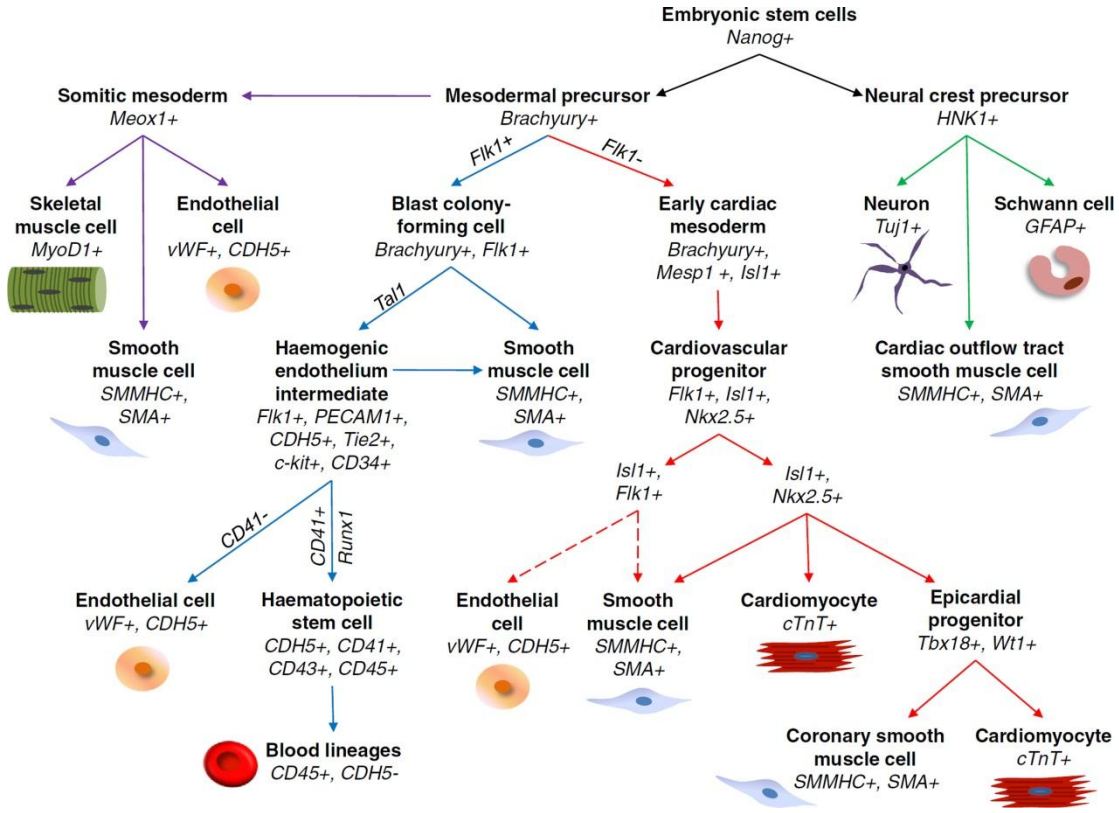

Figure 15. Schematic illustration of diverse origin of vSMC development.

The schematic illustrates the development of vSMCs from paraxial mesoderm, lateral plate mesoderm and neural crest-derived progenitors based on embryological and ESC differentiation studies. Derivatives of cardiac mesoderm, haemangioblast, somitic mesoderm and neural crest are indicated by red, blue, purple and green arrows respectively. Dotted arrows denote speculative differentiation pathways where there is still insufficient evidence at present. *Source: Adapted with permission from (Cheung and Sinha, 2011)*

2.4.1.1. Proepicardial mesothelium

Fate mapping studies have shown that vSMCs present in the walls of coronary arteries seem to arise from progenitors present in the proepicardial mesothelium (Majesky, 2007). Evidence suggests that precursors cells within the proepicardium give rise to epicardium, coronary endothelium and coronary SMCs (Mikawa and Gourdie, 1996). The coronary SMCs seem to arise through EMT of certain subset of epicardial cells. Mouse knock-in models have revealed that expression of Tbx18 and Wt1 marks the proepicardial progenitors that give rise to coronary SMCs (Cheung and Sinha, 2011). Similar to the proepicardial mesothelium evidence also suggest that vSMCs of the vasculature in the gut, lungs and liver, arise from mesothelial cells (Armulik et al., 2011; Majesky, 2007).

2.4.1.2. Secondary heart field

Studies using lineage tracers in avian embryos and Isl1-cre transgenic mice have revealed the origin of vSMCs within the base of aorta and pulmonary trunk to a subset of progenitors within the secondary heart field (Moretti et al., 2006; Waldo et al., 2005). Islet-1 (Isl1) is a transcription factor expressed in the secondary heart field. vSMCs in the fetal heart co-express Isl1 and smooth muscle myosin heavy chain (SM-MHC) suggesting the origin from secondary heart field (Moretti et al., 2006). Further using mouse ESCs they demonstrated that ESC-derived $Isl1^+$ cardiac progenitors co-expressed Nkx2.5 and Flk1. These $Isl^+Nkx2.5^+Flk1^+$ were multipotent cardiac progenitors capable differentiating towards cardiac, endothelial and smooth muscle lineages. Similarly, certain other studies have shown that $Nkx2.5^+$ population consists of two subsets consisting of $Nkx2.5^+Flk1^-$ subpopulation that gives rise to cardiomyocytes and SMCs (Wu et al., 2006), while the $Nkx2.5^+Flk1^+$ subpopulation gives rise to ECs (Christoforou et al., 2008). Similarly, Bu et al., used a reporter gene targeting Isl1 locus to track the differentiation of hESCs to $Isl1^+$ cardiovascular progenitors resembling those derived from secondary heart field (Bu et al., 2009). These progenitors yielded subclones that gave rise to vSMCs, cardiomyocytes or ECs. Similarly, Cheung et al., demonstrated the differentiation of hESCs and iPSCs to vSMCs of lateral plate mesoderm origin (Cheung and Sinha, 2011). Using a 2 step induction consisting of treatment with bFGF, LY294002 and BMP4, followed by bFGF and BMP4, PSCs were differentiated towards VEGFR2 expressing lateral plate mesodermal cells which were further differentiated to vSMCs using $PDGF_{bb}$ and TGFβ1. These $VEGFR2^+$ mesodermal cells also expressed Nkx2.5 and Isl1 suggesting these progenitors could be similar to those from secondary heart field.

2.4.1.3. Mesoangioblasts

Mesoangioblasts refer to aorta-derived satellite-like cells that express markers related to myogenic and endothelial lineages and displays potential to differentiate into skeletal muscle, smooth muscle and other mesenchymal cell types (Majesky, 2007). However, the existence of such cell types is controversial. Evseenko et al., reported differentiation of hESCs to multipotent mesoderm-committed progenitor population ($CD326^-CD56^+$ progenitors) in the presence of activin A, BMP4, VEGF, and FGF2 (Evseenko et al., 2010). These $CD326^-CD56^+$ progenitors were shown to be unique in their ability to commit to all mesodermal lineages including hematopoietic, endothelial, smooth muscle, cardiomyocytes, and mesenchymal (bone, cartilage, fat, fibroblast) similar to mesoangioblasts (***Figure 17***).

2.4.2. Origin from paraxial mesoderm (somitic mesoderm)

The SMCs of the descending aorta seems to be "segmental" in terms of their origin, as they appear to be derived from individual somites (Majesky, 2007). Each somite is derived from

the paraxial mesoderm and consists of sclerotome, myotome and dermatome. The somite-derived SMCs appear to arise from progenitors within the sclerotome. These paraxial mesoderm progenitors are reported to be marked by various markers that include MEOX1, PAX1, TCF1, TBX6, PDGFRα, and PDGFRβ (Cheung et al., 2012; Cheung and Sinha, 2011). Cheung et al., demonstrated the differentiation of hESCs and iPSCs to vSMCs of paraxial mesoderm origin (Cheung and Sinha, 2011). Using a 2 step induction consisting of treatment with bFGF, LY294002 and BMP4, followed by bFGF and LY294002, PSCs were differentiated towards $TCF15^+$ paraxial mesodermal cells which were further differentiated to vSMCs using $PDGF_{bb}$ and TGFβ1. These $TCF15^+$ mesodermal cells also expressed paraxial mesoderm markers MEOX1 and PAX1 suggesting these progenitors could be similar to those from somatic mesoderm. Similarly, Tan et al., reported differentiation of hESCs to paraxial mesoderm progenitors marked by expression of PDGFRα that were negative for CD31 and VEGFR2 (Tan et al., 2013a). These $PDGFR\alpha^+$ paraxial mesoderm progenitors were demonstrated to differentiate towards vascular smooth muscle lineage.

2.4.3. Origin from neural crest cells

Lineage mapping studies in chick-quail and mouse embryos have demonstrated that migrating neural crest cells contribute to the origin of vSMCs in the ascending aorta, and the arterial branches arising from arch of aorta namely, ductus arteriosus, subclavian arteries, and common carotid arteries (Jiang et al., 2000; Majesky, 2007; Nakamura et al., 2006). Most of the vSMCs/pericytes in the head and neck region seem to be derived from the neural crest (Armulik et al., 2011).

Compared to vSMC derived from PSCs of mesodermal origin, protocols for directing PSCs to vSMCs through neural crest cells is poorly defined. A few protocols demonstrating the differentiation of human PSCs to neural crest stem cells have showed their smooth muscle differentiation potential. Lee et al., described a protocol to derive smooth muscle cells through a mesodermal phenotype derived from hESC-derived neural crest stem cells (Lee et al., 2007). In this protocol, hESCs were differentiated to $CD75^+$ neural crest stem cells that were differentiated to $CD73^+$ mesenchymal precursor cells, and subset of these cells expressing NCAM was sorted and differentiated to αSMA^+ smooth muscle phenotype. Other protocols have demonstrated direct differentiation of vSMCs from hESCs-derived neural crest precursors. Colleoni et al., demonstrated the differentiation of hESC-derived neural crest precursors to SMCs (Colleoni et al., 2010). Similarly, $Frizzled3^+Cadherin11^+$ hESC-derived cranial neural crest cells were demonstrated to differentiate towards smooth muscle phenotype in the presence of insulin-like growth factor-1 (IGF-1) and TGFβ1 (Zhou and Snead, 2008). Cheung et al., demonstrated differentiation of hESCs and iPSCs to vSMCs of

neuroectoderm, lateral plate and paraxial mesoderm origin (Cheung and Sinha, 2011). Using bFGF and TGFβ inhibitor SB431542 PSCs were differentiated towards NESTIN and PAX6 expressing neuroectodermal cells which were further differentiated to vSMCs using $PDGF_{bb}$ and TGFβ1.

2.4.4. Origin through endothelial-mesenchymal transition

Certain subsets of endocardial cells and ECs of the aorta and pulmonary arteries are reported to lose their endothelial phenotype and attain mesenchymal or smooth muscle-like characteristics through a process termed as endothelial-mesenchymal transition (EndMT) (Cheung and Sinha, 2011). Similar findings are reported in *in-vitro* ESC models wherein ESC-derived ECs are reported to transdifferentiate to vSMCs under the influence of $PDGF_{bb}$ and TGFβ1 (Hill et al., 2010; Marchetti et al., 2002). Many of the protocols demonstrate that hESC and iPSC-derived $CD34^+$ cells differentiate to ECs and vSMCs depending on the culture conditions (Bai et al., 2010; Ferreira et al., 2007; Hill et al., 2010; Levenberg et al., 2010; Li et al., 2009; Park et al., 2010). Though most of the $CD34^+$ population that exhibit smooth muscle differentiation ability also co-express CD31 (an endothelial marker), bipotent differentiation potential has not been demonstrated at clonal level. EndMT of ECs to vSMCs has been reported to occur through SNAI1-mediated TGFβ1 signaling (Kokudo et al., 2008). In fact, such EndMT of ECs have been increasing implicated in cardiovascular pathologies especially atherosclerosis (Arciniegas et al., 2007).

2.5. In-vitro differentiation of PSCs to smooth muscle progenitors

Various approaches to guide the differentiation of hESCs towards vSMC lineage involve one or combination of following methods: (1) EB-based differentiation (Ferreira et al., 2007; Levenberg et al., 2010; Vazao et al., 2011; Vo et al., 2010), (2) co-culture over murine/ human stromal cells like OP9 (Oyamada et al., 2008; Sone et al., 2007; Taura et al., 2009; Yamahara et al., 2008), MEFs (Bu et al., 2009), M2-10B4 (Hill et al., 2010), human foreskin fibroblasts (Lee et al., 2007), (3) culture of hESCs or iPSCs as monolayers over ECM proteins like Matrigel (Colleoni et al., 2010), and collagen IV (Oyamada et al., 2008; Sone et al., 2007; Taura et al., 2009; Wanjare et al., 2013; Xie et al., 2007; Yamahara et al., 2008), and/or (4) growth factor, cytokines or small molecule mediated differentiation in serum containing/ serum-free conditions (Bai et al., 2010; Cheung et al., 2012; Huang et al., 2006; Lee et al., 2007; Park et al., 2010; Tan et al., 2013a) (***Figure 12, Table 4***). These methodologies are similar to endothelial differentiation of PSCs discussed earlier.

Most of these protocols rely on the use of serum and do not involve lineage-specific differentiation strategies (Huang et al., 2006; Vo et al., 2010; Xie et al., 2007). Certain other protocols demonstrate the differentiation of hESCs towards bi-potent vascular progenitors ($CD34^+$, $VEGFR2^+$ and/or $CD31^+$ cells) capable of differentiation towards endothelial and smooth muscle lineages (Bai et al., 2010; Ferreira et al., 2007; Hill et al., 2010; Levenberg et al., 2010; Vazao et al., 2011; Wanjare et al., 2013). As $CD34^+$, $VEGFR2^+$ and/or $CD31^+$ is expressed by lateral mesodermal subsets, protocols utilizing these markers could be assumed to be yielding vSMCs of lateral plate mesoderm origin. vSMCs have also been demonstrated to be derived through a hESC/iPSC-derived mesenchymal stem cell (MSCs) intermediates (Bajpai et al., 2012; Guo et al., 2013). Recently, Cheung et al., reported differentiation of hPSCs to vSMCs through lateral plate mesoderm, paraxial mesoderm and neural crest progenitors (Cheung et al., 2012). Similarly, Tan et al., had recently demonstrated the differentiation of hESCs to vSMCs through paraxial mesoderm intermediates ($PDGFR\alpha^+CD34^-$) (Tan et al., 2013a). Few protocols have demonstrated the derivation of vSMCs through neural crest progenitors (Colleoni et al., 2010; Lee et al., 2007; Zhou and Snead, 2008). Hence, the differentiation of PSCs towards vSMCs demonstrates the multi-lineage origin of these cells observed during embryonic development.

Various surface markers have been used to identify the progenitors that could be directed towards smooth muscle lineage. Various markers associated with these progenitors are highlighted by the schematic illustrations provided by Cheung and Sinha, Descamps and Emanueli, and Evseenko et al. (Cheung and Sinha, 2011; Descamps and Emanueli, 2012; Evseenko et al., 2010) (***Figures 15-17***, ***Table 4***).

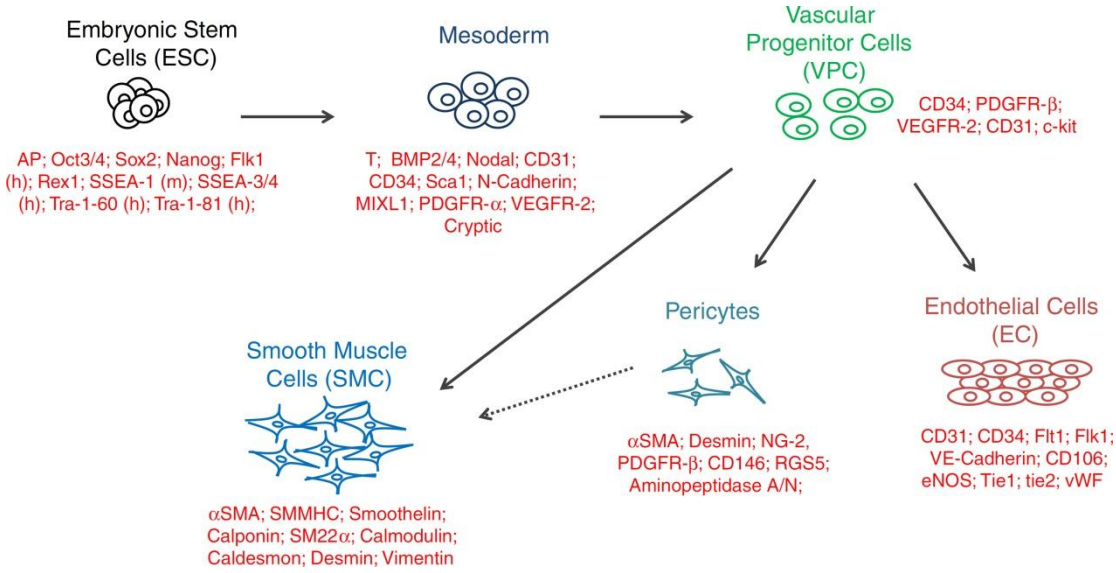

Figure 16. Differentiation of ESCs towards vascular lineage progenitors and their associated markers.

Schematic representation of cell surface marker expression during specification towards vascular lineage from ESCs. *Source: Adapted with permission from (Descamps and Emanueli, 2012)*

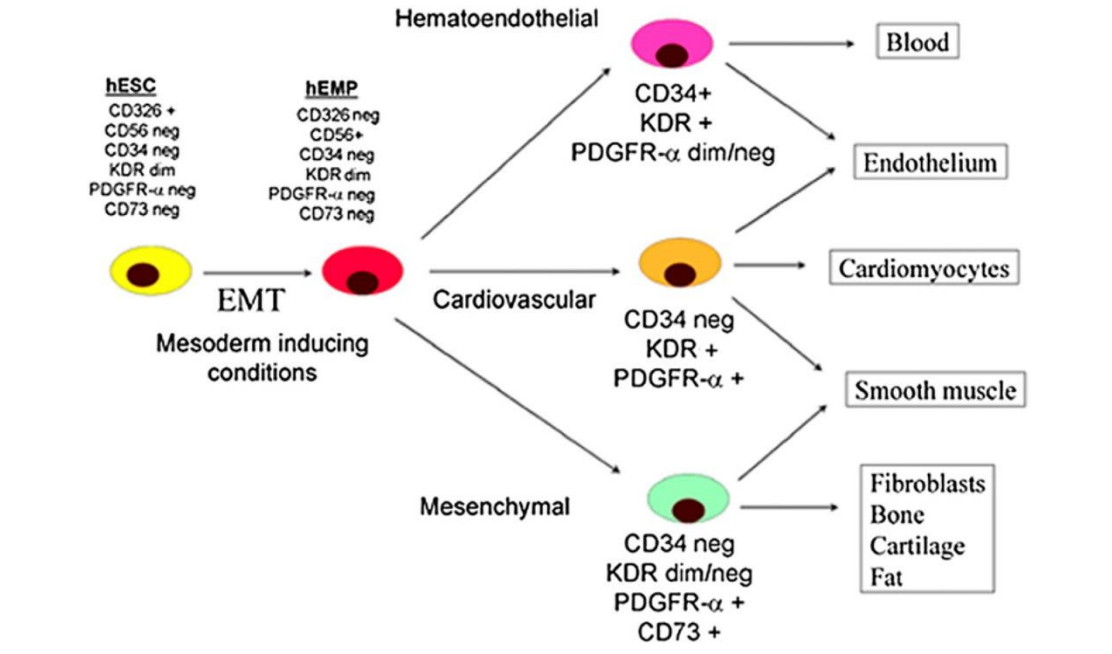

Figure 17. Differentiation of hESCs towards mesenchymal and cardiovascular lineage progenitors and their associated markers.

Schematic representation of the expression of various cell surface markers during specification towards mesenchymal and cardiovascular lineage from ESCs. The schema proposes a common progenitor for mesenchymal and cardiovascular lineages, and identifies the progenitor as mesenchymoangioblast. *Source: Adapted with permission from (Evseenko et al., 2010)*

Table 4. Differentiation of human PSCs to vSMCs.

Cell type	Differentiation Method	Supplemental Factors	Marker Profile of Progenitors (Other markers)	Progenitor Isolation (day of isolation)	Progenitor yield	Inducers for SMC differentiation from Progenitors	*In-vitro* characterization	Other Differentiation Potential	Reference
hESCs (H9.2)	2D monolayer (Collagen IV)	Serum	-	Mechanical-40µm strainer (6d)	-	Collagen IV; DM + $PDGF_{bb}$ (+Serum)	Expression of αSMA, Calponin, MYH11.	ECs	(Gerecht-Nir et al., 2003; Vo et al., 2010; Wanjare et al., 2013)
hESCs (HUES3)	2D monolayer (Gelatin)	Serum + RA	-	-	-	-	Expression of αSMA, SM22a, calponin, desmin, MYH11; contractility assays.	-	(Huang et al., 2006)
hESCs (H1, H9, H13)	Spontaneous EB differentiation	Serum	CD34+ (CD31+, αSMA+, VEGFR2+/-, SSEA4+, CD45-)	MACS (10d)	~10%	Gelatin; EM + $PDGF_{bb}$ (+ Serum)	Expression of αSMA, Calponin, MYH11.	ECs	(Chen et al., 2007b; Ferreira et al., 2007; Levenberg et al., 2010)
hESCs (H1, H9)	EB outgrowth	Gelatin/ Matrigel; SMC Medium (+Serum);	-	-	-	-	Expression of αSMA, caldesmon, MYH11; Contractility assays.	-	(Xie et al., 2007)
hESCs hiPSCs	Co-culture (MS-5)	N2 medium; - Cytokines (Shh, FGF8, BDNF, ascorbic acid) - Polyornithine/ laminin; Cytokines (bFGF, BDNF, ascorbic acid)	Neural crest intermediates p75+ (HNK1+ AP2+)	FACS (~30-40d)	~30%	DM (+Serum)	Expression of SM22α, calponin.	Peripheral Neurons, schwann cells, osteoblasts, chondrocytes, adipocytes	(Lee et al., 2010; Lee et al., 2007; Wang et al., 2012a)

Table 4. Differentiation of human PSCs to vSMCs. (Continued-1).

Cell type	Differentiation Method	Supplemental Factors	Marker Profile of Progenitors (Other markers)	Progenitor Isolation (day of isolation)	Progenitor yield	Inducers for SMC differentiation from Progenitors	*In-vitro* characterization	Other Differentiation Potential	Reference
hESC (H9, HUES-1, HUES-3)	EB	KO serum	Neural crest intermediates Frizzled3+/ Cadherin11+	FACS (10d)	~1%	SFM + EGF + bFGF + NGF; +IGF-1 + TGFβ1	Expression of αSMA.	Neurons, glia, osteoblasts, chondrocytes	(Zhou and Snead, 2008)
hESCs (HES3, khES-1) hiPSCs	Co-culture (OP9)	Serum	VEGF-R2+/ TRA1-60-/ VE-Cad- (Flt1+, cKit-PDGFRα/β+, CD133+, CD34+)	FACS (8d)	~10-15%	Collagen IV, DM+ $PDGF_{bb}$ (+ Serum)	Expression of αSMA, Calponin.	ECs	(Oyamada et al., 2008; Sone et al., 2007; Taura et al., 2009; Yamahara et al., 2008)
hESCs (H1, hES2)	EB + Cytokines	SFM; BMP4 + bFGF + VEGF + DKK1 + Activin-A	VEGFR2+ c-kit- (ISL+ TBX5+ NKX2.5+)	FACS (6d)	?	Matrigel; SFM + VEGF + bFGF + DKK1	Expression of αSMA, Caldesmon, MYH11.	ECs, Cardiomyocytes	(Yang et al., 2008a)
hESCs (many cell lines)	EB + Cytokines	SFM; BMP4 + VEGF + SCF + thrompbopoietin + Flt3	Blast colonies (Oct4+, Brachyury+, VEGFR2+, Isl1+, Nkx2.5+, Mesp+)	-	-	Fibronectin; SMCM (+Serum)	Expression of αSMA, Calponin, SM22α; Contractility assays.	Hematopoietic lineage, Cardiomyocytes, ECs	(Lu et al., 2009)
hESCs (H9, HUES3)	Spontaneous EB differentiation	Serum; *ISL1-cre* knock-in	ISL+ (NKX2.5+, VEGFR2-)	FACS (8d)	?	Fibronectin/ Gelatin/ MEF feeders	Expression of smoothelin	Cardiomyocytes, ECs	(Bu et al., 2009)
hESCs (CHA4) hiPSCs	2D monolayer (Matrigel)	KO serum + PD98059 + BMP4 + VEGF + BMPF	CD34+ (CD31+, CD73+, CD90+, CD105+, CD45-)	MACS (10-15d)	~10-25%	EM + $PDGF_{bb}$ + bFGF (+Serum)	Expression of αSMA, Calponin.	ECs, Hematopoietic cells	(Park et al., 2010)

Table 4. Differentiation of human PSCs to vSMCs. (Continued-2).

Cell type	Differentiation Method	Supplemental Factors	Marker Profile of Progenitors (Other markers)	Progenitor Isolation (day of isolation)	Progenitor yield	Inducers for SMC differentiation from Progenitors	*In-vitro* characterization	Other Differentiation Potential	Reference
hESCs (HEUS-1, HUES-3)	EB outgrowth	Matrigel; SFM + bFGF + EGF	Neural crest intermediates (p75+, Nestin+, Slug+, Sox10+, FoxD3+)	Mechanical isolation	-	Serum	Expression of αSMA.	Neuron, pigmented cell, cartilage	(Colleoni et al., 2010)
hESCs (H9)	Co-culture (S17 and M210)	Serum	CD34+ (CD31+, VEGFR2+)	MACS (13-15d)	~10%	Fibronectin; DM (+ Serum) + $PDGF_{bb}$ + TGFβ1	Expression of αSMA, SM22, Calponin, smoothelin, SM1; response to calcium signaling agonists	SMCs	(Hill et al., 2010; Xiong et al., 2011)
hESCs (H1, H9)	Co-culture (Hs27)	SFM; Cytokines (BMPs, VEGF, bFGF, TGFβ1)	CD34+, CD31+	MACS/ FACS (d10-12)	~15-20%	Collagen-I; SFM + EGF + bFGF + $PDGF_{bb}$	Expression of αSMA, calponin, desmin, caldesmon.	ECs	(Bai et al., 2010)
hiPSCs	EB outgrowth + Cytokines + Feeders	MEF feeders; B27+ BMP2 + FGFR inhibitor	Nkx2.5+ VEGFR2+	FACS (6d)	~6%	B27+ VEGF + Ascorbic acid	Expression of MYH11.	Cardiomyocytes, ECs	(Moretti et al., 2010)
hESCs (H9)	EB	Serum	CD34+ VEGFR2-	MACS (10d)	~2%	Gelatin; SMC medium + $PDGF_{bb}$ + TGFβ1 (+Serum)	Expression of αSMA, calponin, SM22α, MYH11; contractility assays; angiocrines/ cytokine secretion assays.	-	(Vazao et al., 2011)
hESCs hiPSCs	Spontaneous EB differentiation	Serum	CD31- CD105+ CD146+/CD73+	FACS (14d)	~3-8%	Fibronectin/ Gelatin; DM+EM (+ Serum)	Expression of Calponin, PDGFRβ, NG2, CD146, CD90, CD73, Support tube formation by ECs.	ECs	(Dar et al., 2012)

Table 4. Differentiation of human PSCs to vSMCs. (Continued-3).

Cell type	Differentiation Method	Supplemental Factors	Marker Profile of Progenitors (Other markers)	Progenitor Isolation (day of isolation)	Progenitor yield	Inducers for SMC differentiation from Progenitors	*In-vitro* characterization	Other Differentiation Potential	Reference
hiPSCs	2D monolayer (Matrigel; Gelatin/ Collagen IV)	ACTA2 promoter-driven gene expression; SMC medium (+Serum)	MSC intermediates (CD73+ CD90+ CD49b+ CD44+ CD105+ CD45- CD34-)	-	-	Gelatin/ Collagen IV; SMC Medium + TGFβ1 + heparin (+Serum)	Expression of αSMA, Calponin, caldesmon, MYH11, SM22; Contractility assays..	-	(Bajpai et al., 2012)
hESCs (H1, H9) hiPSCs	2D monolayer (Matrigel)	SFM + SB431542 + bFGF	Neuroectoderm intermediates Pax6+, Nestin+	FACS (7d)	~90%	SFM + $PDGF_{bb}$ + TGFβ1	Expression of αSMA, Calponin, smoothelin, MYH11, SM22; contractility assays; Response to cytokines and calcium agonists; expression of ECM	-	(Cheung et al., 2012)
hESCs (H1, H9) hiPSCs	2D monolayer (Matrigel)	CDM + bFGF + LY294002 + BMP4; +bFGF+BMP4	Lateral plate mesoderm intermediates VEGFR2+	FACS (5d)	~80%	SFM + $PDGF_{bb}$ + TGFβ1	Expression of αSMA, Calponin, smoothelin, MYH11, SM22; contractility assays; Response to cytokines and calcium agonists; expression of ECM	-	(Cheung et al., 2012)
hESCs (H1, H9) hiPSCs	2D monolayer (Matrigel)	CDM + bFGF + LY294002	Paraxial mesoderm intermediates TCF15+	FACS (5d)	~70%	SFM + $PDGF_{bb}$ + TGFβ1	Expression of αSMA, Calponin, smoothelin, MYH11, SM22; contractility assays; Response to cytokines and calcium agonists; expression of ECM	-	(Cheung et al., 2012)
hESCs	-	-	MSC intermediates	-	-	SFM + TGFβ1	Expression of αSMA, Calponin, caldesmon, MYH11, SM22α; Contractility assays; Support tube formation by ECs.	-	(Guo et al., 2013)

Table 4. Differentiation of human PSCs to vSMCs. (Continued-4).

Cell type	Differentiation Method	Supplemental Factors	Marker Profile of Progenitors (Other markers)	Progenitor Isolation (day of isolation)	Progenitor yield	Inducers for SMC differentiation from Progenitors	*In-vitro* characterization	Other Differentiation Potential	Reference
hESCs (H9)	EB outgrowth + Cytokines	Gelatin; Hypoxia; Cytokines (BMP4, VEGF, Activin-A) (+ Serum)	CD34+ (CD31+/-)	FACS (15d)	~3-7%	SMC medium + $PDGF_{bb}$ + TGFβ1 (+ Serum)	Expression of αSMA, SM22α; gene expression profiles.	ECs	(Song et al., 2013)
hESCs (H1, H9)	2D monolayer (Matrigel)	CDM + CHIR99021 + BMP4 +VEGF	Paraxial mesoderm intermediates CD34+ VEGFR2-PDGFRα+	FACS (4d)	~50%	Collagen IV; EM+VEGF (+Serum)	Expression of αSMA, calponin, SM22α, PDGFRβ.	ECs	(Tan et al., 2013a)
hESCs hiPSCs	Co-culture (OP9)	Serum + Cytokines (BMP4, VEGF, bFGF)	CD34+ CD31+ (VE-Cad+, VEGFR2+)	FACS (8d)	~10-15%	Fibronectin/ Collagen IV; SMC medium + $PDGF_{bb}$ + TGFβ1 (+Serum)	Expression of αSMA, calponin, PDGFRβ, CD105, caldesmon, NG2; Contractility studies.	ECs	(Marchand et al., 2013)

Notes: CDM: animal component-free, chemically defined medium. DM: minimum essential medium + FBS. EM: standard endothelial media containing serum (2-5%), VEGF, bFGF and EGF. FACS: flow cytometry assisted cell sorting. KO serum: Knockout serum. MACS: magnetic assisted cell sorting. SFM: Serum-free medium. SMC medium: standard smooth muscle media containing serum (2-5%), bFGF and EGF.

2.6. Isolation of endothelial/ vascular/ smooth muscle progenitors

Strategies to isolate the endothelial and/or vascular progenitors from mixed differentiating PSC culture systems are needed to eliminate any contaminating PSCs and any other undesired cell populations, so as to minimize the risk of tumor formation and obtain a homogeneous cell population. A homogeneous cell population is also needed if global gene expression profiles of the differentiated cells needs to be investigated. Various cell isolations methods have been developed to purify the endothelial and/or vascular progenitors from differentiating cultures which include physical, genetic and non-genetic (antibody-mediated) methods.

2.6.1. Physical methods

Physical methods involve manually selecting the appropriate population of cells for further differentiation. These methods were commonly used in isolation of differentiating cardiomyocytes by manual dissection and dissociation of spontaneously contracting EBs. Similar methods have been reported to isolate vascualr progenitor populations. Gerecht et al., reported isolation of mesodermal cells using a 40µm strainer. They observed that the smaller cells that pass through the 40µm strainer had ability to differentiate to ECs and vSMCs upon induction with VEGF and $PDGF_{bb}$ respectively (Gerecht-Nir et al., 2003). Similarly, Kim et al., reported a 2-step enzymatic approach to isolate ECs from differentiating hESCs (Kim et al., 2007). Using gene expression, immunostaining and flow cytometry, they observed that the center regions of EB outgrowths had higher EC markers. The center regions of the EB outgrowths were detached from the outgrowth cells using trypsin followed by dissociation of the center region using cell dissociation buffer. Though the manual selection methods resulted in enrichment of ECs/ vSMCs, they were contaminated with other unknown cell populations and would require further purification steps. Additionally, these methods are labor intensive and subjective.

2.6.2. Genetic (Promoter-based) isolation methods

This method involves expression of a reporter gene under the control of a vascular lineage-specific promoter. These methods have been used commonly in developmental biology to track the differentiation and migration of cells *in-vivo*. Marchetti et al., using plasmid containing enhanced green fluorescent protein (eGFP) or puromycin resistance gene under the control of Tie1 promoter, isolated ECs from differentiating mouse ESCs based on eGFP expression or resistance to puromycin (Marchetti et al., 2002). ECs were tracked in using the expression of Tie1 that is expressed by the cells of the endothelial lineage. Similarly Rufaihah et al., reported efficient differentiation of hESCs to ECs based on induction of VEGF expression using a adenoviral vector expressing VEGF gene (Rufaihah et al., 2007). James et al., reported tracking and isolation of endothelial cells using a bacterial artificial chromosome

containing eGFP and a genomic locus of human EC specific gene, VE-Cadherin (James et al., 2010). This resulted in endothelial specific expression of eGFP. Using the VE-Cadherin mediated eGFP expression, they tracked the kinetics of emergence of endothelial cells within the differentiating hESCs EBs. Further, they used the VE-Cadherin mediated eGFP expression to screen a panel of small molecules that aid vascular development. Bu et al., used *ISL1-β-geo* bacterial artificial chromosome transgenic hESCs to genetically tag $ISL1^{+}$ progenitors (Bu et al., 2009). Additionally, they employed a Cre/*loxP* system to mark *ISL1* expressing cells and their differentiated progeny to track the cells during the process of cardiac differentiation. Lineage tracking studies showed that ISL expressing cells differentiated into cells of the cardiovascular lineage including cardiomyocytes, ECs and vSMCs.

The use of promoter-driven reporter genes enables identification, lineage tracking, and selection of vascular cells/ progenitors within the pool of differentiating ESCs and also tracking the cells *in-vivo* after transplantation in animal models. However, it is labor intensive and is associated with dangers related to genetic modification when these cells are intended for clinical therapy.

2.6.3. Antibody-mediated selection methods

Currently, the most commonly used method to isolate ECs, vSMCs or their progenitors rely on the use of antibodies against various cell surface antigens. Either fluorescent molecules or magnetic beads conjugated to antibodies against surface markers are used to isolate the cells using flow cytometry assisted cell sorting (FACS) or magnetic assisted cell sorting (MACS). Commonly used cell surface markers to identify endothelial or smooth muscle populations are illustrated in ***Figures 15-17***, ***Tables 1-4***.

2.7. Terminal differentiation to ECs and their characterization

hESC and iPSC-derived endothelial progenitors are commonly sorted using MACS or FACS and differentiated to mature endothelial cells through culture in commercially available endothelial growth medium with or without additional supplementation with high concentrations of VEGF and bFGF. VEGF and bFGF are commonly used as endothelial inducing agents for their crucial role in angiogenesis (Cross and Claesson-Welsh, 2001). Commercially available endothelial growth medium typically consists of basal media and endothelial cytokine cocktail (2-5% FBS, VEGF, bFGF, EGF, IGF1, heparin, ascorbic acid, hydrocortisone and/or bovine pituitary extract). In addition to the growth medium and angiogenic growth factors, extracellular matrix also plays an important role. Commonly used matrix substrates for differentiation and culture of PSC-derived ECs include gelatin (Levenberg et al., 2010; Moon et al., 2011; Wang et al., 2007), fibronectin (Hill et al., 2010; Park et al., 2013; White et al., 2013) and collagen IV (Yamahara et al., 2008).

2.7.1. Endothelial associated markers

The PSC-derived ECs upon culture acquire a typical cobblestone morphology *in-vitro*. These ECs express CD31 (PECAM1), CD34, VEGFR2 (KDR/Flk1), VEGFR1 (Flt1), VE-Cadherin (CD144), endoglin (CD105), vascular cell adhesion protein (VCAM-1, CD106), endothelial nitric oxide synthase (eNOS), Tie-1, Tie-2 (tyrosine kinase with immunoglobulin-like and EGF-like domains) and vWF in a time-dependent manner (Kane et al., 2010). VEGFR2 and CD34 are regarded as the earliest marker to appear during the induction and development of endothelial phenotype (Vittet et al., 1996). On the other hand, VE-cadherin, Tie1 and vWF appear later and are regarded as markers of late or mature ECs. vWF and angiopoietin-2 are stored within cytoplasmic organelles that are visible through transmission electron microscopy as electron-dense striated structures termed as Wiebel-Palade bodies (Adams et al., 2013). These bodies also stain positive for vWF upon immune-gold staining.

However, most of these markers are not endothelial specific and are expressed by other cells like hematopoietic stem cells. Hence, a panel of endothelial markers along with functional assays is needed to reliably characterize PSC-derived ECs. Additionally, functional assays indicate the maturation of ECs.

2.7.2. In-vitro characterization of ECs

In-vitro functional assays to characterize ECs include uptake of Dil (1,1'-dioctadecyl-3,3,3',3'-tetramethylindo-carbocyanine perchlorate) acetylated low density lipoprotein (Dil-Ac-LDL), ability to synthesize nitric oxide (NO), form tube-like structure over Matrigel (Glaser et al., 2011). Additional functionality assays include wound healing assays, response of ECs to

activation with inflammatory cytokines like tumor necrosis factor-α (TNFα), ability to bind lectins, production of ECM, migratory response towards angiogenic signals and ability to regulate permeability (Glaser et al., 2011; Huang et al., 2013).

2.7.2.1. Dil-Ac-LDL uptake assay

Dil-Ac-LDL uptake assay relies on the phagocytosis of LDL molecules by endothelial cells. ECs lining the blood vessels take up LDL that is present in the bloodstream and plays a role in transport of lipoproteins and cholesterol (Glaser et al., 2011). LDL is phagocytized by other cells that include macrophages and vSMCs/ pericytes. However, the uptake of LDL is rapid in ECs and macrophages, and hence the assay relies on the ability of ECs to uptake Dil-Ac-LDL upon incubation for 4 hours (Voyta et al., 1984). Ability of hESC- and hiPSC-derived ECs to uptake Dil-Ac-LDL has been demonstrated by various reports (Bai et al., 2010; Levenberg et al., 2010; Park et al., 2010; Rufaihah et al., 2013a; Wang et al., 2007).

2.7.2.2. Matrigel tube formation assay

ECs and progenitors are well recognized in forming new blood vessels by the process of vasculogenesis and angiogenesis. Vasculogenesis is the formation of vascular networks de-novo by ECs and progenitors, while angiogenesis is the formation of new vascular channels from existing vessels (Bai and Wang, 2008). The ability of ECs to forms cords and tube-like structures *in-vitro* upon culture over on a basement membrane matrix, Matrigel, derived from the Engelbreth-Holm-Swarm tumor. It is considered as a measure of vasculogenic and angiogenic potential of ECs (Glaser et al., 2011). Hence, Matrigel tube formation assay is one of the most commonly used assays to investigate angiogenesis and anti-angiogenesis (McGonigle and Shifrin, 2008). However, other cells like fibroblasts, MSCs also exhibit a response on Matrigel (Auerbach et al., 2003). The classic Matrigel tube formation assay involves seeding ECs directly over Matrigel in a 96/48/24 well tissue culture plate. However, the technique is limited by difficulty in imaging the vascular networks due to meniscus effect. To overcome this limitation, a novel slide/ 96 well plate angiogenesis product termed µ-slide/plate angiogenesis (ibidi) is available, which uses a well within a well feature to produce a flat Matrigel interface resulting in a flat surface for imaging (***Figure 18***).

The ability of hESC- and iPSC-derived ECs to form vascular tube-like structures has been demonstrated by various reports (Adams et al., 2013; Kane et al., 2010; Kurian et al., 2013; Sone et al., 2007; Tan et al., 2013a). Using Matrigel tube formation assay, the interactions between hESC-derived ECs and vSMCs have also been reported (Hill et al., 2010; Vo et al., 2010). These studies have demonstrated the circumferential orientation of hESC-derived vSMCs over cords/ tubes formed by hESC-derived ECs. Additionally, these studies have

demonstrated the variation in tube length, tube thickness and branch points depending on the ratio of ECs to vSMCs.

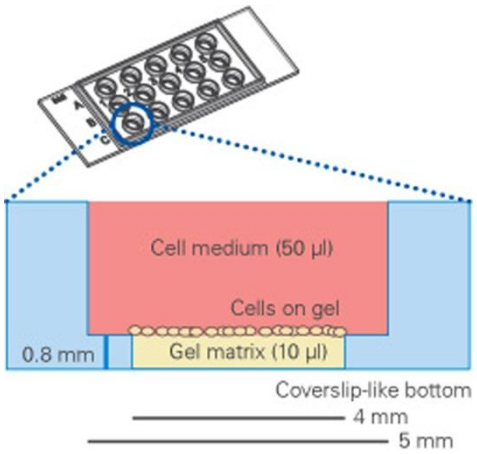

Figure 18. µ-slide angiogenesis (ibidi).

µ-slide angiogenesis is a specialized slide with 15 wells. Cross-sectional view of each well shows the presence of two compartments within it. The smaller lower compartment holds the gel matrix, while the upper compartment holds the media. The specialized slide provides a flat gel surface for better visualization and photomicrography. *Source: Adapted with permission from ibidi GmbH.*

2.7.2.3. NO and eNOS assay

ECs regulate the blood flow and vascular tone through release of vasodilators (like NO, prostacyclin) and vasoconstrictors (like endothelin, platelet activating factor) (Glaser et al., 2011). ECs among other cells synthesize NO by eNOS, and constitutively express NO and eNOS. Similar to primary ECs, hESC- and iPSCs-derived ECs constitutively express NO and eNOS (Wagner et al., 2010; White et al., 2013). eNOS expression has been reported to be absent in PSC-derived endothelial progenitors, while maturation of the progenitors to mature ECs was associated with marked cytoplasmic expression of eNOS (Kusuma et al., 2013). Costa et al., reported perinuclear localization of eNOS within golgi apparatus of hESC-derived ECs when cultured under serum-free conditions, while transfer to serum-containing conditions resulted in a localization in the caveolae (Costa et al., 2013).

2.7.2.4. Proinflammatory endothelial activation

Inflammation is associated with recruitment of leukocytes to the site of inflammation. Leukocyte trafficking through the vessel wall involves the expression of various selectins, chemokines & integrins. In-vitro the endothelium could be activated with inflammatory cytokines like TNFα, IL1β, interferon-γ or microbial components like lipopolysaccharides (LPS). Activation of ECs leads to upregulation and expression of cell adhesion molecules like E-selectin, ICAM, VCAM; and chemokines like IL6, IL8. Activation of iPSC-ECs with IL1β,

TNFα and LPS has been reported to induce the expression of adhesion molecules (E-selectin, ICAM1, VCAM-1) and secretion of proinflammatory cytokines (like monocyte chemotactic protein-1 (MCP1), IL8, RANTES) (Adams et al., 2013).

2.7.2.5. ECM production by ECs

Endothelial cells are separated from the vSMCs/ pericytes by a basement membrane that is composed of various ECM molecules that include collagen IV, laminin, fibronectin, entactin and heparin sulfate proteoglycans (Kusuma et al., 2012). Collagen IV is the most abundant form of ECM produced by ECs which aids in providing structural stability to the blood vessels (Anderson and Hinds, 2012; Glaser et al., 2011). Laminin especially, laminin-8 and -10 isoforms are produced by the ECs, which play a role in maturation of vSMCs (Glaser et al., 2011).

2.7.2.6. Wound healing assay

Angiogenesis involves formation of new blood vessels from existing vascular channels. During the process of angiogenesis, the ECs sprout and migrate to angiogenic signals to form new blood vessels. Wound healing assay is one of various methods to assess migration of ECs *in-vitro*. The assay involves creation of a wound by denuding a part of the endothelial monolayer, followed by observation of migration of the ECs into the wound/ denuded area over a period of time (Liang et al., 2007). These assays could also be used to study directional migration of cells in response to cellular, extracellular matrix and growth factors. The ability of hESC- and iPSC- derived ECs to migrate has been demonstrated using wound healing assays (Huang et al., 2013; Kane et al., 2010).

2.7.2.7. Regulation of vascular permeability

An important role of ECs is to maintain a tight dynamic barrier to regulate the transport of fluids, molecules and cells between the intraluminal and extraluminal compartments of the blood vessels. Monolayer of ECs are relatively impermeable to macromolecules (1-100kDa) with <1% flux (Glaser et al., 2011). To assess the barrier properties of ECs the flux of test compounds could be measured using electrical resistance across the monolayer of ECs termed as trans-endothelial electrical resistance (TEER). Alternatively, the permeation of fluorescently/ radioisotope labeled chemicals could be used to assess the movement of the chemicals across the endothelial monolayer. Adams et al., reported changes in permeability of human iPSC-derived ECs in response to histamine, VEGF, prostaglandin E2, spingosine-2-phosphate and cyclic adrenomedullin (cAMP) analog similar to primary ECs (Adams et al., 2013).

2.7.2.8. Lectin binding

The carbohydrates present on the surface of ECs act as ligands for various mammalian lectins. The L-fucose moieties present on endothelial surface bind to *Ulex europaeus* I (UEA-1) lectin and this is selective for all primate ECs (Gomez and Thorgeirsson, 1998). On the contrary, *Griffonia simplicifoha* lectin binds to ECs of murine origin and many other species except humans (Gomez and Thorgeirsson, 1998). Hill et al., demonstrated the binding of lectins *Helix Pomatia*, *Griffonia simplicifolia* and *Ulex europaeus* by hESC-derived ECs (Hill et al., 2010).

2.7.3. In-vivo characterization of ECs

Therapeutic angiogenesis is a promising application of PSC-derived ECs for treatment of ischemia associated with peripheral arterial diseases, myocardial infarction, diabetic retinopathy and stroke. Most commonly hESC- and iPSC-derived ECs are assayed for their *in-vivo* functionality using Matrigel plug angiogenesis assay and hind limb ischemia model (Cho et al., 2007; Rufaihah et al., 2011; Yamahara et al., 2008). Other *in-vivo* functionality assays and therapeutic models include transplantation with various biomaterials, mouse ischemic retinal angiogenesis assay, incorporation into retinal vasculature of diabetic rats, myocardial ischemia model, stroke and vascularization in dermal wounds (Azhdari et al., 2013; Kim et al., 2013; Kraehenbuehl et al., 2011; Levenberg et al., 2010; Li et al., 2009; Lu et al., 2007; Oyamada et al., 2008; Rufaihah et al., 2010; Wang et al., 2007).

2.7.3.1. Matrigel plug angiogenesis assay

Matrigel plug angiogenesis involves the injection of ECs with or without supporting stromal cells (vSMCs, fibroblasts, MSCs) encapsulated within Matrigel into subcutaneous depots of immunodeficient mice. Upon injection into the mice, the Matrigel undergoes gelation and forms a plug of extracellular matrix. Matrigel plug usually is harvested after 2 weeks for histological evaluation of blood vessel formation and integration with host circulation. hESC- and iPSC-derived ECs form human $CD31^+$ positive capillaries with red blood cells within them, indicating the connectivity with host circulation (Ferreira et al., 2007; Rufaihah et al., 2011).

2.7.3.2. Hind limb ischemia model

Murine hind limb ischemia model is a commonly used model to mimic peripheral arterial disease. The model involves induction of ischemia in one of the hind limbs through ligation of the femoral artery, followed by transplantation of the ECs into gastrocnemius muscle (Huang et al., 2009; Niiyama et al., 2009). Reperfusion of the ischemic hind limb through neovascularization by transplanted ECs is investigated using visual signs of recovery, laser

Doppler spectroscopy, bioluminescence imaging, and/or histology. The potential of hESC- and iPSC-derived ECs in association with mural cells to augment neovascularization and aid in reperfusion of the ischemic hind limbs have been demonstrated by various research groups (Cho et al., 2007; Rufaihah et al., 2011; Sone et al., 2007; Yamahara et al., 2008).

2.8. Arterial-venous differentiation of endothelial cells

The progenitors that give rise to endothelial cells form a primitive vascular plexus by the process of vasculogenesis. The endothelial progenitors (angioblasts) adjacent to the endodermal somites are directed towards arterial lineage and form the first artery (the dorsal aorta in zebrafish), while the endothelial progenitors adjacent to neural tube migrate dorsally and form the first vein (posterior cardinal vein in zebrafish) (Swift and Weinstein, 2009) (***Figure 19***). The angioblasts develop into arterial or venous ECs depending on the signals in the surrounding microenvironment. The plexus of arterial and venous ECs undergo a series of maturational events and give rise to functional blood vessels termed as arteries, arterioles, capillaries, venules and veins (Tan et al., 2013b). In general, the arteries arise from the heart and transport blood that is rich in oxygen to the peripheral tissues, while the veins terminate in the heart and transport oxygen-depleted blood from the peripheral tissues to the heart. The arteries are exposed to high hemodynamic forces, and hence are thick-walled with multiple layers of vSMCs. On the other hand, the veins are exposed to lower hemodynamic forces and are thin-walled with few layers of vSMCs. The veins also exhibit valves projecting into the lumen of the vascular channels to prevent the backflow of blood. Various phenotypic differences between arterial, venous and capillary ECs are highlighted in ***Figure 20***.

Two models have been proposed for the specification of arterial and venous identity. Atleast till late 1990s, the key factor involved in arterial-venous specification of ECs, was believed to be the exposure of ECs to blood flow and the accompanied mechanical forces (shear stress and pressure). Recent evidences however, show that the arterial-venous identity is specified well before the onset of circulation, leading to genetic or molecular-based mechanisms of specification.

2.8.1. Mechanical determinants of arterial-venous identity

As the arteries arise from the heart, they are exposed to significant hemodynamic forces shear stress and pressure. Due to the differences in flow speeds and lumen size, the various parts of the vascular bed is exposed to varying shear stress. The arteries and veins are exposed to varying blood pressure levels ranging from 100 mmHg in large arteries to 6-8 mmHg in large veins (Sato, 2013) (***Figure 21***). These large differences in the blood pressure between arteries and veins are found only in the adults, while in the embryonic vasculature the differences are significantly smaller in the range of 1-2 mmHg. Hence, the vascular channels adapt to differences in the hemodynamic forces by differences in their structure. The arteries are thick-walled with multiple layers of vSMCs, while the veins are thin-walled with few layers of vSMCs.

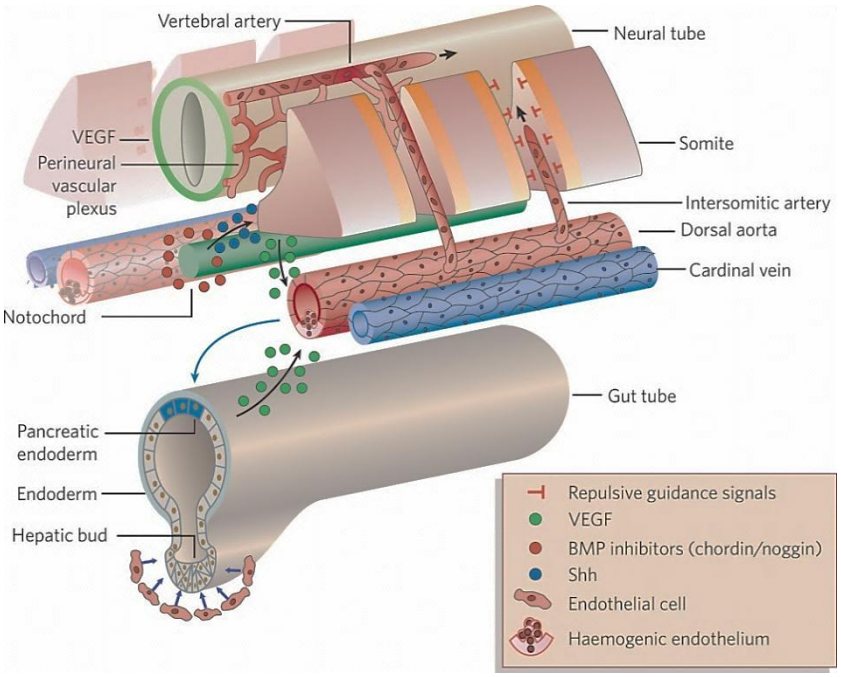

Figure 19. Role of endoderm and notochord in mammalian arterial-venous specification.

VEGF secreted from endoderm results in *de novo* aggregation of angioblasts leading to formation of dorsal aorta and cardinal veins. In response to the Shh secreted by notochord, the developing somites (endoderm) secrete VEGF. The angioblasts in the immediately vicinity of somites are exposed to high concentrations of VEGF, resulting in commitment to arterial lineage and formation of dorsal aorta, while the angioblasts that are away from the somites and notochord commit towards venous phenotype resulting in formation of cardinal veins. Additionally, the notochord secretes BMP inhibitors (noggin and chordin) which results in an avascular midline zone. *Source: Adapted with permission from (Coultas et al., 2005).*

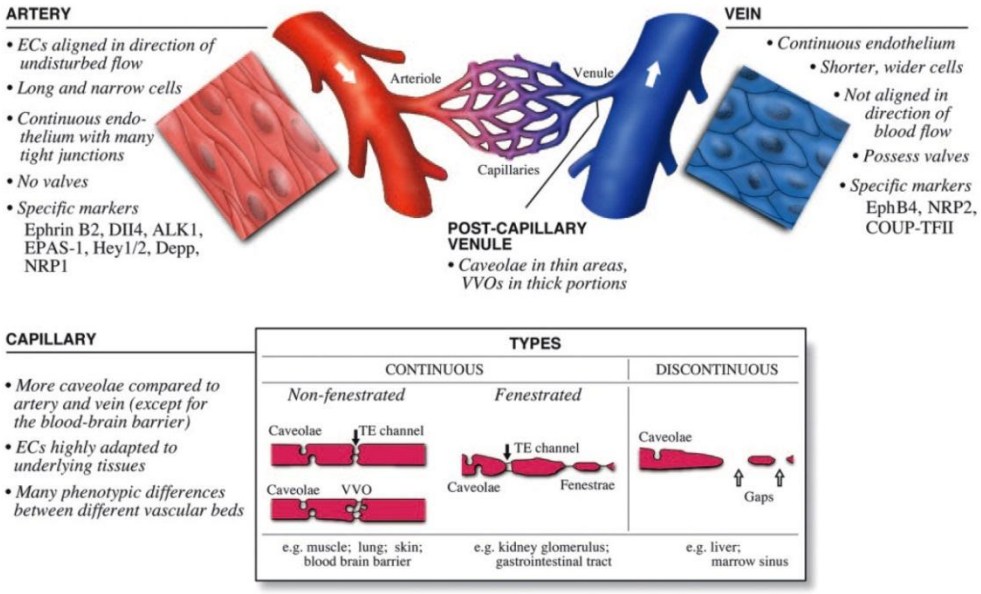

Figure 20. ECs in arterial, venous and capillary systems.

The illustration highlights the phenotypic differences among arterial, venous and capillary ECs. *Source: Adapted with permission from (Aird, 2007b)*

To investigate the role of hemodynamics in arterial-venous specification, "no-flow" models were developed. These "no-flow" *in-vivo* models indicate the downregulation of arterial markers in the arterial channels and no significant differences in the markers between arteries and veins (Sato, 2013). However, to understand whether the hemodynamic forces play a role in specification or in maintenance of arterial-venous identity needs further investigation.

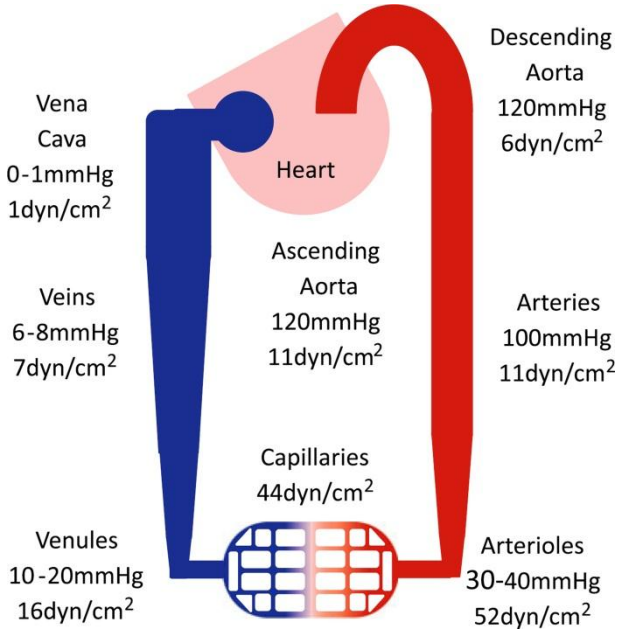

Figure 21. Differences in hemodynamic forces in various parts of the vascular system.

The illustration represents the two types of hemodynamic forces, shear stress and blood pressure among various vascular beds. Shear stress is expressed as (dyn/cm2) and blood pressure as (mmHg). *Source: Adapted with permission from (Sato, 2013)*

2.8.2. Genetic determinants of arterial-venous identity

Investigations on the role of EphrinB2-EphB4 ligand receptor system in the development of nervous system by Wang et al., in 1998 showed that EphrinB2 was expressed only in the arterial system, and the expression of EphB4 was exactly complimentary to that of EphrinB2 expression i.e., in the veins (Wang et al., 1998) (***Figures 10 & 22***). Additionally, this complimentary expression of EphrinB2 and EphB4 was found to be present even before the initiation of blood circulation (Adams et al., 1999; Wang et al., 1998). These findings lead to doubts on the mechanical specification theory of arterial-venous specification and further lead to rigorous molecular studies.

Since the finding of complimentary expression of EphrinB2 and EphB4 within the arterial-venous system, various arterial-venous markers have been identified. Arterial ECs are characterized by expression of high levels of Ephrin-B2, Notch and Notch-related molecules

(Notch-1, Notch-4, Hey-1, Hey-2), Notch ligands (Delta-like 4 (Dll4), Jag-1 and Jag-2), neuropilin-1 (NRP1), chemokine receptor-4 (CXCR4), gap junction proteins (Connexin-37 and Connexon-40); while the venous ECs express EphB4, COUP-TFII Lefty-1, Lefty-2, neuropilin-2 (NRP2) and apelin receptor (APJ receptor) (Aird, 2007b; Kume, 2010; Swift and Weinstein, 2009; Torres-Vazquez et al., 2003; Yamamizu and Yamashita, 2011). Most of the understanding about the molecular mechanisms of arterial-venous specification is based on studies in zebrafish and mice embryos, and a few studies using stem/progenitor cells.

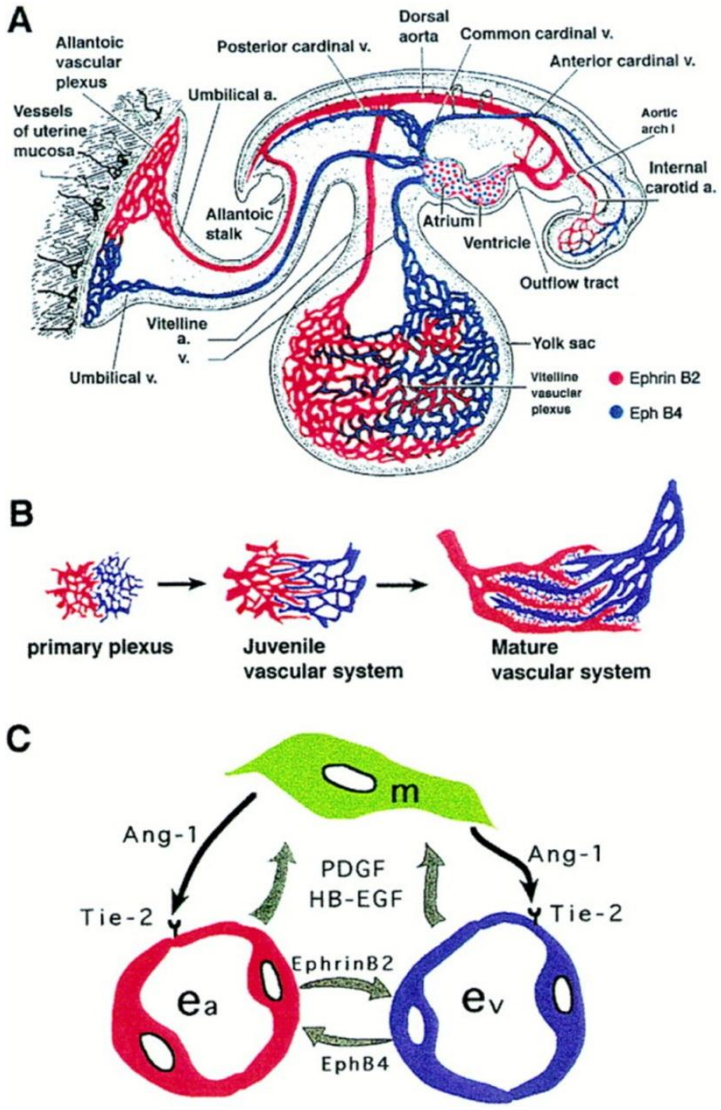

Figure 22. Pattern of EphrinB2 and EphB4 expression in the vascular system.

(A) The schematic shows the distinct pattern of ephrinB2 and ephB4 expression in mouse embryo. The arterial system expresses ephrinB2, while the venous system EphB4 and both are co-expressed in the heart. **(B)** Formation of arterial-venous interaction in the yolk sac. **(C)** shows the cell-cell interactions between ECs (arterial, e_a and venous, e_v) and mesenchymal cells (m). *Source: Adapted with permission from (Wang et al., 1998)*

2.8.2.1. Role of EphrinB2/EphB4 interaction in arterial-venous specification

EphrinB2 and EphB4 were the first set of genes to be identified in the regulation of arterial-venous specification of ECs. These genes encode for transmembrane proteins that belong to Eph-Ephrin subclass of tyrosine kinases. The Ephs represent the receptors and the Ephrins the ligand. Eph-Ephrin signaling occurs through cell-to-cell contact resulting in binding of the Ephrin ligand to the Eph receptors. The Eph-Ephrin signaling is bidirectional, wherein the forwards signaling represents Ephrin ligand to Eph receptor signaling, while reverse signaling represents Eph receptor to Ephrin ligand signaling.

The role of molecular signals in arterial-venous specification was based on study by Wang et al., which showed that EphrinB2 was expressed only in the arterial system and EphB4 in the venous system (Wang et al., 1998). Additionally, this complimentary expression of EphrinB2 and EphB4 was found to occur even before the initiation of blood circulation (Adams et al., 1999; Wang et al., 1998). Though the expression of ephrinB2 is restricted to arterial system, mice knockouts for EphrinB2 exhibit defects in angiogenesis of both arterial and venous systems (Wang et al., 1998). Findings from ephrinB2 knockouts suggest that the reciprocal signaling between arterial and venous system is needed for the integrated development of both the systems. Though, the expression of ephrinB2 and EphB4 only labels the arterial and venous systems respectively, and they are not required for the arterial-venous specification of ECs during vasculogenesis. The various molecular pathways involved in the arterial-venous specification are discussed below and summarized in ***Figure 23***.

2.8.2.2. Role of VEGF in arterial-venous specification

VEGF family of proteins plays a fundamental role in the vascular development through endothelial commitment, differentiation, proliferation, survival and migration. In mammals, VEGF family is composed of VEGF-A, VEGF-B, VEGF-C, VEGF-D, and placental growth factor (PlGF) (Hirashima, 2009). VEGF-A acts through various receptor tyrosine kinases that include VEGFR2 (also known as flk1), VEGFR1 (also known as flt1), VEGFR3 (also known as flt4), and NRP1. VEGF-A exists as three isoforms; $VEGF_{120}$, $VEGF_{164}$ and $VEGF_{188}$ in mice; and $VEGF_{121}$, $VEGF_{165}$ and $VEGF_{185}$ in humans. Expression of the VEGF receptors and co-receptors also show differences in their expression patterns. The VEGFR1 and VEGFR2 are expressed in all vascular ECs, VEGFR3 is mainly expressed in lymphatic ECs (but is an early marker for venous commitment), NRP1 in arterial ECs, and NRP2 in venous and lymphatic ECs (Herzog et al., 2001; Swift and Weinstein, 2009).

Selective expression of single isoforms of VEGF in transgenic mice, showed impaired arterial development only in mice with $VEGF_{188}$, while those expressing $VEGF_{120}$ and $VEGF_{164}$

displayed normal arterial development (Ng et al., 2001). Similarly, loss of $VEGF_{164}$ expression was associated with downregulation of EphrinB2 expression (Ng et al., 2001). These findings suggest the role of $VEGF_{164}$ in arterial differentiation and $VEGF_{188}$ in venous development.

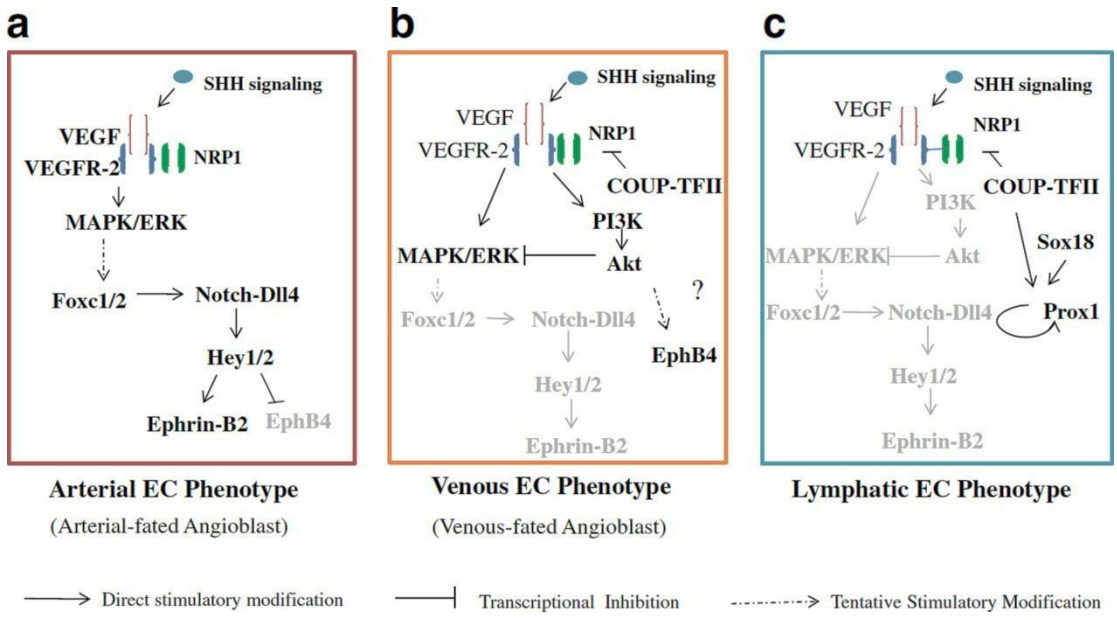

Figure 23. Signaling pathways involved in endothelial phenotype specification.

(a) Shh signaling induces VEGF which interacts with VEGFR2 and NRP1 resulting in activation of Notch-Dll4 downstream pathways to activate expression of arterial phenotype. (b) In contrast, in venous fated ECs, the presence of COUP-TFII suppress the expression of NRP1 and Notch-Dll4 pathways resulting in upregulation of genes related to venous phenotype. (c) Transcription factor Sox18 in co-operation with COUP-TFII activates the expression of Prox1 resulting in lymphatic endothelial phenotype. *Source: Adapted with permission from (Tan et al., 2013b).*

In Zebrafish embryos, injection of morpholinos targeted against *vegf* results in significant downregulation of arterial *ephrinB2* expression and arterial commitment; and upregulation of venous marker *vegfr3* (Swift and Weinstein, 2009). Similarly, sonic hedgehog (shh) deficient embryos display strong downregulation of arterial *ephrinB2* expression that could be rescued by injection of *vegf* mRNA (Atkins et al., 2011). *vegf* expression by somites is dependent on *shh* signals form the notochord (Swift and Weinstein, 2009). The somites in $shh^{-/-}$ embryos or cyclopamine-treated embryos fail to express *vegf* that could be rescued by injection of *shh* mRNA (Lawson et al., 2002). However, injection of *vegf* mRNA does not rescue the arterial differentiation observed in *Notch*-deficient embryos. Instead the injection of Notch intracellular domain (NICD) into *vegf* morpholino-injected embryos, rescues the ephrinB2 expression and arterial differentiation (Lawson et al., 2002). These results indicate that VEGF functions downstream of Shh and upstream of Notch for arterial fate specification. Hence the

hierarchical manner of arterial differentiation involves the expression of Shh by the notochord inducing the expression of *vegf* in the adjacent somite, which in turn induces Notch signaling in the adjacent ECs resulting in arterial specification and suppression of venous fate (Swift and Weinstein, 2009) (***Figures 19 & 23***).

The diffusion of VEGF expressed by somites towards the developing vascular channels results in a VEGF gradient. In zebrafish embryos, the vascular channel developing into dorsal aorta is exposed to higher levels of VEGF, while the blood vessel developing into posterior cardinal vein is exposed to lower levels of VEGF (Atkins et al., 2011) (***Figure 19***). This indicates the gradient effect of VEGF in arterial-venous specification of ECs, with higher levels favoring arterial fate. Binding of VEGF to its receptors like VEGFR2 results in activation of several targets that include phospholipase Cγ1 (PLCγ1), which in turn activates mitogen-activated protein kinase (MEK) and extracellular signal-regulated kinase (ERK) signaling pathways (Atkins et al., 2011; Swift and Weinstein, 2009). Further, in zebrafish embryos the activated form of ERK (phosphorylated form) is preferentially expressed in angioblasts fated towards arterial phenotype in early stages of vascular development; and is localized to arterial ECs in later stages of vascular development (Swift and Weinstein, 2009).

2.8.2.3. Role of Notch in arterial-venous specification

Notch family is composed of 4 receptors (Notch1-4) and 6 ligands (Dll1-4, Jag1-2). Activation of Notch results in cleavage of the NICD which translocates to the nucleus where it upregulates various target genes. In mice, the *ephrinB2*$^{+}$ arterial ECs specifically express Notch1, Notch4, Dll4, Jag1, and Jag2 (Swift and Weinstein, 2009). Mice lacking Notch1 display defects in vascular remodeling (especially axial vessels), reduced size of dorsal aorta and embryonic lethality, while Notch4 knockouts display no major vascular manifestations. However, Notch1/Notch4 double knockout mice show abnormal development of axial vessels that is severe than Notch1 mutants (Krebs et al., 2000). In zebrafish embryos, inhibition of Notch signaling by injection of a dominant negative Su(H) (suppressor of hairless) leads to downregulation of arterial markers (ephrinB2) and corresponding ectopic expression of venous markers (ephB4 and flt4) (Lawson et al., 2001). On the other hand, forced expression of NICD results in downregulation of venous markers (Lawson et al., 2001). Similarly, mice heterozygous & homozygous for Dll4 exhibit severe vascular malformations, downregulation of arterial markers (ephrinB2, Connexin 37, Connexin 40) and upregulation of ephB4 expression indicative of failure in arterial specification (Duarte et al., 2004). All these findings indicate the role of Notch signaling in induction of arterial specification and suppression of venous fate in early vascular development.

2.8.2.4. Role of Hedgehog in arterial-venous specification

Hedgehog (Hh) belongs to a family of secreted morphogens that includes sonic hedgehog (*shh*) and Indian hedgehog (*ihh*). Hh signaling occurs through interaction with a transmembrane receptor (Patched) that leads to patched-mediated inhibition of a transmembrane protein called Smoothened (smo) which leads to activation of target genes (Swift and Weinstein, 2009). The developing endoderm (proximal to the developing vascular network) expresses shh and the receptor for shh signal (patched-1) is expressed in ECs (Swift and Weinstein, 2009). In mice, *shh* induces expression of *vegf* and angiopoietins which in turn induces the development of coronary vessels (Pola et al., 2001). Inhibition of *shh* signaling using cyclopamine in mouse embryos results in underdeveloped vessels in the yolk sac and downregulation of *vegf* and *Notch1* (Pola et al., 2001). Further, mouse embryos lacking *shh* or those treated with cyclopamine, exhibit development of a single large axial vessel instead of a pair and the vessel shows expression of venous markers instead of arterial markers (Lawson et al., 2002). Similarly, zebrafish embryos injected with *vegf* anti-sense morpholinos exhibit downregulation of arterial specific markers like ephrinB2 (Lawson et al., 2002). On the otherhand, injection of vegf mRNA into zebrafish embryos that lacks activity of shh, rescues arterial specification (Lawson et al., 2002). These findings indicate that *shh* acts upstream of *vegf* and *Notch* in regulating in arterial specification (***Figure 23***).

2.8.2.5. Role of COUP-TFII in arterial-venous specification

Chicken ovalbumin upstream-transcription factor II (COUP-TFII) is an orphan nuclear receptor specifically expressed in venous ECs and is a genetic determinant of venous specification (Atkins et al., 2011). Unlike arterial specification, the molecular mechanisms into venous specification are poorly understood. Exposure to low concentrations of VEGF seems to be a negative regulator of arterial specification. Phosphatidylinosito-3-kinase/Akt pathway and retinoic acid is hypothesized to induce COUP-TFII which leads suppression of Notch and Nrp1 signaling, expression of EphB4, Nrp2, Vegfr3 and induction of a venous phenotype (You et al., 2005). In endothelial specific COUP-TFII knockout mice, the vessels are thin and dilated; and the venous ECs express arterial markers (Nrp1, Jag1, Notch1, Hey1, and EphrinB2) suggesting suppression of Notch1 and Nrp1 signaling (You et al., 2005). Further, endothelial specific overexpression of COUP-TFII in mouse embryos results in downregulation of Jag1 in aortic ECs (You et al., 2005). Hence, it seems that COUP-TFII expression in venous fated ECs leads to suppression of Notch and Nrp1 signaling, and hence leading to maintenance of venous endothelial phenotype (***Figure 23***).

2.8.3. Arterial-venous differentiation of ECs derived from PSCs

Subculture of mouse ESC-derived Vegfr2+ mesodermal cells on collagen IV coated plates in the presence of high concentrations of VEGF (50ng/ml) yielded ECs with upregulation of arterial markers like *Dll4, Notch4, EphrinB2,* and *Nrp1;* while in the presence of low concentrations of VEGF (10ng/ml) the ECs displayed upregulation of venous marker *COUP-TFII* (Lanner et al., 2007). Further inhibition of Notch signaling resulted in downregulation of arterial markers and upregulation of venous markers implying the role of Notch signaling in arterialization of ECs. Similarly, directed differentiation of mouse ESCs and iPSCs-derived *Vegfr2+* mesodermal cells to arterial, venous and lymphatic ECs by modulation of the concentration VEGF and cAMP was reported (Narazaki et al., 2008). However, in their study high concentration of VEGF (50-100ng/ml) resulted in venous ECs, and supplementation with cAMP in addition to VEGF was needed for arterial differentiation (Narazaki et al., 2008; Yurugi-Kobayashi et al., 2006). Aranguren et al., reported high concentration of VEGF (100ng/ml) induced arterial differentiation of human bone marrow-derived multipotent adult progenitor cells (Aranguren et al., 2007). Further, the arterial induction was reported to be enhanced by supplementation with Dll4 and Shh, while blockade of Notch and/or Shh led to attenuation of arterial differentiation and upregulation of venous markers similar to data from animal studies (Aranguren et al., 2007). Similarly, Rufaihah et al., demonstrated high concentration of VEGF (50ng/ml) in the presence of cAMP aided differentiation of human iPSCs-derived EBs towards ECs of arterial phenotype; and low concentration of VEGF (10ng/ml) resulted in venous differentiation (Rufaihah et al., 2013a). Interestingly, the role of VEGF and Notch signaling in arterial-venous specification was reported using human bone marrow-derived MSCs (Zhang et al., 2008b). Endothelial differentiation of MSCs in the presence of high concentration of VEGF (100ng/ml) resulted in upregulation of arterial markers and low concentration (50ng/ml) resulted in upregulation venous markers. Further the upregulation of arterial markers were abrogated upon inhibition of Notch signaling.

In contrast to these studies, certain studies have analyzed the expression of arterial, venous and lymphatic markers in the pool of PSC-derived ECs. Glaser et al., analyzed mouse ESC-derived ECs differentiated in the presence of VEGF (50ng/ml) and serum for proportion of ECs expressing arterial, venous and lymphatic markers (Glaser et al., 2011). Almost 60% of the mouse ESC-derived ECs expressed venous marker EphB4, while only 20% of the cells expressed arterial markers Notch1 and Dll4. Based on these observations the authors hypothesized that venous specification is the default differentiation pathway similar to early embryonic development. In another study from the same group, reported ~60% of mouse ESC-derived ECs expressed arterial markers (EphrinB2, Notch1, Dll4) and almost 90% of ECs expressed venous marker COUP-TFII, indicating the heterogeneous expression of

arterial and venous markers (Hatano et al., 2013). Kurian et al., recently reported conversion of fibroblasts to ECs through a plastic intermediate state, and these ECs exhibited expression of arterial, venous and lymphatic markers (Kurian et al., 2013).

In aggregate, studies in mouse and human *in-vitro* models indicate the dose-dependent effect of VEGF and Notch signaling in arterial-venous specification of ECs.

2.9. Terminal differentiation to vSMCs and their characterization

Early reports on differentiation of hESCs to vSMCs employed a direct differentiation to vSMC bypassing identification/ purification of a defined progenitor stage (Gerecht-Nir et al., 2003; Huang et al., 2006; Vo et al., 2010; Xie et al., 2007). Currently, hESC and iPSC-derived smooth muscle progenitor cells are commonly sorted using MACS or FACS and differentiated to mature vSMCs through culture in the presence of FBS or commercially available smooth muscle growth medium with or without additional supplementation with retinoic acid, $PDGF_{bb}$ and/or TGFβ1 (Cheung and Sinha, 2011). Commercially available smooth muscle growth medium typically consists of basal media and smooth muscle cytokine cocktail (2-5% FBS, bFGF, EGF, IGF1, heparin, ascorbic acid, and/or hydrocortisone). Alternative media used is DMEM supplemented with 10% FBS. In addition to the growth medium and growth factors, extracellular matrix also plays an important role. Commonly used matrix substrates for differentiation and culture of PSC-derived vSMCs include gelatin (Levenberg et al., 2010), fibronectin (Hill et al., 2010; Lu et al., 2007) and collagen IV (Oyamada et al., 2008; Vo et al., 2010; Yamahara et al., 2008).

2.9.1. Smooth muscle associated markers

To isolate the smooth muscle progenitors various markers have been reported in the literature (***Table 4***, ***Figures 15-17***), however the commonly employed markers are VEGFR2, CD34, PDGFRs, and ISL1. vSMC usually display a typical spindle-shaped morphology similar to fibroblasts and MSCs. vSMCs exist as contractile and synthetic phenotypes with the ability to switch phenotypes. The contractile vSMCs have a spindle-shaped morphology while the synthetic vSMCs are short and exhibit epitheloid morphology (Kane et al., 2011). As the synthetic phenotype is associated with modulation of ECM, it displays higher growth and migratory activities. The contractile phenotype being associated with contractile role contains large quantities of contractile filaments, while the synthetic phenotype has organelles associated with protein synthesis (Hao et al., 2003).

PSC-derived vSMCs are defined by expression of intracellular contractile proteins like α-smooth muscle actin (αSMA), calponin (CNN1), smoothelin (SMTN), transgelin (TAGLN/SM22a), smooth muscle myosin heavy chain (MYH11/ SM1a), calmodulin (CALM), and h-caldesmon (Cheung and Sinha, 2011; Descamps and Emanueli, 2012). αSMA is considered as the most early marker of smooth muscle differentiation, while CNN1, desmin, TAGLN are considered as intermediate and MYH11, SMTN are late stage markers of differentiation towards smooth muscle lineage. αSMA is the most commonly used marker for defining differentiation towards smooth muscle lineage (Kane et al., 2011). It is also the most abundant protein present in the vSMCs occupying almost 40% of the total cellular protein

content (Fatigati and Murphy, 1984). Among the various SMC marker, MYH11 and SMTN are considered as the best markers of mature vSMCs. Although these markers are present in vSMCs, they are not definitive for vSMCs as they are also expressed in other cell types like myofibroblasts, skeletal muscle, cardiac muscle and visceral smooth muscle cells (Owens et al., 2004; Shepro and Morel, 1993). Vascular and visceral SMCs are very closely related and could be distinguished using spice variants of myosin heavy chain, and smoothelin (Cheung and Sinha, 2011).

In addition to the expression of intracellular contractile proteins, various cell surface associated markers are used to identify, sort and characterize progenitors and mature SMCs/ pericytes (Wang et al., 2012b). These markers include PDGFRα, PDGFRβ, NG2 (neuroglial 2), CD90, CD73, CD105, CD146, CD13 and alkaline phosphatase (Armulik et al., 2011; Bergers and Song, 2005; Dar et al., 2012; Wang et al., 2012b). Other markers identified to mark the vSMCs/pericytes include RGS5 (regulator of G protein signaling 5), SUR2 (ATP-binding cassette, subfamily C), Kir6.1 (potassium inwardly rectifying channel), endosialin, DLK1 (delta-like 1 homolog) (Armulik et al., 2011). However, these additional markers need validation. PDGFRβ is tyrosine kinase receptor, expressed by developing vSMCs (Hellstrom et al., 1999). Its expression by the developing vSMCs is extremely crucial for their recruitment onto developing nascent endothelial channels resulting in stabilization and maturation of the vascular networks. NG2 is a chondroitin sulfate proteoglycan (also referred to as high molecular weight melanoma associated antigen) is especially expressed in pericytes (Bergers and Song, 2005).

Both the intracellular and surface markers of developing and mature vSMCs are not specific to vSMCs, and hence a panel of smooth muscle markers along with functional assays are needed to reliably characterize vSMCs derived from PSCs.

2.9.2. Characterization using functionality assays

Functional assays to characterize vSMCs include contractility assays, ability to support endothelial vessels *in-vitro* and *in-vivo*, and synthesis of ECM.

2.9.2.1. Contractility assays

vSMCs maintain the tone of blood vessels and control the flow of blood through their ability to contract. In-vitro equivalent of inducing contraction of vSMCs involve stimulation with agonists that include carbachol, histamine, bradykinin, angiotensin II norepinephrine, oxytocin, serotonin, endothelin, ATP and potassium chloride (Vazao et al., 2011). The assay typically involves stimulation with the agonist (most commonly carbachol) followed by time-lapse microscopy to monitor the contraction of the cells over a period of 30 minutes.

Additionally, relaxation of the cells is induced with atropine before inducing carbachol for negative control experiments. The change in area of the cells is used as a measure to quantify the amount of contraction (Marchand et al., 2013; Vo et al., 2010). Alternatively, flux of intracellular calcium (Ca^{2+}) is also used to quantify the contractility of PSC-derived vSMCs (Cheung et al., 2012; Hill et al., 2010; Vazao et al., 2011).

2.9.2.2. Support maturation of endothelial vessels

Formation of mature and functional microvascular network relies on the interaction between ECs and mural cells. Without the mural cells, the nascent endothelial vessels would undergo regression (Jain, 2003). Hence, the vSMCs play a crucial role in providing structural and functional support to the nascent endothelial vessels.

In-vitro tubulogenesis of ECs using Matrigel tube formation is used to investigate the supportive role of PSC-derived vSMCs *in-vitro* (Hill et al., 2010; Kim et al., 2013; Marchand et al., 2013; Vo et al., 2010). These studies have demonstrated the circumferential orientation of PSC-derived vSMCs over cords/ tubes formed by PSC-derived ECs. Additionally, these studies have demonstrated the variation in tube length, tube thickness and branch points depending on the ratio of ECs to vSMCs. In general, vSMCs supported formation of longer and thicker vascular tubes with less complex networks.

For *in-vivo* functional assessments, the PSC-derived vSMCs are co-implanted along with PSC-derived ECs. Subcutaneous injection of the two cells encapsulated within Matrigel and other biomaterials has been reported by various groups. Co-implantations have demonstrated higher density of vascular structures with host connectivity in the presence of vSMCs have been demonstrated (Ferreira et al., 2007; Kim et al., 2013; Kusuma et al., 2013; Levenberg et al., 2010; Lu et al., 2007). Similarly using cranial window models, formation of stable, perfused vascular networks by PSC-derived ECs in the presence of PSC-derived vSMCs have been demonstrated (Samuel et al., 2013; Wang et al., 2007). Further the supportive role of vSMCs in neovascularization have been demonstrated in hindlimb ischemia (Yamahara et al., 2008), myocardial infarction (Kraehenbuehl et al., 2011) and dermal wound models (Kim et al., 2013).

2.9.2.3. Synthesis of ECM proteins

To support the formation of mature vascular networks, vSMCs secrete various ECM molecules around the nascent endothelial channels. The expression of collagen and fibronectin has been investigated using hESC-derived vSMCs (Vo et al., 2010). vSMCs demonstrate upregulation of collagen and fibronectin. However, the effects on other matrix proteins are yet to be explored.

2.10. Engineering vascularized tissue equivalents

Tissue engineering provides a great platform to build functional tissues and organs to build, replace or repair lost, damaged or diseased tissues and also provides a platform for designing *in-vitro* test systems. Although considerable advancement has taken place in the field of tissue engineering in the past few decades, success has been limited to thin, avascular tissues like cartilage, cornea and skin that depend on nutrient and oxygen supply by diffusion (Novosel et al., 2011; Tian and George, 2011). Due to the limited success in engineering complex tissues, development and testing of pharmaceutical products are limited to use of conventional monolayer cell culture systems and/or animal experiments.

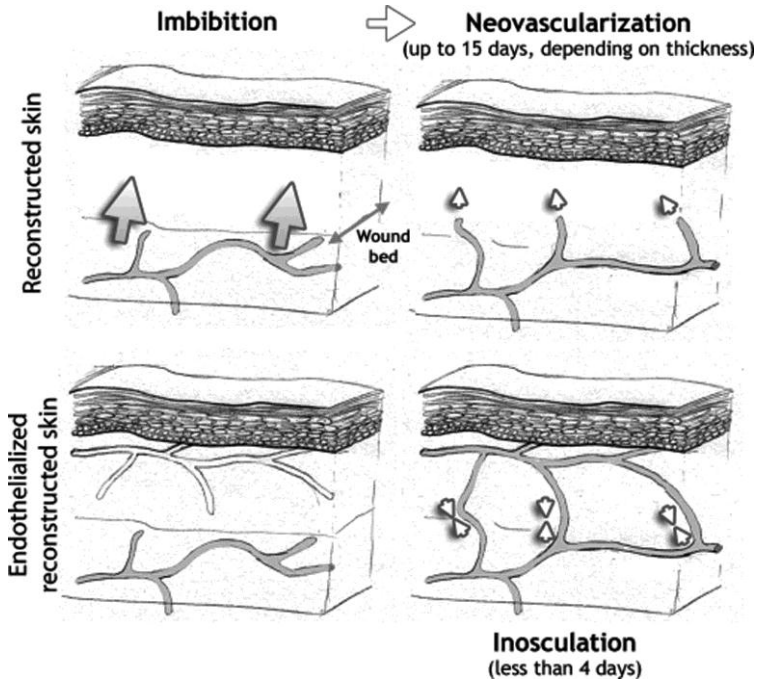

Figure 24. Schematic representation of graft nutrition after transplantation.

The schematic illustrates the three different mechanisms of nutrient supply to a graft after transplantation, which includes diffusion (imbibition), neovascularization, and inosculation. Imbibition is a passive diffusion of nutrients from the host and hence is has a limited range, while neovascularization is an active process involving migration of new blood vessels from the host into the graft. But neovascularization is a slow process taking upto 15 days depending on the thickness of the graft. On the other hand, inosculation is process of anastomosis of pre-existing graft vasculature with the host vasculature resulting rapid supply of nutrition within 4 days. *Source: Adapted with permission from (Tremblay et al., 2005)*

Fabrication of complex tissues needs delivery of nutrients and oxygen through perfusion, rather than diffusion alone. To enable the perfusion of thick, complex tissues a network of blood vessel system within the tissue constructs are needed. Young et al., described three mechanisms of nutrient supply to a tissue construct after implantation, namely (1) diffusion,

(2) neovascularization and (3) inosculation (Montano et al., 2010; Young et al., 1996) (***Figure 24***). Diffusion of the nutrients through the tissue construct is an inefficient process limited to a maximum distance of 200µm (Novosel et al., 2011). Neovascularization is the formation of new blood vessels through the process of vasculogenesis and/or angiogenesis. But, this process takes time and hence, is not the mechanism by which the graft survives during the initial days after implantation. Inosculation is the anastomosis of preexisting graft vasculature with the host vessels. The process of inosculation occurs rapidly, and would result in early supply of nutrients to the graft after implantation.

To vascularize engineered tissue several possible approaches have been explored over the past few decades. These approaches include (1) vascularization using (a) angiogenic factors and adhesion molecules, (b) incorporation of ECs and mural cells, (c) biomaterials or decellularized matrices; and (2) prevascularization by formation of *de novo* vascular channels before implantation (***Figure 25***).

2.10.1. Neovascularization using angiogenic factors and adhesion molecules

Vascularization of acellular or cellular tissue constructs could be aided by incorporation of angiogenic factors and adhesion molecules. Adhesion molecules like RGD, REDV, YIGSR sequences are commonly used with synthetic biomaterials to aid adhesion, recruitment, migration and differentiation of cells (Novosel et al., 2011). The angiogenic factors are aimed to activate the endothelial progenitors or ECs to migrate, proliferate and assemble to form a vascular network within the tissue construct.

VEGF and bFGF are the commonly growth factors used for upregulating the angiogenic process (Kaully et al., 2009; Novosel et al., 2011). Other angiogenic factors investigated include PDGF, TGFβ, hepatocyte growth factor and angiopoietins (Novosel et al., 2011). Hence, various scaffolds have been designed to incorporate and release various growth factor(s). Administration of single growth factor is generally insufficient, as several growth factor combinations are involved in the process of formation and maturation of vascular network. Hence, a cocktail of growth factors are needed that needs to be delivered in a spatial and temporal manner. Additionally, these growth factors generally suffer from very short-half-lives and hence require scaffolds capable of controlled-release of growth factors to enable local delivery for a prolonged period of time (Kaully et al., 2009). Further controlling the dose, rate of release and possible uncontrolled effects at distant sites is a huge challenge.

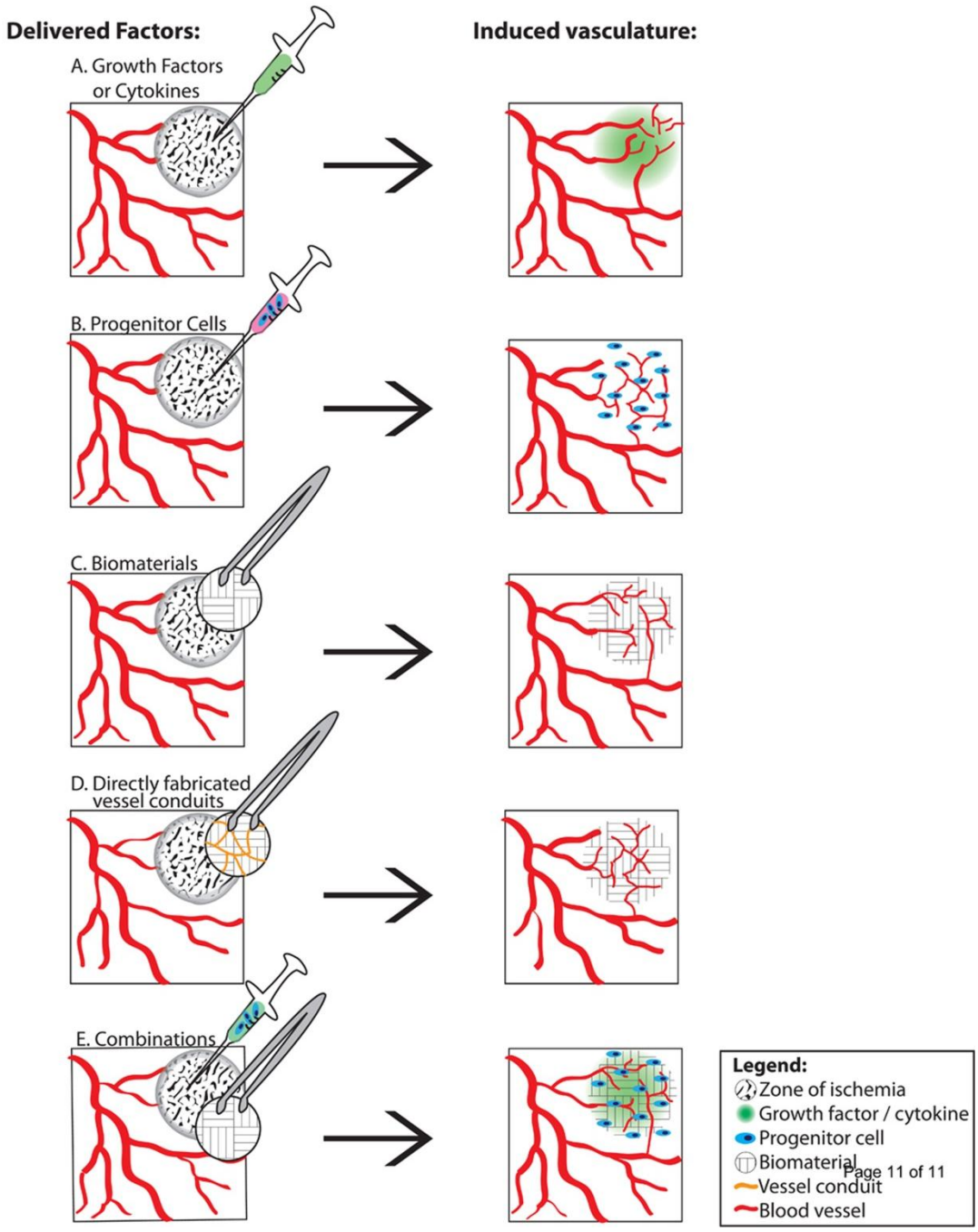

Figure 25. Common strategies for vascularization in tissue engineering.

Common strategies for engineering vascularized tissues include the delivery of **(A)** angiogenic factors like VEGF, bFGF, gene vectors, small molecules; **(B)** vascular cells like ECs, vSMCs, MSCs, fibroblasts; **(C)** biomaterials ranging from natural, synthetic to hybrid materials, **(D)** prefabricated/ prevascularized constructs; and **(E)** combination of one or more of the above methods. *Source: Adapted with permission from (Phelps and Garcia, 2010)*

Dual factor release system for temporal delivery of VEGF and $PDGF_{bb}$ was demonstrated to promote angiogenesis through endothelial sprouting under the control of VEGF followed by

maturation with pericytes under the control of $PDGF_{bb}$ (Carmeliet and Conway, 2001; Richardson et al., 2001). Similarly, incorporation and dual delivery of VEGF and bFGF within collagen-heparin and fibrin scaffolds was demonstrated to enhance the formation of mature vascular structures *in-vivo* (Hall, 2007; Nillesen et al., 2007). Recently, multifactor delivery was demonstrated using co-immobilization of VEGF and angiopoietin-1 as well as VEGF, IGF1 and stromal cell-derived factor-1 facilitated rapid and functional neovascularization compared to any individual factor (Sun et al., 2011). Another alternative method to deliver growth factors is to use genetically modified cells that overexpress these angiogenic factors (Novosel et al., 2011). hESC-derived endothelial progenitors expressing VEGF under the influence of adenoviral vector was reported to aid regeneration of infarct region in a rat myocardial infarct model (Rufaihah et al., 2010). Similarly, bone substitutes seeded with MSCs overexpressing VEGF was demonstrated to enhance angiogenesis and osteogenesis (Geiger et al., 2007).

2.10.2. Scaffolds for enhancing neovascularization

Advantage of using scaffolds primarily lies in providing the initial encapsulation of the donor cells that provides physical, chemical or mechanical cues that gradually preconditions the cells to the local biological environment upon implantation. Delivery of progenitors/ cells encapsulated within biomaterials with controlled release of pro-angiogenic factors may provide the ideal microenvironment for neovascularization (Kraehenbuehl et al., 2009; Saif et al., 2010). Though significant advancements have been achieved in the past decade, there are only a few studies that employ a biomaterial-based generation of *in-vitro* or *in-vivo* vascularized grafts using human PSC-derived vascular cells.

2.10.2.1. Natural biomaterials

Natural biomaterials offer several advantages as they provide both physical and chemical cues for cell adhesion, proliferation, migration and differentiation (Tian and George, 2011). Further they are biocompatible, biodegradable and biologically active. Various biological materials are available, but only those relevant to fabrication of vascularized tissues would be discussed below. Though natural biomaterials offer promising biological properties, they generally degrade rapidly, can cause immune reaction (except collagen), have batch-to-batch variation and may harbor infectious agents (Tian and George, 2011). To overcome these issues, the natural biomaterials are used in combination with synthetic biomaterials.

Collagen

Collagen is the most abundant protein present in the mammalian extracellular matrix. It has high mechanical strength and low antigenicity. Compared to most synthetic biomaterials, it

degrades faster. The degradation kinetics, pore size and mechanical properties of collagen scaffolds could be controlled by conjugation with various polymers. Collagen and hybrid collagen scaffolds promote angiogenesis as evidenced by the ability of various ECs to form functional vascularized tissue upon implantation into subcutaneous tissues of mouse. Collagen is commonly used in combination with fibronectin to fabricate vascularized tissues. Human umbilical vein endothelial cells (HUVECs) and murine fibroblasts encapsulated within collagen-fibronectin gels formed functional vessels integrated with the host vasculature and was durable for 1 year *in-vivo* (Koike et al., 2004). *In-vivo* the ECs formed long, branching vascular channels stabilized by recruitment of murine fibroblasts as pericytes. Similarly, hESC-derived ECs and murine fibroblasts encapsulated within collagen-fibronectin gels and implanted into cranial windows in severe combined immunodeficient (SCID) mice integrated with mouse vasculature and were functional for 150 days (Wang et al., 2007). Further, the microvessels derived from hESC-derived ECs without pericytes failed to anastomose with host vasculature and regressed within 7 days, underscoring the role of mural cells in maturation and stabilization of endothelial microvessels. In another study, hESC-derived ECs encapsulated within collagen-Matrigel gel constructs and cultured *in-vitro* for 5 days upon transplantation into infarcted nude rat hearts formed vascular networks that integrated with host vasculature (Nourse et al., 2010). Human iPSC-derived ECs and supporting perivascular cells (MSCs or iPSC-derived mesenchymal cells) encapsulated within collagen-fibronectin gels and transplanted into cranial windows or dorsal skin chamber models, formed functional, perfused blood vessels (Samuel et al., 2013).

Fibrin

Fibrin is a natural polymer of the monomer fibrinogen and is formed during the final phases of coagulation cascade. Fibrin-based materials are biocompatible, and biodegradable. It can be easily obtained from patient's blood, and hence eliminating the issues related to xenogenic products, foreign body reaction and disease transmission (Aper et al., 2007). Using this advantage, Aper et al., demonstrated fabrication of autologous blood vessels using endothelial progenitor cells and fibrin obtained from patient's peripheral blood (Aper et al., 2007). Fibrin and its degradation products support cellular attachment, cellular proliferation, angiogenesis and tissue repair (Ahmed et al., 2008; Shaikh et al., 2008). As a natural polymer involved in healing, fibrin has excellent biological properties for vascular tissue engineering (Chen et al., 2009; Lesman et al., 2011). Additionally, fibrinogen/ fibrin acts as a growth factor sink by providing binding sites for angiogenic factors VEGF and bFGF, and further protects them proteolytic degradation (Sahni et al., 2000; Sahni and Francis, 2000; Sahni et al., 2006). Hence, use of fibrin-based scaffolds for vascularization holds a great promise. However, fibrin lacks mechanical stiffness and undergoes rapid degradation both *in-vitro* and *in-vivo*

(Dikovsky et al., 2006). Stiffness of the fibrin hydrogels could be controlled by using fibrin in conjugation with collagen or synthetic polymers like polyglycolic acids (PGA), poly-L-lactic acid (PLLA), polylactic-glycolic acid (PLGA) or crosslinking with synthetic polymers like polyethylene glycol (PEG) (Dikovsky et al., 2006; Gonen-Wadmany et al., 2011; Lesman et al., 2011; Natesan et al., 2011). Similarly, the degradation rates could also be modulated using enzyme inhibitors like aprotinin (Wozniak, 2003). Additionally, the porosity of fibrin gels could also be modulated by varying the concentration of fibrinogen, with higher concentrations yielding gels with lower porosity and higher stiffness.

One of the well documented methods of controlling the limitations of fibrin scaffolds is through crosslinking the fibrin with PEG (PEGylation) and this has been employed for various tissue engineering applications. PEGylation has been reported to introduce the ability to photopolymerize, improve the degradation rates and structural properties like porosity and mechanical strength (Zhang et al., 2006; Zhu, 2010). Additionally, PEG is biocompatible, non-immunogenic and is resistant to protein adsorption (Zhu, 2010). On the other hand, crosslinking could be detrimental to biological activity of fibrin due to certain alterations to the protein during the process of PEGylation (Barker et al., 2001). However, certain other studies have found no effect on the biofunctionalilty of fibrin in PEG-fibrin hydrogels (Zhang et al., 2008a; Zhang et al., 2006). The contradicting findings may be due to differences in the PEGylation process.

Excellent pro-angiogenic properties has led to fibrin-based gels been extensively used for fabrication of vascularized tissue equivalents for skin (Lugo et al., 2011; Montano et al., 2010), bone (Steffens et al., 2009), adipose tissue (Borges et al., 2006; Frerich et al., 2001; Natesan et al., 2012; Natesan et al., 2011), skeletal muscle (Lesman et al., 2011) and cardiovascular (Birla et al., 2005; Plotkin et al., 2014) applications. Using fibrin, an *in-vitro* 3D-model for assessing the permeability of capillary networks was recently reported (Grainger and Putnam, 2011).

HUVECs or endothelial progenitor cells encapsulated with fibrin-based tissue constructs cultured *in-vitro* for a week aided the formation of patent capillary network that upon transplantation into mouse anastomosed with mouse blood vessels within 1-4 days (Chen et al., 2009; Chen et al., 2010). Similarly, *in-vitro* triculture of ECs, fibroblasts and skeletal myoblasts within fibrin gels alone or in combination with synthetic PLLA/PLGA sponges resulted in formation of network of vessels within 7 days (Lesman et al., 2011). Further, the maturity levels of the vessel networks were dependent on the concentration of fibrinogen. Although the utility of fibrin gels in aiding vascularization has been extensively studied, no reports are available using PSC-derived vascular cells.

Matrigel

Matrigel is a basement membrane extracted from Engelbreth-Holm-Swarm mouse sarcoma cells (Tian and George, 2011). It is most extensively used extracellular matrix especially for assaying angiogenesis and vasculogenesis both *in-vitro* and *in-vivo*. ECs including human PSC-derived ECs form tube-like structures when seeded over Matrigel, and also form perfused vascular structures when injected subcutaneously (Ferreira et al., 2007; Rufaihah et al., 2011). However, from a clinical stand point, use of Matrigel is limited by its xenogenic and tumor-origin, and batch variability (Tian and George, 2011).

Hyaluronic acid hydrogels

Hyaluronic acid (HA) is a glycosaminoglycan made of nonsulfated linear polysaccharide of (1-β-4)D-glucuronic acid and (1-β-3)N-acetyl-D-glucosamine. HA has been reported to aid EC attachment, proliferation, migration and sprouting through surface receptors CD44 and CD168 (Yee et al., 2011). Using HA hydrogels, Gerecht and colleagues, developed a 3D *in-vitro* vascularized construct to study the events during the process of vascular morphogenesis (Hanjaya-Putra et al., 2011).

Decellularized matrices

Engineering the natural architecture of the vascular tree *in-vitro* and rebuilding the vascular networks within is challenging. Decellularization of mammalian tissues, a naturally-derived 3D-architecture of the vascular system could be obtained. Decellularized matrix exposes the ECM and also maintains its 3D architecture like that of vasculature that could be repopulated with desired ECs and/or mural cells to rebuild the vascular tree *in-vitro* (Novosel et al., 2011). Additionally, the process of decellularization removes most, if not all, antigens that might invoke a host-immune response. For instance, *in-vitro* vascularized heart and liver-like tissues were reported utilizing the intact geometry of the vasculature after decellularization of rat heart and porcine jejunal segment with ECs (Linke et al., 2007; Ott et al., 2008).

2.10.2.2. Synthetic biomaterials

Numerous synthetic biomaterials have been investigated for tissue engineering purposes, but the most essential features to consider while designing or choosing a suitable scaffold for vascularization include (1) ability to aid attachment, proliferation and migration of ECs, (2) adequate porosity for vessel infiltration, and (3) sufficient pore interconnectivity to allow for the branching and anastomoses of microvascular channels. Synthetic biomaterials are advantageous in terms of the ability to tune their mechanical properties, degradation rates, pore size, and pore interconnectivity. Additionally, they can be reproduced consistently and do not pose risk of infectious disease transmission. However, they are limited by lack of

surface ligands for cell attachment and fate of degradation products. Many synthetic biomaterials have been used for fabrication vascularized tissue equivalents, but the most commonly used include PEG and PLGA-based hydrogels. In addition to conventional methods of engineering vascularized constructs, microfabrication techniques like rapid prototyping and solid free form techniques are used to engineer scaffolds with required vascular tree architecture (reviewed by Kaully et al., (Kaully et al., 2009) and Novosel et al., (Novosel et al., 2011)). However, the challenges include the micron-scale of the vessels that vary from few nanometers to few micrometers, and biological qualities for adequate adhesion, proliferation and growth of cells within the architecture.

Polyethylene glycol (PEG)

PEG is an inert hydrophilic polyether that is biocompatible and approved by US Food Drug and Administration (FDA) for clinical use (Barker et al., 2001). PEG has an extremely simple structure (HO(CH2CH2O)*n*CH2CH2OH) that is either linear or branched with hydroxyl ends that could be functionalized through conjugation with other polymers, drugs, peptides and proteins (Banerjee et al., 2012). Due to the hydrophilic nature of PEG, it attracts water molecules forming hydrogels that is resistant to protein adsorption and cell attachment (Tian and George, 2011). However, for purpose of vascularization applications, PEG must be modified to enhance cell attachment, migration and endothelial sprouting. The most common chemical approach for conjugating PEG with proteins or peptide sequences involves addition of an electrophilic functional group to the hydroxyl ends. The electrophilic functional group is used to couple with amine ($-NH_2$) groups present in proteins/ peptides, and the process is termed as PEGylation (Banerjee et al., 2012). For the purpose of engineering vascularized tissue equivalents, PEG is commonly conjugated with fibrinogen resulting in PEGylated-Fibrinogen that could be used to encapsulate ECs or other cells. Two commonly reported PEG-Fibrin gels for vascularization use PEG molecules functionalized using diacrylate or succinimidyl groups (Gonen-Wadmany et al., 2011; Seetharaman et al., 2011). In the former, bifunctional PEG-diacrylate is conjugated with fibrinogen using a complex process and the PEG-fibrin hydrogel is formed by photopolymerization using UV light exposure in the presence of a photoinitiator (Irgacure) (Almany and Seliktar, 2005; Gonen-Wadmany et al., 2011). While in the later, bifunctional PEG-succinimidylglutarate is conjugated to fibrinogen by a simple process of incubation wherein the electrophilic groups at both ends of PEG react with amine groups present in fibrinogen at 37^0C to produce stable amide linkages (Natesan et al., 2011; Seetharaman et al., 2011). PEG-fibrin hydrogel is formed using thrombin-assisted enzymatic gelation.

Seliktar and colleagues, demonstrated that PEG-fibrin hydrogels aided the recovery of cardiac function and cardiac neovascularization in a myocardial infarct model (Plotkin et al., 2014; Rufaihah et al., 2013b). Additionally, they demonstrated the ability to modulate the matrix stiffness by varying the concentration of PEG and its effect on cardiac recovery (Plotkin et al., 2014). Further, they have demonstrated the use of PEG-fibrin hydrogel as a delivery system for controlled release of VEGF (Rufaihah et al., 2013b). Same group using PEG-Collagen hydrogels demonstrated *in-vitro* capillary morphogenesis of ECs and fibroblasts (Singh et al., 2013). Similarly, Suggs and colleagues developed a PEG-Fibrin hydrogel for various cell delivery applications. They demonstrated differentiation of bone marrow and adipose-derived MSCs encapsulated within PEG-fibrin gels towards ECs without the need for additional growth factor supplementation (Natesan et al., 2011; Zhang et al., 2010). Further, using PEG-Fibrin hydrogels they developed wound dressing for cell delivery with antimicrobial and angiogenic properties (Seetharaman et al., 2011; Zhang et al., 2006). Similarly Kraehenbuehl et al., developed an injectable MMP-responsive PEG hydrogels for dual delivery of pro-angiogenic and pro-survival factor, thymosinβ4 and hESC-derived vascular cells for restoration of cardiac function in a rat myocardial infarct model (Kraehenbuehl et al., 2011).

Polylactic-glycolic acid (PLGA)

Polylactic-glycolic acid (PLGA) is a co-polymer of polylactic acid and polyglycolic acid. It is one of the most commonly used synthetic biomaterial in tissue engineering applications. Upon transplantation *in-vivo*, the polymer degrades to non-toxic naturally occurring compounds (glycolic acid and lactic acid) by hydrolysis and hence is biodegradable and biocompatible. Other advantages include tunable degradation rates and mechanical properties, ability to absorb proteins, and ability to functionalize using peptide sequences. PLGA is commonly used as a composite in combination with PLLA. The degradation rate of the polymer could be controlled by varying the molecular weight of the polymers and their ratios. The PLGA component of the composite polymer (PLGA/PLLA) degrades quickly and allows cellular ingrowth, while the PLLA degrades slowly providing mechanical strength.

PLGA/PLLA composite is commonly used in combination with natural biomaterials like collagen, fibronectin, Matrigel for fabrication of 3D vascularized tissue constructs. hESC-derived ECs encapsulated within a PLGA/PLLA + Matrigel formed perfused $CD31^+$ vascular channels upon subcutaneous implantation into SCID mice (Levenberg et al., 2010; Levenberg et al., 2002). Similarly, implantation of a triculture of hESC-derived cardiomyocytes, ECs and fibroblasts within PLGA/PLLA porous scaffolds into rat heart demonstrated formation of perfused donor (human) and host (rat)-derived vasculature (Lesman et al., 2010). A PLGA/PLLA-Matrigel scaffold has been used to engineer vascularized skeletal muscle

construct using hESC-derived ECs and mouse myoblasts that resulted in stable vascular structures surrounded by myoblasts (Levenberg et al., 2005). Further, addition of embryonic fibroblasts to the system resulted in dramatic increase in vascularization. Another study utilized co-seeding of ECs and MSCs encapsulated within collagen-fibronectin gel into PLGA to engineer vascularized bone graft *in-vivo* that integrated with host vasculature (Tsigkou et al., 2010). Hence, hybrid scaffolds of PLGA/PLLA along with natural biomaterials are a promising option for engineering vascularized scaffolds.

2.10.3. Engineering prevascularized tissue equivalents

Since long term survival of the cells within engineered tissue equivalents depends on adequate nutrient and oxygen supply, rapid establishment of vascular channels immediately after implantation is critical. Implantation of vascular cells encapsulated within biomaterials has shown promising results in establishment of vascular supply by process of vasculogenesis and neovascularization. However, this process takes atleast 7-15 days depending on the thickness of the construct (Tremblay et al., 2005). During this period of neovascularization, the cells in the center of the scaffold are dependent on mass transport (diffusion) which leads to a central zone of apoptosis (Johnson et al., 2011; Tsigkou et al., 2010). Hence, the ideal approach to provide rapid supply of nutrients would be to transplant tissue constructs with preformed vasculature that would anastomose with the host vasculature. This process of anastomoses of host and graft vasculature is termed as inosculation. In addition to clinical use, establishment of 3D prevascularized tissue equivalents would aid in development and testing of pharmaceutical products which otherwise are limited to use of conventional monolayer cell culture systems and/or animal experiments.

2.10.3.1. Role of preformed vascular network

Preformed vascular channels are believed to play a fundamental role of rapid establishment of nutrient supply to the tissue construct. In addition to this fundamental role, the preformed vascular channels also play passive and active roles in the success of the tissue construct after implantation. Vascularization of the implanted tissue equivalents (graft) could occur by (1) a simple anastomoses of the graft and host vessels, (2) ingrowth of host vasculature into the graft (internal inosculation), (3) outgrowth of graft vasculature (external inosculation) (***Figure 26***), and/or (4) recruitment of host derived-endothelial progenitors in the process of neovascularization. To determine how the vascularization of a transplanted full-thickness skin graft occurs, Capla et al., transferred grafts between transgenic tie2/lacZ mice and wild-type FVB/N mice (Capla et al., 2006). To differentiate the host and donor-derived ECs they employed lacZ expression under the control of endothelial specific tie2 promoter. Their results indicate the gradual regression of the graft vascular channels beginning at the

periphery of the graft on day 3 towards center of the graft through day 21. In parallel to the regression of graft vascular channels, ingrowth of the host vasculature was found to replace the regressing vessels. Additionally, bone marrow-derived endothelial progenitor cells were recruited and contributed to ~20% of the host ECs that invaded the graft. Hence, it seems that the prevascularization of tissue equivalents plays a passive role in the process of neovascularization by providing an outline for the ingrowth of new host-derived blood vessels. This process of ingrowth of host vasculature into the channels formed by regressing graft vasculature is termed as internal inosculation (***Figure 26***).

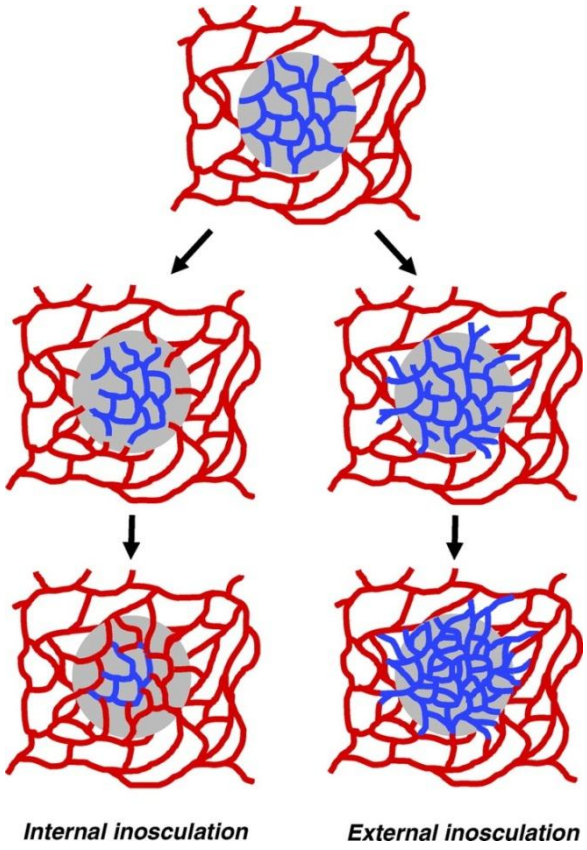

Figure 26. Schematic representation of internal and external inosculation.

The schematic illustrates the process of internal and external inosculation. The grey circular region represents the graft with its vasculature (blue network) surrounded by host vasculature (red network). Implantation of a graft with preformed vasculature could aid in vascularization of the graft by two processes: internal and external inosculation. In the process of internal inosculation the graft vasculature regresses, and is followed by invasion of host microvasculature into the graft. In external inosculation, the graft vasculature grows out into the host tissue and anastomoses with host vasculature. In parallel, the graft vasculature undergoes sprouting angiogenesis within the graft leading to increased density of the graft microvasculature. *Source: Adapted with permission from (Laschke et al., 2009)*

Recent studies demonstrate that preformed vascular channels play an active role in the process of neovascularization. Laschke et al., transplanted PLGA scaffolds prevascularized

within GFP-transgenic mice into dorsal skinfold chamber of wild-type recipient mice (Laschke et al., 2008). They observed that GFP^+ microvessels grew out of the graft into the surrounding host tissue and interconnected with GFP^- host vasculature. Further, they observed that the graft vasculature instead of regressing contributed to more vasculature by means of sprouting angiogenesis. This process of outgrowth of graft vasculature into the host tissue and anastomoses external to the graft is termed as external inosculation (***Figure 26***). Similarly, Shepherd et al., using prevascularized collagen gels demonstrated that anastomoses of graft and host vasculature predominantly occurred through external inosculation; and internal inosculation was restricted to the periphery of the graft (Shepherd et al., 2004).

The contradicting results demonstrate that the role of preformed vascular channels in the process of neovascularization is yet to be understood. However, the role of preformed vascular channels seems to be more than providing a framework for the ingression of host vasculature.

2.10.3.2. Approaches to prevascularize tissue equivalents

Tissue equivalents could be prevascularized *in-vitro* by seeding/ encapsulating ECs or endothelial progenitor cells with or without supporting mural cells (like vSMCs, fibroblasts, MSCs) within a suitable biomaterial. This approach is termed as *in-vitro* prevascularization. Secondly, a tissue construct could be prevascularized *in-vivo* by using body as a natural bioreactor and is termed as *in-vivo* prevascularization approach to engineering the microcirculation (***Figure 27***).

In-vitro prevascularization

To prevascularize tissue equivalents *in-vitro* angiogenic cells are seeded/ encapsulated within a 3D angiogenic matrix. This approach utilizes the ability of ECs and endothelial progenitors to self-assemble into microvascular networks. After the cells form a preliminary microvascular network, the *in-vitro* prevascularized tissue equivalent could either be used for *in-vivo* implantation or for *in-vitro* studies.

In one of the earliest attempts, Black et al., co-cultured keratinocytes, HUVECs, and dermal fibroblasts in a chitosan-collagen-chondroitin sulfate sponge to engineer the first endothelialized human tissue engineered skin equivalent (Black et al., 1998). Further, they demonstrated that the endothelialized skin equivalent accelerated graft revascularization by means of inosculation. Later the same group developed a human endothelialized skin equivalent by co-culturing keratinocytes, fibroblasts and HUVECs in a collagen sponge and demonstrated the rapid vascularization of the endothelialized skin equivalent in less than 4 days compared to 14 days in a non-endothelialized skin equivalent. Similarly, Levenberg et

al., developed vascularized skeletal muscle constructs *in-vitro* by co-culturing mouse myoblasts, embryonic fibroblasts and HUVECs/ hESC-derived ECs. They demonstrated that ECs organized into $CD31^+$ vascular channels in between the skeletal myoblasts. Further, in the presence of embryonic fibroblasts the ECs formed more vascular structures underscoring the role of mural cells. The vascular channels within *in-vitro* vascularized skeletal muscle constructs were stable for 1 month.

Chen et al., reported fabrication of fibrin-based *in-vitro* prevascularized tissue constructs by co-culturing HUVECs or endothelial progenitor cells with fibroblasts (Chen et al., 2009). Further, they demonstrated that prevascularization aided rapid vascularization by anastomosis with host vasculature within 1-4 days compared to non-prevascularized tissue constructs (8-14 days) (Chen et al., 2009; Chen et al., 2010). Further, the density of fibroblasts was demonstrated to play a role in establishing anastomoses with higher densities favoring rapid anastomoses (Chen et al., 2010). The optimal concentration and superior angiogenic properties of fibrin over collagen was demonstrated by Montano et al. (Montano et al., 2010). 3D culture of human microvascular ECs within fibrin (fibrinogen: 10-11mg/ml) resulted in formation of capillary networks, while the ECs remained as spherical aggregates in collagen matrices. Using the fibrin gels, they recapitulated the early stages of capillary morphogenesis i.e., (1) aggregation of single ECs into solid cords, (2) deposition of basement membrane, (3) formation of intracellular vacuoles through pinocytosis (pinocytotic vesicles), (4) formation of intracellular lumen by fusion of the intracellular vacuoles, and (5) formation of patent vascular channels by fusion of intracellular vacuoles of adjacent ECs (***Figure 28***). Further, the rudimentary vascular channels underwent maturation by recruitment of mural cells upon implantation into a mouse.

Grainger and Putnam developed 3D in-vitro vascularized tissue equivalents using HUVECs supported by fibroblasts, adipose derived-stem cells or MSCs in a fibrin gel (Grainger and Putnam, 2011). Further, they developed a novel 3D *in-vitro* model to assess the permeability of endothelial vessels and role of different mural cells in the modulation of capillary permeability.

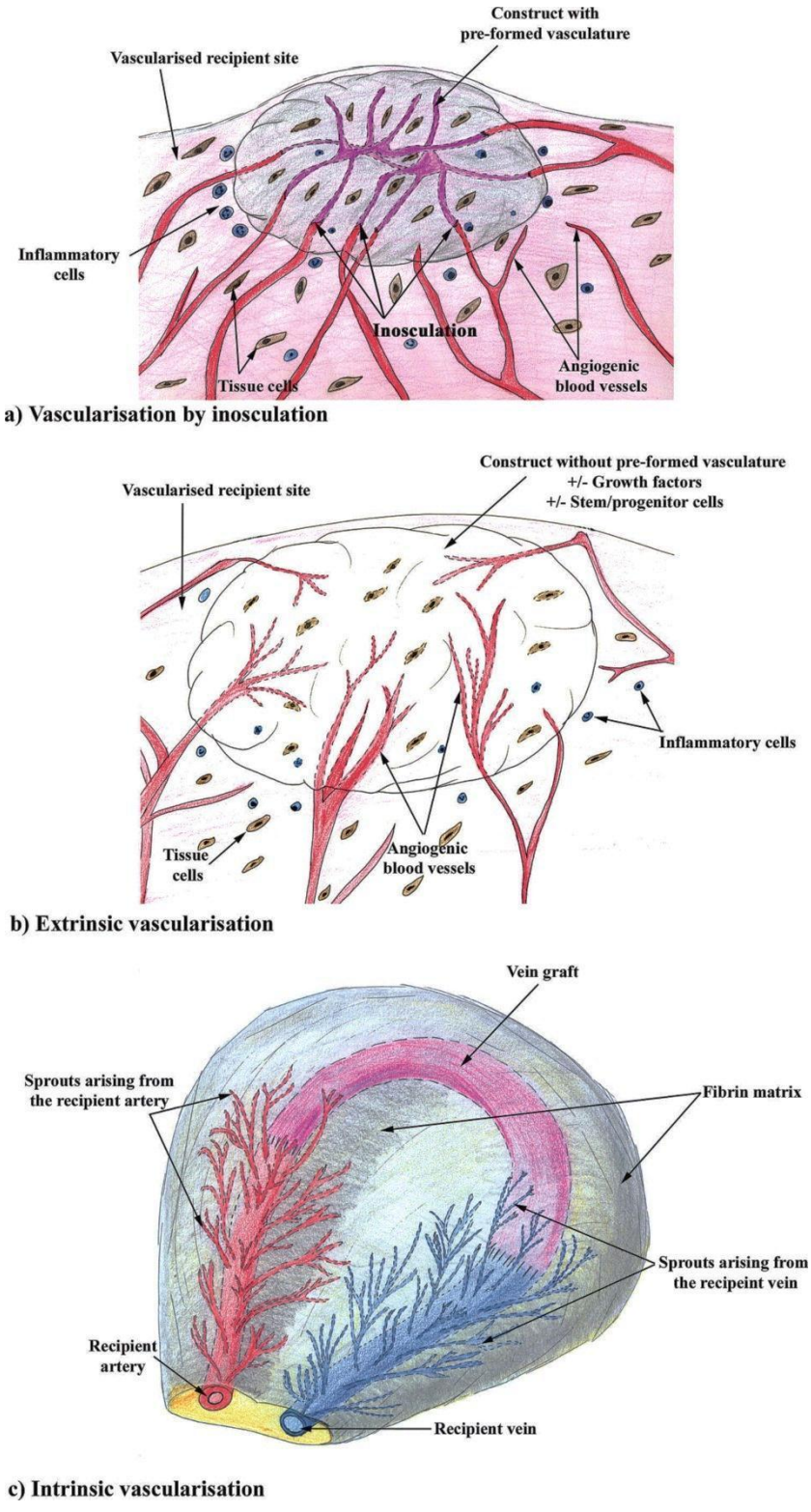

Figure 27. Approaches to prevascularize tissue constructs.

Tissue engineering constructs could be prevascularized *in-vitro* which upon implantation could inosculate with the host circulation **(a)**. Alternatively, the tissue constructs could be vascularized *in-vivo* involving extrinsic and intrinsic vascularization approaches. In the extrinsic approach, the tissue construct is vascularized by host vasculature outside of the construct **(b)**; while in the intrinsic approach, the host vasculature is included within the tissue to be constructed **(c)**. *Source: Adapted with permission from (Lokmic and Mitchell, 2008)*

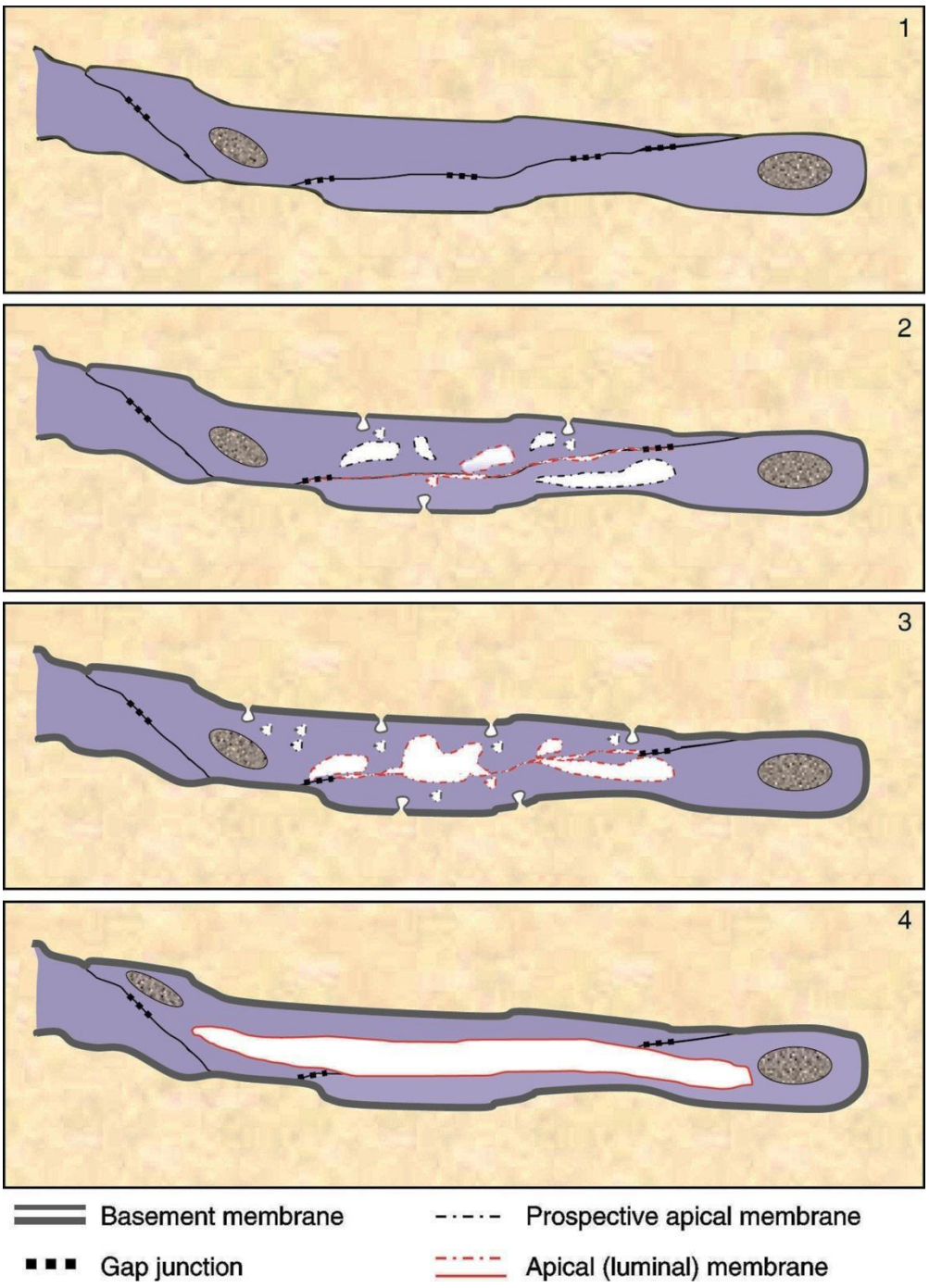

Figure 28. Schematic illustration of early morphogenetic events in formation of lumenized endothelial channels.

The schematic illustrates the early events in capillary morphogenesis i.e., **(1)** aggregation of single ECs into solid cords mediated by junctional complexes, **(2)** deposition of early basement membrane and formation of intracellular vacuoles through pinocytosis (pinocytotic vesicles), **(3)** formation of intracellular lumen by fusion of the intracellular vacuoles, and **(4)** formation of patent vascular channels by fusion of intracellular vacuoles of adjacent ECs. *Source: Adapted with permission from (Montano et al., 2010)*

In-vivo prevascularization

In-vivo prevascularization of tissue constructs utilizes the inherent angiogenic capacity of body, and could be achieved by two ways termed as extrinsic and intrinsic vascularization (Lokmic and Mitchell, 2008; Novosel et al., 2011) (***Figure 27***). Both the approaches involve a preliminary implantation of a non-vascularized construct into the host body, when vascularization of the construct occur *de novo*. After vascularization, the construct is harvested and reimplanted in the region of need. This methodology could be used to prevascularize large scaffolds but is limited by the need for multiple surgeries and donor-site morbidity.

Extrinsic vascularization

This method of *in-vivo* prevascularization involves the ingrowth of host vasculature into the implanted construct. It involves implantation of a cellular/ acellular porous scaffold into vascularized areas like adipose tissue, kidney capsule, and subdermis (Lokmic and Mitchell, 2008). Ingrowth of blood vessels into the porous scaffold vascularizes the construct.

Intrinsic vascularization

This approach is based on the provision of an artery or vein as a source of new blood vessels. Tissue construct to be vascularized is implanted within a chamber along with pedicle flap or an arteriovenous loop, which results in spontaneous angiogenic sprouting from the pedicle or loop. Then the vascularized construct with the feeder vessel is harvested and implanted into the site of need. This approach is commonly used to engineer vascularized bone grafts (Wang et al., 2010). In a landmark study, this methodology was used to fabricate a custom-made vascularized mandible by implantation of a titanium mesh filled with autologous bone chips and BMP4 in the latissimus dorsi muscle (Warnke et al., 2004). Hence, using this approach individually tailored, large 3D tissue constructs could be fabricated. However, the disadvantage lies in the time lag, need for multiple surgeries, and donor site morbidity.

Chapter 3

Rationale and study design

3. Rationale and study design

This doctoral study was designed to address the following objectives:

1. Develop protocols to efficiently differentiate hESCs to endothelial lineage through efficient commitment to primitive streak (PS), lateral plate mesoderm, endothelial progenitors and ECs.
2. Investigate the commitment of endothelial progenitors to arterial and venous endothelial phenotypes.
3. Develop protocols to efficiently differentiate hESCs to vascular smooth muscle lineage through efficient commitment to PS, paraxial mesoderm and vSMCs.
4. To engineer *in-vitro* 3D vascularized tissue equivalents using hESC-derived vascular progenies in a suitable biomaterial.
5. Reduce the use of xenogeneic products throughout the process of differentiating hESCs to progenitors and terminally differentiated ECs and vSMCs; and fabrication of vascularized tissue equivalents.

These objectives were approached in a phased manner as summarized below and in ***Figure 29***.

Phase 1: Differentiation of hESCs to PS through modulation of Wnt/β-Catenin signaling pathway using an inhibitor of glycogen synthase kinase-3 (GSK3) under feeder- and serum-free conditions (***Chapter 4***).

Phase 2: Differentiation of PS to lateral plate mesoderm and endothelial lineage through modulation of mesoderm and vascular lineage inducing factors that include bFGF, BMP4, and VEGF under feeder- and serum-free conditions (***Chapter 4***).

Phase 3: Differentiation of hESC-derived endothelial progenitors to ECs, in particular arterial and venous phenotypes under feeder- and serum-free conditions (***Chapter 5***).

Phase 4: Differentiation of PS to paraxial mesoderm intermediates through modulation of mesoderm and vascular lineage inducing factors that include bFGF and VEGF under feeder- and serum-free conditions (***Chapter 6***).

Phase 5: Differentiation of hESC-derived paraxial mesoderm intermediates to vSMCs under feeder- and serum-free conditions (***Chapter 6***).

Phase 6: Engineer *in-vitro* 3D vascularized tissue equivalents using hESC-derived arterial ECs and -vSMCs using PEG-Fibrin as a scaffold material under serum-free conditions (***Chapter 6***).

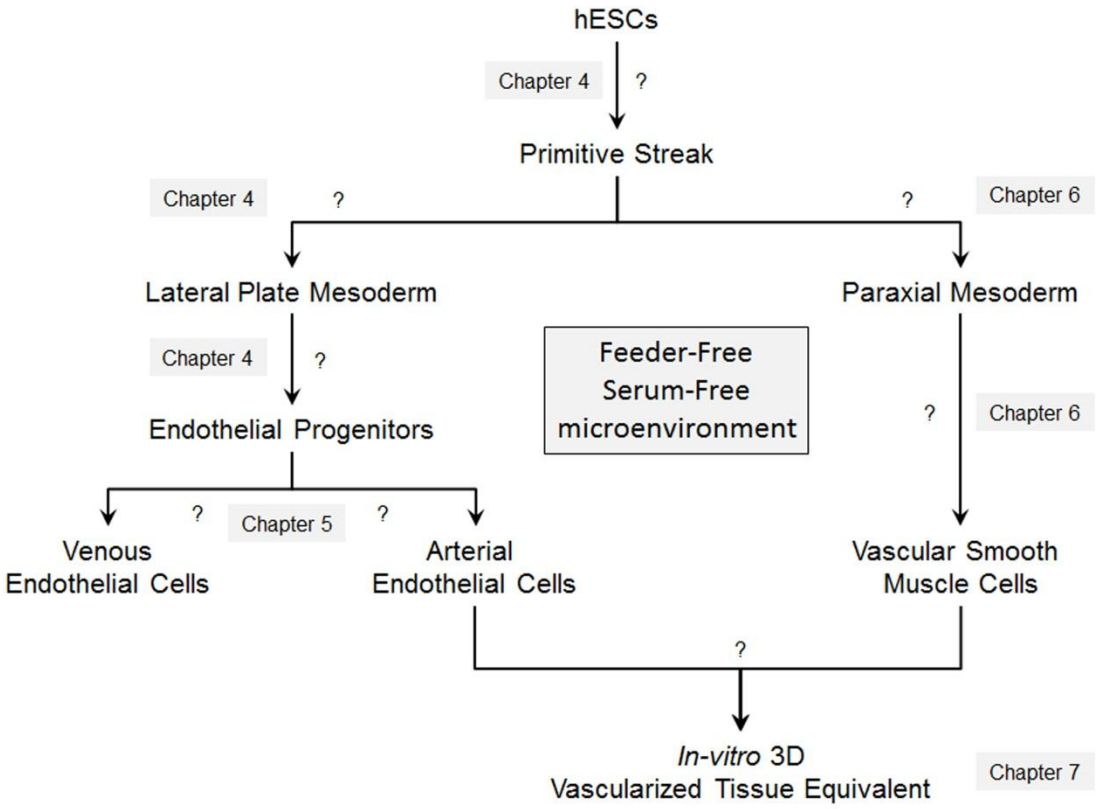

Figure 29. Schematic representation of the study design.

The schematic summarizes the findings demonstrated in this study. Refer to the text for detailed explanations. Briefly, the study aims to develop protocols to efficiently differentiate hESCs towards primitive streak-like cells that could be further directed towards lateral plate and paraxial mesoderm subtypes. Further, the differentiation of lateral plate mesoderm to endothelial progenitors that could be differentiated to venous and arterial endothelial phenotypes is studied. Similarly, the differentiation of paraxial mesoderm intermediates to vSMCs is investigated. Further, the utility of hESC-derived arterial ECs and vSMCs to engineer in-vitro 3D vascularized tissue equivalents is investigated.

Chapter 4

Efficient differentiation of hESCs to endothelial progenitors under feeder-free, chemically-defined conditions

4. Efficient differentiation of hESCs to endothelial progenitors under feeder-free, chemically-defined conditions

4.1. Introduction

Efficient differentiation of pluripotent stem cells (PSCs) that include human embryonic stem cells (hESCs) and induced pluripotent stem cells (iPSCs) towards specific lineages is a critical step towards obtaining sufficient amounts of clinically relevant cell populations for cell therapy, drug screening and developing models to study human development or disease. Since the pioneering report of Levenberg et al., (Levenberg et al., 2002) several protocols to differentiate hPSCs towards endothelial lineage have been reported till date (Kane et al., 2011). These protocols involve: (1) embryoid body-based differentiation, (2) co-culture of hPSCs over murine stromal cells, , (3) culture of hESCs or iPSCs as monolayers over extracellular matrix proteins like Matrigel, and collagen IV, and/or (4) growth factor, cytokines or small molecule mediated differentiation in serum containing/ serum-free conditions (***Figure 12***). However, these protocols are either inefficient or involve the use of xenogeneic (animal-derived) products such as fetal bovine serum (FBS), murine feeder cells and/or extracellular matrix. These xenogeneic components limit the clinical translation potential of these cells owing to the potential risk of transmission of animal pathogens and xenogeneic rejection (Kaupisch et al., 2012). Additionally, undefined nature of serum limits the ability to tune the cellular microenvironment. Hence, major challenges in the current differentiation models for endothelial differentiation include elimination of xenogeneic products and developing strategies for efficient differentiation.

Vascular cells that include the endothelial progenitor cells are derived from the mesoderm lineage. Formation of three germ layers including mesoderm begins with the formation of PS. The formation of PS is considered as the central structural marker for mesodermal and endodermal precursors (Tam and Beddington, 1987). The mesoderm further differentiates into paraxial, intermediate and lateral mesodermal subtypes (***Figures 3-5***). Embryologically, the endothelial lineage develops from the lateral mesoderm, while the vSMCs have diverse origins that include the lateral plate mesoderm, paraxial mesoderm and neuroectoderm. Hence, efficient differentiation of hESCs to vascular cells may also require the efficient differentiation towards specific mesodermal subtypes. Since, the formation of PS is the first event that marks the generation of mesodermal lineages, efficient differentiation towards PS would be an essential step to achieve maximal commitment of hESCs towards mesodermal subtypes.

4.2. Objectives

To efficiently differentiate hESCs to endothelial progenitors with minimal use of xenogeneic products.

4.3. Materials and Methods

4.3.1. Culture of hESCs under feeder-free and serum-free conditions

For feeder- and serum-free culture, H1- and H9- hESCs (WiCell Research Institute, Madison, WI) were cultured in chemically-defined medium (mTeSR™1; Stemcell Technologies) on growth factor reduced Matrigel (BD Biosciences)-coated plates (Nunc). Briefly, 70-80% confluent hESCs were passaged after treatment with 1mg/ml dispase (Invitrogen) for 5 min at 37^0C. The hESC colonies were dispersed into small clumps and re-plated onto Matrigel-coated plates.

4.3.2. Directed Differentiation of hESCs under chemically-defined conditions

To achieve the objective of minimal use of xenogeneic products, hESCs were differentiated under feeder-free and chemically-defined conditions as follows. hESCs cultured as described above were passaged using dispase, dispersed into small clusters (~300-500 cells per colony) and seeded onto 4µg/cm^2 human plasma fibronectin (GIBCO) coated plates. These hESC colonies were maintained in mTeSR™1 for 24 hours, after which the cells were gently washed with DMEM:F12 (Invitrogen) and differentiated in chemically-defined, serum-free, animal component-free basal medium (STEMdiff™ APEL™, Stemcell Technologies) supplemented with appropriate factors as depicted in ***Figures 32, 35-37***. Briefly, to induce hESCs towards PS, the hESCs were exposed to glycogen synthase kinase-3 inhibitor (GSKi; CHIR99021, 5µM, Stemgent) for 24 hours as previously reported (Tan et al., 2013a). Following induction of PS, mesodermal and endothelial induction was carried out in the presence of basic fibroblast growth factor (bFGF; 50ng/ml; R&D systems) for 24 hours followed by 72 hours of bone morphogenic protein-4 (BMP4; 25ng/ml; R&D systems) and/or vascular endothelial growth factor-A (VEGF; 50ng/ml; GIBCO). For validating the mesodermal differentiation potential of PS, hESCs after 24 hour treatment with CHIR99021 was treated with bFGF (50ng/ml) with or without FGF receptor inhibitor (PD173074; 0.1µM) as illustrated in ***Figure 35***. Similarly, validation of endodermal differentiation potential of PS was verified by induction with Activin A (50ng/ml) with or without Activin and TGF-β signaling inhibitor SB431542 (10µM) as illustrated in ***Figure 36***.

4.3.3. RNA extraction and real-time PCR

Total cellular RNA was isolated from harvested cells using RNeasy Plus Mini kit (Qiagen) and reverse transcribed using iScript™ cDNA synthesis kit (BioRad) according to manufacturer's instructions. Real-time PCR was performed in triplicates using Fast SYBR Green PCR master mix (Applied Biosystems) and Stepone Plus real-time PCR system (Applied Biosystems) as per manufacturer's instructions. Real-time PCR reaction mixtures were denatured at 94^{o}C for 20s and cycled for 40 cycles at 95^{o}C for 3s, 60^{o}C for 30s, followed by melt curve stage. Based on our previous studies (Rufaihah et al., 2010; Rufaihah et al., 2007) and others (Hill et al., 2010; Vo et al., 2010), we had chosen *β-ACTIN* as the internal control. The expression levels of specific genes were quantified by normalization against corresponding internal control gene *β-ACTIN* and expressed as the fold change relative to control sample (undifferentiated hESCs). Details of related primer sequences used in this study are presented in ***Appendix I***. The results are presented as mean ± standard deviations of two or more independent experiments.

4.3.4. Flow cytometry analysis

hESCs and differentiated cells were harvested using accutase, resuspended in FACS buffer (1xPBS/ 0.5% BSA) and incubated with FcR blocking agent (1:10; Miltenyi Biotec) for 10 minutes at 4^{o}C to block non-specific binding of antibodies. For labeling of cell surface antigens (VEGFR2, CD34, CD31), the cells were incubated with the antibodies for 10 minutes at 4^{o}C. The details of the antibodies used are presented in ***Appendix II***. After labeling with appropriate antibodies, the cells were washed thrice with FACS buffer to remove unbound antibodies and resuspended in FACS buffer for analysis and/or sorting. The labeled cells were analyzed for surface-marker expression using Dako Cytomation CyAn ADP. The flow cytometry data was further analyzed using FlowJo v7.6.5 (TreeStar).

4.3.5. Immunocytochemistry

hESCs and differentiated cells were fixed with 4% paraformaldehyde (Sigma) for 20 minutes at room temperature. The fixed cells were permeabilized using PBS/ 0.1% TritonX-100 (Sigma) for 10 minutes, washed thrice with PBS/0.05% Tween-20 (Sigma) and blocked with PBS/5% goat serum for 60 minutes to block non-specific binding. Subsequently, the cells were labeled with appropriate primary antibodies (OCT4, SSEA4, TRA-1-60, TRA-1-81, Alkaline phosphatase, BRACHYURY, β-Catenin; details of these antibodies are listed in ***Appendix III***) at 4^{o}C overnight. After thorough washing, the cells were fluorescently labeled using appropriate secondary antibodies (listed in ***Appendix III***) for 60 minutes. For nuclear labeling, the cells were washed and labeled with 4`,6-diamidino-2-phenylindole (DAPI;

Sigma) for 3 minutes. After washing thrice, the cells were observed using fluorescence microscope (Olympus IX70).

4.3.6. Statistical Analysis

All real time RT-PCR experiments were performed in duplicates with duplicate readings each. Student's t-test was performed to determine significance using Microsoft Excel Data Analysis ToolPak.

4.4. Results

To study the specification of hESCs towards mesodermal subtypes, H1-hESC line was used and the robustness of the protocol verified using H9-hESCs. The pluripotency status of H1-hESCs maintained on Matrigel and mTeSR1 were confirmed by immunocytochemical staining for expression of OCT4, SSEA4, TRA-1-60, TRA-1-81 and Alkaline Phosphatase (AP) (***Figure 30***). One day prior to differentiation, hESCs were passaged onto human plasma fibronectin coated plates. The pluripotent status of hESCs cultured upon fibronectin for 24 hours was confirmed by RT-PCR and immunocytochemical staining. Real time RT-PCR analysis revealed the hESCs cultured upon Matrigel and fibronectin had similar expression levels of pluripotent genes (*OCT4, SOX2, NANOG*) (***Figure 31***). Further, the hESCs cultured over fibronectin also expressed OCT4, SSEA4, TRA-1-60, TRA-1-81 and AP (***Figure 31***). Hence, the hESCs grown over fibronectin for 24 hours maintained pluripotent status.

4.4.1. Temporal emergence of primitive streak (PS)

During gastrulation in early embryogenesis, the mesoderm that gives rise to cells of the vascular lineage arises through an epithelial-mesenchymal transition of epiblast cells in the region of PS. Hence, we believe that efficient differentiation of hESCs to endothelial lineage depends on effective commitment of hESCs towards PS-like stage. Canonical Wnt pathway is one of various signaling pathways implicated in playing a critical role in the formation of PS. For differentiation towards PS, we adopted our previously published protocol (Tan et al., 2013a), using inhibition of glycogen synthase kinase-3 (GSKi) with CHIR99021 (5µM) under feeder-free, chemically-defined conditions. Since Matrigel is of animal-origin, and we aimed to reduce the use of xenogenic products, we modified our previous protocol by replacing Matrigel with human plasma fibronectin. During the induction of PS in hESCs, we observed that GSKi induced a marked decrease in pluripotency gene *SOX2* within 24 hours, followed by *OCT4* and *NANOG*; and the neuroectoderm-associated genes (*PAX6, SOX1*) (***Figure 32***). In contrast to the downregulation of neuroectodermal genes, the PS-related genes (*BRACHYURY, MIXL1*) were upregulated synchronously along with anterior PS genes (*FOXA2, GSC*) and peaked at day 1 of differentiation (***Figure 32***). The temporal expression

of PS-related genes was accompanied by steady upregulation of gene involved in epithelial-mesenchymal transition (*SNAI1*). The expression of BRACHYURY and OCT4 after 24 hours of GSKi was confirmed by immunofluorescence (***Figure 33***). As the cells migrate out of the colony by day 2, OCT4 was downregulated with persistent expression of BRACHYURY in the migrating cells. Further, the hESCs treated with CHIR99021 displayed nuclear accumulation of β-catenin as the cells differentiated; while the β-catenin was localized to the cell periphery in hESCs and no-GSKi control cells (***Figure 34***).

We further analyzed the expression of ectoderm, mesoderm and endoderm related transcripts. In the absence of GSKi, upregulation of neuroectodermal genes (*PAX6* and *SOX1)* around 3rd day of differentiation indicates the probable neuroectodermal induction (***Figure 32***). On the other hand, under the influence of GSKi, the expression levels of these neuroectodermal genes remained downregulated throughout the time-course of differentiation, suggesting a non-ectodermal differentiation (***Figure 32***). With prolonged treatment of hESCs with GSKi, only genes indicative of paraxial mesoderm (*PDGFRα, PDGFRβ*) and endoderm (*CXCR4)* were upregulated, while that of lateral plate mesoderm (*VEGFR2*) was downregulated (***Figure 32***). These findings suggest that prolonged GSKi treatment possibly favors differentiation towards paraxial mesoderm and endoderm fate.

Collectively, these findings suggest that treatment of hESCs with GSKi is unable to maintain pluripotency, and instead triggers differentiation towards a non-ectodermal lineage. Further, short-term treatment (24 hours) of hESCs with GSKi results in emergence of PS-like cells.

4.4.2. hESC-derived PS-like cells have potential to commit towards mesoderm and endoderm

Cells of the PS have the ability to commit to mesoderm and endodermal progenies depending on the balance between bFGF, Activin and BMP4 signaling (Huber et al., 1998; Pick et al., 2007; Tan et al., 2013a). We next sought to ascertain the bipotential differentiation capacity of PS towards mesoderm and endoderm. During embryonic development, FGF signaling is involved in specification, migration and patterning of mesoderm (Ciruna and Rossant, 2001). Hence, commitment of mesodermal lineage was investigated after exposure to bFGF. After 24-hour treatment of hESCs with CHIR99021, mesodermal induction was carried out using bFGF (50ng/ml) with or without FGF receptor inhibitor (PD173074; 0.1μM) as illustrated in ***Figure 35***. During early stages of induction towards mesoderm, mesodermal subsets could be identified by expression of VEGFR2 and PDGFR receptors.(Tan et al., 2013a; Yamashita et al., 2000; Zhang et al., 2008c). Real-time PCR analysis revealed that induction of GSKi treated-hESCs with bFGF resulted in modest upregulation of *VEGFR2*, *PDGFRα* and

PDGFRβ transcripts accompanied by steady downregulation of PS (*BRACHYURY*, *MIXL1*) and endoderm-related transcripts (*FOXA2*, *GSC*, *CXCR4*) (***Figure 35***). On the other hand, absence of bFGF or presence of FGF inhibitor resulted in marked downregulation of PS, endoderm, lateral plate mesoderm and EMT-related transcripts; and upregulation paraxial mesoderm-related transcripts (*PDGFRα, PDGFRβ*). These findings indicate the commitment of hESC-derived PS-like cells towards mesoderm subtypes.

Activation of Nodal pathway using high concentrations of Activin A in mouse and human ESCs induces specification of PS towards endoderm fate (D'Amour et al., 2005; D'Amour et al., 2006; Kubo et al., 2004; Vallier et al., 2009). Hence, endodermal differentiation was induced using Activin A (50ng/ml) with or without Activin and TGF-β signaling inhibitor SB431542 (10μM) as illustrated in ***Figure 36***. Treatment of GSKi treated-hESCs with Activin A resulted in marked upregulation of endoderm genes (*FOXA2*, *GSC*, *CXCR4*) and downregulation of PS, EMT and mesoderm-related transcripts (***Figure 36***). To confirm the involvement of Activin/Nodal signaling in the commitment to endoderm fate, the GSKi treated-hESCs were treated with Activin A and SB431542 (a selective inhibitor of TGFβ type I activin receptor-like kinases). The upregulation of endodermal genes and the downregulation of mesodermal genes were abolished in the absence of Activin A and in the presence of SB431542 (***Figure 36***).

Collectively, these observations demonstrate the potential of hESCs differentiated to PS under the influence of GSK-3 inhibition (for 24 hours) to commit towards mesoderm or endoderm depending on the culture milieu provided.

4.4.3. Synergistic differentiation to endothelial progenitor cells using BMP and VEGF signaling

Inhibition of GSK-3 followed by bFGF exposure drives the hESCs towards lateral plate mesoderm as evidenced by the upregulation of *VEGFR2* and downregulation of PS and endoderm-related genes (***Figure 35***). We next sought to investigate the potential of these lateral plate mesoderm cells to commit towards endothelial lineage. Earlier studies have reported the ability of BMP4 and VEGF in the induction of hESCs to endothelial and smooth muscle lineages (Bai et al., 2010; Ferreira et al., 2007; Hill et al., 2010; Levenberg et al., 2010; Tan et al., 2013a). The kinetics of differentiation towards endothelial lineage was monitored using *VEGFR2* (an early marker for lateral plate mesoderm-derived progenitors), *CD34* (early marker for progenitors with potential to differentiate towards endothelial lineage), and *CD31* (pan-endothelial lineage marker). Differentiation was performed in a step-wise approach wherein the hESCs exposed to CHIR99021 and bFGF for 24 hours each, were exposed to BMP4 (25ng/ml) and/ or VEGF (50ng/ml) as illustrated in ***Figure 37***. Real-time

PCR analysis (***Figure 37***) revealed BMP4 (Gi.F.B) supplementation resulted in modest upregulation of *VEGFR2* and a marked upregulation of *PDGFRβ*, but had minimal effect on the expression levels of *CD34* and *CD31*. On the contrary, treatment with VEGF (Gi.F.V) resulted in modest increase in the transcript levels of *CD34*, *CD31*, *VEGFR2 and PDGFRβ*. While combined modulation with BMP4 and VEGF (Gi.F.BV) resulted in marked upregulation of all the three markers related to lateral plate mesoderm and endothelial lineage (*VEGFR2*, *CD34*, *CD31*) and downregulation of paraxial mesoderm-related transcript (*PDGFRβ*) (***Figure 36***).

In accordance with the real-time RT-PCR data, time-course flow cytometry analysis (***Figure 38, 39***) revealed the gradual emergence of $VEGFR2^+$ population with BMP4 supplementation (G.F.B), but only a small subset of this population co-express CD34. While addition of VEGF (G.F.V) results in gradual appearance of $CD34^+$ cells that co-express VEGFR2 and CD31 and account for ~54% of the differentiated cells by the 5^{th} day of differentiation. Combined treatment with BMP4 and VEGF (G.F.BV) resulted in a robust emergence of $VEGFR2^+CD34^+CD31^+$ cells which accounted for ~55% and 95% of the differentiated cells by 3^{rd} and 5^{th} day of differentiation respectively (***Figure 38, 39***).

Further, the emergence of $VEGFR2^+CD34^+$ population starting from 3^{rd} day of differentiation under the influence of BMP4 and/or VEGF demonstrate the emergence of lateral plate mesoderm. In all the three differentiation conditions, time-course flow cytometry plots also reveal the temporal emergence of $VEGFR2^+$ population that gradually attain CD34 and CD31 positivity (***Figure 38, 39***). These findings suggest the role of BMP4 in induction of lateral plate mesoderm progenitors ($VEGFR2^+$ cells) followed by initiation towards endothelial lineage by VEGF. Additionally, we verified the robustness of the protocol using H9-hESCs which also yielded ~90% of cells positive for VEGFR2, CD34 and CD31 (***Figure 40***). In conclusion, BMP4 synergizes the endothelial induction potential of VEGF resulting in a robust protocol that yields ~90-95% of endothelial progenitor cells co-expressing VEGFR2, CD34 and CD31.

4.5. Discussion

The *in-vitro* differentiation of hESCs in most cases recapitulates the sequential stages of development observed in embryological studies. In the developing embryo, the cells of the hematopoietic and cardio-vascular lineage arise from subpopulations of mesoderm in a defined temporal sequence. Hence, the development of successful human hESC-based therapies would require an understanding of the complex signaling pathways controlling the lineage commitment during embryonic development to establish robust, efficient, and reproducible differentiation protocols. Though various differentiation protocols have been

devised, most of these involve spontaneous and/or single-step approaches under undefined conditions, and/or require long-term culture resulting in low yields of the desired cell population (Descamps and Emanueli, 2012; Kane et al., 2011). We previously developed a directed differentiation of hESCs over Matrigel, to efficiently generate lateral plate and paraxial plate mesoderm derivatives through short term inhibition of GSK-3 (Tan et al., 2013a). In the present study we modified the differentiation microenvironment using human plasma fibronectin as substrate instead of Matrigel, and investigated the sequence, timing and combination of growth factors needed to efficiently drive the differentiation towards endothelial lineage. In the current approach, a step-wise modulation of Wnt-βcatenin, FGF, BMP and VEGF signaling pathways led to sequential and efficient induction of hESCs towards PS, lateral plate mesoderm and endothelial progenitors.

Mesoderm induction starts with formation of primitive streak (PS) from the epiblast which gives rise to the progenitors related to cells of the mesoderm and endoderm germ layers. In this part of the study, we demonstrate that short-term inhibition of GSK-3 efficiently drives the differentiation of hESCs towards a PS/mesendoderm-like state. Inhibition of GSK-3 leads to stabilization, accumulation and translocation of β-catenin to the nucleus. In the nucleus, the β-catenin binds to members of T-cell factors (TCF) family of transcription factors and activates the target genes (Kimelman, 2006; Sokol, 2011b). Among the different PS-related genes, *BRACHYURY* is reported as a direct target of Wnt-βcatenin pathway (Arnold et al., 2000; Yamaguchi et al., 1999). The concurrent upregulation of *BRACHYURY* and other PS-related genes (*MIXL1, FOXA2, GSC*) within 24 hours of GSKi and their subsequent downregulation is indicative of the transient and temporal emergence of PS observed during early embryogenesis. Furthermore, these short-term GSKi treated cells show evidence of commitment towards mesoderm upon induction with bFGF and towards endoderm in response to Activin A. The rapid induction of PS in response to GSKi is comparable to the *in-vivo* events described in the study by Kemler et al., (Kemler et al., 2004). In transgenic mouse models constitutive expression of stabilized β-catenin induces premature EMT of epiblasts to mesodermal progenitors (Kemler et al., 2004). Hence, we demonstrate that these hESC-derived PS/mesendoderm-like cells have the bipotent differentiation towards mesoderm or endoderm depending on the culture milieu.

The role of Wnt/β-catenin signaling in mouse and human ESCs has been controversial due to contradictory findings. Studies have reported the activation of Wnt/β-catenin signaling maintains pluripotency of both mouse and human ESCs (Hao et al., 2006; Miyabayashi et al., 2007; Ogawa et al., 2006; Sato et al., 2004; Singla et al., 2006; Takao et al., 2007; ten Berge et al., 2011; Wagner et al., 2010). On the other hand, activation using either Wnt3a or GSK-3

inhibitors induces differentiation of ESCs towards PS, mesoderm and endoderm (Bone et al., 2011b; Davidson et al., 2012; Nakanishi et al., 2009a; Tan et al., 2013a). These controversial observations may be due to differences in dose and duration of Wnt activation, differences in differentiation methods, and presence of serum or other factors like bFGF in the differentiation medium. In one of the studies, it has been observed that Wnt3a maintains pluripotency of hESCs wherein MEF-conditioned media was used as differentiation media (Dravid et al., 2005). It could be argued that the presence of anti-differentiation factors like bFGF in the conditioned media could aid in the pluripotency in-spite of Wnt signaling. In support of this argument are studies that demonstrate Wnt signaling aids pluripotency of hESCs under the influence of FGF signaling, while aids differentiation in the absence of FGF signaling (Cai et al., 2007; Ding et al., 2010b). However, this was contradicted by another study that uses mTeSR1 as differentiation media that is known to contain high concentrations of bFGF (Bone et al., 2011a). In this study, the authors demonstrate the differentiation towards endoderm upon inhibition of GSK-3. In the present study, we demonstrate activation of Wnt/β-catenin signaling using CHIR99021 in feeder-free, chemically-defined conditions without the addition/ presence of additional growth factors/ cytokines drives the differentiation of hESCs towards PS.

Previous studies (Bai et al., 2010; Ferreira et al., 2007; Hill et al., 2010; Park et al., 2010; Tan et al., 2013a) have demonstrated that hESC-derived $CD34^+CD31^+$ cells could serve as endothelial progenitors. Under serum-free conditions, bFGF, BMP4 and VEGF have been reported to facilitate the differentiation of hESCs towards endothelial lineage (Bai et al., 2010). Similar to the findings of Bai et al., (Bai et al., 2010) we found that BMP4 alone is not sufficient to induce hESCs towards $CD34^+CD31^+$ cells, while VEGF alone or in combination with BMP4 causes a significant increase in the commitment to endothelial lineage. However, Bai et al., (Bai et al., 2010) could achieve only ~13% of hESCs induced to $CD34^+CD31^+$ cells, while we could achieve around 90-95% of the cells being positive for CD34 and CD31. This could be due to efficient induction of hESCs towards PS and mesoderm before stimulation with BMP4 and VEGF. Currently available protocols to differentiate hESC and hiPSCs towards endothelial lineage generally requires 10-15 days of differentiation to achieve a modest 2-40% of cells committed to endothelial lineage (Kane et al., 2011). In contrast, our findings suggest a robust commitment (90-95%) towards endothelial lineage within a differentiation span of 5 days compared to those previously reported (Bai et al., 2010; Ferreira et al., 2007; Hill et al., 2010; James et al., 2010; Levenberg et al., 2010; Park et al., 2010). The shortening of the differentiation period could be due to various reasons which include the following:

1. Monolayer differentiation of hESCs instead of EB/co-culture methods. In EB method of differentiation, the addition of growth factors would result in a gradient effect within the differentiating EBs which in turn could have dose-dependent effect and reduce the differentiation efficiency or reduce the abi;lity to tune/ precisely control the differentiation.
2. hESCs were differentiated immediately (24 hours) after seeding, instead of waiting of the hESC colonies to grow larger. When the hESC colonies are small, they are more uniformly spread and remain almost as a monolayer of cells. In this state, the addition of growth factors/ small molecules could theoretically result in equal induction of all the cells.
3. The differentiation of hESCs was carried out based on a developmental biology approach wherein the differentiation through various developmental stages like PS, mesoderm (lateral plate/ paraxial), endoderm and endothelial lineages were closely monitored.
4. Differentiation of hESCs under chemically defined conditions could be a reason which allows for fine tuning of the differentiation microenvironment.

In conclusion, we dissected the early signaling pathways leading to a novel, step-wise differentiation approach to efficiently drive the commitment of hESCs towards endothelial lineage. The ability to generate endothelial progenitors efficiently may provide opportunities to study endothelial commitment using hESCs as an *in-vitro* model. Additionally, efficient generation of endothelial progenitors under defined conditions could pave way towards scalable production of clinically competent ECs.

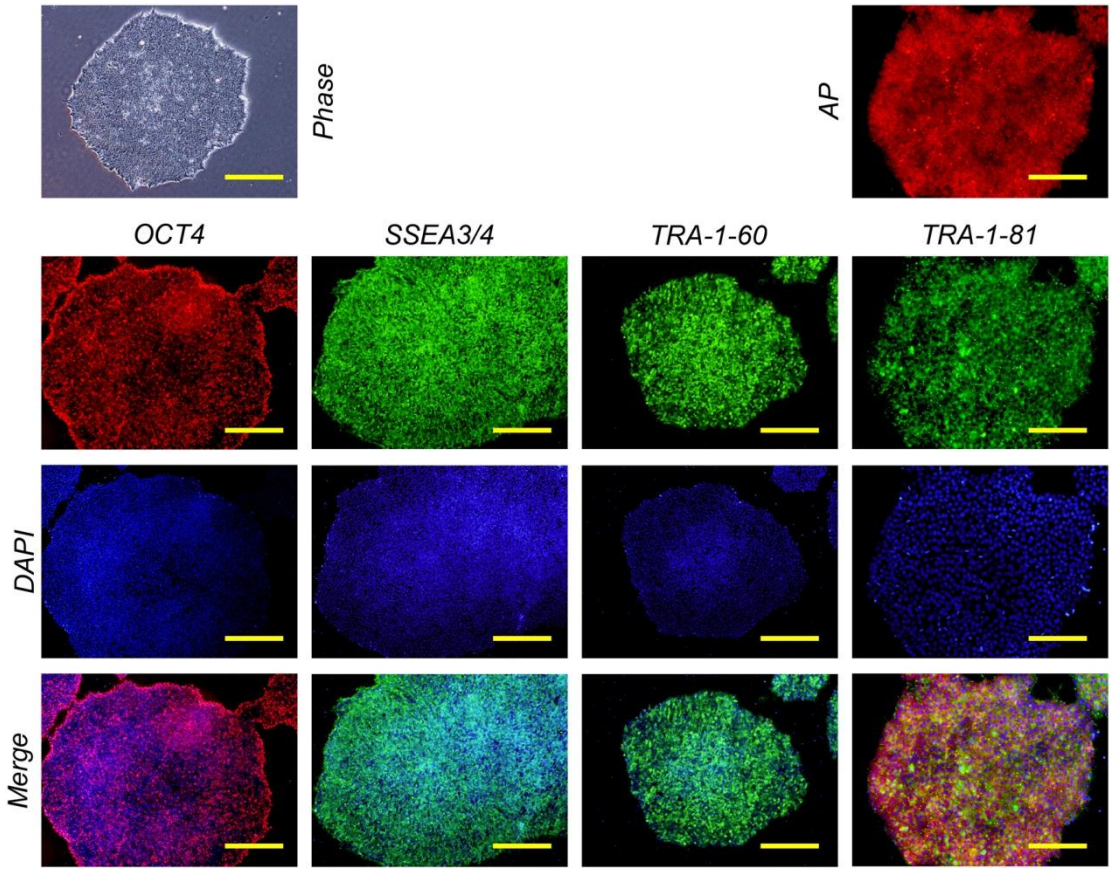

Figure 30. Analysis of pluripotency status of hESCs cultured over Matrigel.

Top left photomicrograph shows the compact, well defined morphology of hESC colony upon culture over Matrigel and mTeSR1. Immunofluorescence micrographs show the expression of pluripotency markers OCT4, SSEA4, TRA-1-60, TRA-1-81 and alkaline phosphatase (AP). Scale bars: 500µm.

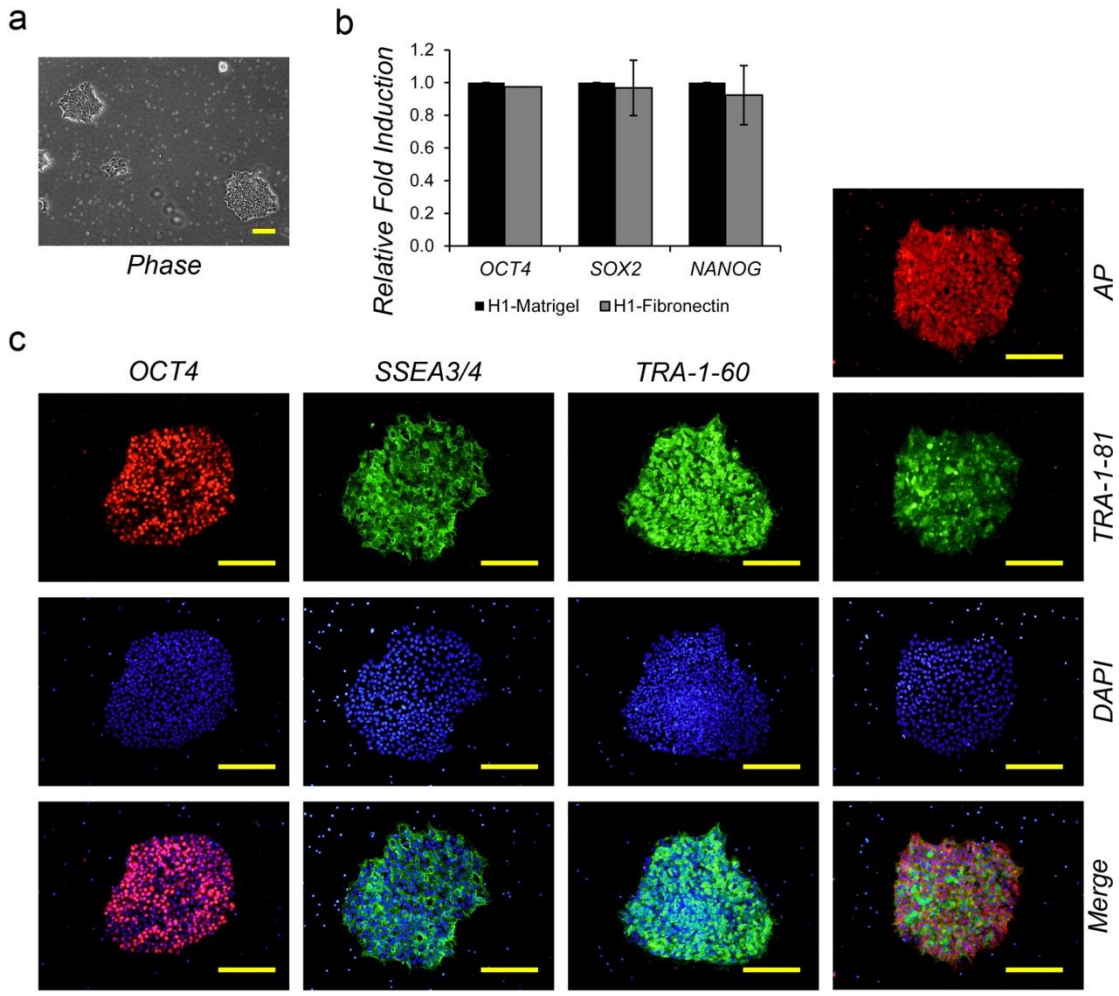

Figure 31. Analysis of pluripotency status of hESCs cultured over fibronectin.

(a) Photomicrograph shows the compact, well defined morphology of hESC colony upon culture over fibronectin and mTeSR1 for 24 hours. **(b)** Real time RT-PCR comparison of expression of pluripotency genes (*OCT4*, *SOX2*, *NANOG*) by the hESCs cultured over Matrigel and fibronectin. The plots show no significant difference in the gene expression between the cells grown on Matrigel and fibronectin. For gene expression plots, the levels of expression were normalized to corresponding *β-ACTIN* values and are shown as relative to that of undifferentiated hESCs cultured over Matrigel. **(c)** Immunofluorescence micrographs show the expression of pluripotency markers OCT4, SSEA4, TRA-1-60, TRA-1-81 and alkaline phosphatase (AP). Scale bars: 200µm.

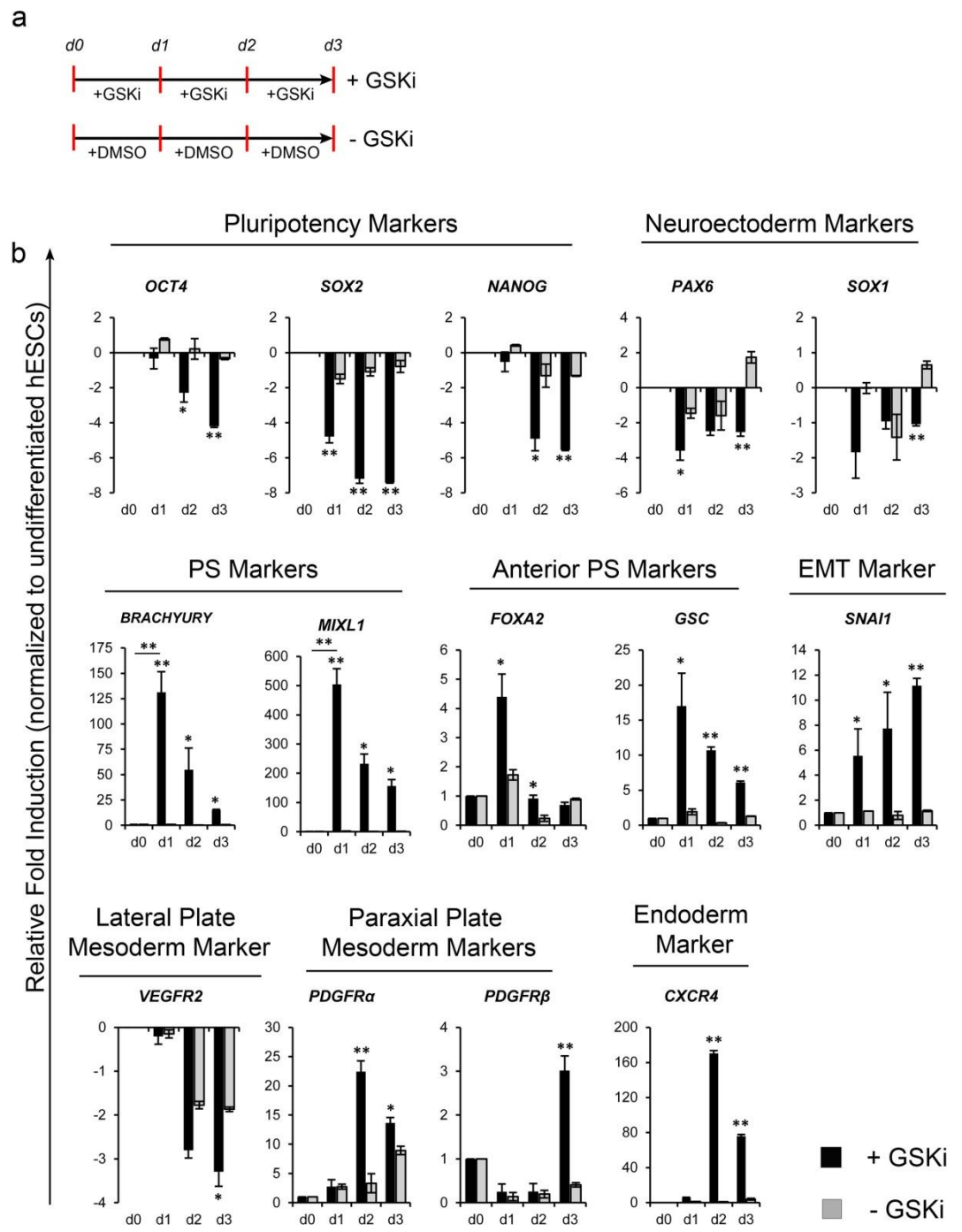

Figure 32. Time course analysis of expression of genes associated with pluripotency and early differentiation of hESCs in response to inhibition of GSK-3.

(a) Schematic representation of differentiation of hESCs with or without the inhibition of GSK-3 using CHIR99021 (±GSKi). **(b)** Real time RT-PCR analysis of gene expression kinetics of markers associated with pluripotency and neuroectoderm, primitive streak (PS/ mesendoderm), epithelial-mesenchymal transition (EMT), anterior PS/ endoderm, and mesodermal subsets after differentiation of hESCs with (■) or without (■) GSKi. For all gene expression plots, the levels of expression were normalized to corresponding *β-ACTIN* values and are shown as relative to that of undifferentiated hESCs. The expression levels of *OCT4*, *SOX2*, *NANOG*, *PAX6*, *SOX1* and *VEGFR2* were log-normalized to reveal the amount of downregulation in relation to undifferentiated hESCs. Error bars: s.d. (n≥2). *p<0.05. **p<0.01. p values represent the levels of significance in relation to differentiation without GSKi.

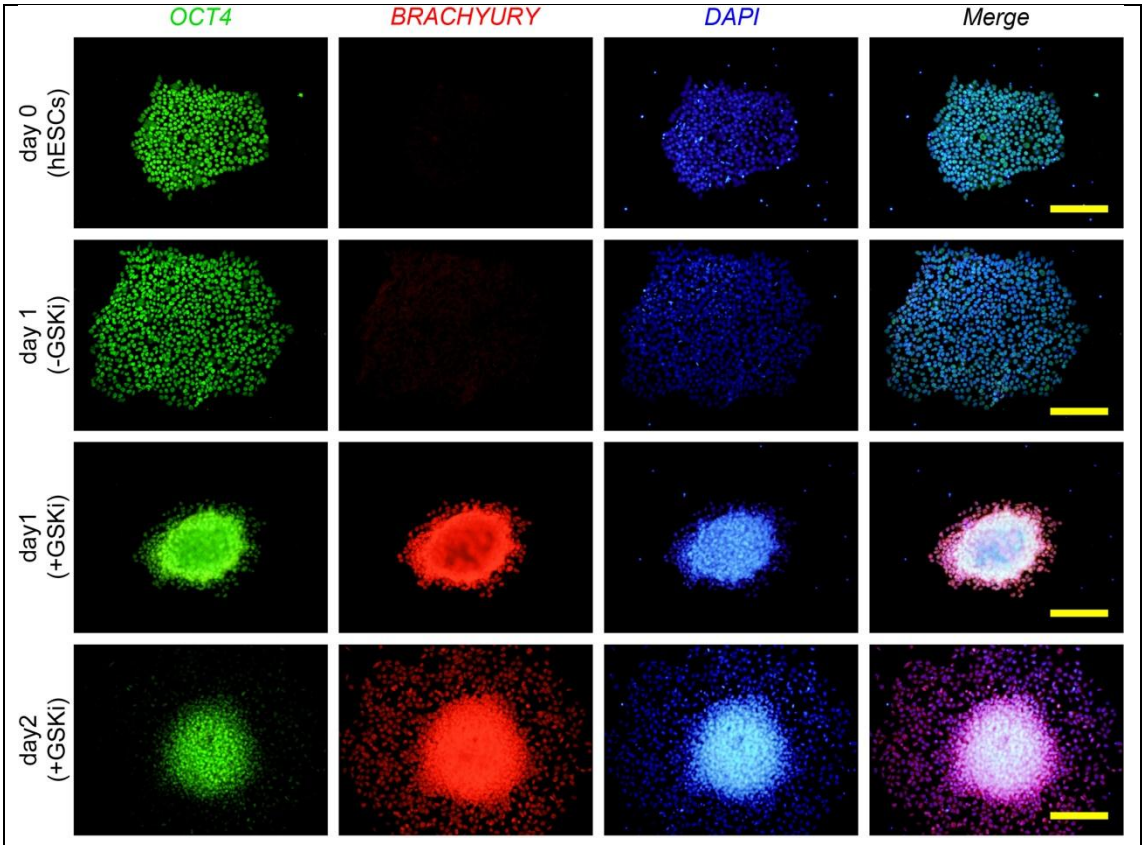

Figure 33. Immunocytochemical analysis of expression of BRACHYURY and OCT4 in response to inhibition of GSK-3.

Immunofluorescence micrographs display the expression of OCT4 and BRACHYURY after differentiation with or without GSKi. (green-OCT4; red-BRACHYURY; blue-nuclear stain DAPI). Scale bars: 200µm.

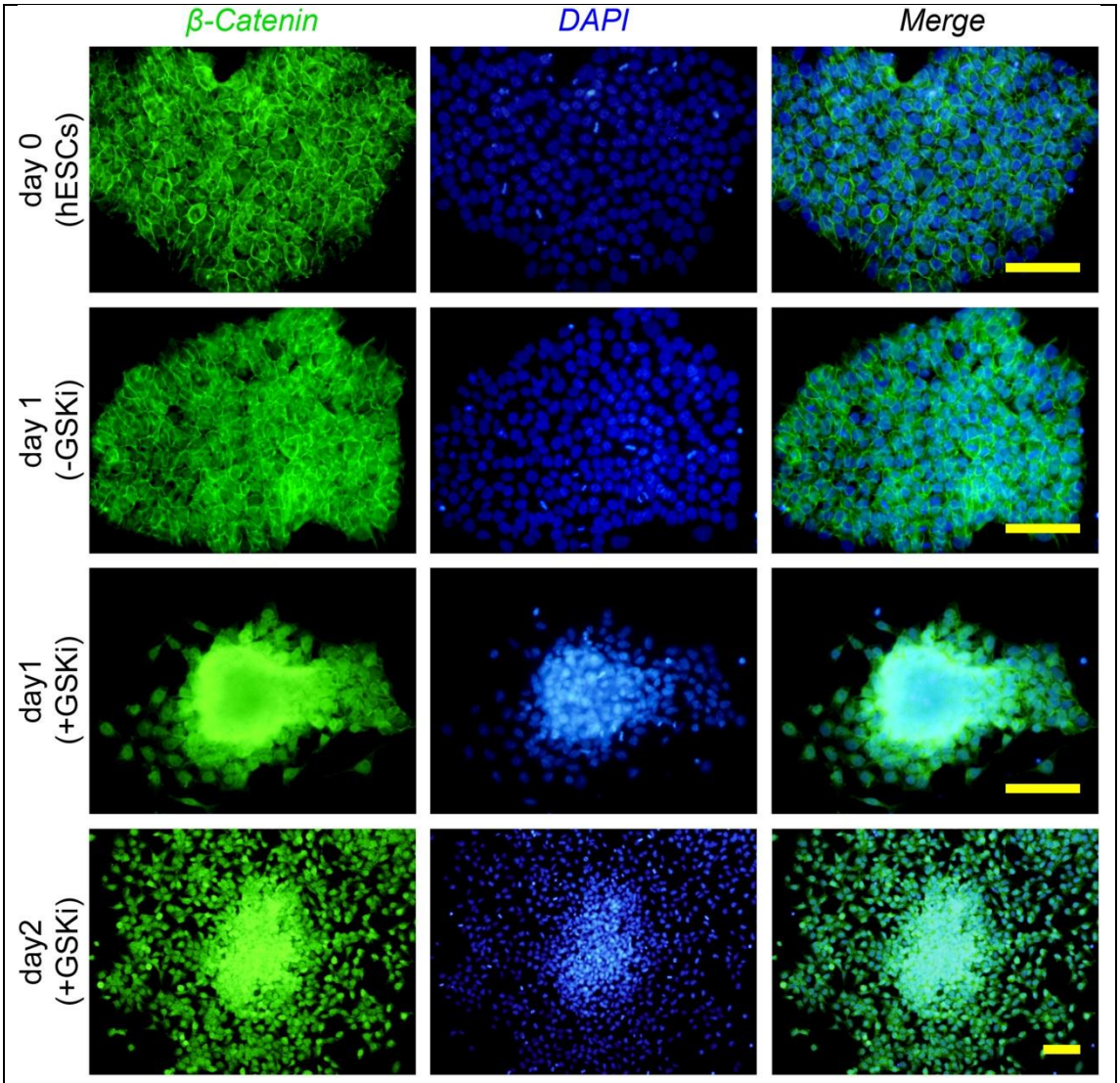

Figure 34. Immunocytochemical analysis of expression of β-Catenin in response to inhibition of GSK-3.

Immunofluorescence micrographs display the expression of OCT4 and BRACHYURY after differentiation with or without GSKi. (green-OCT4; red-BRACHYURY; blue-nuclear stain DAPI). Scale bars: 100μm.

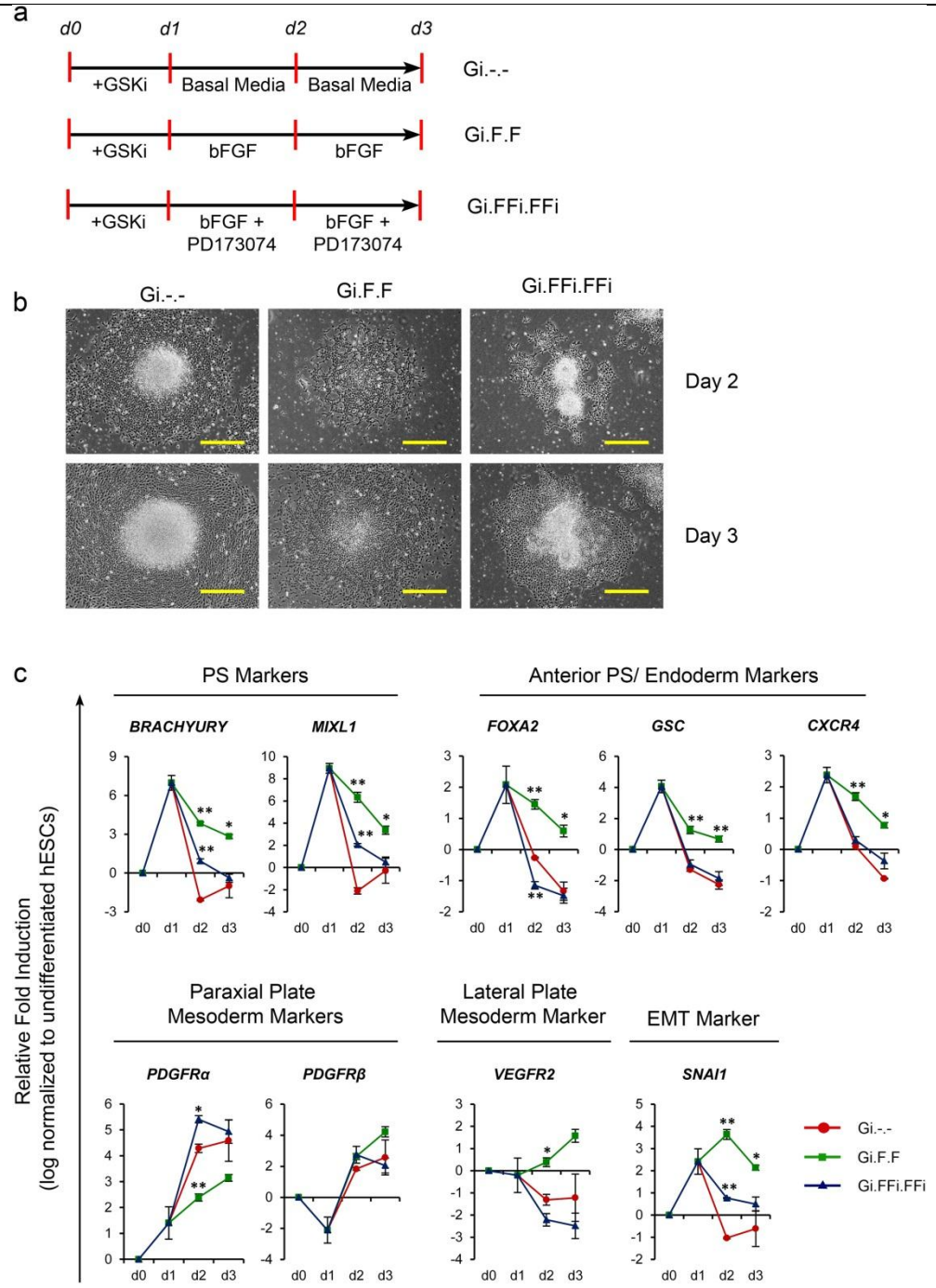

Figure 35. Time course analysis of early differentiation of hESCs towards mesoderm lineage.

(a) Schematic representation of differentiation of hESCs towards mesoderm using bFGF (Gi.F.F) after 24 hours of treatment with CHIR99021 (+GSKi). Condition without bFGF (Gi.-.-) and the one with bFGF+FGF receptor inhibitor PD173074 (Gi.FFi.FFi) were used as controls. **(b)** Representative photomicrographs display the change in the morphology of the hESC colonies under different differentiation conditions after 2 and 3 days of differentiation. The cells can be seen spreading and migrating away from the center of the colony similar to early migratory events observed in early embryonic development. **(c)** mRNA expression kinetics of markers associated with PS, anterior PS/ endoderm, mesodermal subsets and EMT after differentiation of hESCs under the three different conditions. For all gene expression plots, levels of expression were log normalized to corresponding *β-ACTIN* values and are shown as relative to that of undifferentiated hESCs. Scale bars: 500µm. Error bars: s.d. (n≥2). *p<0.05. **p<0.01. p values represent the levels of significance in relation to (Gi.-.-).

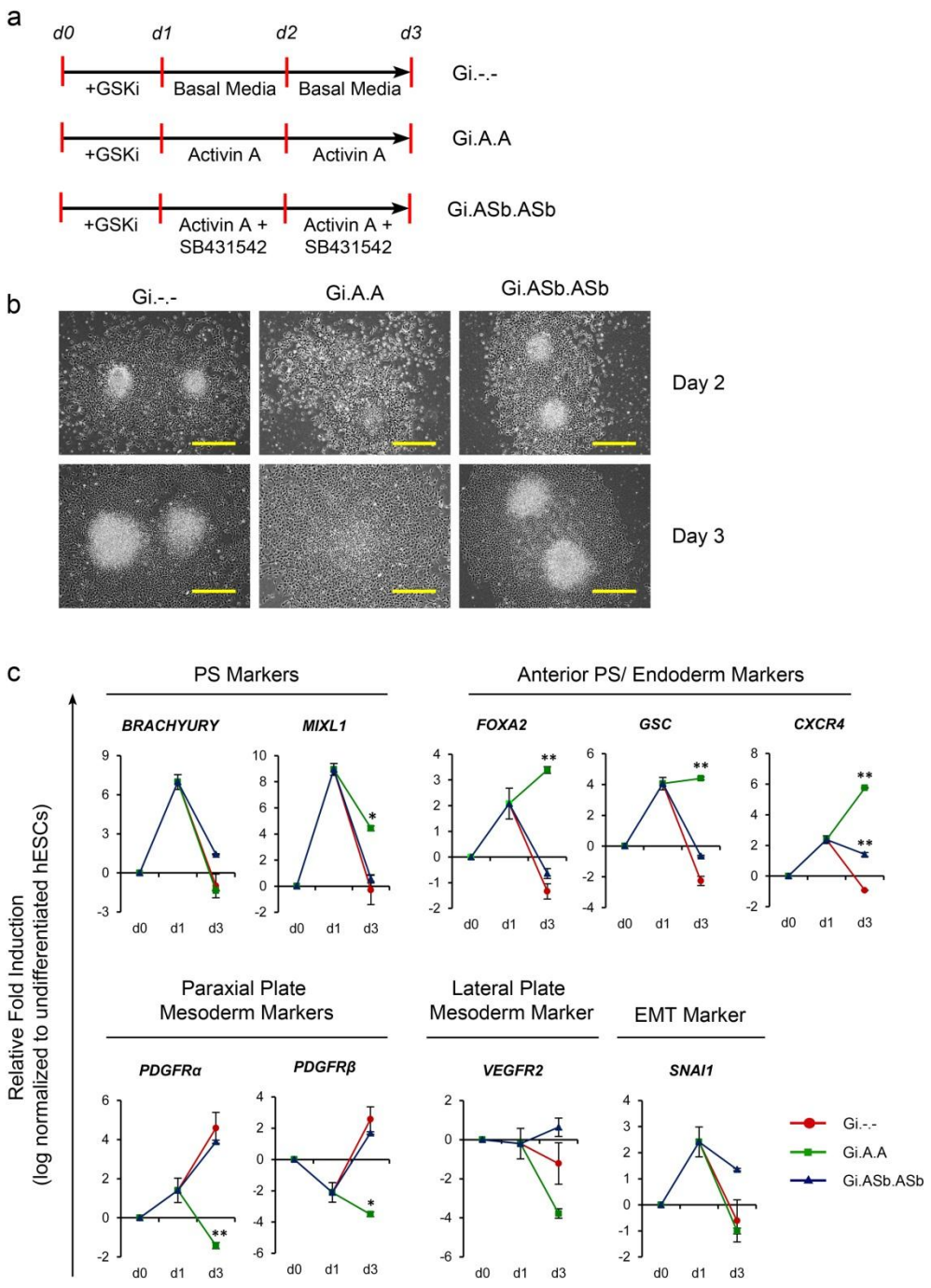

Figure 36. Time course analysis of early differentiation of hESCs towards endoderm lineage.

(a) Schematic representation of differentiation of hESCs towards endoderm using Activin A (Gi.A.A) after 24 hours of treatment with CHIR99021 (+GSKi). Condition without Activin A (Gi.-.-) and the one with Activin+TGFβ inhibitor SB431542 (Gi.ASb.ASb) were used as controls. **(b)** Representative photomicrographs display the change in the morphology of the hESC colonies under different differentiation conditions after 2 and 3 days of differentiation. The cells can be seen spreading and migrating away from the center of the colony similar to early migratory events observed in early embryonic development. **(c)** mRNA expression kinetics of markers associated with PS, anterior PS/ endoderm, mesodermal subsets and EMT after differentiation of hESCs under the three different conditions. For all gene expression plots, the levels of expression were log normalized to corresponding *β-ACTIN* values and are shown as relative to that of undifferentiated hESCs. Scale bars: 500µm. Error bars: s.d. (n≥2). *p<0.05. **p<0.01. p values represent the levels of significance in relation to (Gi.-.-).

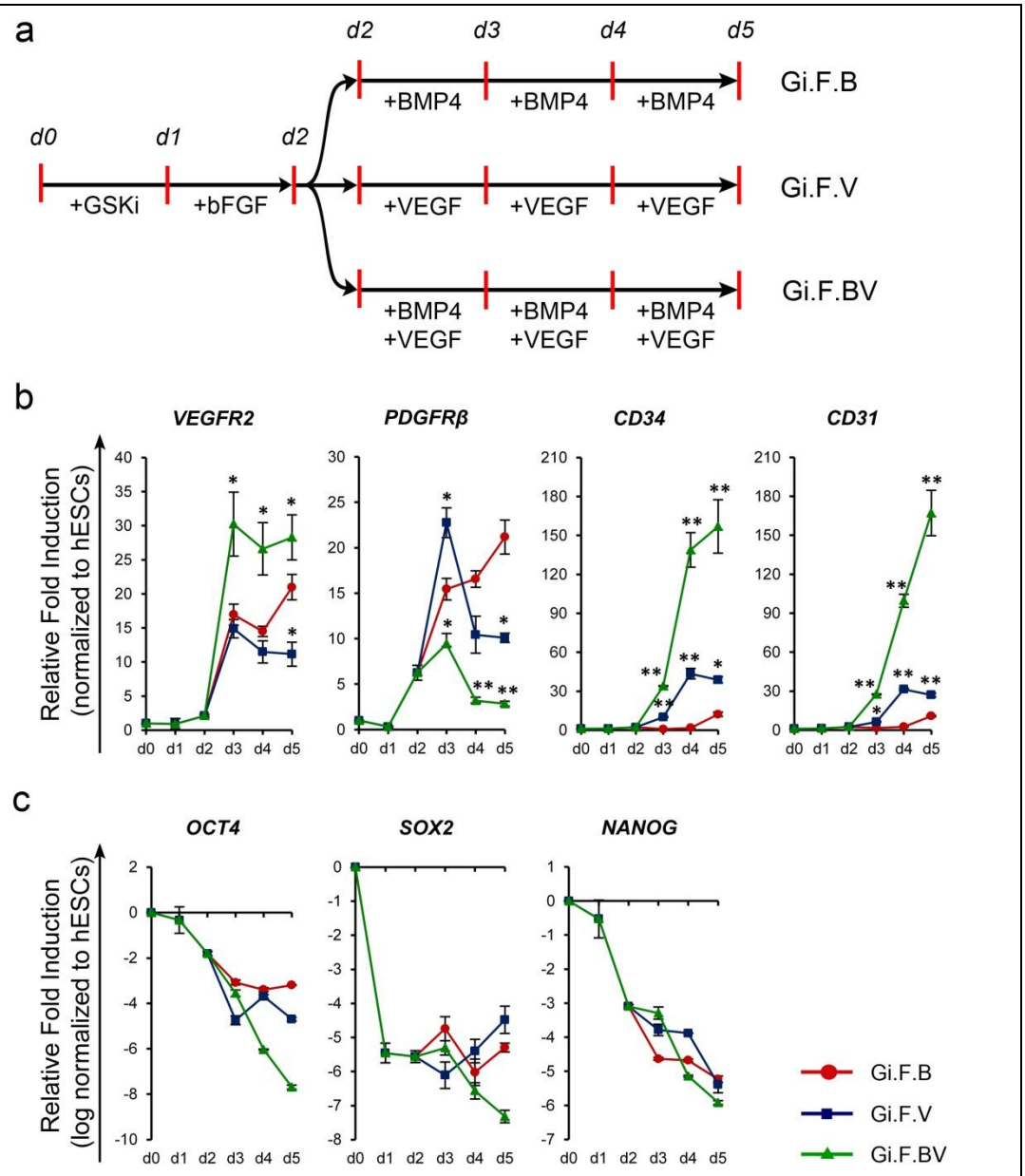

Figure 37. Time course analysis of differentiation of hESCs towards endothelial lineage.

(a) Schematic representation of differentiation of H1-hESCs towards endothelial progenitors by sequential treatment with CHIR99021 (+GSKi) and bFGF for 24 hours each followed by exposure to BMP4 and/or VEGF. **(b)** Kinetics of expression of *VEGFR2* (an early marker for lateral plate mesoderm-derived progenitors), *CD34* (early marker for progenitors with potential to differentiate towards endothelial lineage), and *CD31* (pan-endothelial lineage marker) upon induction with BMP4 (Gi.F.B), VEGF (Gi.F.V) and BMP4 + VEGF (Gi.F.BV) over a differentiation period of 5 days. **(c)** Time course expression kinetics of pluripotency genes (*OCT4*, *SOX2*, *NANOG*) over 5 days of differentiation among the three differentiation conditions. For gene expression plots in **(b)**, the levels of expression were normalized to corresponding *β-ACTIN* values and are shown as relative to that of undifferentiated hESCs; while for those in **(c)** the expression levels were log-normalized to reveal the amount of downregulation in relation to undifferentiated hESCs. Error bars: s.d. ($n \geq 2$). *$p<0.05$. **$p<0.01$. p values represent the levels of significance in relation to (Gi.F.B) in **(b)** and **(c)**.

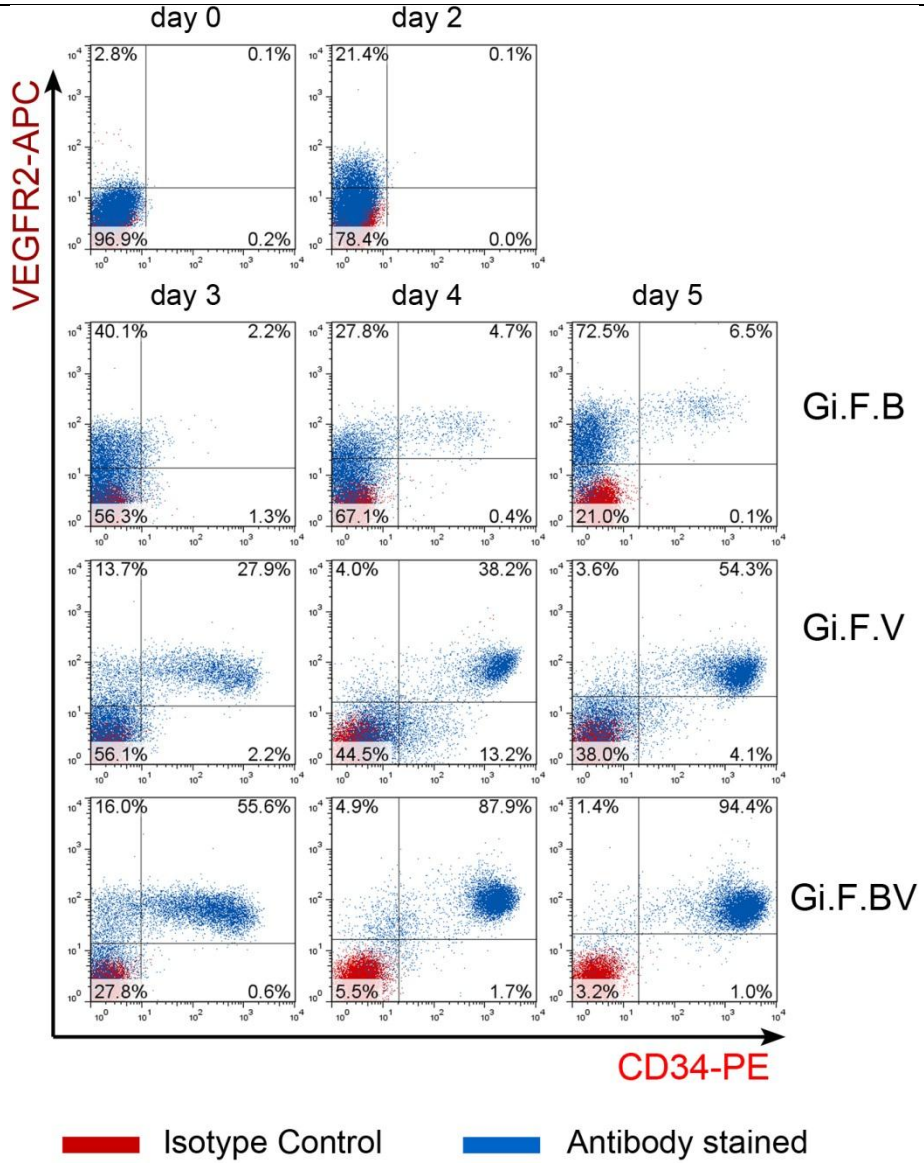

Figure 38. Flow cytometry analysis CD34 and VEGFR2 expression upon differentiation of hESCs towards endothelial lineage.

Representative flow cytometry overlays display the kinetics of co-expression of VEGFR2 and CD34 over 5 day period of differentiation of H1-hESCs, in the presence of BMP4 and/or VEGF after initial treatment with GSKi and bFGF for 24 hours each.

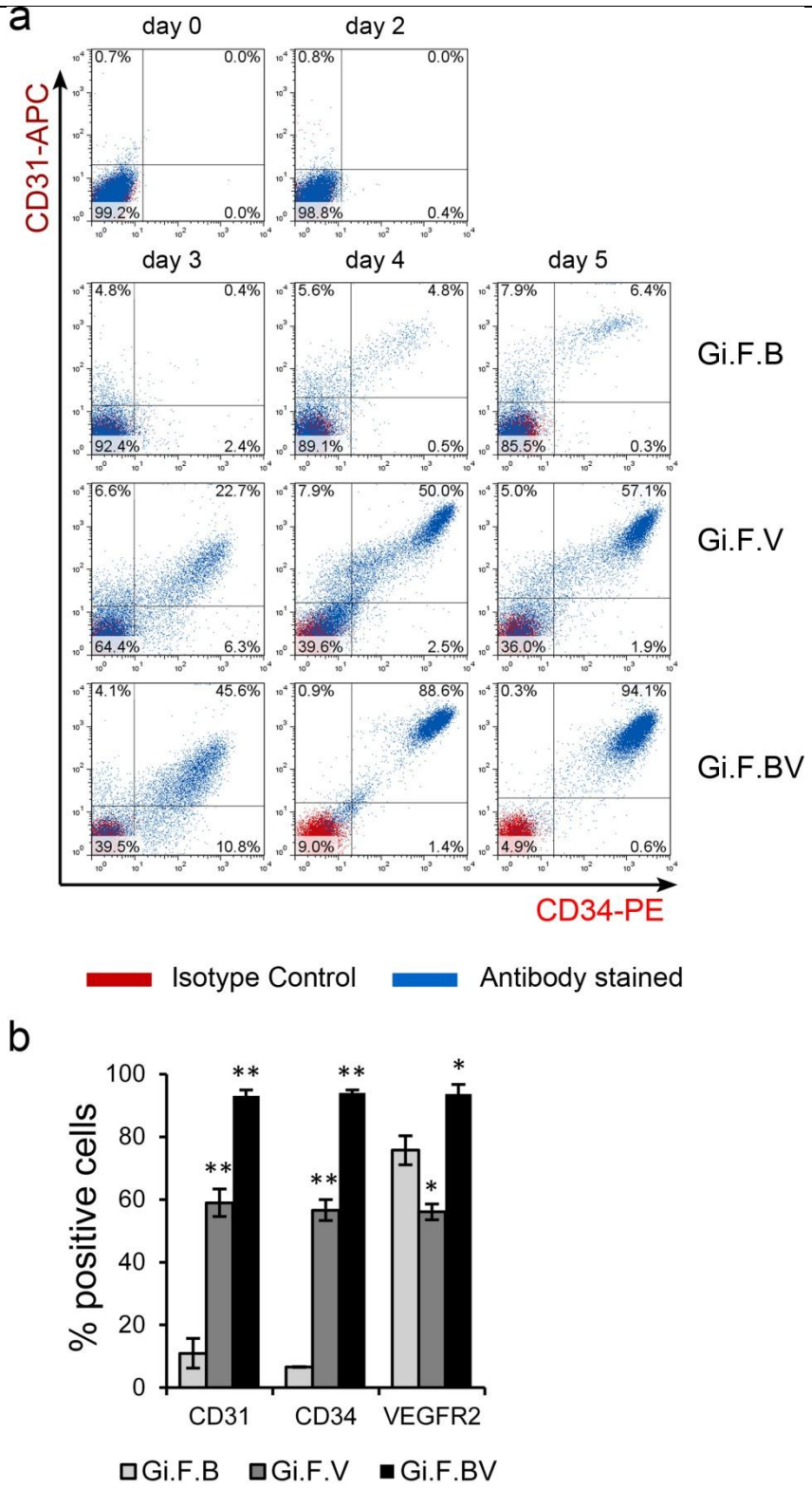

Figure 39. Flow cytometry analysis CD34 and CD31 expression upon differentiation of hESCs towards endothelial lineage.

(a) Representative flow cytometry overlays display the kinetics of co-expression of CD34 and CD31 over 5 day period of differentiation of H1-hESCs, in the presence of BMP4 and/or VEGF after initial treatment with GSKi and bFGF for 24 hours each. **(b)** Graphical representation comparing the percentage of $CD31^+$, $CD34^+$, and $VEGFR2^+$ cells after 5 days of differentiation in the presence of BMP4 and/or VEGF. Error bars: s.d. of 2 independent experiments. Error bars: s.d. (n=3). *p<0.05. **p<0.01. p values represent the levels of significance in relation to (Gi.F.B).

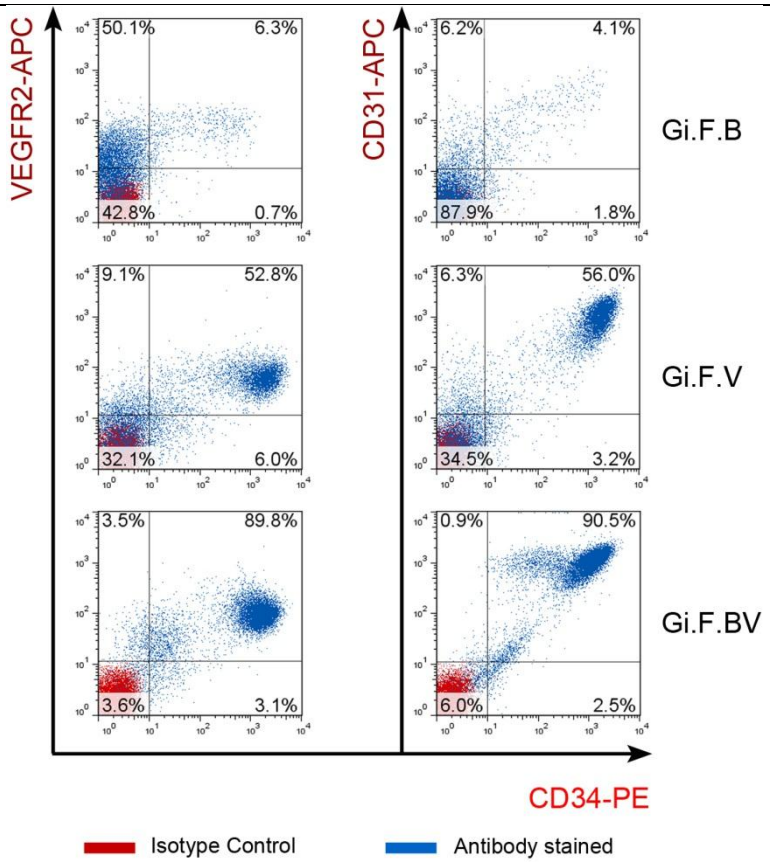

Figure 40. Flow cytometry validation of differentiation of H9-hESCs towards endothelial lineage.

Representative flow cytometry overlays display the co-expression of VEGFR2 and CD34, CD31 and CD34 after 5 days of differentiation of H9-hESCs, in the presence of BMP4 and/or VEGF, after initial treatment with GSKi and bFGF for 24 hours each.

Chapter 5

Differentiation of hESC-derived endothelial progenitors to arterial and venous endothelial cells

5. Differentiation of hESC-derived endothelial progenitors to arterial and venous endothelial cells

5.1. Introduction

Endothelial cells (ECs) are a unique population of cells that share many common morphological and functional features, and yet present significant heterogeneity in different vessels and organs. The vascular system in a broad sense consists of a complex network of arteries and veins. These arteries and veins share certain features and have several morphological, molecular and functional differences (Aird, 2007b; Dyer and Patterson, 2010; Kume, 2010; Swift and Weinstein, 2009; Torres-Vazquez et al., 2003). Although, arterial and venous ECs share certain common molecular signatures like the expression of pan-endothelial markers (CD31, VE-Cad, and vWF), they do possess certain distinct molecular profiles (Torres-Vazquez et al., 2003). Such molecular distinction seems to occur quite early in the development even before the onset of blood flow; while other factors like hemodynamic stress, oxygen tension and interplay of various signaling cues such as VEGF, Notch, and COUP-TFII also play a significant role (Aird, 2007b; Kume, 2010; Swift and Weinstein, 2009; Torres-Vazquez et al., 2003).

Arterial ECs are characterized by expression of high levels of Ephrin-B2, DLL4, Hey-1, Hey-2, NRP1, NOTCH-1, NOTCH-4, CXCR4, JAG-1 and JAG-2; while the venous ECs express EphB4, Lefty-1, Lefty-2, NRP2 and COUP-TFII (Aird, 2007b; Kume, 2010; Swift and Weinstein, 2009; Torres-Vazquez et al., 2003). Previous studies have reported differentiation of hPSCs towards mature and functional ECs (Ferreira et al., 2007; Hill et al., 2010; James et al., 2010; Kane et al., 2010; Kaupisch et al., 2012; Levenberg et al., 2010; Li et al., 2009; Margariti et al., 2012; Rufaihah et al., 2011; Tan et al., 2013a; White et al., 2013), but very limited data is available on how these stem cells could be coaxed into arterial or venous ECs. Recent studies have observed the heterogenous expression of arterial and venous markers within the pool of PSC-derived ECs (Hatano et al., 2013; Margariti et al., 2012; Samuel et al., 2013). Limited reports using mouse ESCs (Lanner et al., 2007; Yurugi-Kobayashi et al., 2006), mouse iPSCs (Narazaki et al., 2008) and human iPSCs (Rufaihah et al., 2013a) have shown the specification towards arterial or venous fate by modulation of VEGF, Notch and/or cyclic adenosine monophosphate (cAMP) pathways.

5.2. Objective

To efficiently differentiate hESC-derived endothelial progenitors to arterial and venous ECs under feeder- and serum-free conditions.

5.3. Materials and Methods

5.3.1. Differentiation of endothelial progenitors ($CD34^+CD31^+$ cells) to endothelial subtypes in feeder-free, serum-free conditions

After 5 days of differentiation in STEMdiff™ APEL™, $CD34^+CD31^+$ cells were isolated by flow cytometry assisted sorting (FACS), and plated onto 2µg/cm^2 human plasma fibronectin coated plates (12,000 cells per cm^2) and cultured in endothelial serum-free medium (ESFM, Invitrogen) with medium changes every 2-3 days (***Figure 41***). For differentiation towards venous endothelial cells, the medium was supplemented with 10ng/ml EGF (R&D Systems), 20ng/ml bFGF (R&D Systems) (***Figure 41***). While, arterial differentiation was induced using 10ng/ml EGF, 20ng/ml bFGF, and 10ng/ml VEGF (GIBCO) (***Figure 41***). The resulting endothelial cells were passaged using accutase (Invitrogen) when 70-80% confluent and characterized after 3 to 5 passages.

5.1.1. RNA extraction and real-time PCR

Total cellular RNA was isolated, reverse transcribed and quantitated using real-time PCR as described previously under Section 4.3.3.

5.1.2. Flow cytomerty analysis and sorting

Flow cytometry analysis of differentiated cells for cell surface antigens (CD34, CD31, VE-Cad, NRP1, DLL4, CXCR4, NRP2, EphB4) were performed and analyzed as previously described under Section 4.3.4.

5.1.3. Immunocytochemistry

Immunocytochemical staining of differentiated cells for appropriate primary antibodies (CD31, VE-Cad, vWF) were performed and documented as previously described under Section 4.3.5.

5.1.4. Acetylated-low density lipoprotein uptake assay

To demonstrate the ability of ECs to phagocytize low-density lipoprotein (LDL), hESC-derived arterial and venous ECs, were incubated with 10µg/ml of Dil-acetylated-LDL (Dil-Ac-LDL; Molecular Probes) for 4h. The cells were washed with PBS and the nuclei

counterstained with Hoescht 33258 (Sigma) and observed using fluorescence microscope (Olympus IX70).

5.1.5. Matrigel tube formation assay

Ability of the ECs to form vascular tube-like structures over Matrigel™ was analyzed as previously described (Tan et al., 2013a). Briefly, $7.5x10^3$ ECs were seeded onto each well of ibidi µ-angiogenesis slides that is coated with 10µl of Matrigel. After incubation for 18h, the vascular tube-like structures were labeled with 1µM Calcein-AM (Sigma) as per manufacturer's instructions and visualized using fluorescence microscope (Olympus IX70).

5.1.6. Annexin V-Propidium Iodide (PI) apoptosis assay

Analysis of live cells and apoptotic cells were performed using Alexa Fluor® 488 Annexin V/Dead Cell Apoptosis Kit (Molecular Probes). Briefly, after 24 hour exposure to varying concentrations of VEGF, the cells in the culture supernatant and culture plate were collected, washed and resuspended in 1x annexin-binding buffer. Then, the cells were incubated with Alexa Fluor® 488 annexin V and PI for 15 minutes at room temperature as per manufacturer's instructions. After the incubation period, the cells were analyzed immediately using Dako Cytomation CyAn ADP and FlowJo v7.6.5.

5.1.7. Wound closure assay

Monolayers of H1-hESC derived arterial and venous ECs were scraped with a 200µl pipette tip to create a "wound" as described previously (Liang et al., 2007). Following the creation of the wound, the cells were washed with PBS to remove debris and floating cells. The cells were incubated for a period of 24 hours at 37^0C in endothelial serum-free media supplemented with EGF (10ng/ml) and bFGF (20ng/ml). The Art-ECs were not supplemented with VEGF to eliminate the bias that could be created otherwise. Photomicrographs of the same field were acquired every 3 hours starting from 0 hours to 24 hours. The closure of the wound by migration of the cells was analyzed using TScratch program (Geback et al., 2009), available from www.cse-lab.ethz.ch/software.html. The results are tabulated as mean ± standard deviations of three independent experiments.

5.1.8. Human angiogenesis antibody array

Human Angiogenesis Proteome Profiler™ antibody array (R&D Systems) was used to survey the levels of 55 different angiocrines secreted by H1-hESC derived Art-ECs and Ven-ECs into culture supernatants. Arterial and venous ECs were seeded onto fibronectin coated plates at a seeding density of $1.2x10^4/cm^2$ in their respective media. After 24 hours, the media was changed to endothelial serum-free media without any additional supplements and incubated

for 24 hours. After the incubation the culture supernatants were collected and stored at -80^{0}C. Total protein concentration within cell-free culture supernatants were quantified using Micro BCA™ Protein Assay Kit (Thermoscientific) as per manufacturer's instructions. Cell culture supernatant containing 200µg of protein was used for the antibody array as per manufacturer's instructions. The membranes were developed using 10 minute exposure to X-ray film. The array data was quantified by densitometry analysis using Image J (NIH, USA). The various angiocrines in the protein blot are listed in ***Appendix IV***.

5.1.9. Statistical Analysis

All real time RT-PCR and angiogenesis antibody array experiments were performed in duplicates with duplicate readings each. Student's t-test was performed to determine significance using Microsoft Excel Data Analysis ToolPak. For angiogenesis antibody arrays, the density of each protein blot was quantified by a densitometry analysis using Image J software. The pixel densities corresponding to the negative control spots within each array was used as controls to normalize the density corresponding to each protein spot. These pixel density values were used as relative pixel density measurements to compare the expression levels of the proteins between different blots.

5.4. Results

To study the specification towards arterial and venous endothelial subtypes, H1-hESC line was used and the robustness of the protocol verified using H9-hESCs.

5.4.1. Differentiation of hESCs to endothelial progenitors

hESCs were differentiated to endothelial progenitors expressing VEGFR2, CD34 and CD31 using sequential modulation of Wnt/β-catenin, FGF, BMP and VEGF signaling pathways as described under ***Section 4.4.3***. Briefly, differentiation was performed in a step-wise approach wherein the hESCs exposed to CHIR99021 and bFGF for 24 hours each, were treated with BMP4 (25ng/ml) and VEGF (50ng/ml) as illustrated in ***Figure 41***. This sequential differentiation of H1- and H9-hESCs resulted in 90-95% of the cells co-expressing VEGFR2, CD34 and CD31 (***Figure 38-40***). These cells expressing CD34 and CD31 would be termed as endothelial progenitors.

5.4.2. Terminal differentiation of $CD34^+CD31^+$ endothelial progenitors to arterial and venous endothelial cells under serum-free conditions

Under serum-containing conditions, high concentrations (50ng/ml) of VEGF have been reported to aid arterial differentiation, while lower concentrations (10ng/ml) aid venous commitment (Lanner et al., 2007; Rufaihah et al., 2013a; Yurugi-Kobayashi et al., 2006).

However, such dose-dependent role of VEGF under serum-free conditions is not reported so far. Differentiation of mouse ESCs and human iPSCs towards arterial and venous ECs have been reported. However, differentiation of arterial-venous specification of hESCs has not been reported so far. The $CD34^{+}CD31^{+}$ endothelial progenitors obtained after 5 days of differentiation were sorted using FACS and further differentiated towards endothelial subtypes in serum-free conditions, using commercially available endothelial serum-free medium (ESFM, GIBCO). Serum-containing endothelial medium typically requires the supplementation with bFGF, EGF and VEGF but the serum-free endothelial medium as per manufacturer's instructions, requires supplementation with bFGF and EGF only. Hence we initially carried out the differentiation of the $CD34^{+}CD31^{+}$ cells in ESFM supplemented with bFGF (20ng/ml) and EGF (10ng/ml) for 3-6 passages (***Figure 41***). Differentiation under these conditions yielded 98-99% CD34, CD31 and VE-CAD positive ECs (***Figure 41***). Real-time PCR analysis demonstrated upregulation of all transcripts associated with endothelial lineage (*CD31*, *VE-CAD*, VEGFR-2, *CD34*, *vWF*, *GATA2*, *eNOS*, *TIE2*) (***Figure 42***). Additionally, immunocytochemistry revealed the characteristic membrane expression of CD31 and VE-CAD, and cytoplasmic expression of vWF (***Figure 43***). Further analysis into the arterial and venous phenotype markers showed almost 85-90% of the cells to be positive for venous markers (NRP2, COUP-TFII) while only ~7% of the cells expressed NRP1 and DLL4, and ~17% expressed CXCR4 (***Figure 41***). These observations suggest the commitment of $CD34^{+}CD31^{+}$ cells towards venous endothelial phenotype and these would be referred to Ven-ECs. Expression of arterial markers by a minor subset of the differentiated cells might indicate either presence of arterial phenotype or co-expression of arterial markers.

VEGF has been reported as critical for vascular patterning governing the specification towards arterial phenotype through a cascade of signaling events involving Shh, Notch, Dll4 and Ephrin-B2 (Coultas et al., 2005; Lawson et al., 2001; Lawson et al., 2002; Yamamizu et al., 2010). Similar studies on mouse ESCs (Lanner et al., 2007; Yamamizu et al., 2010), human adult progenitors (Aranguren et al., 2007) and human iPSCs (Rufaihah et al., 2013a) have shown high concentrations of VEGF favor arterial specification. To ascertain if the $CD34^{+}CD31^{+}$ cells had the potential to commit towards arterial phenotype, we additionally supplemented the ESFM with VEGF in addition to EGF and bFGF. Surprisingly, when the $CD34^{+}CD31^{+}$ cells were exposed to high concentrations of VEGF (50ng/ml), some of the cells underwent apoptosis (***Figure 44***). To ascertain the effect of VEGF, we analyzed apoptotic cell death using Annexin-V/ dead cell apoptosis kit. Titration of VEGF concentration using Annexin V-PI staining revealed the occurrence of cellular apoptosis in a dose-dependent manner with the optimal concentration around 5-10ng/ml VEGF (***Figure 44***). Upon differentiation of $CD34^{+}CD31^{+}$ cells in the presence of 10ng/ml of VEGF for 3-6

passages, yielded almost 99% of $CD34^+$, $CD31^+$ and VE-Cad^+ ECs (***Figure 41***). Flow cytometry analysis showed that these ECs were also positive for arterial markers (NRP1, DLL4, CXCR4) and only 5-6% of the cells positive for venous markers (NRP2, EPH-B4) (***Figure 41***). When compared to Ven-ECs, the cells differentiated under the influence of VEGF, displayed significantly higher levels of *CD31*, *vWF*, *eNOS* and *Tie2* transcripts (***Figure 42***). Real-time PCR analysis also revealed that these cells had significantly higher levels of arterial-related transcripts (*NRP1*, *EPHRIN-B2*, *DLL4*, *NOTCH1, CXCR4*) and lower levels of venous endothelial-related transcripts (*NRP2*, *EPH-B4*, *COUP-TFII*) (***Figure 42***). The expression profile of the cells differentiated under the influence of low concentrations of VEGF indicate the commitment of $CD34^+CD31^+$ cells towards arterial endothelial phenotype and these would be referred to as Art-ECs.

Further, the differentiation of $CD34^+CD31^+$ cells towards arterial and venous phenotype under serum-free conditions with or without VEGF was validated using H1- and H9-hESCs, and both these cell lines yielded similar results (***Figure 42***). The *in-vitro* functionality of hESC-derived Art-ECs and Ven-ECs was assessed by their ability for uptake of acetylated low-density lipoprotein (LDL) uptake, a characteristic of mature ECs and by their ability to self-organize into cord-like structures over Matrigel. Both the Art-ECs and Ven-ECs were functional in terms of their ability for LDL uptake and formation of cord-like structures over Matrigel (***Figure 43***). In summary, these findings indicate the efficient differentiation of hESCs-derived $CD34^+CD31^+$ endothelial progenitors to arterial and venous ECs under feeder- and serum-free conditions. Moreover, under serum-free conditions low concentrations of VEGF drives arterial differentiation, while the absence of VEGF drives commitment towards venous phenotype.

5.4.3. Intrinsic differences in cell migration and angiocrine secretory profile of hESC-derived arterial and venous ECs

ECs interact with the local micro-environment and support tissue regeneration after injury through revascularization of the newly healed tissue and expression of various trophic growth factors, known as angiocrine factors (Ding et al., 2010a). To revascualrize the regenerating tissue, ECs proliferate and migrate from pre-existing blood vessels. To assess cell migration, *in-vitro* wound closing assays were performed over a period of 24 hours. Compared to Ven-ECs, the Art-ECs displayed faster closure of the wound area resulting in a complete wound closure by Art-ECs in ~15 hours in contrast to ~24 hours taken by Ven-ECs (***Figure 45***).

ECs pertaining to distinct vascular beds have recently been reported to express diverse signatures of angiocrine factors (Nolan et al., 2013). However, the distinct expression of various endothelial phenotypes still needs exploration. To probe into the profile of various

angiocrine factors secreted by hESC-derived endothelial phenotypes, we used angiogenesis antibody array of 55 different proteins related to angiogenesis, inflammation, and extracellular matrix. Both arterial and venous ECs showed similar protein secretion profiles with certain dissimilarities (***Figure 46, 47***). Both Art-ECs and Ven-ECs displayed marked induction of endothelin-1, insulin-like growth factor-binding protein-2 (IGFBP-2), monocyte chemoattractant protein-1 (MCP-1), pentraxin-3, serpin-E1, and tissue inhibitor of matrix metalloproateinase-1 (TIMP-1). However, the media conditioned by Art-ECs had significantly higher levels of IGFBP-1, interleukin-8 (IL-8), matrix metalloproteinase-8 (MMP-8), platelet-derived growth factor-AA (PDGF-AA) and thrombospondin-1 (TSP-1) compared to that of Ven-ECs (***Figure 46***). On the contrary, the conditioned media of Ven-ECs had significantly higher levels of activin-A, IGFBP-3, interleukin-1β (IL-1β), and placenta-derived growth factor (PlGF) compared to Art-ECs (***Figure 46***). These results emphasize the existence of functional differences between the two endothelial phenotypes in addition to the differences in their molecular expression profiles.

5.5. Discussion

In this part of the study, we demonstrate for the first time the differentiation of hESCs towards arterial and venous ECs under feeder- and serum-free conditions. Inhibition of GSK-3 followed by stepwise stimulation with bFGF, BMP4 and VEGF led to robust differentiation of hESCs towards $CD34^{+}CD31^{+}$ endothelial progenitors. These $CD34^{+}CD31^{+}$ endothelial progenitors were differentiated to ECs of arterial and venous phenotype under serum-free conditions by modulating the concentration of VEGF. Further, we validated the differences between the two endothelial phenotypes at molecular and functional levels.

In the last few decades, our understanding regarding heterogeneity among various endothelial phenotypes in terms of their function, molecular signatures and the underlying pathways controlling their specification has increased tremendously (Aird, 2007a; Coultas et al., 2005; Kume, 2010; Lanner et al., 2007; Lawson et al., 2001; Lawson et al., 2002; Nolan et al., 2013; Swift and Weinstein, 2009; Torres-Vazquez et al., 2003; Yamamizu et al., 2010). Distinction of arterial and venous endothelial phenotypes seems to occur quite early in the development, wherein VEGF, Shh, and Notch signaling has been suggested to play a crucial role (Lawson et al., 2001; Lawson et al., 2002). Current understanding on the specification of arterial and venous endothelial phenotypes is based predominantly on animal studies. *In-vitro* studies using mouse PSCs (Lanner et al., 2007; Narazaki et al., 2008) indicate the expression of arterial markers like *Dll4*, *EphrinB2* and *Notch4* in response to high concentrations of VEGF (50ng/ml), while lower concentrations (10ng/ml) resulted in upregulation of venous marker

COUP-TFII. Additionally, the VEGF-mediated arterialization was reported to be further enhanced by the addition of adrenomedullin (Narazaki et al., 2008; Yurugi-Kobayashi et al., 2006) and these effects were blocked in the absence of Notch signaling (Lanner et al., 2007; Yurugi-Kobayashi et al., 2006). These findings from *in-vitro* models correlate with the findings of *in-vivo* animal models highlighting the coordinated activation of VEGF-Notch signaling in arterial specification.

Towards obtaining data from human models, several groups have used human stem cells to study the early developmental events in the specification of endothelial lineage. Though tremendous amounts of information have been obtained from these *in-vitro* human models, the heterogeneity of ECs has been investigated by very few studies. Kurian et al., (Kurian et al., 2013) reported conversion of fibroblasts to ECs through a plastic intermediate state, wherein they found the pool of ECs as being heterogeneous in terms of expression of arterial, venous and lymphatic markers. Similarly, Samuel et al., *(Samuel et al., 2013)* reported differentiation of human iPSCs to NRP1 (an arterial marker) expressing progenitors which further differentiated to ECs expressing markers related to both arterial and venous phenotypes. These studies indicate the expression of arterial and venous endothelial markers by a pool of differentiated ECs, however distinct specification towards either phenotype is not investigated. Only two studies using human adult progenitors (Aranguren et al., 2007) and human iPSCs (Rufaihah et al., 2013a) have elucidated the arterial-venous specification of human progenitor/ stem cells till date. Aranguren et al., (Aranguren et al., 2007) reported high concentration of VEGF (100ng/ml) induced arterial differentiation of human bone marrow-derived multipotent adult progenitor cells. Further, the arterial induction was reported to be enhanced by supplementation with Dll4 and Shh, while blockade of Notch and/or Shh led to attenuation of arterial differentiation and upregulation of venous markers. Similarly, Rufaihah et al., (Rufaihah et al., 2013a) using human iPSCs model demonstrated the arterial differentiation by high VEGF concentration coupled with cAMP and induction of venous specification under low concentrations of VEGF. In aggregate, all the above studies in mouse and human *in-vitro* models indicate the dose-dependent effect of VEGF in arterial-venous specification of endothelial cells. However, all these studies were performed under serum-containing conditions.

Inclusion of xenogeneic products (like Matrigel, FBS, murine stromal cells) in the culture milieu could influence the differentiation outcome and limit the ability to tune the microenvironment due to the presence of unknown/ poorly defined factors (Kaupisch et al., 2012). Additionally, these xenogeneic components could limit the clinical translation potential, owing to the potential risk of transmission of animal pathogens and xenogeneic

rejection (Kaupisch et al., 2012). Towards eliminating or reducing the use of xenogeneic products, we have developed a novel feeder- and serum-free protocol for differentiation of hESCs to endothelial subtypes. Under serum-free conditions, we found higher concentrations of VEGF (25-100ng/ml) causes apoptosis of the cells, while at lower concentrations (10ng/ml) directs arterial phenotype and its absence favors venous fate. This is in contrast to the findings previously reported under serum-containing conditions. The contradictory results could be due the presence of serum in the culture milieu. The novel insights into the arterial-venous specification under serum-free conditions would provide clues for developing clinically competent vascular cells in the future. In addition, access to robust differentiation of hESCs to arterial and venous ECs under defined conditions could provide a potential human model to study arterial-venous specification and for various clinical, research and pharmaceutical applications.

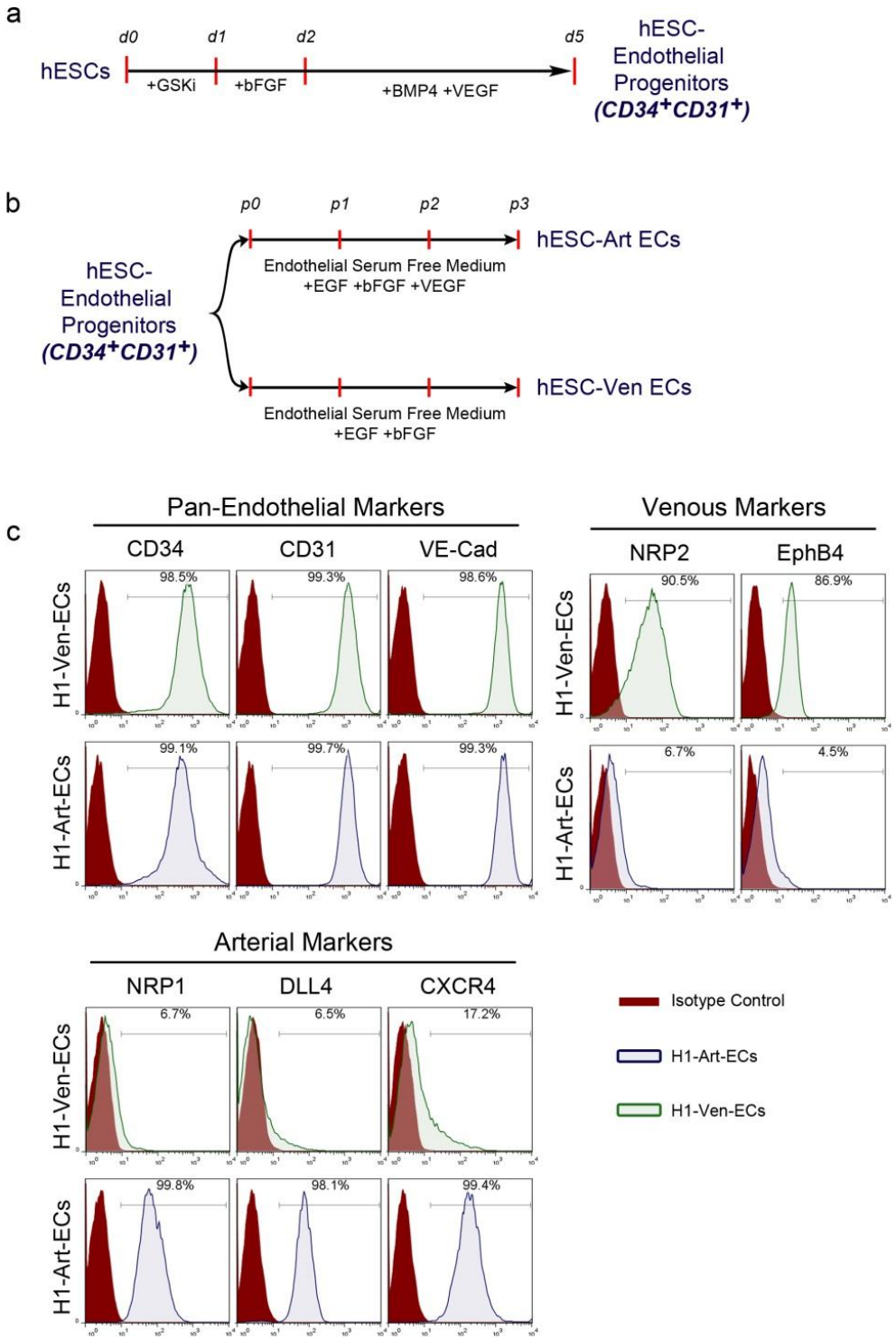

Figure 41. Flow cytometry analysis of terminal differentiation of $CD34^+CD31^+$ endothelial progenitors to venous and arterial endothelial cells under serum-free conditions.

(a) Schematic representation of differentiation of hESCs to endothelial progenitors ($CD34^+CD31^+$) cells by sequential treatment with CHIR99021 (+GSKi), bFGF, followed by combined treatment with BMP4 and VEGF. **(b)** The hESC-derived $CD34^+CD31^+$ cells were sorted using flow cytometry after 5 days of differentiation and further differentiated towards venous ECs (hESC-Ven-ECs) and arterial ECs (hESC-Art-ECs). **(c)** Representative flow cytometry histogram overlays represent the expression of pan-endothelial markers, arterial markers and venous markers among H1-hESC derived Ven-ECs **(b)** and Art-ECs **(c)**.

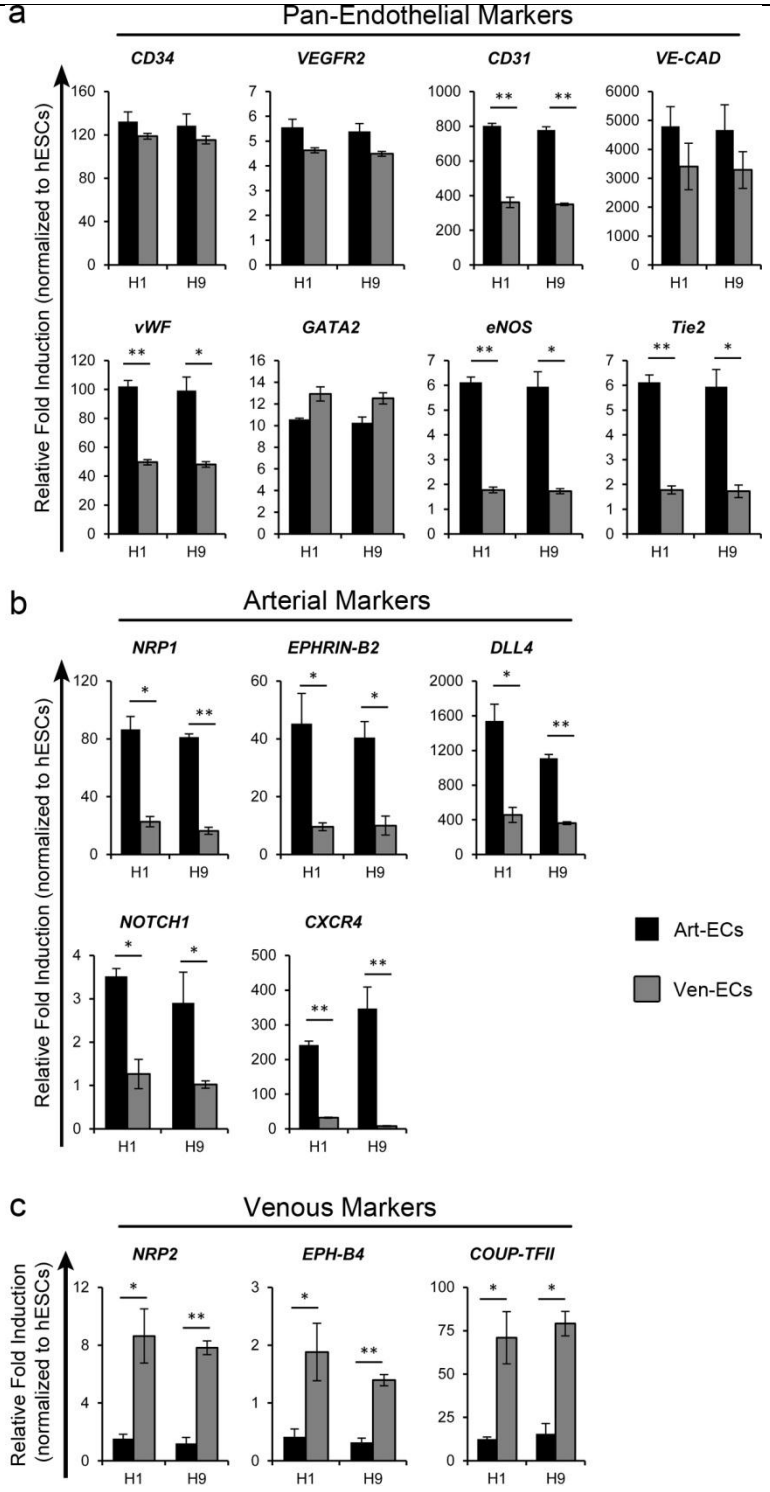

Figure 42. RT-PCR analysis of terminal differentiation of CD34+CD31+ endothelial progenitors to venous and arterial endothelial cells under serum-free conditions.

mRNA profiles of pan-endothelial **(a)**, arterial **(b)**, and venous **(c)** endothelial related transcripts **(e)** among Art-ECs and Ven-ECs derived from H1- and H9-hESCs. For gene expression plots, the levels of expression were normalized to corresponding *β-ACTIN* values and are represented as relative to that of undifferentiated hESCs. Error bars: s.d. (n≥2). *p<0.05. **p<0.01.

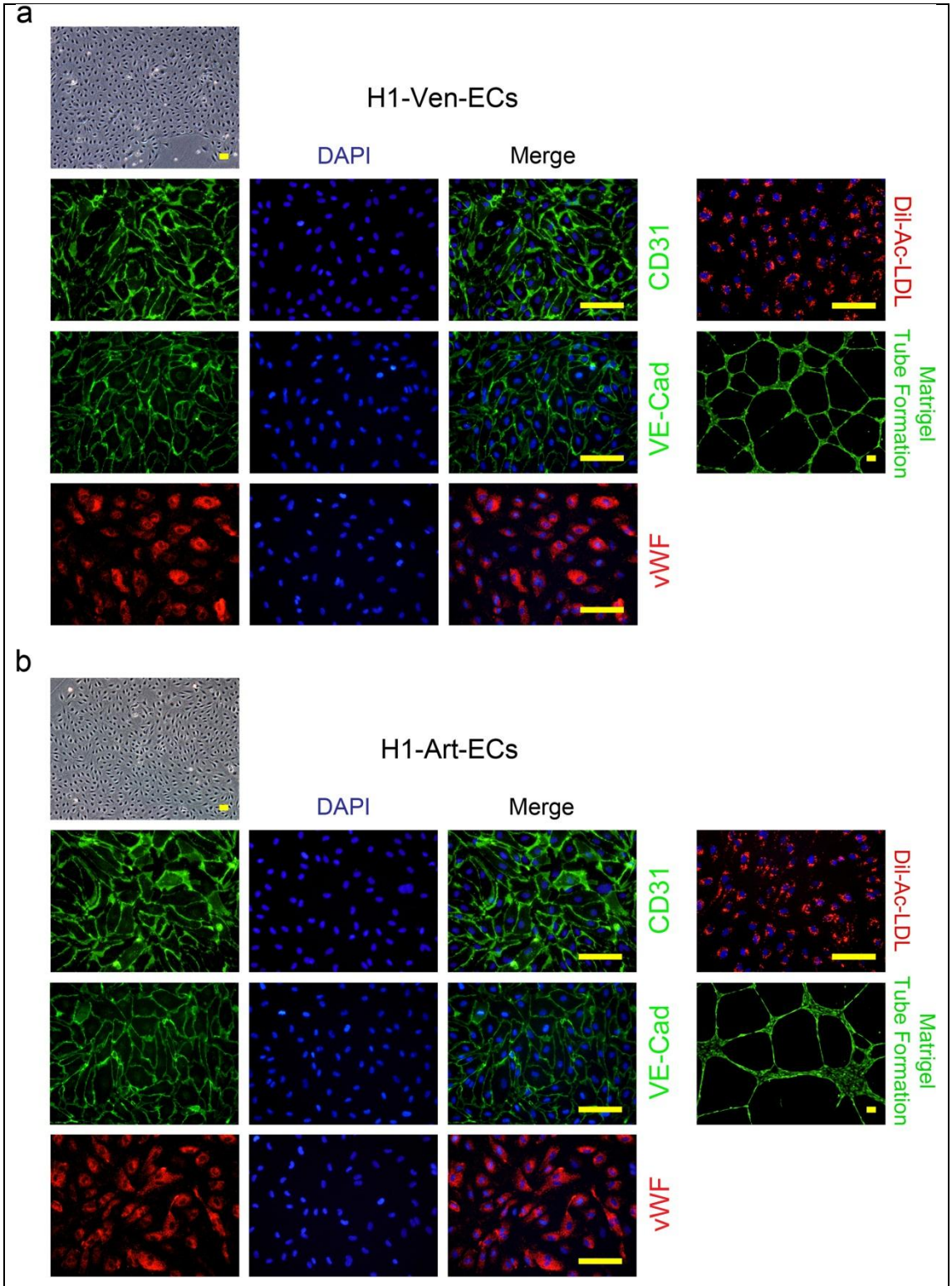

Figure 43. Immunocytochemical analysis of expression of endothelial markers by hESC-derived venous and arterial endothelial cells.

Representative photomicrographs of ECs differentiated under venous **(a)** and arterial **(b)** differentiation conditions. Photomicrographs show the cobblestone morphology of ECs under phase contrast microscopy, and immunofluorescence images demonstrate the expression of endothelial markers CD31, VE-Cadherin, and vWF; uptake of Dil-acetylated low density lipoprotein (Dil-Ac-LDL) and formation of anastomosing network of cord-like structures over Matrigel. Scale bar: 100µm.

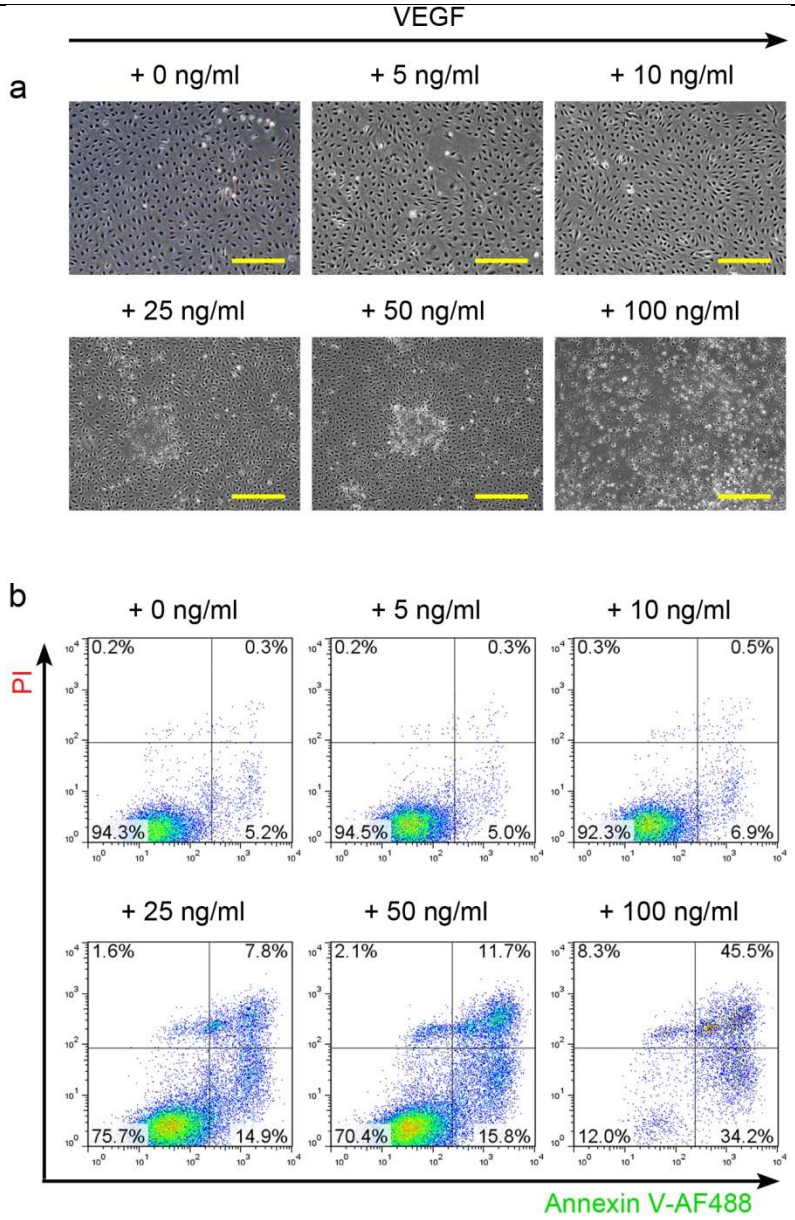

Figure 44. Effect of VEGF on endothelial cells.

(a) Representative photomicrographs of endothelial cells after 24 hour exposure to increasing concentrations of VEGF reveal the apoptosis of cells at higher VEGF concentrations. (b) Representative flow cytometry plots displaying the Annexin V/ PI staining to quantify the apoptotic cell death with increasing concentrations of VEGF. Scale bar 500µm.

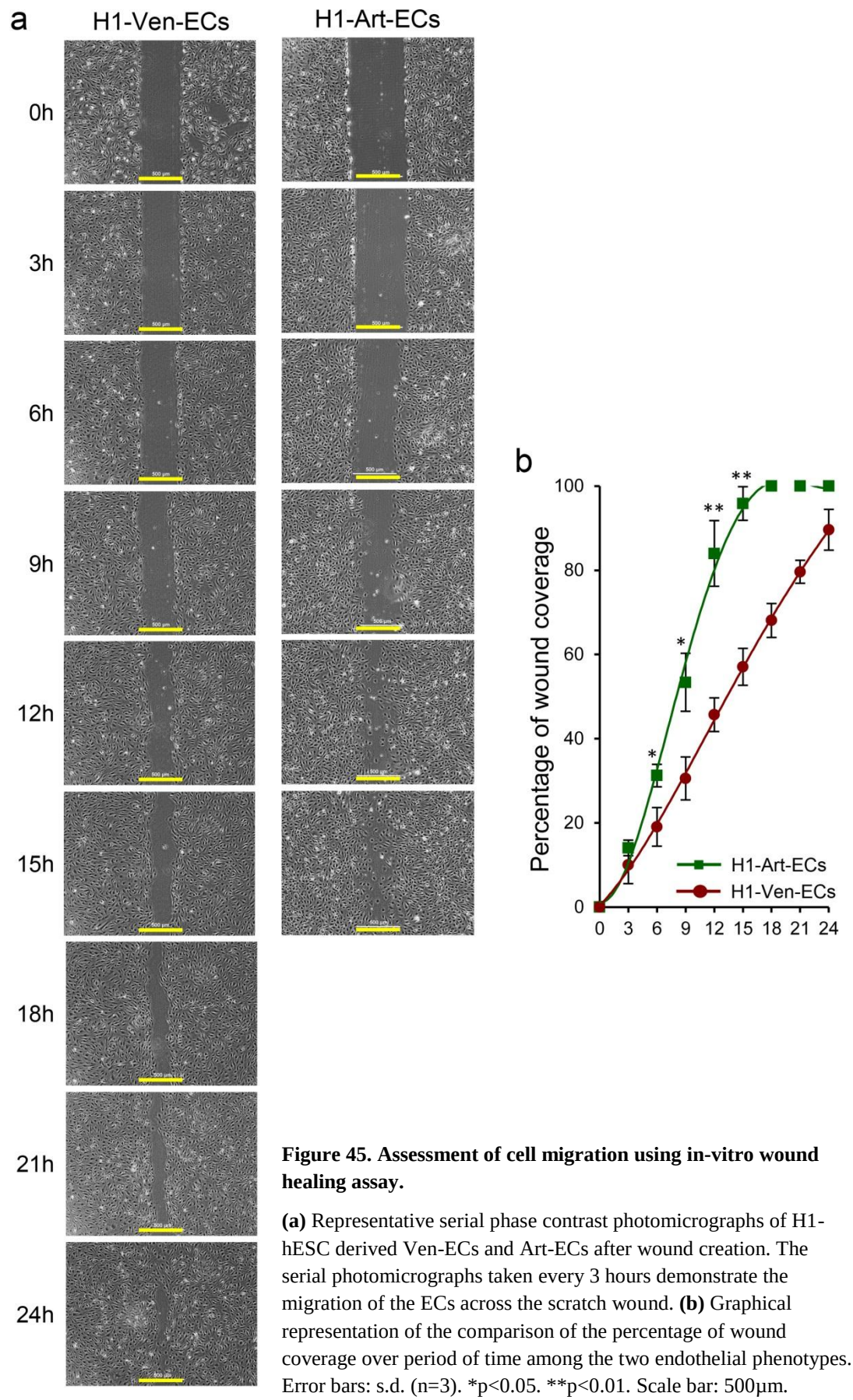

Figure 45. Assessment of cell migration using in-vitro wound healing assay.

(a) Representative serial phase contrast photomicrographs of H1-hESC derived Ven-ECs and Art-ECs after wound creation. The serial photomicrographs taken every 3 hours demonstrate the migration of the ECs across the scratch wound. **(b)** Graphical representation of the comparison of the percentage of wound coverage over period of time among the two endothelial phenotypes. Error bars: s.d. (n=3). *p<0.05. **p<0.01. Scale bar: 500µm.

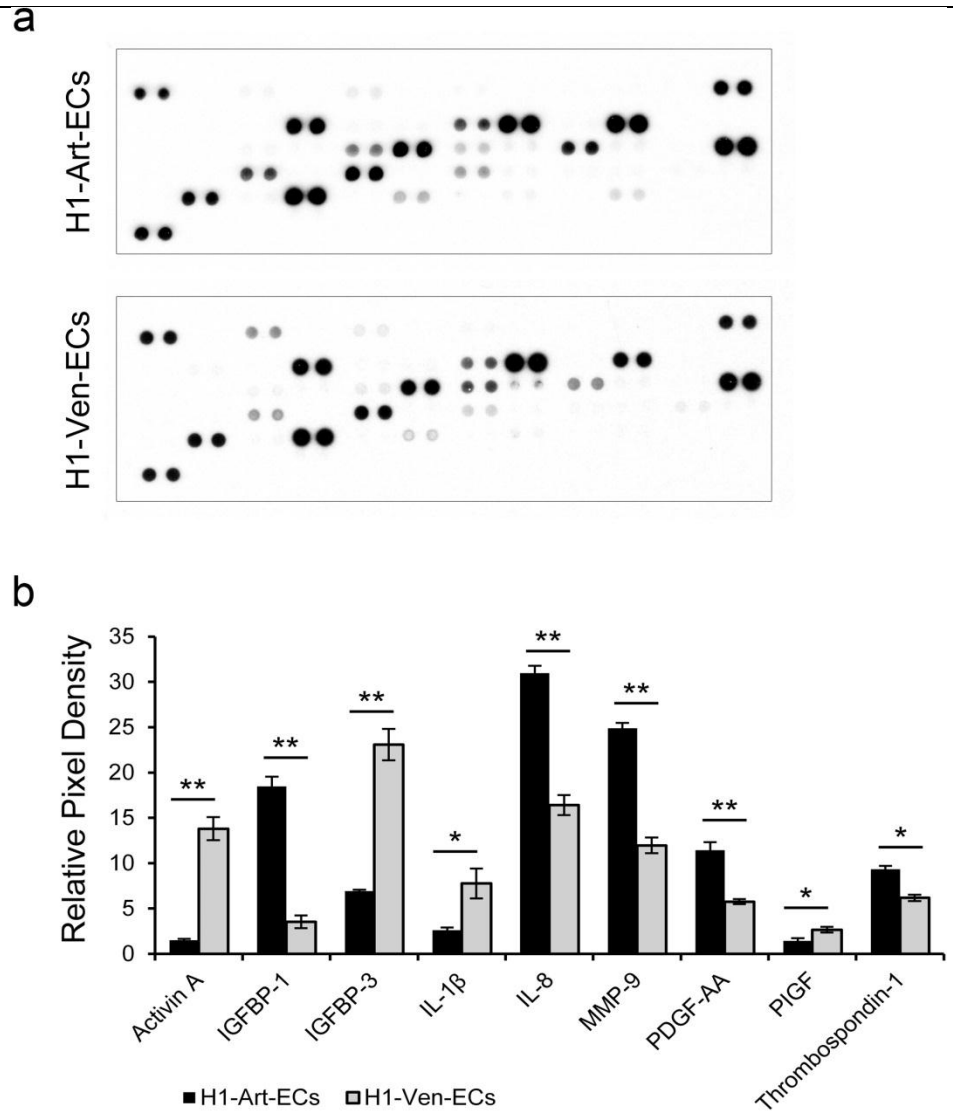

Figure 46. Angiocrine secretory profile of hESC-derived arterial and venous ECs using angiogenesis antibody array.

(a) Representative scans of angiogenesis antibody arrays demonstrating the secretion of various angiocrine factors by arterial and venous ECs. Array images are obtained from 10-minute exposure of X-ray film. **(b)** Graphical representation of the relative amounts of selected angiocrine factors that show significant difference among the arterial and venous ECs. The bars represent relative amounts of factors secreted based on densitometric analysis of relative pixel density of the blots. ***Figure 46*** provides the complete densitometric analysis of all the 55 angiocrine factors analyzed using antibody arrays. Error bars: s.d. (n=2). *p<0.05. **p<0.01.

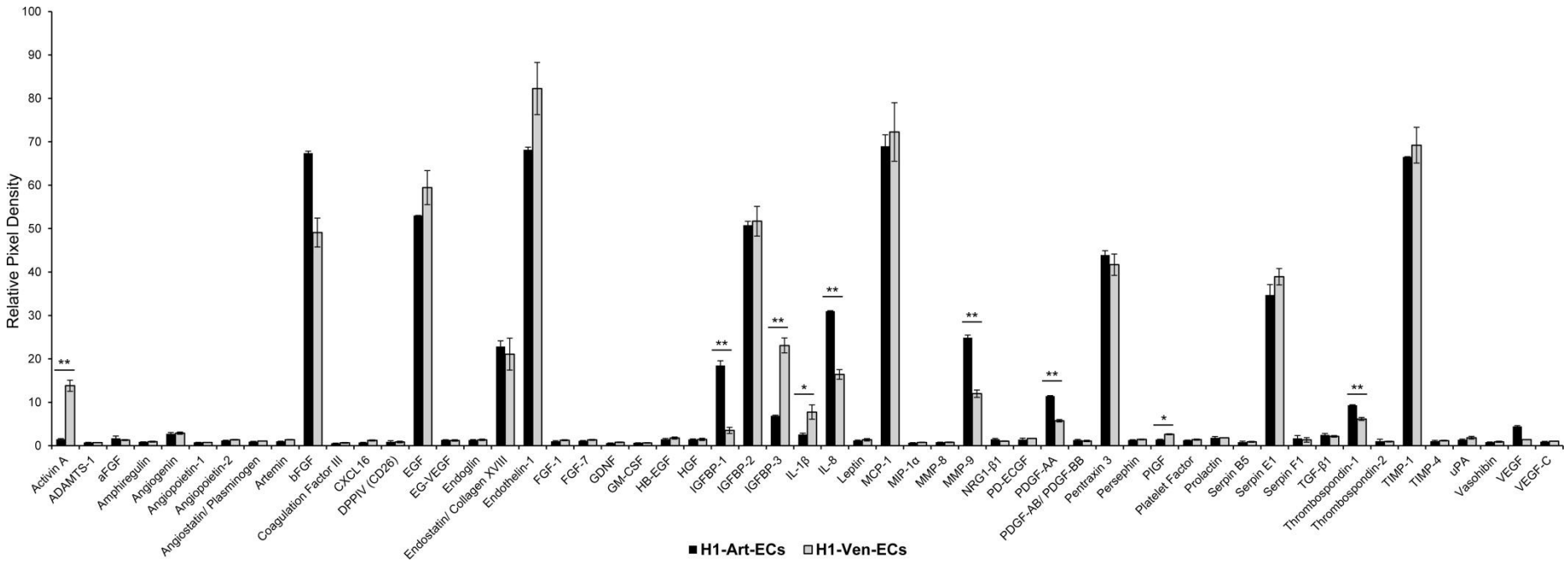

Figure 47. Survey of secretory profile of 55 angiocrines by hESC-derived arterial and venous ECs using angiogenesis antibody array.

Graphical representation of the relative amounts of 55 angiocrine factors secreted by H1-hESC derived Art-ECs and Ven-ECs analyzed using angiogenesis antibody array. The bars represent relative amounts of factors secreted based on densitometric analysis of relative pixel density of the blots. Error bars: s.d. (n=2). *p<0.05. **p<0.01.

Chapter 6

Differentiation of hESCs to vascular smooth muscle cells under feeder-free, serum-free conditions

6. Differentiation of hESCs to vascular smooth muscle cells under feeder-free, serum-free conditions

6.1. Introduction

Formation of mature and functional microvascular network relies on the interaction between ECs and vSMCs. In early embryogenesis and in adult life, newly formed endothelial vessels recruit mural cells (pericytes and vSMCs) resulting in a complex network of arteries, arterioles, capillaries, venules and veins (Coultas et al., 2005; Flamme et al., 1997). These vSMCs and/or pericytes are heterogeneous group of cells derived from diverse embryological origins ranging from lateral plate mesoderm (secondary heart field, splanchnic mesoderm), paraxial mesoderm (somites) and neural crest (Majesky, 2007). Various approaches to guide the differentiation of PSCs towards vSMC lineage involves one or combination of following methods: (1) EB-based differentiation (Ferreira et al., 2007; Levenberg et al., 2010; Vazao et al., 2011; Vo et al., 2010), (2) co-culture over murine/ human stromal cells like OP9 (Oyamada et al., 2008; Sone et al., 2007; Taura et al., 2009; Yamahara et al., 2008), MEFs (Bu et al., 2009), M2-10B4 (Hill et al., 2010), human foreskin fibroblasts (Lee et al., 2007), (3) culture of hESCs or iPSCs as monolayers over ECM proteins like Matrigel (Colleoni et al., 2010), and collagen IV (Oyamada et al., 2008; Sone et al., 2007; Taura et al., 2009; Wanjare et al., 2013; Xie et al., 2007; Yamahara et al., 2008), and/or (4) growth factor, cytokines or small molecule mediated differentiation in serum containing/ serum-free conditions (Bai et al., 2010; Cheung et al., 2012; Huang et al., 2006; Lee et al., 2007; Park et al., 2010; Tan et al., 2013a) (***Figure 12, 15-17, Table 4***). Most of these protocols rely on use of serum and do not involve lineage-specific differentiation strategies. Recently, Cheung et al., using serum-free media and specific lineage restriction methods reported differentiation of hPSCs were differentiated to lateral plate mesoderm, paraxial mesoderm and neural crest progenitor-derived vSMCs (Cheung et al., 2012). Similarly, Tan et al., had recently demonstrated the differentiation of hESCs to vSMCs through paraxial mesoderm progenitors ($PDGFR\alpha^{+}CD34^{-}$) (Tan et al., 2013a). In this study, the hESCs were differentiated to paraxial mesoderm intermediates in chemically-defined media conditions using Matrigel as substrate and sequential modulation of Wnt/β-catenin, BMP and VEGF signaling pathways. Further, these paraxial mesoderm intermediates were sorted and differentiated into vSMCs under the influence of platelet-derived growth factor-BB ($PDGF_{bb}$) and serum.

Using human plasma fibronectin as substrate and chemically defined medium (Stemdiff APEL medium), we developed a feeder-free, and chemically-defined differentiation system for directing hESCs towards PS and mesodermal subsets (***Chapter 4***). In this chapter, we

further investigated the differentiation towards paraxial mesoderm intermediates followed by differentiation towards vSMCs.

6.2. Objective

To differentiate hESCs to paraxial mesoderm intermediates and vSMCs with minimal use of xenogeneic products.

6.3. Materials and Methods

6.3.1. Culture of hESCs under feeder-free and serum-free conditions

H1- and H9- hESCs were cultured as perviosly described under Section 4.3.1.

6.3.2. Directed Differentiation of hESCs to paraxial mesoderm intermediates under chemically-defined conditions

hESCs were passaged using dispase, dispersed into small clusters (~300-500 cells per colony) and seeded onto 4μg/cm^2 human plasma fibronectin (GIBCO) coated plates. These hESC colonies were maintained in mTeSR™1 for 24 hours, after which the cells were gently washed with DMEM:F12 (Invitrogen) and differentiated in chemically-defined, serum-free, animal component-free basal medium (STEMdiff™ APEL™, Stemcell Technologies) supplemented with appropriate factors as depicted in (***Figure 48***). Briefly, to induce hESCs towards PS, the hESCs were exposed to glycogen synthase kinase-3 inhibitor (CHIR99021, 5μM, Stemgent) for 24 hours. Following induction of PS, mesodermal and vascular induction was carried out in the presence of bFGF (50ng/ml; R&D systems) for 24 hours followed by 72 hours of VEGF (50ng/ml; GIBCO).

6.3.3. Differentiation of paraxial mesoderm intermediates (CD34$^-$CD31$^-$PDGFRβ$^-$ cells) to vSMCs in feeder-free, serum-free conditions

After 5 days of differentiation in STEMdiff™ APEL™, *CD34$^-$CD31$^-$PDGFRβ$^-$* cells were isolated by flow cytometry assisted sorting (FACS), and plated onto 2μg/cm^2 human plasma fibronectin coated plates (12,000 cells per cm^2) and cultured in serum-free medium (SFM) with media changes every 2-3 days. The SFM consists of Opti-MEM (GIBCO, Invitrogen) supplemented with insulin, transferrin, selenium (ITS) supplement (GIBCO, Invitrogen), 0.1mM β-mercaptoethanol (Sigma), 1% (5mg/ml) bovine serum albumin (Sigma). For differentiation towards vSMCs, the SFM was further supplemented with EGF (10ng/ml), bFGF (20ng/ml) and $PDGF_{bb}$ (GIBCO; 10ng/ml). The vSMCs were passaged using accutase (Invitrogen) when 70-80% confluent and characterized after 3 to 5 passages.

6.3.4. RNA extraction and real-time PCR

Total cellular RNA was isolated, reverse transcribed and quantitated using real-time PCR as described previously under Section 4.3.3.

6.3.5. Flow cytomerty analysis and sorting

Flow cytometry analysis of differentiated cells for cell surface antigens (VEGFR2, CD34, CD31, PDGFRβ, NG2, CD73, CD90, CD105) were performed and analyzed as previously described under Section 4.3.4.

For intracellular antigens, the cells were harvested, fixed and permeabilized using BD Cytofix/Cytoperm™ fixation/permeabilization solution for 20 minutes at 4^{o}C as per manufacturer's instructions. After fixation/permeabilization, the cells were washed and non-specific staining blocked with PBS/5% goat serum (30 minutes). Subsequently, the cells were labeled with appropriate primary antibodies (αSMA, CNN1, MYH11; details of the antibodies listed in ***Appendix III***) diluted in BD Perm/Wash™ staining buffer for 15 minutes at 4^{o}C, washed and fluorescently labeled using appropriate secondary antibodies (listed in ***Appendix III***) for 15 minutes at 4^{o}C. After washing thrice, the cells were resuspended in FACS buffer for analysis.

The labeled cells were analyzed for surface marker and intracellular protein expression using Dako Cytomation CyAn ADP. For sorting paraxial mesoderm intermediates, the cells labeled with surface markers were sorted using a Dako Cytomation MoFlo high speed flow cytometer. The flow cytometry data was further analyzed using FlowJo v7.6.5 (TreeStar).

6.3.6. Immunocytochemistry

Immunocytochemical staining of differentiated cells for appropriate primary antibodies (αSMA, CNN1; details listed in ***Appendix III***) were performed and documented as previously described under Section 4.3.5.

6.3.7. Contractility assays

Agonist-induced contraction of the hESC-differentiated cells was assessed as previously described (Ferreira et al., 2007; Vo et al., 2010). Briefly, the hESC-derived CD34^{-}CD31^{-} PDGFRβ^{+} progenitor cells differentiated under smooth muscle inducing conditions for 3-6 passages were stimulated with 10^{-5}M carbachol (Sigma) in Opti-MEM for 30 minutes. In a separate experiment, the cells were treated with muscarinic antagonist 10^{-4} atropine (Sigma) in Opti-MEM for 1 hour before induction with carbachol. The cells were visualized using time-lapse phase contrast microscopy (Olympus IX70).

6.3.8. Human angiogenesis antibody array

Human Angiogenesis Proteome Profiler™ antibody array (R&D Systems) was used to survey the levels of 55 different angiocrines secreted by H1-hESC derived vSMCs into culture supernatants. vSMCs were seeded onto fibronectin coated plates at a seeding density of $1.2x10^4/cm^2$. After 24 hours, the media was changed to SFM without any additional supplements and incubated for 24 hours. After the incubation the culture supernatants were collected and stored at -80^0C. Total protein concentration within cell-free culture supernatants were quantified using Micro BCA™ Protein Assay Kit (Thermoscientific) as per manufacturer's instructions. Cell culture supernatant containing 200µg of protein was used for the antibody array as per manufacturer's instructions. The membranes were developed using 10 minute exposure to X-ray film. The array data was quantified by densitometry analysis using Image J (NIH, USA). The various angiocrines in the protein blot are listed in ***Appendix IV***.

6.3.9. Statistical Analysis

All real time RT-PCR and angiogenesis antibody array experiments were performed in duplicates with duplicate readings each. Student's t-test was performed to determine significance using Microsoft Excel Data Analysis ToolPak. For angiogenesis antibody arrays, the density of each protein blot was quantified by a densitometry analysis using Image J software. The pixel densities corresponding to the negative control spots within each array was used as controls to normalize the density corresponding to each protein spot. These pixel density values were used as relative pixel density measurements to compare the expression levels of the proteins between different blots.

6.4. Results

6.4.1. Directed Differentiation of hESCs to paraxial mesoderm intermediates under chemically-defined conditions

A variety of markers have been used to identify/ track the progenitors that give rise to vSMCs, including *CD34*, *CD31*, *VEGFR2*, *PDGFRα*, *PDGFRβ*, *NKX2.5*, *ISL1*, *TCF15*, and *p75* (Cheung and Sinha, 2011). In early embryonic development, *PDGFRα*, *PDGFRβ*, and *TCF15* indicate commitment towards paraxial mesoderm (Cheung et al., 2012; Sakurai et al., 2006; Sakurai et al., 2012; Takakura et al., 1997; Yang et al., 2008b); and PDGF receptors are associated with progenitors for cardiac, smooth muscle, and mesenchymal lineages (Evseenko et al., 2010). We utilized paraxial mesoderm marker *PDGFRβ* in association with lateral plate mesoderm markers (*VEGFR2, CD34, CD31*) to track the commitment towards paraxial mesoderm. Differentiation of hESCs was performed under feeder-free and chemically-defined

conditions as previously mentioned in ***Section 4.3 and 4.4***. Briefly, the hESCs were differentiated by sequential modulation of Wnt/β-catenin using CHIR99021 followed by FGF and VEGF signaling pathways (***Figure 48***). This step-wise modulation resulted in ~55% of the differentiated cells positive for VEGFR2, CD34, and CD31 after 5 days of differentiation (***Figure 48***). Analysis of CD34, CD31 and PDGFRβ expression showed that almost 35% of the differentiated cells were positive for PDGFRβ, but this subset was negative for CD34 and CD31 (***Figure 48***). Further, almost 96% of CD34 and CD31 negative population expressed PDGFRβ, while only ~8% of CD34 and CD31 positive cells expressed PDGFRβ (***Figure 49***). Expression of PDGFRβ (paraxial mesoderm marker) and simultaneous absence in the expression of lateral plate mesoderm markers (VEGFR2, CD34, CD31) among the subset of differentiated cells is indicative of potential commitment of the subpopulation towards paraxial mesoderm.

6.4.2. Terminal differentiation of PDGFRβ^{+}CD34^{-}CD31^{-} paraxial mesoderm intermediates towards vascular smooth muscle lineage under serum-free conditions

During early embryonic development, paraxial mesoderm is a potential source of vSMCs. During vasculogenesis and angiogenesis, $PDGF_{bb}$ induces the differentiation of mesenchymal progenitors towards vSMC lineage (Flamme et al., 1997; Jain, 2003). To terminally differentiate hESC-derived paraxial mesoderm progenitor population towards vascular smooth muscle lineage, the PDGFRβ^{+}CD34^{-}CD31^{-} was FACS sorted after 5 days of differentiation. The sorted population was seeded onto fibronectin coated plates and cultured in SFM supplemented with EGF, bFGF and $PDGF_{bb}$ (***Figure 50***). Within one passage, the PDGFRβ^{+}CD34^{-}CD31^{-} cells attained a spindle-shaped morphology and were observed for over 10 passages (***Figure 50***). These cells were characterized for vSMC phenotype by real time RT-PCR, flow cytometry and immunocytochemistry after 3-6 passages.

Real time RT-PCR analysis showed the PDGFRβ^{+}CD34^{-}CD31^{-} cells expressed early SMC markers (*αSMA, CNN1, TAGLN*), late SMC markers (*MYH11, SMTN*) and *PDGFRβ* (***Figure 50***). On the other hand, these cells showed down-regulation of endothelial-associated genes (*CD34, CD31, VE-CAD*). Flow cytometry analysis for cell surface marker expression profile displayed that the PDGFRβ^{+}CD34^{-}CD31^{-} cells were negative for CD34 and CD31, while ~65% of the cells were positive for PDGFRβ (***Figure 51***). Analysis of pericyte markers showed that ~96% of the cells were positive for pericyte marker, NG2 with ~62% of the cells double positive for PDGFRβ and NG2 (***Figure 51***). Analysis of mesenchymal/ perivascular markers showed that almost all of the cells were positive for CD73 and CD105, while only ~32% of the cells were positive for CD90 (***Figure 51***). Flow cytometry analysis of SMC-associated intracellular antigens displayed that >95% of the cells were positive for early SMC

markers (αSMA, CNN1) and late SMC marker (MYH11) (***Figure 51***). Immunocytochemical analysis also displayed the cytoplasmic, filamentous expression of αSMA and CNN1 (***Figure 51***). Expression of perivascular markers at mRNA and protein levels indicates the terminal differentiation to vSMC phenotype and these cells would be referred to as H1-vSMCs.

6.4.3. In-vitro functionality of H1-vSMCs

vSMCs/ pericytes are heterogeneous group of mesenchymal cells that exhibit phenotypes ranging from contractile to synthetic phenotype. The *in-vitro* functionality of H1-vSMCs in terms of their ability to contract was investigated upon stimulation with cholinergic (muscarinic) agonist, carbachol and muscarinic antagonist atropine. Stimulation of H1-vSMCs with 30 minute exposure to carbachol showed marked contraction of most of the cells that was abolished by preincubation with atropine (***Figure 52***).

To investigate the synthetic function of these H1-vSMCs, the production of extracellular matrix components (Collagen IV, fibronectin, laminin) and various proteinases was analyzed. Immunohistochemical staining revealed that H1-vSMCs produce their own extracellular matrix proteins fibronectin, laminin and traces of collagen IV (***Figure 52***). Further, culture supernatants of H1-vSMCs were screened for matrix metalloproteinase (MMPs; MMP8, MMP9), ADAMTS (**A** **D**isintegrin **A**nd **M**etalloproteinase with **T**hrombospondin **M**otifs), serpins (**ser**ine **p**rotease **in**hibitors; serpin-B5, E1, F1) and tissue inhibitor of metalloproteinases (TIMP; TIMP1, TIMP4) using angiogenesis protein array. Protein blots of the culture supernatants displayed the secretion of MMP9, Serpin-E1, Serpin-F1 and TIMP-1 (***Figure 53, 54***). H1-vSMCs, in comparison to H1-Art-ECs and H1-Ven-ECs, display higher levels of secretion of Serpin-E1, Serpin-F1 and TIMP1; and in comparison to H1-Art-ECs, secrete significantly lower levels of MMP9 (***Figure 55***).

Analysis angiogenesis protein array also revealed the secretion of various angiocrine and pro-inflammatory factors by H1-vSMCs that include Activin A, angiogenin, endostatin, IGFBP (-1,2,3), IL-8, monocyte chemoattractant protein (MCP-1), $PDGF_{aa}$, pentraxin 3, urokinase type-plasminogen activator (uPA), and VEGF (***Figure 53, 54***). Levels of secretion of most of these factors are significantly higher compared to H1-Art-ECs and H1-Ven-ECs (***Figure 55***). Further, the H1-vSMCs secreted significantly high amounts of angiogenic factors that include activin A, angiogenin, IGFBP (1-3), IL-8, VEGF, and uPA. However, the H1-vSMCs also secreted significantly high amounts of certain anti-angiogenic factors that include Serpin F1, thrombospondin-1 (TSP-1), and TIMP1. Hence, the various angiocrines factors secreted by H1-vSMCs might provide a balanced angiogenic and anti-angiogenic signals for H1-Art-ECs and H1-Ven-ECs.

6.5. Discussion

In this part of the study, we developed a feeder- and serum-free differentiation system to efficiently generate origin-specific vSMCs from hESCs. Inhibition of GSK-3 followed by stepwise stimulation with bFGF and VEGF led to robust differentiation of H1-hESCs towards two distinct population, PDGFRβ^{-}CD34^{+}CD31^{+} (lateral plate mesoderm/ endothelial progenitors) and PDGFRβ^{+}CD34^{-}CD31^{-} (paraxial mesoderm intermediates). The PDGFRβ^{+}CD34^{-}CD31^{-} cells were further differentiated to vSMCs under serum-free conditions. The H1-vSMCs were characterized for expression of vSMC-related markers, secretion of ECM proteins and their ability to contract upon stimulation with cholinergic (muscarinic) agonist, carbachol and muscarinic antagonist atropine. Further, the expression profile of angiocrine factors were surveyed and compared with those of H1-hESC derived arterial and venous ECs.

vSMCs are a heterogeneous group of vascular cells derived from diverse developmental origins that include lateral plate mesoderm, paraxial mesoderm and neural crest (Majesky, 2007). Interestingly, vSMCs derived from different origins are reported to display distinct functional properties. For instance, SMCs derived from neural crest and mesoderm display different growth and transcriptional responses to the stimulation with morphogenetic factors such as TGFβ1 (Topouzis and Majesky, 1996). Similarly, hPSC-derived vSMCs of different origin exhibit differences in activation of MMPs & TIMPs in response to IL-1β (Cheung et al., 2012). Protocols to differentiate hESCs towards vSMCs initially relied on differentiation towards spindle-shaped cells that express vSMC-related markers without due consideration for their diverse developmental origin (Huang et al., 2006; Vo et al., 2010; Xie et al., 2007). Developmental insights, lead to protocols demonstrating the differentiation of hESCs towards bi-potent vascular progenitors (CD34^{+}, VEGFR2^{+} and/or CD31^{+} cells) capable of differentiation towards endothelial and smooth muscle lineages (Bai et al., 2010; Ferreira et al., 2007; Hill et al., 2010; Levenberg et al., 2010; Vazao et al., 2011; Wanjare et al., 2013). As CD34^{+}, VEGFR2^{+} and/or CD31^{+} is expressed by lateral mesodermal subsets, protocols utilizing these markers could be assumed to be yielding vSMCs of lateral plate mesoderm origin. Similarly, certain groups have reported the differentiation towards vSMCs through a hESC/iPSC-derived mesenchymal stem cell (MSCs) intermediates (Bajpai et al., 2012; Guo et al., 2013). Recently, Cheung et al., reported differentiation of hPSCs to vSMCs through lateral plate mesoderm, paraxial mesoderm and neural crest progenitors (Cheung et al., 2012). Similarly, Tan et al., had recently demonstrated the differentiation of hESCs to vSMCs through paraxial mesoderm intermediates (PDGFRα^{+}CD34^{-}) (Tan et al., 2013a). Hence, the recent studies based on PSCs, highlight the focus towards developing protocols for lineage-specific derivation of vSMCs.

In the current study, we modified our earlier protocol to differentiate hESCs to paraxial mesoderm and then to vSMCs (Tan et al., 2013a). We replaced Matrigel used in the previous study with human plasma fibronectin with the aim of reducing the use of xenogeneic products. Secondly, we used PDGFRβ instead of PDGFRα to track paraxial mesoderm intermediates, as studies in mouse embryos have demonstrated the selective expression of PDGFRβ by developing vSMCs; and the expression of PDGFRβ by the developing vSMCs was crucial for their recruitment onto the embryonic blood vessels (Hellstrom et al., 1999). Further, $PDGF_{bb}$ is well documented to induce the differentiation of vascular progenitors towards smooth muscle lineage (Cheung et al., 2012). For the cells to respond to $PDGF_{bb}$, they should express the receptors for the same i.e., PDGFRβ. Hence, we believe that it is more prudent to track cells that express PDGFRβ, than the α-subtype (though the cells might express both the subtypes).

Differentiation of the $PDGFR\beta^{+}$ cells in the presence of $PDGF_{bb}$ under serum-free conditions yielded cells with spindle-shaped morphology reminiscent of the mesenchymal cells like vSMCs, fibroblasts, and MSCs. However, gene expression, flow cytometry and immunocytochemical studies revealed the expression of various vSMC-related markers indicating the commitment to vSMC phenotype. Mature vSMCs are specialized type of vascular cells that can perform both synthetic function (to support blood vessels) and contractile function (to regulate vessel hemodynamics) (Majesky, 2003). Further, the vSMCs interact with the ECs to stabilize the nascent endothelial channels through cytokine interactions and production of ECM (Carmeliet, 2005; Jain, 2003). Hence, engineering functional vascular networks requires the presence of both the synthetic and contractile phenotypes. In this study, immunocytochemical evidence shows that hESC-vSMCs secrete ECM proteins fibronectin, laminin and traces of collagen IV. Similarly, analysis of hESC-vSMC conditioned media using angiogenic antibody array show the production of MMP8, MMP9, Serpins (E1, F1) and TIMP-1. Additionally, the hESC-vSMCs also secrete various other angiogenic and antiangiogenic factors. These findings indicate the synthetic function of hESC-vSMCs. Contraction of hESC-vSMCs upon stimulation with carbachol is reminiscent of their contractile function. These results suggest that hESC-vSMCs possess the essential characteristics needed to support the formation of *in-vitro* microvasculature.

In summary, improved protocols for differentiation of hESCs could yield highly purified cultures of hESC-vSMCs. These hESC-vSMCs display the molecular and functional characteristics of vSMCs, and hence have the potential to support engineered vascular networks.

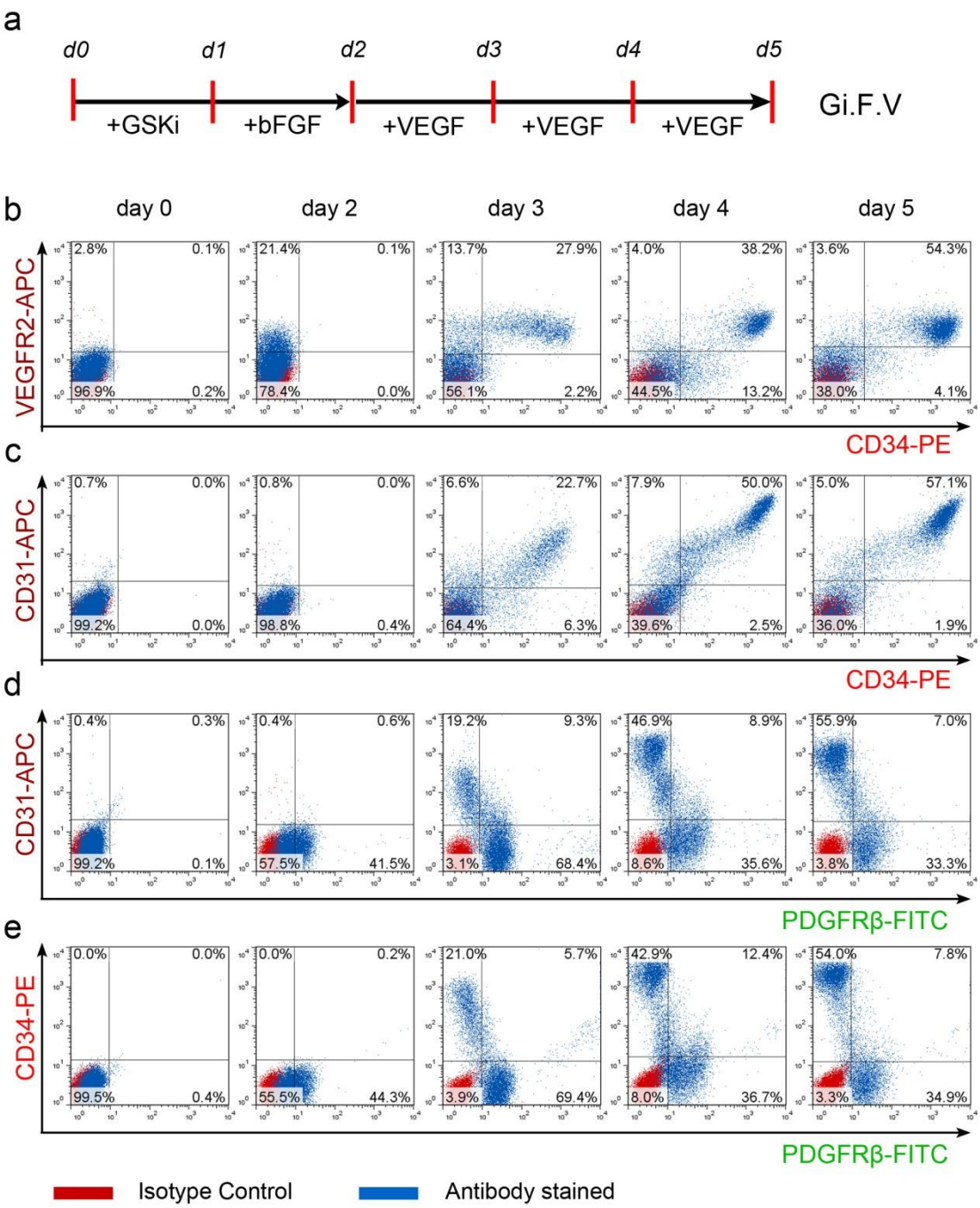

Figure 48. Flow cytometry analysis VEGFR2, CD34, CD31 and PDGFRβ expression upon differentiation of hESCs towards paraxial mesoderm lineage.

(a) Schematic representation of differentiation of H1-hESCs towards paraxial mesoderm by sequential treatment with CHIR99021 (+GSKi) and bFGF for 24 hours each followed by exposure to VEGF for 3 days. Representative flow cytometry overlays display the kinetics of co-expression of VEGFR2 and CD34 **(b)**, CD31 and CD34 **(c)**, CD31 and PDGFRβ **(d)**, and CD34 and PDGFRβ **(e)** over 5 day period of differentiation of H1-hESCs, in the presence of VEGF after initial treatment with GSKi and bFGF for 24 hours each.

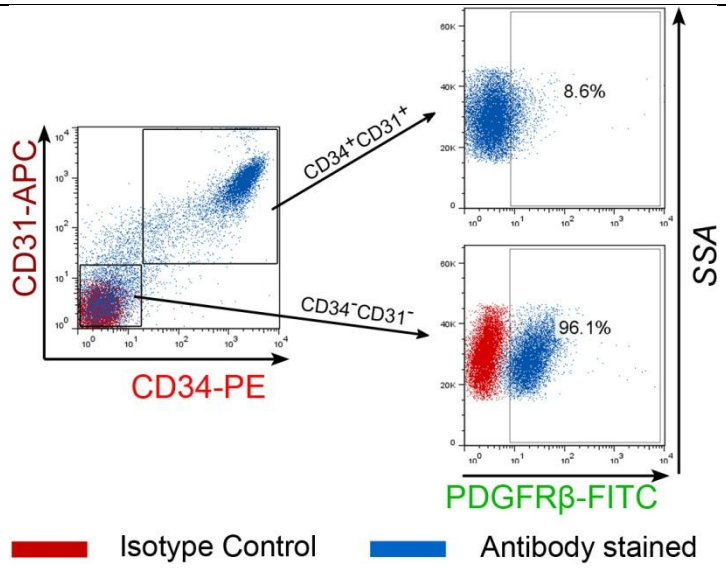

Figure 49. Flow cytometry analysis of co-expression of CD34, CD31 and PDGFRβ upon differentiation of hESCs towards paraxial mesoderm lineage.

Representative flow cytometry overlays display the kinetics of co-expression of CD31, CD34 and PDGFRβ after 5 days of differentiation of H1-hESCs, in the presence of VEGF for 3 days after initial treatment with GSKi and bFGF for 24 hours each. Left panel shows the co-expression of CD31 and CD34. The right panel shows the expression of PDGFRβ among $CD34^{+}CD31^{+}$ and $CD34^{-}CD31^{-}$ subsets.

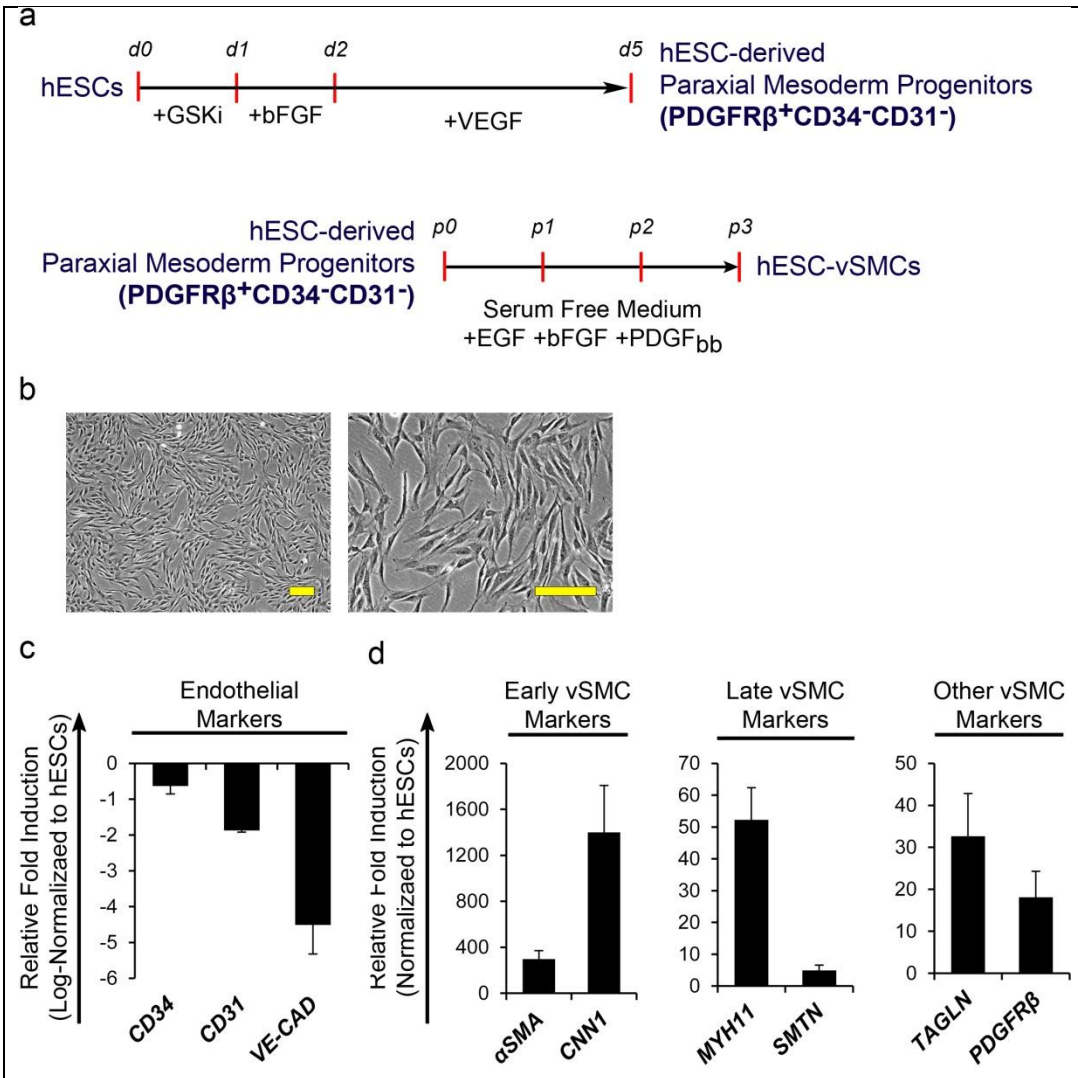

Figure 50. Terminal differentiation of PDGFRβ^{+}CD34^{-}CD31^{-} paraxial mesoderm intermediates to vSMCs under serum-free conditions.

(a) Schematic representation of differentiation of hESCs to paraxial mesoderm intermediates (PDGFRβ^{+}CD34^{-}CD31^{-}) cells by sequential treatment with CHIR99021 (+GSKi), bFGF, followed by VEGF. The hESC-derived CD34^{+}CD31^{+} cells were sorted using flow cytometry after 5 days of differentiation and further differentiated towards vSMCs under the influence of $PDGF_{bb}$ under serum-free conditions. **(b)** Representative photomicrographs show the spindle-shaped morphology of H1-vSMCs. mRNA profiles of pan-endothelial **(c)**, and vSMC markers **(d)** after differentiation of H1-hESCs towards vSMCs. For gene expression plots, the levels of expression were normalized to corresponding *β-ACTIN* values and are represented as relative to that of undifferentiated hESCs. Error bars: s.d. (n≥2). Scale bars: 200µm.

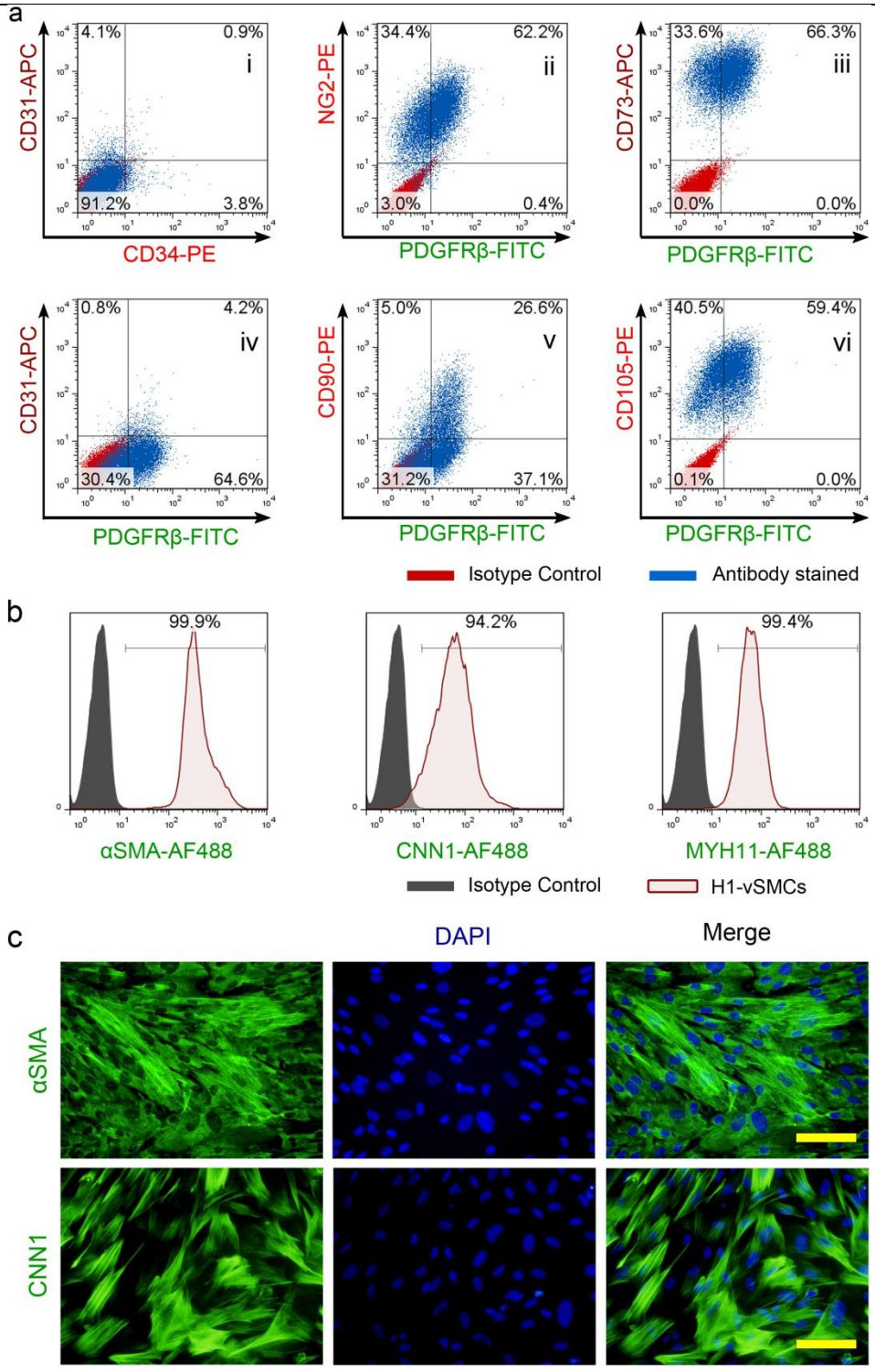

Figure 51. Flow cytometry and immunocytochemical analysis of hESC-derived vSMCs.

(a) Representative flow cytometry overlays display the expression of surface markers related to endothelial (CD34, CD31), vSMC/pericytes (PDGFRβ, NG2), and mesenchymal (CD73, CD90, CD105) cells. The overlays show co-expression of (**i**) CD34 and CD31; (**ii**) NG2 and PDGFRβ; (**iii**) CD73 and PDGFRβ; (**iv**) PDGFRβ and CD31; (**v**) CD90 and PDGFRβ; and (**vi**) CD105 and PDGFRβ. **(b)** Representative flow cytometry histogram overlays show the expression of intracellular protein αSMA, calponin (CNN1) and smooth muscle myosin heavy chain (MYH11). **(c)** Photomicrographs display the intracytoplasmic expression of smooth muscle-related proteins αSMA and CNN1 by H1-vSMCs. Scale bars: 200µm

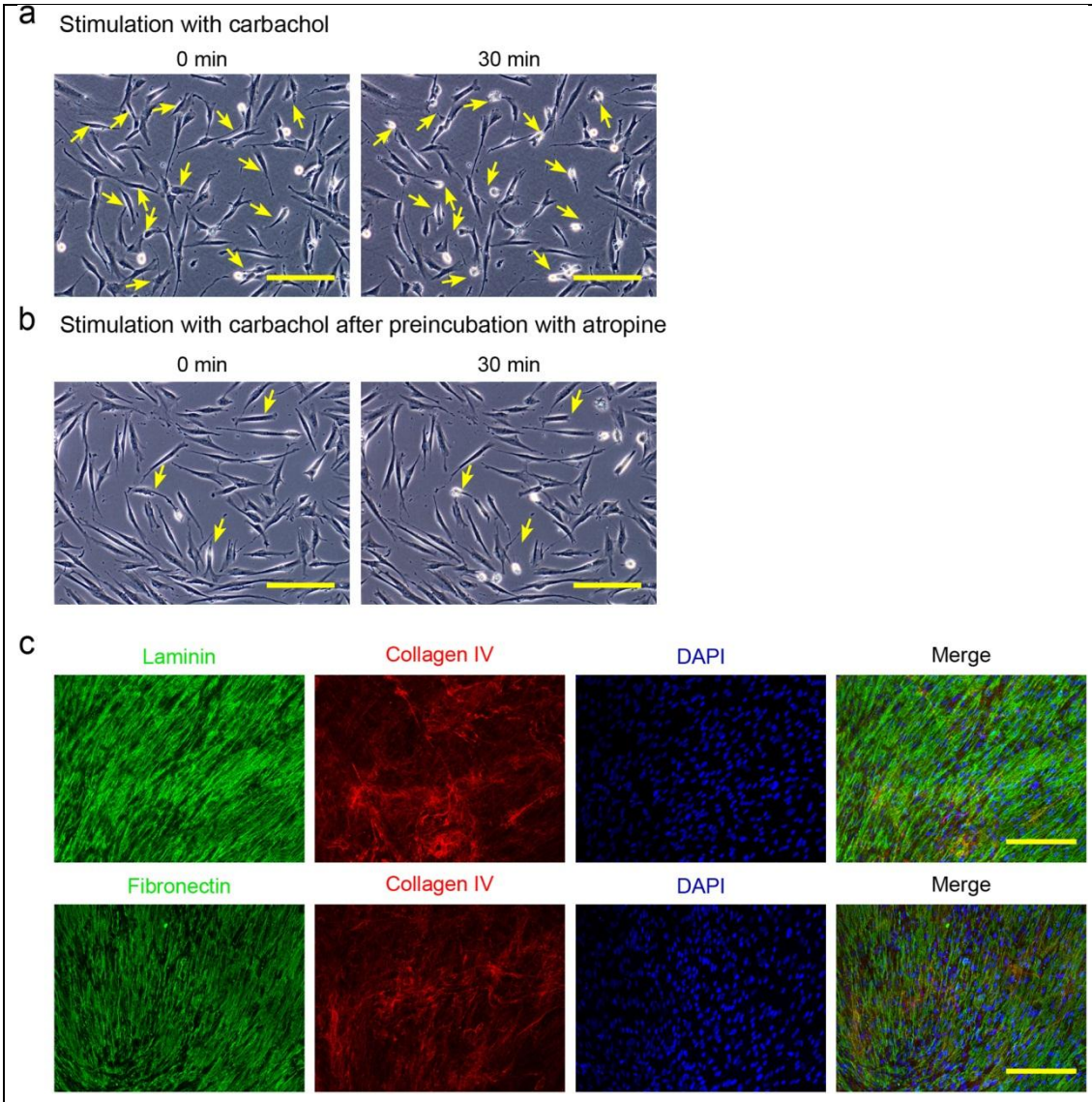

Figure 52. Contractility and ECM production by hESC-derived vSMCs.

The photomicrographs show the contractility of H1-vSMCs after 30 minute stimulation with carbachol **(a)** and lack of contraction when stimulated with carbachol after 1 hour preincubation with atropine **(b)**. The photomoicrographs on the left and right side represent the pictures taken before and after stimulation with carbachol and arrows point at the cells that have contracted. **(c)** Photomicrographs display the expression of ECM proteins laminin, collagen and fibronectin by H1-vSMCs. Scale bars: 500µm

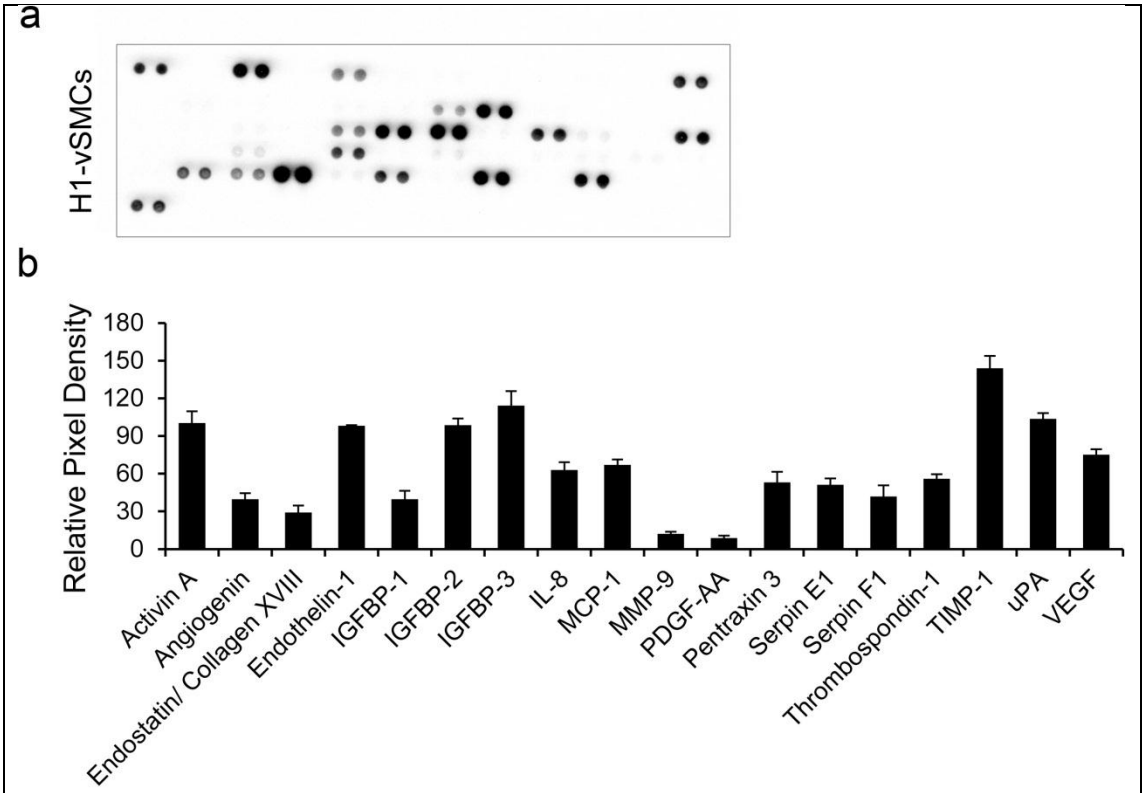

Figure 53. Angiocrine secretory profile of hESC-derived vSMCs using angiogenesis antibody array.

(a) Representative scan of angiogenesis antibody arrays demonstrating the secretion of various angiocrine factors by H1- vSMCs. Array images are obtained from 10-minute exposure of X-ray film. **(b)** Graphical representation of the relative amounts of angiocrine factors secreted by H1-vSMCs. The bars represent relative amounts of factors secreted based on densitometric analysis of relative pixel density of the blots. ***Figure 54*** provides the complete densitometric analysis of all the 55 angiocrine factors analyzed using antibody arrays. Error bars: s.d. (n=2).

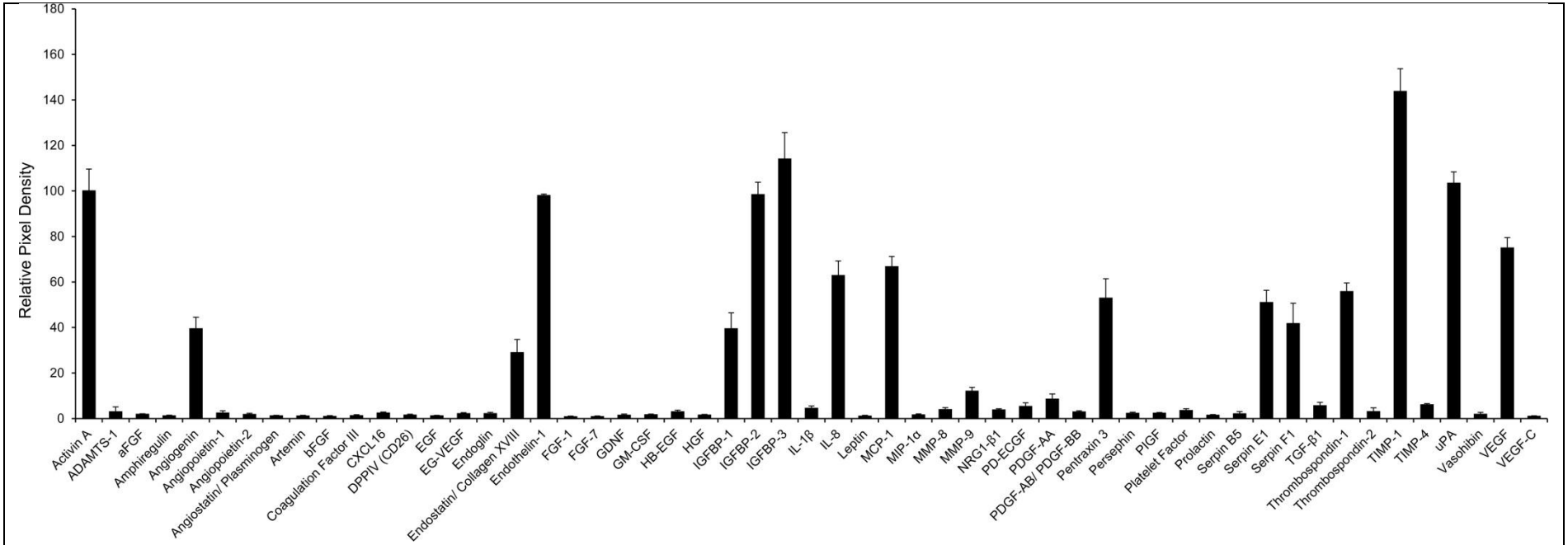

Figure 54. Survey of secretory profile of 55 angiocrines by hESC-derived vSMCs using angiogenesis antibody array.

Graphical representation of the relative amounts of 55 angiocrine factors secreted by H1-vSMCs analyzed using angiogenesis antibody array. The bars represent relative amounts of factors secreted based on densitometric analysis of relative pixel density of the blots. Error bars: s.d. (n=2).

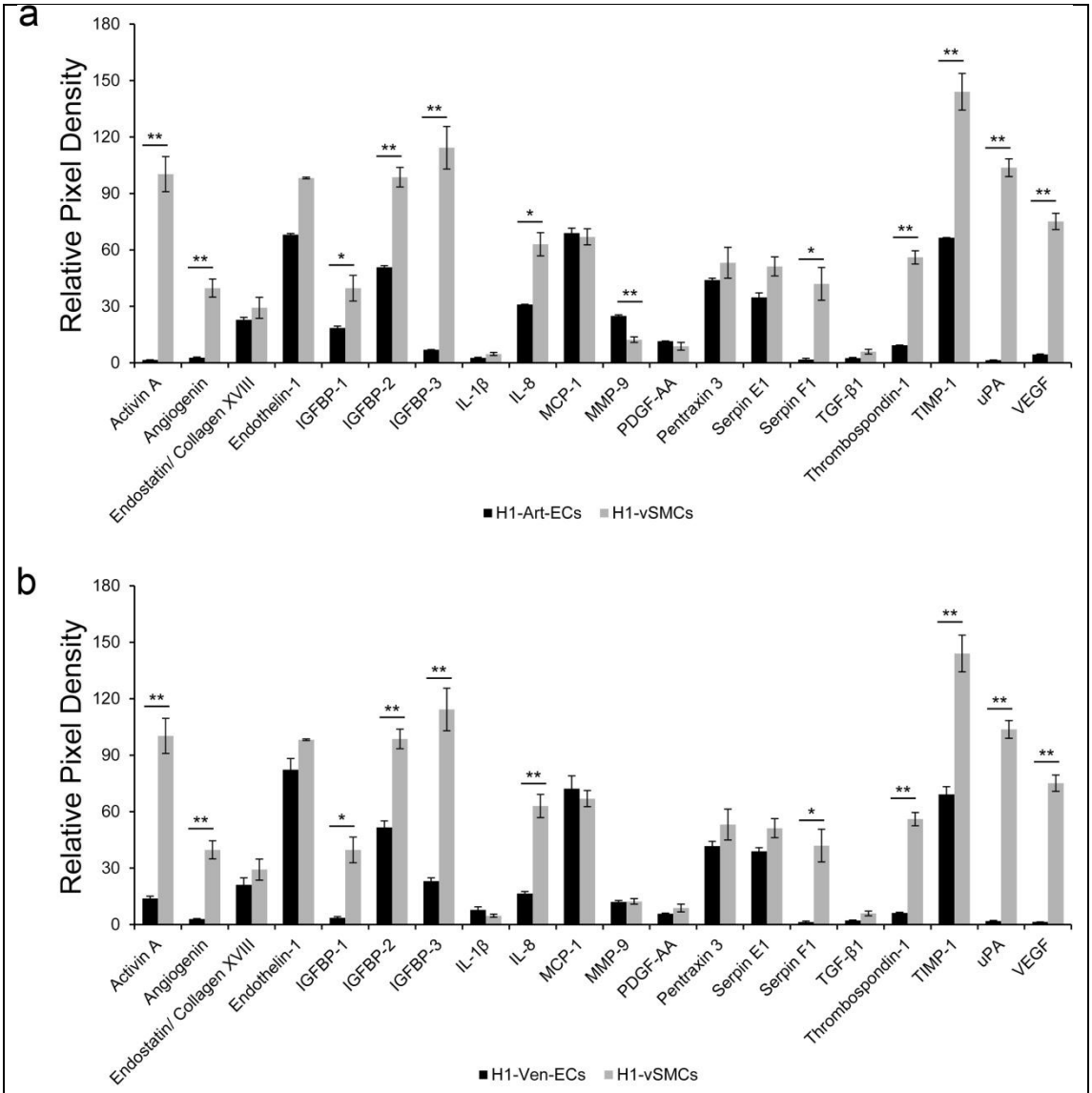

Figure 55. Comparison of angiocrines secreted by hESC-derived vSMCs and hESC-derived ECs using angiogenesis antibody array.

Graphical representation of the relative amounts of selected angiocrine factors among H1-vSMCs and H1-Art-ECs **(a)**, H1-vSMCs and H1-Ven-ECs **(b)**. The bars represent relative amounts of factors secreted based on densitometric analysis of relative pixel density of the blots. Error bars: s.d. (n=2). *p<0.05. **p<0.01.

Chapter 7

Fabrication of in-vitro vascularized tissue equivalents using hESC-derived arterial ECs and vSMCs

7. Fabrication of *in-vitro* vascularized tissue equivalents using hESC-derived arterial ECs and vSMCs

7.1. Introduction

One of the major obstacles challenging successful tissue engineering is the scaffold vascularization that can support the survival of implanted cells *in-vivo* (Novosel et al., 2011). Tissue constructs could be vascularized, either by promoting the invasion of host vasculature into the graft or by using vascular cells within the graft that could form vascular networks and integrate with the host vasculature (Kaully et al., 2009; Rivron et al., 2008). However, studies have shown that prevascularization of the tissue construct enables accelerated engraftment of the implanted tissues by anastomoses of graft vasculature with host vasculature (Chen et al., 2009; Tremblay et al., 2005). Additionally, protocols to fabricate *in-vitro* 3D vascularized tissue equivalents could provide an *in-vitro* platform to study vascular morphogenesis, angiogenesis modulating factors, barrier properties of ECs (permeability) and also aid in development and testing of various vascular pharmaceutical products.

7.2. Objective

To investigate the potential of,

1. hESC-Art-ECs to self-assemble into microvascular networks within a 3D microenvironment under serum-free conditions.
2. hESC-vSMCs to support and stabilize the microvascular networks formed by hESC-Art-ECs.
3. PEG-Fibrin gels to support the fabrication of *in-vitro* vascularized tissue equivalents.

7.3. Materials and Methods

7.3.1. Fluorescent labeling of hESC-derived arterial ECs and vSMCs

To enable visualization of cells within a 3D culture system, the hESC-derived vascular cells were fluorescently labeled. To fluorescently label H1-Art-ECs, H1-hESCs expressing enhanced green fluorescent protein (eGFP) was used. The H1-hESCs expressing eGFP was established by members of A/P Cao Tong. Briefly, H1-hESCs grown on mouse embryonic fibroblasts were single cell dissociated using accutase and transfected with a plasmid construct consisting of pAcGFP1-1 backbone with pCAG-GFP promoter (Clontech) using X-tremeGENE HP DNA Transfection Reagent (Roche). The transfected H1-hESCs were seeded onto mouse embryonic fibroblast feeders and medium was supplemented with Y27632 (Inhibitor of Rho-associated protein kinase, ROCK; Stemgent) to aid cell survival and

attachment. With every passage colonies expressing eGFP were manually selected and passaged to obtain H1-hESC colonies with homogeneous expression of eGFP. These H1-hESCs expressing eGFP were then transferred to feeder-free system over Matrigel (BD Biosciences) and mTeSR1 (StemCell Technologies). After the H1-hESCs were adapted to feeder-free system for more than 5 passages were differentiated using sequential modulation of Wnt, FGF, BMP and VEGF signaling pathways as described earlier in ***Chapter 5***. After 5 days of differentiation, H1-hESCs expressing eGFP, CD34 and CD31 were sorted using FACS and differentiated further towards arterial ECs in ESFM supplemented with EGF, bFGF and VEGF as described in ***Chapter 5***. The H1-Art-EC^{eGFP+} were cultured for at least 3 passages before characterization and use for co-culture studies.

To fluorescently label hESC-derived vSMCs, the H1-hESCs were differentiated to vSMCs as described in ***Chapter 6***. The H1-vSMCs were then transduced with a reporter lentiviral construct encoding DsRed2 gene. This part of the research was done in collaboration with Dr. Gan Shu Uin (Department of Surgery, National University of Singapore). Briefly, WPT-DsRed2 lentivirus was produced by transient transfection of $5x10^6$ 293T cells seeded in 10cm tissue culture plates 24 hours before transfection via polyethylenimine-mediated transfection method with 5μg pWPT-DsRed2 vector, 3.75μg helper plasmid pPax2, and 1.75 μg of MD2G envelope plasmids (gifts from Dr. D Trono, University of Geneva, Geneva, Switzerland). Fresh medium was added 14-16 hours after transfection. Following supernatant filtration through a 0.45μm filter, the viral titer on 293T cells was determined using flow cytometry. SMCs were infected with supernatant containing pWPT-DsRed2 at a multiplicity of infection (MOI) of 5, and sorted for DsRed2 positivity subsequently. The H1-vSMC^{DsRed+} were cultured for at least 3 passages before characterization and use for co-culture studies.

7.3.2. Flow cytomerty analysis and sorting

Flow cytometry analysis of differentiated cells for cell surface antigens (CD34, CD31, VEGFR2, PDGFRβ, NG2, CD90, CD73, CD105) were performed and analyzed as previously described under Section 4.3.4. The labeled cells were analyzed using Dako Cytomation CyAn ADP. For sorting paraxial mesoderm intermediates, the cells labeled with surface markers were sorted using a Dako Cytomation MoFlo high speed flow cytometer. The flow cytometry data was further analyzed using FlowJo v7.6.5 (TreeStar).

7.3.3. Fabrication and culture of 3D tissue equivalents

Fibrinogen from bovine plasma (MP Biomedicals, Cat. No. 154165) and polyethylene glycol-4-arm, succinimidyl glutarate terminated (Sigma, Cat No. 565768; 10,000 Da; PEG) were used for the fabrication of PEG-fibrin gels. PEG-fibrin gels were fabricated as previously

published (Natesan et al., 2012; Natesan et al., 2011). Briefly, fibrinogen was reconstituted at a concentration of 80mg/ml in 0.1 M sodium bicarbonate (pH8.3) at room temperature with gentle shaking for 1 hour and aliquots stored at -80^{0}C (***Appendix V***). PEG was reconstituted at a concentration of 8mg/ml at aliquots stored at -20^{0}C. To fabricate PEGylated fibrin gels, fibrinogen and PEG were mixed in a ratio of 40:1 such that the final concentrations of fibrinogen and PEG in the gel would be 10 mg/ml and 0.25 mg/ml respectively. The resultant PEG-fibrinogen solution was incubated at 37^{0}C for 20 minutes. Then the cells (H1-Art-ECs^{eGFP+} and/or H1-vSMCs^{DsRed+}) were suspended in appropriate volumes of media and mixed with PEG-Fibrinogen solution (***Appendix VI***). Thrombin (Sigma) was used to aid the gelation of PEG-fibrinogen solution. Thrombin (100U/ml) was mixed with calcium chloride (40mM) in a ratio of 1:3 to yield a final concentration of 12.5U/ml in the gel. The PEG-fibrinogen-cell suspension was allowed to undergo gelation by addition of equal volume of thrombin-calcium chloride solution. The cell-gel mixture was pipetted into a 12-well culture insert (9mm) or into angiogenesis µ-slides (ibidi), incubated at 37^{0}C for 10 minutes for complete gelation. After the incubation, the gels were incubated with ESFM supplemented with bFGF (20ng/ml), EGF (10ng/ml) and VEGF (10ng/ml).

7.3.4. Optimization of density of ECs in the 3D co-culture system

To determine the optimal concentration of ECs and vSMCs within the co-culture system different densities of ECs were used. The ratio of vSMCs/ pericytes to ECs is reported to vary from 1:1 to 1:100 depending on the tissue in the body (Shepro and Morel, 1993). We used a fixed vSMCs to ECs ratio of 1:10 for all the experiments. For optimization experiments, H1-Art-ECs^{eGFP+} were used at densities of 1x10^6, 1.5x10^6, 2x10^6 and 2.5x10^6 ECs per ml of PEG-fibrin gel with H1-vSMCs^{DsRed+} at a density corresponding to a ratio of 1:10 (vSMCs:ECs). For these experiments, the 3D PEG-fibrin gels were casted into angiogenesis µ-slides (ibidi). Images of microvascular networks were captured using laser scanning confocal microscope at a 10x magnification after 6 days of culture. The individual z-stacks of the resultant images were stacked into a single two-dimensional image using Olympus Fluoview ver.3.0 viewer.

7.3.5. Confocal Imaging of 3D tissue equivalents

To facilitate imaging of 3D tissue equivalents, the PEG-fibrin gels were casted into angiogenesis µ-slides (ibidi). µ-slide angiogenesis is a special slide with 15 microwells available primarily for assessing endothelial tube formation over Matrigel (***Figure 18***). Each microwell of the µ-slide is of 5mm in diameter and contains another smaller microwell compartment of 4mm diameter and 0.8 mm depth. The inner well is designed to hold the matrix/ 3D scaffold (volume=10mm^3), and the upper compartment for holding the media (volume=50mm^3).

The 3D tissue equivalents with H1-Art-ECs^{eGFP+} with or without H1-vSMCs^{DSR+} were imaged by confocal microscope (Olympus FluoView™ FV1000). Imaging fields consisted of 4-5 randomly selected fields within each microwell of the 3D co-culture. Z-stacks were obtained at 4x, 10x, 20x and 60x magnifications at various time points that include 0, 3, 6, 9, 12, 15, and 18 days. The z-stacks obtained were processed using Imaris v6.1.5 software.

7.3.6. In-vitro 3D *permeability assay*

To assess the permeability of vascular channels *in-vitro* in a 3D microenvironment a model using inverse permeability was recently developed (Grainger and Putnam, 2011). Briefly, dextran-Texas Red conjugated (molecular weight of 70kDa, Invitrogen) was used as the tracer dye to assess the permeability of the microvessels. To enable visualization using confocal microscopy, 3D vascularized tissue constructs were fabricated using H1-Art-ECseGFP+ and H1-vSMCs (non-fluorescent). After 18-21 days of culture, the 3D vascularized constructs were incubated with dextran (5mg/ml) in ESFM for 30 minutes at 37^{o}C, washed thrice with PBS (for 10 minutes each) and imaged using laser-scanning confocal microscope. In some experiments, the 3D constructs were preincubated with histamine (100µM, Sigma) for 5 minutes before incubation with dextran.

7.3.7. Statistical Analysis

All tube formation assays were performed in triplicates with duplicate readings each. The total tube length (expressed in pixels), number of tubes and number of branching points were analyzed using WimTube Key Metrics Program (Wimasis GmbH, Munich, Germany). One-way ANOVA with Bonferroni post-hoc test was used to determine significance between groups using GraphPad Prism 4.02.

7.4. Results

7.4.1. Fluorescent labeling of hESC-Art-ECs

To facilitate visualization of the ECs within the 3D environment, the hESC-Art-ECs were differentiated from H1-hESCs expressing eGFP (***Figure 56***). The differentiated cells displayed characteristic cobblestone morphology and almost all of the cells expressed eGFP (***Figure 56***). Using flow cytometry, the proportion of H1-Art-ECs expressing eGFP and endothelial markers were analyzed. Bivariate flow cytometry plots reveal ~100% of the cells express eGFP and these cells co-express CD31 (~100%), CD34 (~92%) and VEGFR2 (~98%) indicating the endothelial characteristic of these cells (***Figure 56***). These eGFP expressing H1-Art-ECs would be referred to as H1-Art-ECs^{eGFP+}.

7.4.2. Fluorescent labeling of hESC-vSMCs

To enable the visualization of vSMCs within the 3D environment, the hESC-vSMCs were differentiated to PDGFRβ^{+}CD34^{-}CD31^{-} cells from H1-hESCs as described earlier in ***Chapter 6***. The PDGFRβ^{+}CD34^{-}CD31^{-} cells were sorted by FACS and differentiated to H1-vSMCs. The H1-vSMCs were then transduced with lentivirus encoding DS-Red2. The H1-vSMCs after transduction were passaged for 2-3 passages before characterization and usage for further studies. The H1-vSMCs after transduction maintained the spindle-shaped morphology and almost all of the cells expressed DS-Red2 (***Figure 57***). However, the intensity of fluorescence was heterogeneous with some of the cells been bright and certain others faint. Using flow cytometry, the proportion of H1-vSMCs expressing DS-Red2, and perivascular markers were analyzed. Bivariate flow cytometry plots reveal almost 100% of the cells express DsRed2, however there were two populations corresponding to the intensity of fluorescence (***Figure 57***). These cells co-expressed CD73 (~100%), CD90 (~48%) and PDGFRβ (~74%) while they lacked the expression of CD34 and CD31 similar to the H1-vSMCs before the transduction (***Figure 57***). These DS-Red2 expressing H1-vSMCs would be referred to as H1-vSMCs^{DsRed+}.

7.4.3. Co-culture of H1-hESC derived ECs and vSMCs within PEG-fibrin gels

To fabricate 3D vascularized tissue equivalents and visualize the self-assembly of ECs into vascular networks by confocal microscopy, H1-Art-ECs^{eGFP+} and H1-vSMCs^{DsRed+} were co-cultured within PEG-fibrin gels casted into angiogenesis µ-slides (ibidi). Each gel occupied the inner well of the µ-slides and occupied a volume of 10mm^3 (4mm x 4mm x 0.8mm). To validate the ability of these cells to form microvascular networks in larger formats, the 3D vascularized tissue equivalents were fabricated within 12-well culture inserts using 300mm^3 of PEG-fibrin gel. Further to provide the serum-free conditions, the 3D tissue equivalents were cultured in ESFM supplemented with EGF, bFGF and VEGF.

7.4.3.1. Optimization of seeding density of ECs within the 3D PEG-fibrin co-culture system

To determine the optimal concentration of ECs and vSMCs within the co-culture system different densities of ECs were used. The ratio of vSMCs/ pericytes to ECs is reported to vary from 1:1 to 1:100 depending on the tissue in the body (Shepro and Morel, 1993). We used a fixed vSMCs to ECs ratio of 1:10 for all the experiments. For optimization experiments, H1-Art-ECs^{eGFP+} were used at densities of 1x10^6, 1.5x10^6, 2x10^6 and 2.5x10^6 ECs per ml of PEG-fibrin gel with H1-vSMCs^{DsRed+} at a density corresponding to a ratio of 1:10 (vSMCs:ECs).

Various parameters related to microvascular networks that include total length of the vascular network, total number of tubes and the number of branching points within the network were used to narrow down on the optimal density of ECs for further experiments. Density optimization studies showed a significant increase in the total tube length, number of tubes, and number of branching points with increase in the seeding density of ECs (***Figure 58***). Based on these experiments, a density of $2.5x10^6$ ECs per ml of PEG-fibrin gels with vSMCs at a ratio of 1:10 (vSMCs:ECs) were used for further studies.

7.4.3.2. Bicellular environment results in stable microvascular networks

To investigate whether H1-Art-ECs could self-assemble into microvascular network, H1-Art-ECs^{eGFP+} at density of $2.5x10^6$ ECs per ml of PEG-fibrin gel were cultured within µ-slides. After 1 day of culture most of the H1-Art-ECs^{eGFP+} were primarily rounded, while some of the ECs had elongated cytoplasm indicating endothelial sprouting. Though, the H1-Art-ECs^{eGFP+} formed short anastomosing cords of ECs after 4 days of culture, by 6^{th} day of culture the endothelial cords started decreasing in number, length and complexity (***Figure 59***). By 8^{th}-9^{th} day of culture no cells were visible for visualization by confocal microscopy.

On the other hand, when H1-Art-ECs^{eGFP+} were co-cultured with H1-$vSMCs^{DsRed+}$, the ECs formed robust microvascular networks that increased in number, length, and complexity with increasing days of culture (***Figure 60***). Further, these bicellular microvascular networks were stable in culture for 3 weeks (***Figure 60***). Furthermore, the size of PEG-fibrin gel constructs remained the same (~zero shrinkage) for the entire 3-week period.

Based on these results we speculate that the inability of H1-Art-ECs to form stable microvascular networks within PEG-fibrin gels is due to the lack of H1-vSMCs within the culture system. While, the addition of H1-vSMCs into the culture milieu, resulted in formation of stable microvascular networks.

7.4.3.3. Vascular morphogenesis within PEG-fibrin gels

We next sought to investigate the morphological changes during the formation and maturation of microvascular networks within PEG-fibrin gels under serum-free conditions. Starting from 1^{st} day after encapsulation of the H1-Art-ECs^{eGFP+} and H1-$vSMCs^{DsRed+}$ within PEG-fibrin gels, z-stack images were obtained over a period of 3 weeks (i.e., days 1, 4, 6, 9, 12, 15, 21) using confocal microscopy. After culturing for 1 day, though most of the cells were rounded, vacuoles were observed within many of these ECs and sprouting of a few ECs, with the vacuolation extending into the sprouts as well (***Figure 61***). On the other hand, the vSMCs were seen to extend fine, branched processes into the surrounding gel (***Figure 60, 61***).

After 4 days of culture, tubulogenesis progressed rapidly resulting in extensive sprouting, network formation and occasional endothelial tubules with open lumen (***Figure 61***). The DsRed2-expressing H1-vSMCs were seen to have longer processes with some of the cells/ cellular processes in close proximity to the eGFP-expressing endothelial tubules. After 6 days of culture, the eGFP-expressing endothelial tubules could be seen to be thicker, with more complex network formation and open, inter-connected lumen-like structure (***Figure 61***). After day 6, the network of endothelial tubules seems to become more complex forming a microvascular network supported by DsRed2-expressing H1-vSMCs. Hence, the H1-Art-ECs^{eGFP+} and H1-vSMCs^{DsRed+} formed bicellular microvascular networks within PEG-fibrin gels within a week, and matured further in terms of thickness, anastomosis and network formation. Further, the bicellular microvascular networks were stable over a period of 3 weeks.

Cross-sectional analysis of Z-stacks of the microvascular networks formed by H1-Art-ECs^{eGFP+} and H1-vSMCs^{DsRed+} reveal the presence of DsRed2-expressing H1-vSMCs just on the periphery of the eGFP-expressing endothelial tubules (***Figure 60, 61***). Also, some of the H1-vSMCs^{DSR+} are seen to encircle the endothelial tubules.

Hence, using ibidi µ-slides we were able to fabricate micro-3D vascularized tissue constructs. To validate the utility of hESC-derived vascular cells in scaling up to a macro-3D constructs, PEG-Fibrin gels were casted within 9mm-culture inserts using 300µl of PEG-fibrin. ***Figure 62*** shows the naked eye view of the construct after 21 days of culture. Confocal imaging of the construct reveals anastomosing network of microvascular channels within the *in-vitro* vascularized tissue equivalent (***Figure 62***). Hence, the hESC-derived vascular cells and PEG-fibrin gels could be utilized to engineer *in-vitro* 3D vascularized tissue equivalents.

7.4.3.4. In-vitro assessment of permeability of the microvascular channels

To assess the permeability of microvascular channels within the *in-vitro* 3D vascularized tissue equivalents, we used the ability of dextran-Texas Red (Molecular weight of 70kDa) to permeabilize the vascular channels. Confocal imaging of the 3D constructs after incubation with the tracer dye revealed that most of the microvessels were impermeable to the dye (***Figure 63***). On the other hand, pre-incubation of the constructs with histamine resulted in marked increase in the permeability of the microvascular channels as evidenced by the presence of aggregates of the tracer dye within the lumen (***Figure 63***). Hence, the microvascular channels within *in-vitro* 3D vascularized tissue equivalents were mature in terms of their barrier function, and also were capable of regulating the permeability in responsive to physiological stimulus like histamine.

7.5. Discussion

All tissues in the body except skin, cartilage and cornea require presence of a vascular network for nutrient and oxygen supply. Hence, tissue engineering and regeneration of tissues and organs require the formation of vascular network within the implant. Various strategies for vascularization using scaffolds, cells and local delivery of angiogenic factors have been investigated to enhance the ingrowth of vessels from the host into the implant (Novosel et al., 2011). However, this process involves considerable amount of time for neovascularization of the implant. Hence, use of large grafts is not clinically feasible as the cells in the core of the implants undergo necrosis due to lack of nutrition (Johnson et al., 2011; Tsigkou et al., 2010). An alternative approach is to prevascularize the tissue construct *in-vitro* or *in-vivo* to expedite the process of blood supply for the implant. Secondly, establishment of 3D prevascularized tissue equivalents would aid in development and testing of pharmaceutical products which otherwise are limited to use of conventional monolayer cell culture systems and/or animal experiments.

ECs have an inherent capability to self-assemble upon 2D direct co-culture or 3D culture within angiogenic biomaterial. However, the development of a vasculature of mature and functional vasculature depends not only on the ECs but also requires the interaction with mural cells (vSMCs/ pericytes) (Carmeliet and Conway, 2001; Ghanaati et al., 2011; Jain, 2003). Additionally, they require the ECM to adhere, migrate and assemble into anastomosing network of vascular channels. In addition to providing a scaffold for the ECs to form vascular networks, the ECM also acts as a growth factor sink by sequestering and releasing various growth factors and other signaling molecules (Kubota et al., 1988; Sahni et al., 2000; Sahni and Francis, 2000; Sahni et al., 2006). Many studies have demonstrated the ability of primary ECs in the presence of supporting cells (pericytes, SMCs, fibroblasts, MSCs) form microvascular networks when cultured within 3D microenvironment (Chen et al., 2009; Grainger and Putnam, 2011; Lesman et al., 2011; Montano et al., 2010; Tsigkou et al., 2010). Recently, self-organization of vascular networks from human PSC-derived vascular cells in a synthetic matrix that integrates with the host circulation has been reported (Kusuma et al., 2013).

In this chapter, we demonstrate that hESC-derived arterial ECs in the presence of hESC-derived vSMCs form mature and stable microvascular networks within PEG-Fibrin gels under serum-free conditions. The presence of hESC-derived vSMCs seems to be a prerequisite for the formation of stable microvascular networks, as the vascular networks formed by hESC-derived arterial ECs undergo early regression in the absence of hESC-derived vSMCs. Hence, the hESC-derived vSMCs seem to play a supportive role for the formation of mature vascular

network similar to the observations *in-vivo* and *in-vitro* (Carmeliet and Conway, 2001; Fuchs et al., 2007; Jain, 2003; Kolbe et al., 2011; Lesman et al., 2011; Montano et al., 2010). The supportive function of the hESC-derived vSMCs could be due to direct contact or through paracrine signaling. Though detailed studies were not carried out to elucidate the mechanism of support, the observation of close proximity of hESC-derived vSMCs and endothelial channels especially at the branch points seems to suggest a supportive role through direct contact. Additionally, in the previous chapter it is shown that hESC-derived vSMCs secrete various positive and negative regulators of angiogenesis (***Chapter 6, Figure 53***). Hence, through these angiocrine molecules the hESC-derived vSMCs could support the formation and maturation of endothelial channels. Various co-culture studies have shown that 2D culture of mural cells and ECs lead to organization of ECs into anastomosing cords over the mural cells indicating the role of direct contact. The paracrine role of mural cell secreted factors in organotypic vessel formation has been reported by various studies (Antonelli-Orlidge et al., 1989; Evensen et al., 2009; Kolbe et al., 2011).

The density and extent of microvascular networks formed seem to depend on the density of hESC-derived ECs within the 3D construct. The number of tubules, branch points and their total length increased with increase in density of ECs seeded within the construct. Based on these observations, hESC-derived ECs were used at a density of $2.5x10^6$ cells/ ml of the construct along with hESC-vSMCs at a ratio of 10:1. Though various seeding densities of ECs were studied the effect of varying densities of hESC-derived vSMCs were not investigated.

Various scaffolds have been used for engineering of vascularized tissues *in-vitro* and *in-vivo*. Scaffold vascularization using primary and hESC-derived vascular cells has been reported in hyaluronic acid, alginate, and dextran-based hydrogels (Hanjaya-Putra et al., 2011; Hanjaya-Putra and Gerecht, 2009), fibrin gels (Chen et al., 2009; Lesman et al., 2011; Montano et al., 2010), PEG-Fibrin gels (Natesan et al., 2012; Natesan et al., 2011), collagen gels (Koike et al., 2004; Wang et al., 2007), PLGA/PLLA scaffolds (Laschke et al., 2008; Levenberg et al., 2005; Tsigkou et al., 2010) and other natural, synthetic and hybrid biomaterials. Fibrin-based scaffolds are an attractive option due to its angiogenic, biocompatible and biodegradable nature. However, fibrin lacks stiffness and undergoes rapid degradation both *in-vitro* and *in-vivo* (Dikovsky et al., 2006). Stiffness of the fibrin hydrogels could be controlled by crosslinking with synthetic polymers like PEG (Dikovsky et al., 2006; Natesan et al., 2011). Hence, we investigated the potential of PEGylated-fibrin based scaffold and hESC-derived vascular cells for fabrication of *in-vitro* vascularized tissue constructs. The hESC-derived vascular cells formed stable microvascular networks within these PEG-fibrin gels.

Additionally, the size of the PEG-Fibrin gel construct remained constant throughout the 3-week culture period indicating the stability of the construct.

Fluorescent labeling of hESC-derived ECs and vSMCs enabled the documentation of the distinct steps in the formation of microvascular networks. The microvascular network formation starts with the formation of intracellular vacuolation, followed by extension of endothelial cytoplasmic processes, organization of adjacent ECs into anastomosing cords, coalescence of the these vacuoles between adjacent ECs, recruitment of vSMCs, formation of endothelial tubules with patent lumen and increase in thickness of the vascular channels. Using PEG-fibrin gels, we found that hESC-derived vascular cells could self-assemble to form microvascular networks within 6-9 days that undergoes further maturation and is stable for 3 weeks *in-vitro*. Some of the earlier studies utilized histology, phase contrast and electron microscopy to study the various morphogenetic events during the formation of microvascular networks (Hanjaya-Putra et al., 2011; Montano et al., 2010). Though fluorescent labeling enabled us to easily track the various morphogenetic events during the formation microvascular network, the early events like basement membrane formation/ disruption, pinocytosis could probably be studied with more details using electron microscopy. Hence, our *in-vitro* vascularized tissue equivalent based on PEG-fibrin gel and hESC-derived vascular cells could provide a valuable platform to study the early morphogenetic events in vasculogenesis and angiogenesis *in-vitro*. Additionally, the fluorescent labeling allowed us to track the formation of vascular networks in a non-invasive manner.

In this part of the study we demonstrate the fabrication of *in-vitro* vascularized tissue equivalent using co-culture of hESC-derived ECs and -vSMCs within PEG-Fibrin gels is possible. Fibrin has been well-demonstrated in the literature as an angiogenic natural biomaterial both *in-vivo* and *in-vitro* (Ahmed et al., 2008; Lesman et al., 2011; Montano et al., 2010; Shaikh et al., 2008). Both fibrin and PEG has been approved by US-FDA for various clinical applications. In the current study, we used bovine fibrinogen to fabricate the PEG-Fibrin gels for economic reasons. However, we believe that the protocol could be replicated using human fibrinogen, but needs further studies for validation.

Functionality of *in-vitro* microvascular networks is usually defined as integration with the host vessels upon *in-vivo* implantation. In addition to the integration, these vessels need to possess sufficient barrier properties and also respond to inflammatory signals that increase/ decrease the permeability of the vessels. To assess the permeability of the implanted microvessels *in-vivo*, studies use fluorescent tracers and/or non-invasive live imaging (Samuel et al., 2013). *In-vitro* equivalent of permeability testing, typically measures the transendothelial resistance across a 2D monolayer of ECs (without the presence of supporting

mural cells) in a transwell system (Adams et al., 2013). To assess the permeability of vascular channels *in-vitro* in a 3D microenvironment, a model using inverse permeability was recently developed (Grainger and Putnam, 2011). The principle behind this model of inverse permeability is that mature microvessels are impermeable to dextrans over a molecular weight of 65kDa, and a tracer would be able to enter inside the lumen of leaky vascular channels, while it cannot enter inside a vascular channel with mature, competent cell-cell endothelial junctions. We adapted this method of inverse permeability to assess the barrier properties of the microvascular networks within hESC-derived *in-vitro* vascularized tissue equivalents. The microvascular channels were generally impermeable to the tracer dye (dextran-texas red), while responded to treatment with histamine resulting in increased leakiness of the microvessels as evidenced by the presence of tracer dye into the lumen of these microvessels. The permeability assessment reveals the maturity and functionality of the hESC-derived microvascular channels *in-vitro*. Though in the original methodology proposed by Grainger and Putnam employed assessment of permeability after fixation, we were able to assess the permeability on live cultures due to the fluorescent labeling of ECs. Hence, we believe that these *in-vitro* vascularized tissue equivalents could be used as a research model to assess/ screen novel compounds for their effect on vascular permeability on a 3D platform.

In conclusion, we demonstrate that *in-vitro* prevascularized tissue equivalents could fabricated using hESC-Art-ECs and hESC-vSMCs co-cultured within PEG-fibrin gels under serum-free conditions. Additionally, the role of hESC-vSMCs in supporting the formation of stable microvascular networks is demonstrated. Further, use of micro 3D constructs using ibidi µ-slides could provide in establishment of an economical and high-throughput platform *in-vitro* to study vascular pharmacological agents in the future.

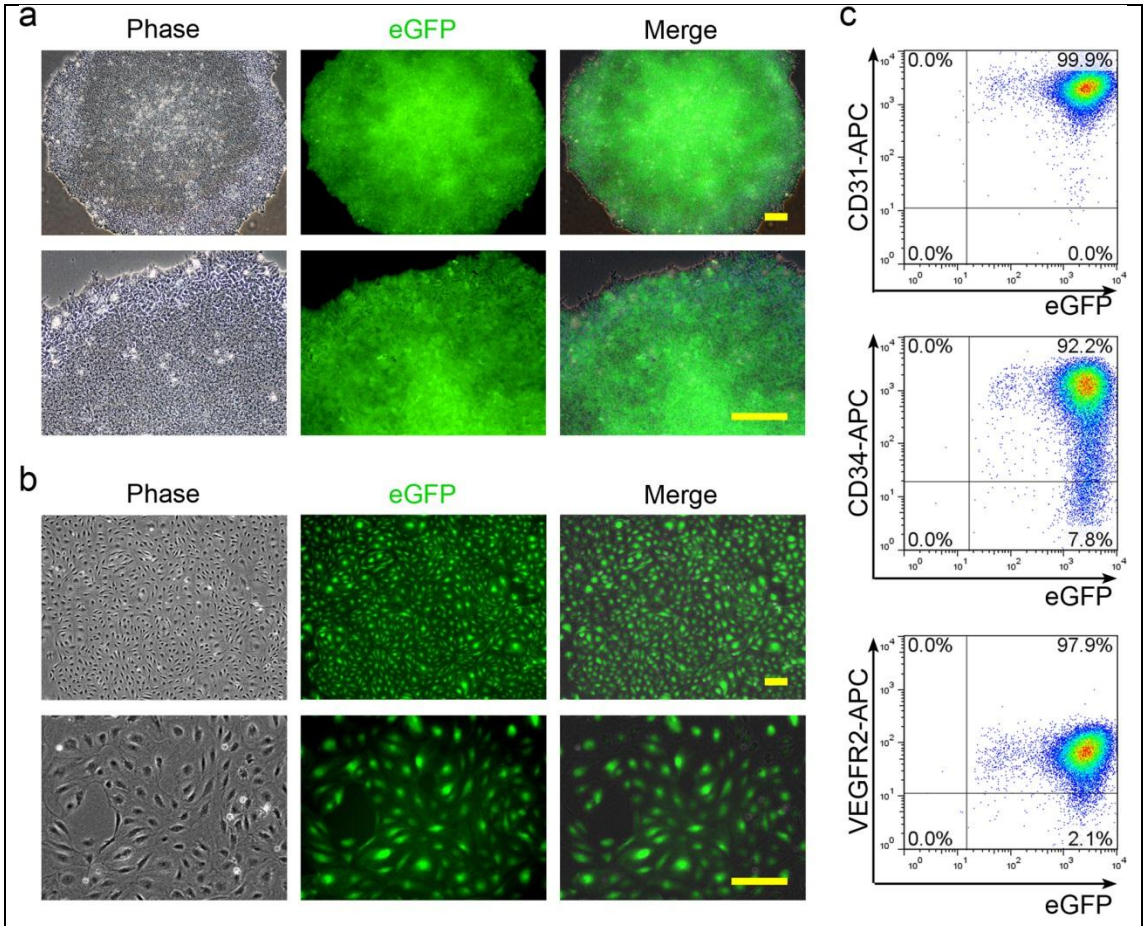

Figure 56. Characterization of hESCs and hESC-derived ECs for eGFP expression.

Photomicrographs display the expression of eGFP by H1-hESCs^{eGFP+} colonies **(a)** and H1-Art-ECs^{eGFP+} cells **(b)** under 4x and 10x magnifications. **(c)** Flow cytometry plots display the co-expression of eGFP and CD31, CD34, VEGFR2 by H1-Art-ECs^{eGFP+}. Scale bars: 200µm.

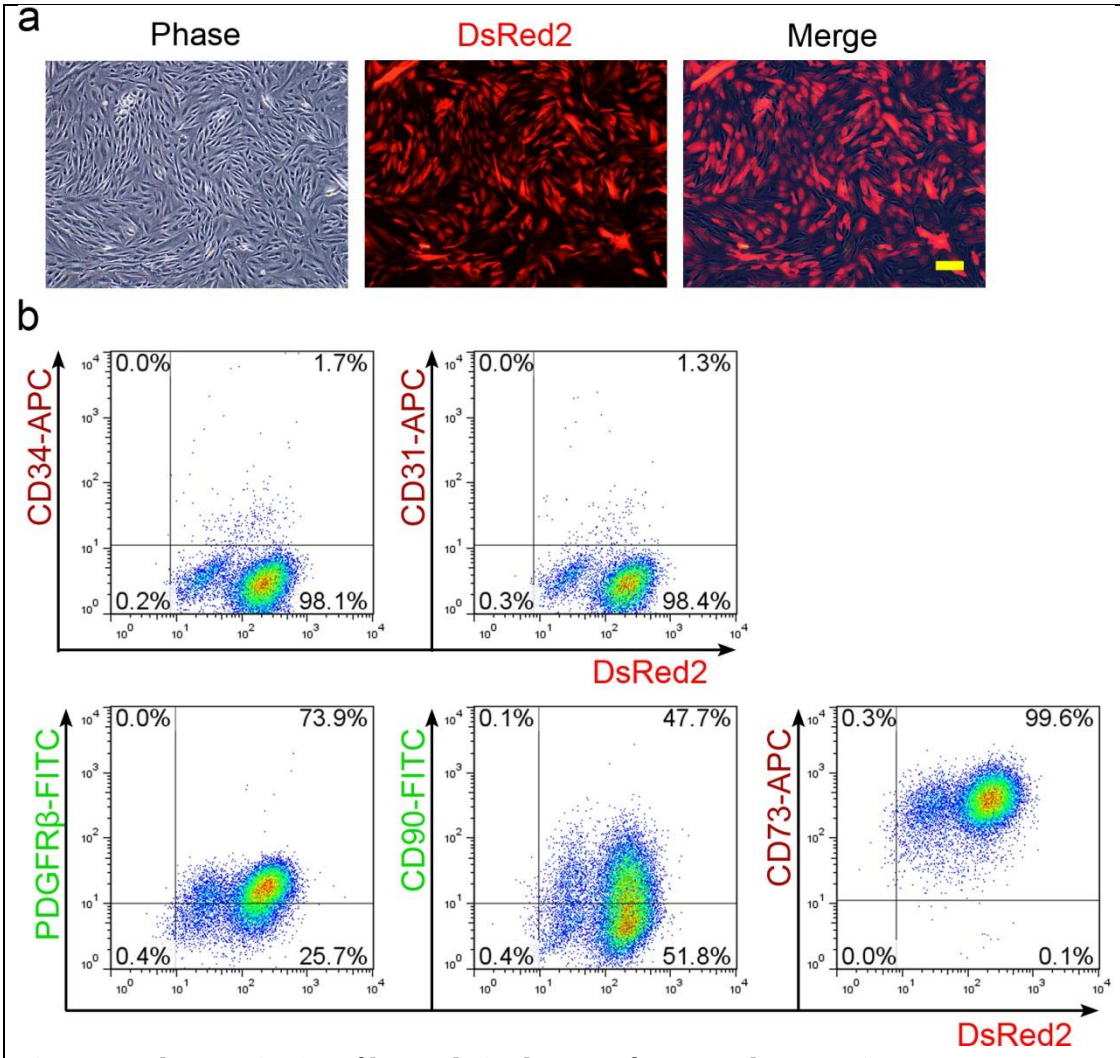

Figure 57. Characterization of hESC-derived vSMCs for DS-Red2 expression.

(a) Photomicrographs display the expression of DsRed2 by H1-vSMCs^{DsRed+} cells. **(b)** Flow cytometry plts display the co-expression of DsRed2 and endothelial-related markers (CD34,CD31), vSMC-related markers (PDGFRβ, CD90, CD73) by H1-vSMCs^{DsRed2}. Scale bars: 200µm

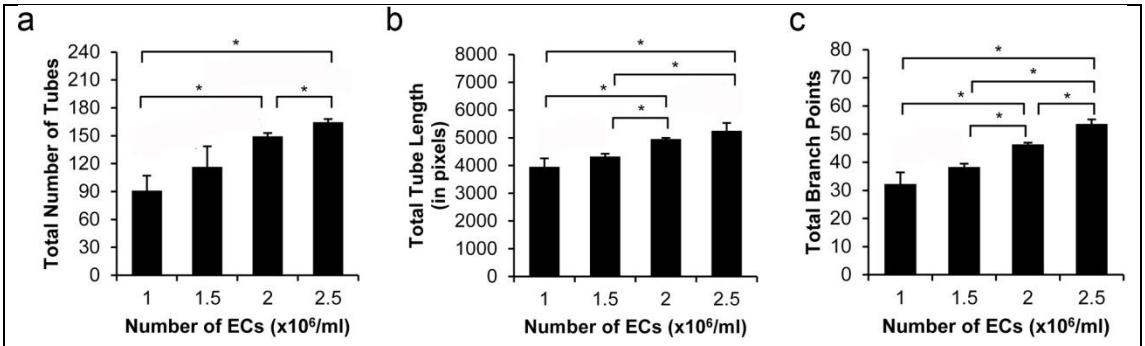

Figure 58. Optimization of seeding density of ECs within the 3D PEG-fibrin co-culture system.

The bar graphs represent the various parameters of microvascular networks formed by H1-Art-ECs^{eGFP+} when seeded with H1-vSMCs$^{DsRed2+}$ at a ratio of 10:1 within PEG-Fibrin gels. The parameters of the microvascular networks represented are **(a)** total length of the vascular network, **(b)** total number of tubes and **(c)** number of branching points within the network. Error bars: s.d. (n=3). *p<0.05.

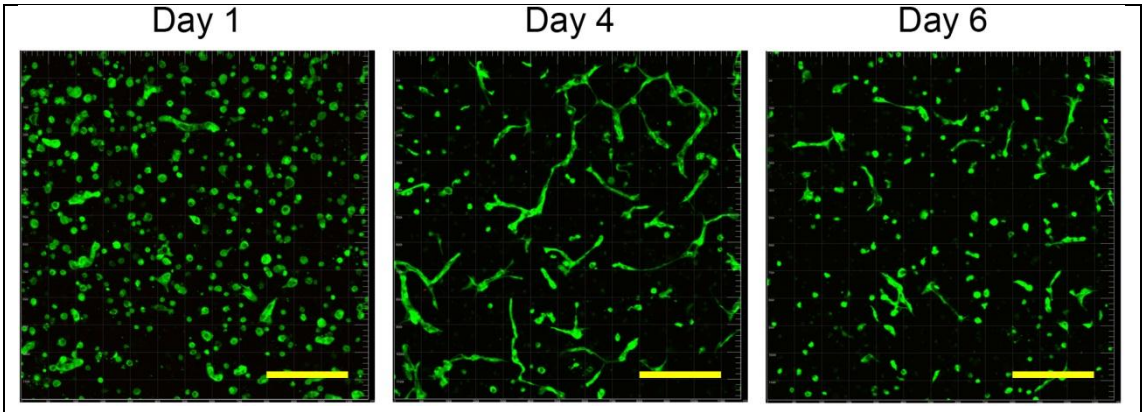

Figure 59. Kinetics of development of microvascular networks by hESC-ECs

The representative photomicrographs display the 3D projection of the confocal z-stack images of the microvascular network formed by H1-Art-ECs^{eGFP+} cells after 3D culture in PEG-Fibrin gels for 1, 4 and 6 days. The series of images show the sprouting of ECs to form anastomosing cords after 4 days of culture, but undergo regression after 6 days. Scale bar: 150µm.

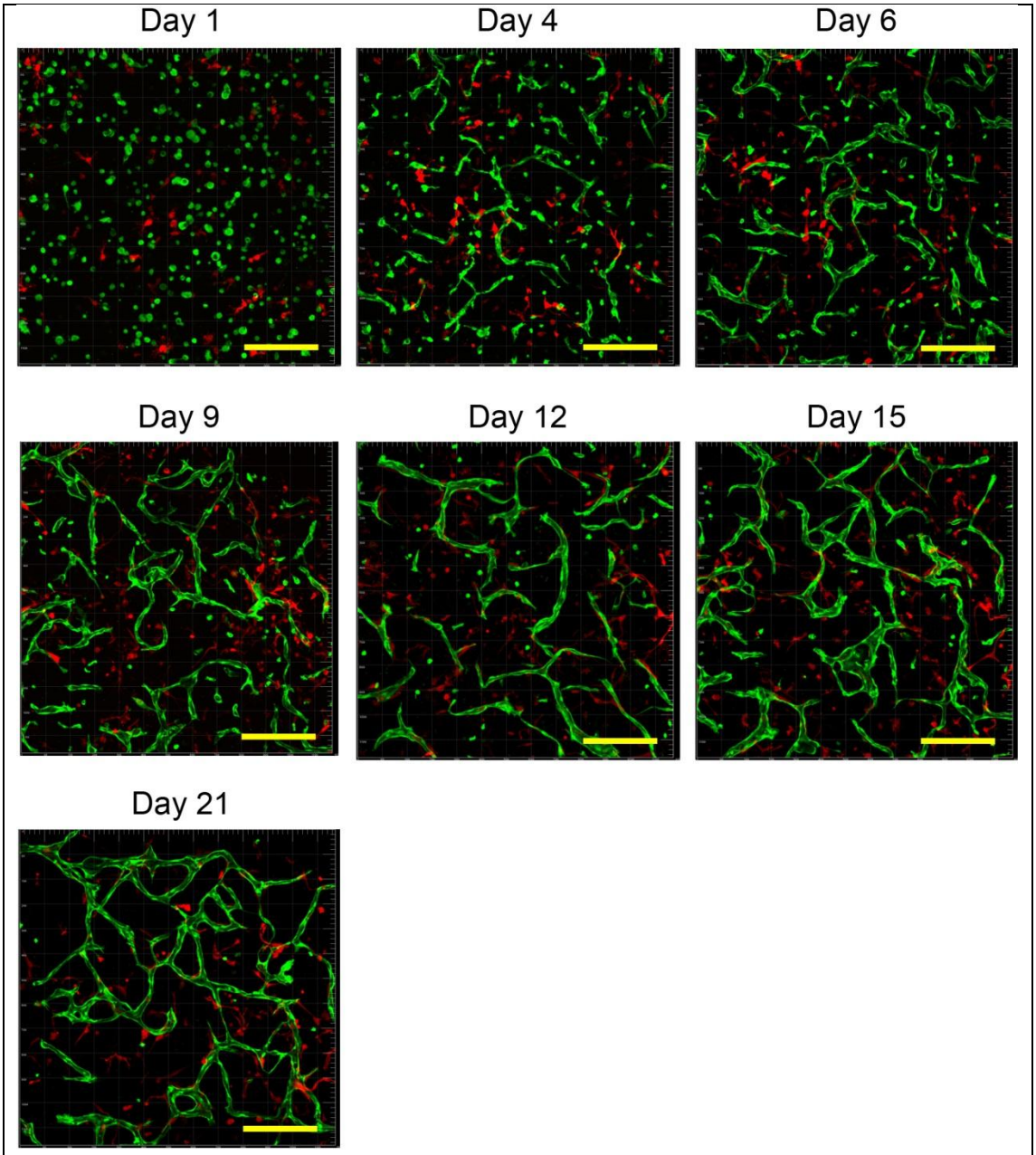

Figure 60. Kinetics of development of microvascular networks by hESC-ECs and –vSMCs.

The representative photomicrographs display the 3D projection of the confocal z-stack images of the microvascular network formed by H1-Art-ECs^{eGFP+} (green) and H1-vSMCs$^{DsRed2+}$ (red) cells after 3D co-culture in PEG-Fibrin gels for 1, 4, 6, 9, 12, 15, and 21 days. The series of images show the sprouting of ECs that forms anastomosing cords after 4-6 days of culture and undergoes maturation in terms of thickness and interconnectivity of the endothelial networks with prolonged culture. Scale bar: each major unit=100µm.

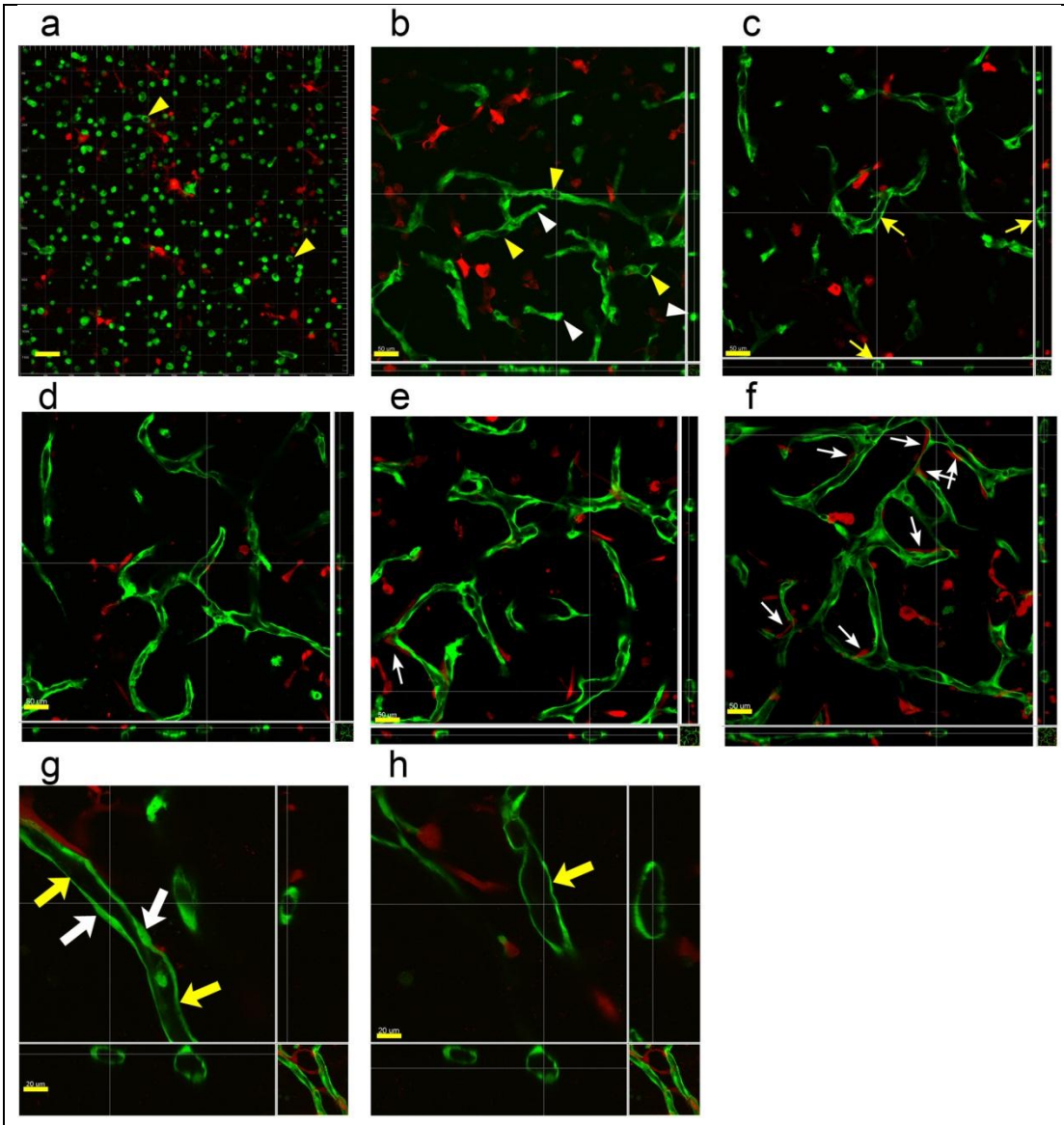

Figure 61. Vascular morphogenesis and maturation of hESC-derived microvascular networks.

The representative photomicrographs display the 3D projection of the confocal z-stack images of the microvascular network formed by H1-Art-ECs^{eGFP+} (green) and H1-vSMCs$^{DsRed2+}$ (red) cells after 3D co-culture in PEG-Fibrin gels for varying periods. All images except **(a)** consist of 4 parts. The upper-left portion represents the image of a single z-plane with corresponding x-z (bottom-left) and y-z (top-right) cross-sectional images of the microvascular networks; and the lower-right corner represents the 3D projection of the confocal z-stack images. **(a)** 1 day after 3D co-culture, most of the ECs were rounded, but a few of the ECs displayed vacuoles (yellow arrowheads). **(b)** After 4 days the ECs displayed tubulogenesis resulting in extensive sprouting, network formation. Some of these endothelial tubules displayed vacuoles/ lumen (yellow arrowheads) and others were resembled cords (white arrowheads). With progression of 3D co-culture **(c-f)** the endothelial networks grew thicker in size and displayed lumen-like structures (thin-yellow arrows). Additionally, the DsRed2-expressing H1-vSMCs (thin-white arrows) are seen in close proximity to the eGFP-expressing endothelial tubules. Further these vSMCs are seen to be on the periphery of the endothelial tubules. Also, the vSMCs are seen in/near the branch points of the endothelial networks. Higher magnification of the endothelial tubules shows a clear lumen **(g, h)**. The photomicrographs in **(g, h)** represent the z-stacks at different layers of the same 3D image. These lumenized structures are surrounded by ECs that display regularly alternating nuclei (thick-white arrows) and cytoplasm (thick-yellow arrows). Scale bar in **(a-f)** 50µm; **(g, h)** 20µm.

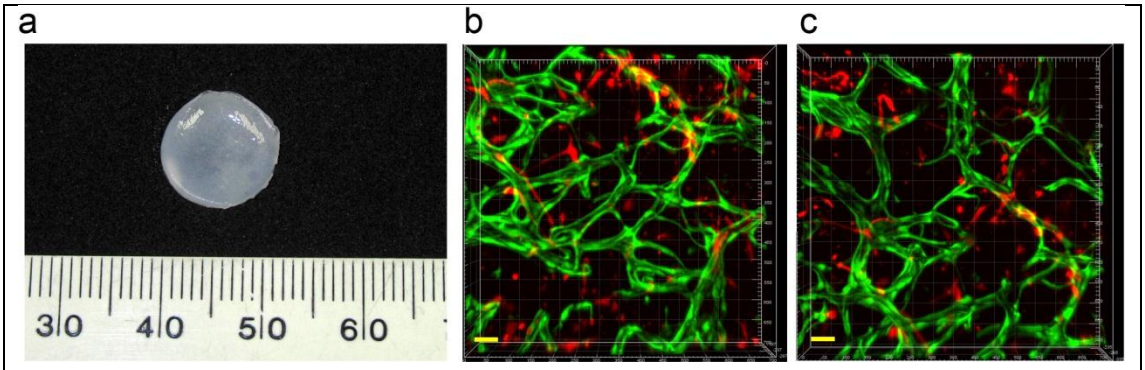

Figure 62. *In-vitro* vascularized tissue equivalent.

The figures show the *in-vitro* vascularized tissue equivalent fabricated within a 9mm-culture insert. **(a)** PEG-Fibrin gel with microvascular networks after 21 day culture period measuring ~9mm in diameter. Scale: each unit equals 1 mm. **(b,c)** The representative photomicrographs display the 3D perspective of the confocal z-stack images of the microvascular network formed by H1-Art-ECs^{eGFP+} (green) and H1-vSMCs$^{DsRed2+}$ (red) cells after 3D co-culture in PEG-Fibrin gels for 21 days within a 9mm-culture insert. Scale bar: 50µm.

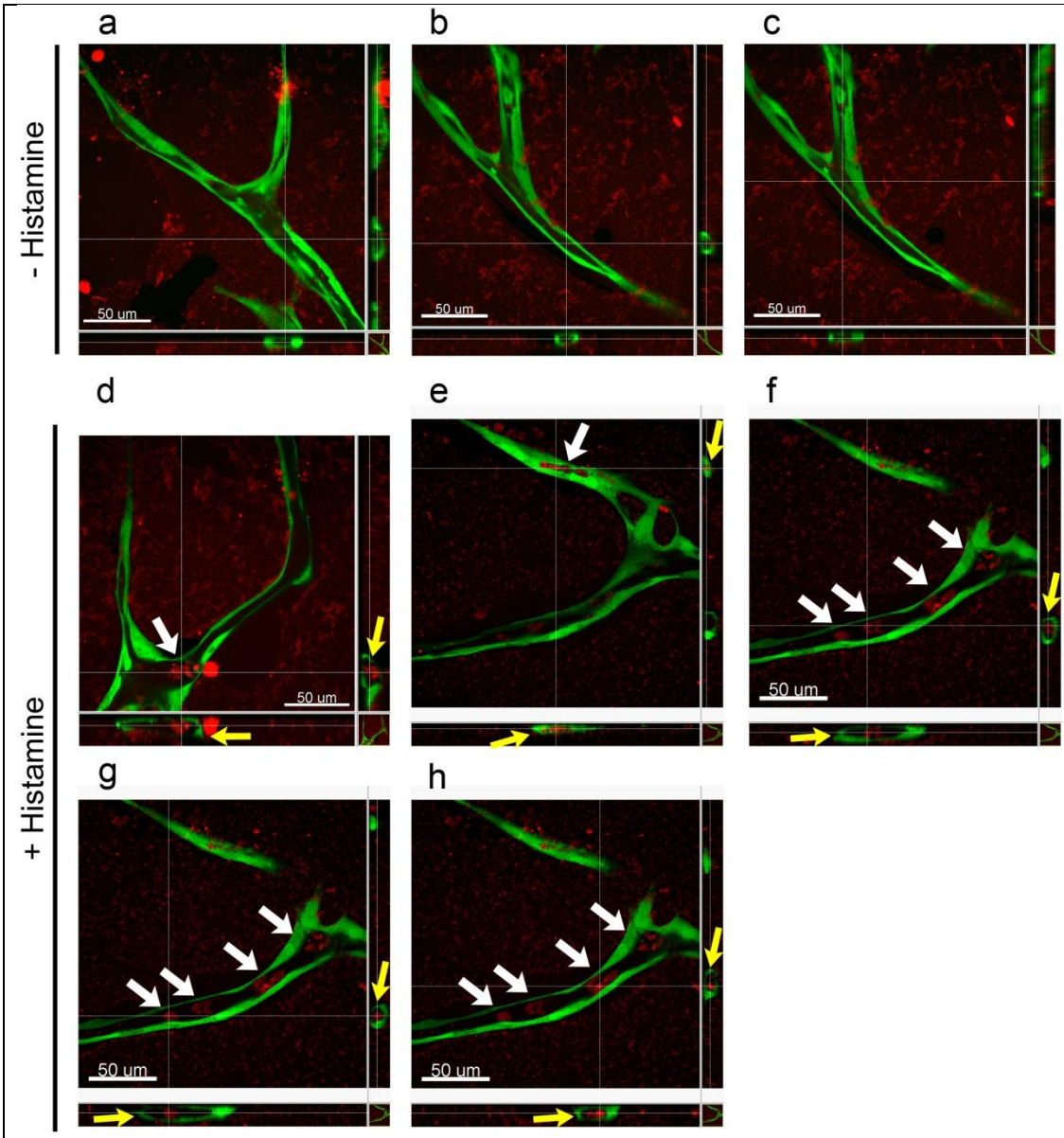

Figure 63. Assessment of vascular permeability of microvascular networks.

The representative photomicrographs display the 3D projection of the confocal z-stack images of the microvascular network formed by H1-Art-ECs^{eGFP+} (green) and H1-vSMCs (not visible) after 3D co-culture in PEG-Fibrin gels. All images except consist of 4 parts. The upper-left portion represents the image of a single z-plane with corresponding x-z (bottom-left) and y-z (top-right) cross-sectional images of the microvascular networks; and the lower-right corner represents the 3D projection of the confocal z-stack images. Permeability of the vascular channels was assessed using dextran-texas red (red particles/ clumps). **(a-c)** The microvascular channels were generally impermeable to the dextran molecule i.e., the dextran molecules are seen outside the vessel wall, and the lumen is clear. **(d-h)** However, upon preincubation of the vascular channels with histamine, resulted in permeabilization of the dextran molecule into the lumen (white arrows) of the microvascular channels, indicating the leakiness in response to histamine. The cross-sectional view of the microvessels shows the presence of the dextran within the lumen (yellow arrows). Scale bar: 50µm

Chapter 8

Conclusions and outlook for the future

8. Conclusions and outlook for the future

In the past few decades, significant advancement has been achieved in the field of tissue engineering and regeneration. However, one of the major obstacles challenging the success of tissue engineering is the vascularization of the tissue construct. Engineered tissue equivalents could be vascularized either *in-vivo* or *in-vitro*. Fabrication of vascularized tissue equivalents *in-vitro* has been shown to offer superior and rapid engraftment after implantation into a host and successful regeneration of tissue. Additionally, *in-vitro* vascularized tissue equivalents could offer potential avenues for developing/ screening new compounds especially in the field of vascular pharmacology.

Engineering vascularized tissue equivalents requires the co-operation of a triad of vascular cells (ECs and mural cells), signaling molecules involved in the angiogenic cascade and biomaterial that supports angiogenesis. ECs and mural cells like vSMCs form the building blocks of the vascular system, while the biomaterials and angiogenic molecules provide the physical, chemical and biological cues/ support needed for the formation of network of vascular channels. ECs and vSMCs could be obtained from various natal and post-natal sources. However, obtaining sufficient quantities of healthy and functional cells from these cell sources especially in the elderly and those with co-morbid diseases are quite challenging. In this regard, hESCs offer a potential alternative and unlimited source of vascular cells. However, differentiating the hESCs towards vascular cells suffers from two major issues: efficient and scalable differentiation towards terminally differentiated cells and avoidance of xenogeneic products in the culture milieu.

This doctoral work has chosen to focus on developing protocols for efficiently directing the differentiation of hESCs to a homogenous population of endothelial subtypes and vSMCs in a relatively animal-product free microenvironment, which could be used to engineer vascularized tissue equivalents. This objective was addressed in phases as summarized below and in ***Figure 64***.

Phase 1: Rapid induction of hESCs towards primitive streak-like stage under feeder-free, chemically-defined conditions (***Chapter 4***):

Efficient commitment of epiblasts cells to PS is a requisite for the formation of mesoderm and endoderm. In this phase, the hESCs were directed towards PS through modulation of Wnt/β-Catenin signaling pathway using an inhibitor of glycogen synthase kinase-3 (GSK3) under feeder-free and chemically-defined conditions. Differentiation of hESCs seeded on human

plasma fibronectin in a chemically-defined media (Stemdiff APEL) under the influence of GSK-3 inhibitor (CHIR99021) resulted in a temporal upregulation of genes related to PS, mesoderm and endoderm accompanied by downregulation of genes related to pluripotency and neuroectoderm. Short-term inhibition of GSK-3 (24 hours) showed maximal upregulation of genes related to PS indicating the emergence of PS-like cells. The identity of PS-like cells was confirmed by their ability to commit towards mesoderm and endoderm under the influence of bFGF and Activin A respectively.

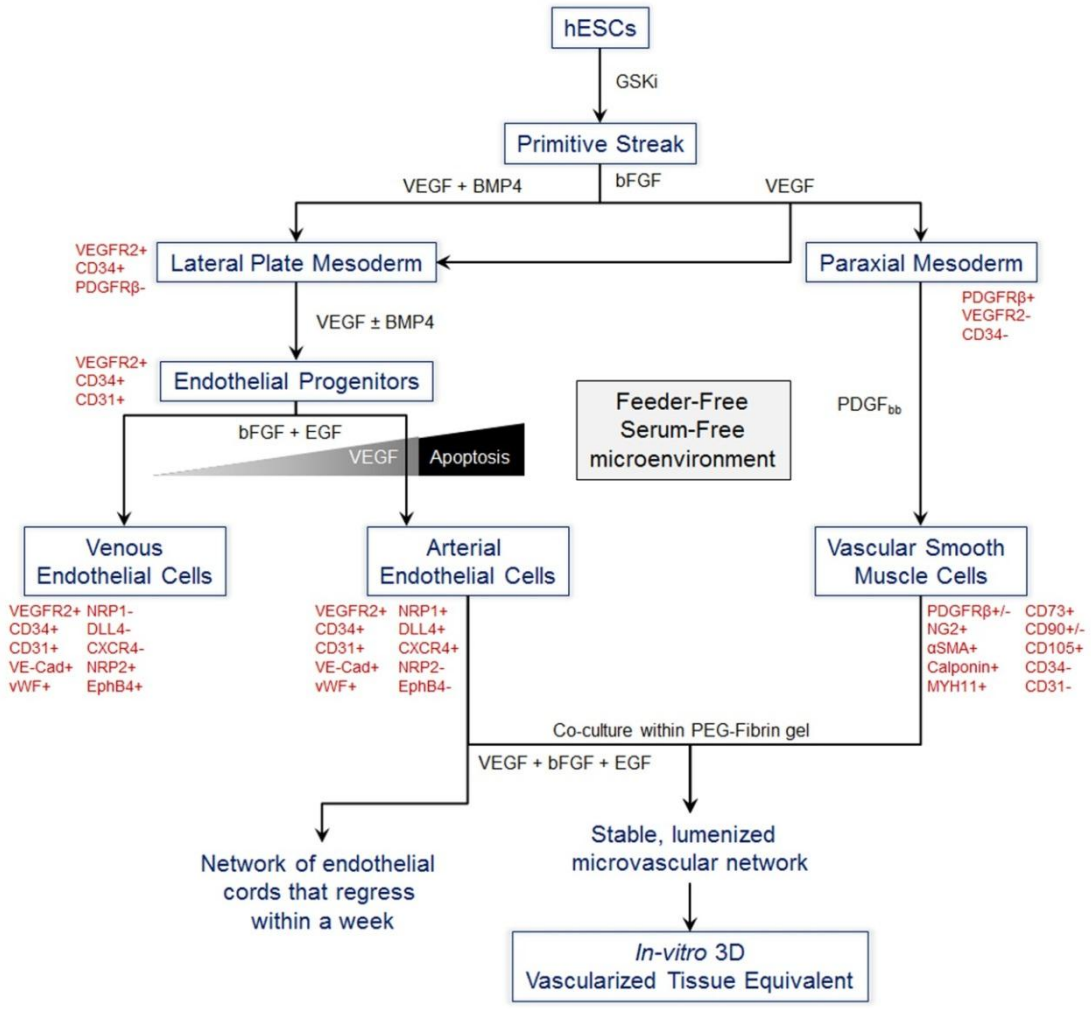

Figure 64. Summary of the findings of the study.

The schematic summarizes the findings demonstrated in this study. Refer to the text for detailed explanations. Briefly, hESCs were directed to primitive streak-like cells using GSKi and these cells could be further directed towards lateral plate and paraxial mesoderm subtypes by modulation of bFGF, BMP4 and VEGF signaling pathways. The lateral plate mesoderm could be further directed to endothelial progenitors that could be differentiated to venous and arterial endothelial phenotypes by modulating the concentration of VEGF. Similarly, the paraxial mesoderm intermediates could be directed to vSMCs. Further, *in-vitro* 3D vascularized tissue equivalents could be engineered using co-culture of arterial ECs and vSMCs within PEG-Fibrin gels.

Phase 2: Differentiation of PS to lateral plate mesoderm and endothelial lineage under feeder-free, chemically-defined conditions (***Chapter 4***):

The hESC-derived PS-like cells were directed towards lateral plate mesoderm and endothelial lineage through modulation of mesoderm and vascular lineage inducing factors that include bFGF, BMP4, and VEGF. Differentiation of GSKi-treated hESCs with bFGF followed by BMP4 and VEGF resulted in a rapid (5 days) and highly efficient induction (90-95%) of H1- and H9-hESCs to VEGFR2, CD34 and CD31 expressing endothelial progenitor cells. This protocol to differentiate hESCs to endothelial progenitors is novel in terms of rapid induction (5days versus 10-15days), high proportion (90-95% versus 2-40%) and minimal use of xenogeneic products. To our knowledge, this is the most rapid and efficient protocol so far to derive endothelial progenitors from hESCs.

In phase 1, 2 and 4, the use of xenogeneic products were reduced by the use of human plasma fibronectin as substrate and chemically-defined animal product-free medium (Stemdiff APEL) for the differentiation. However, components like BSA were used to reconstitute growth factors bFGF and VEGF. The use of BSA could be avoided in the future by use of carrier-free growth factors.

Phase 3: Differentiation of hESC-derived endothelial progenitors to ECs, in particular arterial and venous phenotypes under feeder- and serum-free conditions (***Chapter 5***):

The $CD34^{+}CD31^{+}$ endothelial progenitors derived from hESCs were sorted using FACS and differentiated further over fibronectin coated plates. Differentiation of these cells using endothelial serum-free medium yielded cells with endothelial characteristics. Under serum-containing conditions, VEGF has been reported to have a strong arterialization effect in a dose-dependent manner with higher concentrations favoring arterial fate. However, under serum-free conditions, we found that high concentrations (25-50 ng/ml) resulted in apoptosis of the cells, while at low concentrations (10 ng/ml) aided differentiation towards a homogenous population of ECs expressing arterial markers. While differentiation under the absence of VEGF, resulted in a homogenous population of ECs expressing venous markers. Derivation of arterial and venous ECs from hESCs and use of serum-free endothelial medium has not been reported so far. The hESC-derived arterial and venous ECs showed heterogeneity in terms of their gene expression pattern, ability to migrate and close a scratch wound, and secretion of various angiocrines factors. Additional functional studies, especially *in-vivo* studies are needed to further validate the functional heterogeneity between the hESC-derived arterial and venous ECs. Similarly, protocols to direct the ECs towards lymphatic

phenotype under serum-free conditions might throw more light on the differentiation conditions required.

In this this novel protocol, the use of xenogeneic products were reduced by the use of human plasma fibronectin as substrate and endothelial serum-free medium. Though the components of the endothelial serum-free medium are proprietary, we believe the medium might contain animal-derived components like BSA or insulin commonly present in other serum-free media formulations. To avoid the use of xenogeneic products and derive clinically competent ECs, endothelial medium free of animal-derived components need to be developed in the future.

Phase 4: Differentiation of PS to paraxial mesoderm under feeder-free, chemically-defined conditions (***Chapter 6***).

In this study, the hESCs were differentiated towards paraxial mesoderm through modulation of mesoderm and vascular lineage inducing factors that include bFGF, and VEGF. Treatment of GSKi-treated hESCs with bFGF and VEGF resulted in two distinct population of cells, one expressing lateral plate mesoderm related markers (VEGFR2, CD34 and CD31) and the other lacking them but expressing paraxial mesoderm and vSMC-related marker, PDGFRβ. The later population accounted for ~35% after 5 days of differentiation.

Phase 5: Differentiation of hESC-derived paraxial mesoderm intermediates to vSMCs under feeder- and serum-free conditions (***Chapter 6***).

Differentiation of FACS sorted hESC-derived paraxial mesoderm intermediates ($PDGFR\beta^{+}CD34^{-}CD31^{-}$) under the influence of $PDGF_{bb}$ in a custom-made serum-free media yielded spindle-shaped cells that expressed cell surface and intracellular markers related to vSMCs. These cells exhibited contractile property upon stimulation with carbachol. It is well established that vSMCs interact with ECs to support the formation and maturation of vascular channels (Carmeliet, 2000; Jain, 2003). Hence, the angiocrine secretory profile of hESC-vSMCs was surveyed using angiogenesis antibody array. The results showed that hESC-vSMCs secrete various angiogenic and antiangiogenic factors.

During embryogenesis, vSMCs have a diverse source of origins that include lateral plate mesoderm, paraxial mesoderm and neural crest. Very few protocols employ a lineage-directed approach for vSMC differentiation. The present protocol of differentiation of vSMCs from paraxial mesoderm intermediates is one of the other two publications reported in the literature (Cheung et al., 2012; Tan et al., 2013a).

In this this novel protocol, the use of xenogeneic products were reduced by the use of custom made serum-free media. However, the media still contains xenogeneic components like BSA

and insulin. To avoid the use of xenogeneic products and derive clinically competent vSMCs, smooth muscle medium free of animal-derived components needs to be developed in the future.

Phase 6: Engineer *in-vitro* 3D vascularized tissue equivalents using hESC-derived vascular cells under serum-free conditions (***Chapter 6***).

Though many reports have reported the utility of hESC-derived ECs and vSMCs in aiding neovascularization, very few reports have demonstrated the use of these cells in engineering *in-vitro* vascularized tissue equivalents. To engineer *in-vitro* 3D vascularized tissue equivalents, hESC-derived arterial ECs with or without hESC-vSMCs were cultured within PEG-Fibrin gels under serum-free conditions. hESC-derived arterial ECs formed anastomosing cords within PEG-fibrin gels, but regressed within a week in the absence of support from hESC-vSMCs. In the presence of hESC-vSMCs, the ECs formed anastomosing network of microvessels with patent lumen and were stable for 3 weeks in culture. Additionally, the use of fluorescently labeled hESC-derived vascular cells enabled non-invasive and live visualization of the microvascular networks. Further, we assessed the maturity and functionality of the microvessels by inverse permeability. The hESC-derived microvessels were mature in terms of their barrier function, and also were capable of regulating the permeability in responsive to physiological stimulus like histamine.

Though the use of xenogeneic products in this phase of the study was reduced by use of endothelial serum-free medium, the fibrinogen used was of bovine origin. We used bovine fibrinogen in this study for economic reasons. However, from clinical standpoint future studies are needed to evaluate the vascularization potential using fibrinogen of human origin. Fibrin is well established as being highly angiogenic, biodegradable and biocompatible, but is associated poor mechanical characteristics and degradation. One of the most commonly established approaches to improve fibrin's weak mechanical properties is by conjugating the fibrinogen molecules with PEG. The PEG-Fibrin gels used in this study was stable during the 3 week culture period and displayed no contraction or degradation under serum-free conditions.

Limitations and future outlook

Though our novel and efficient differentiation system for differentiating hESCs towards ECs and vSMCs and the utility of these cells in engineering 3D *in-vitro* vascularized tissue equivalents have several advancements, there are certain limitations that need to be addressed.

1. Though in each phase of the project, we were able to reduce the use of xenogeneic products, certain components like BSA, bovine insulin, bovine fibrinogen needs to be replaced. Hence, further reductions in the use of such xenogeneic products are possible and could advance the research output more close to clinical translation.
2. We found differences in the arterial and venous phenotypes at molecular and *in-vitro* functional levels. However, *in-vivo* studies are needed to establish functional differences between the two phenotypes.
3. In the current study, the ability of hESC-derived arterial ECs to form microvascular networks within PEG-fibrin gels was studied. Studies on the effect of hESC-derived venous ECs in place of arterial ECs are needed, as these two endothelial phenotypes demonstrated differences at molecular and functional levels.
4. In this study, the ECs and vSMCs were used at a fixed ratio of 10:1. However, the ratio of these two cell types varies widely depending on the tissue. Hence, additional studies are needed to fine-tune the ratio of ECs to vSMCs.
5. One of the major concerns with the use of hESC-derived products is the probability of teratoma formation. *In-vivo* studies to validate the safety of hESC-derived ECs and vSMCs are currently under investigation.
6. Further, from a clinical translation point-of-view *in-vivo* studies are needed to investigate the ability of these *in-vitro* vascularized tissue equivalents to integrate with the host tissue.
7. Additionally, investigating the utility of 3D vascularized system in screening novel angiogenic and anti-angiogenic compounds in a 3D microenvironment would be promising.
8. Using ibidi µ-slides we were able to engineer micro-3D constructs. This system could aid in establishment of economic and high-throughput *in-vitro* platform to study/ screen angiogenic and anti-angiogenic compounds in the future.
9. *In-vitro* vascularized tissue equivalents could aid in developing more complex tissues like full thickness skin equivalents and vascularized bone. Currently, work is in progress in investigating the utility of our hESC-derived *in-vitro* vascularized tissue equivalents for engineering vascularized skin and bone tissues.

In conclusion, the hESC-derived 3D *in-vitro* system to fabricate vascularized tissue equivalents is a reproducible system that mimics the natural physiology of ECs to self-assemble into microvascular networks. Thus our novel system provides a step forward towards engineering vascularized tissues/ organs with potential for clinical translational research and pharmaceutical drug discovery research.

Chapter 9

Bibliography

9. Bibliography

Adams, R. H., Wilkinson, G. A., Weiss, C., Diella, F., Gale, N. W., Deutsch, U., Risau, W. and Klein, R. (1999). Roles of ephrinB ligands and EphB receptors in cardiovascular development: demarcation of arterial/venous domains, vascular morphogenesis, and sprouting angiogenesis. *Genes & development* **13**, 295-306.

Adams, W. J., Zhang, Y., Cloutier, J., Kuchimanchi, P., Newton, G., Sehrawat, S., Aird, W. C., Mayadas, T. N., Luscinskas, F. W. and Garcia-Cardena, G. (2013). Functional vascular endothelium derived from human induced pluripotent stem cells. *Stem cell reports* **1**, 105-113.

Ahmed, T. A., Dare, E. V. and Hincke, M. (2008). Fibrin: a versatile scaffold for tissue engineering applications. *Tissue engineering. Part B, Reviews* **14**, 199-215.

Aird, W. C. (2007a). Phenotypic heterogeneity of the endothelium: I. Structure, function, and mechanisms. *Circ Res* **100**, 158-173.

---- (2007b). Phenotypic heterogeneity of the endothelium: II. Representative vascular beds. *Circ Res* **100**, 174-190.

Almany, L. and Seliktar, D. (2005). Biosynthetic hydrogel scaffolds made from fibrinogen and polyethylene glycol for 3D cell cultures. *Biomaterials* **26**, 2467-2477.

Anderson, D. E. and Hinds, M. T. (2012). Extracellular matrix production and regulation in micropatterned endothelial cells. *Biochem Biophys Res Commun* **427**, 159-164.

Antonelli-Orlidge, A., Saunders, K. B., Smith, S. R. and D'Amore, P. A. (1989). An activated form of transforming growth factor beta is produced by cocultures of endothelial cells and pericytes. *Proc Natl Acad Sci U S A* **86**, 4544-4548.

Aper, T., Schmidt, A., Duchrow, M. and Bruch, H. P. (2007). Autologous blood vessels engineered from peripheral blood sample. *European journal of vascular and endovascular surgery : the official journal of the European Society for Vascular Surgery* **33**, 33-39.

Aranguren, X. L., Luttun, A., Clavel, C., Moreno, C., Abizanda, G., Barajas, M. A., Pelacho, B., Uriz, M., Arana, M., Echavarri, A., et al. (2007). In vitro and in vivo arterial differentiation of human multipotent adult progenitor cells. *Blood* **109**, 2634-2642.

Arciniegas, E., Frid, M. G., Douglas, I. S. and Stenmark, K. R. (2007). Perspectives on endothelial-to-mesenchymal transition: potential contribution to vascular remodeling in chronic pulmonary hypertension. *American journal of physiology. Lung cellular and molecular physiology* **293**, L1-8.

Armulik, A., Genove, G. and Betsholtz, C. (2011). Pericytes: developmental, physiological, and pathological perspectives, problems, and promises. *Developmental cell* **21**, 193-215.

Arnold, S., Stappert, J., Bauer, A., Kispert, A., Herrmann, B. and Kemler, R. (2000). Brachyury is a target gene of the Wnt/beta-catenin signaling pathway. *Mechanisms of development* **91**, 249-258.

Atkins, G. B., Jain, M. K. and Hamik, A. (2011). Endothelial differentiation: molecular mechanisms of specification and heterogeneity. *Arterioscler Thromb Vasc Biol* **31**, 1476-1484.

Auerbach, R., Lewis, R., Shinners, B., Kubai, L. and Akhtar, N. (2003). Angiogenesis assays: a critical overview. *Clinical chemistry* **49**, 32-40.

Azhdari, M., Baghaban-Eslaminejad, M., Baharvand, H. and Aghdami, N. (2013). Therapeutic potential of human-induced pluripotent stem cell-derived endothelial cells in a bleomycin-induced scleroderma mouse model. *Stem Cell Res* **10**, 288-300.

Bai, H., Gao, Y., Arzigian, M., Wojchowski, D. M., Wu, W. S. and Wang, Z. Z. (2010). BMP4 regulates vascular progenitor development in human embryonic stem cells through a Smad-dependent pathway. *J Cell Biochem* **109**, 363-374.

Bai, H. and Wang, Z. Z. (2008). Directing human embryonic stem cells to generate vascular progenitor cells. *Gene Ther* **15**, 89-95.

Bajpai, V. K., Mistriotis, P., Loh, Y. H., Daley, G. Q. and Andreadis, S. T. (2012). Functional vascular smooth muscle cells derived from human induced pluripotent stem cells via mesenchymal stem cell intermediates. *Cardiovascular research* **96**, 391-400.

Banerjee, S. S., Aher, N., Patil, R. and Khandare, J. (2012). Poly(ethylene glycol)-Prodrug Conjugates: Concept, Design, and Applications. *Journal of drug delivery* **2012**, 103973.

Barker, T. H., Fuller, G. M., Klinger, M. M., Feldman, D. S. and Hagood, J. S. (2001). Modification of fibrinogen with poly(ethylene glycol) and its effects on fibrin clot characteristics. *J Biomed Mater Res* **56**, 529-535.

Bauwens, C. L., Peerani, R., Niebruegge, S., Woodhouse, K. A., Kumacheva, E., Husain, M. and Zandstra, P. W. (2008). Control of human embryonic stem cell colony and aggregate size heterogeneity influences differentiation trajectories. *Stem Cells* **26**, 2300-2310.

Beddington, R. S., Rashbass, P. and Wilson, V. (1992). Brachyury--a gene affecting mouse gastrulation and early organogenesis. *Dev Suppl*, 157-165.

Bergers, G. and Song, S. (2005). The role of pericytes in blood-vessel formation and maintenance. *Neuro-oncology* **7**, 452-464.

Bernardo, A. S., Faial, T., Gardner, L., Niakan, K. K., Ortmann, D., Senner, C. E., Callery, E. M., Trotter, M. W., Hemberger, M., Smith, J. C., et al. (2011). BRACHYURY and CDX2 mediate BMP-induced differentiation of human and mouse pluripotent stem cells into embryonic and extraembryonic lineages. *Cell Stem Cell* **9**, 144-155.

Birla, R. K., Borschel, G. H., Dennis, R. G. and Brown, D. L. (2005). Myocardial engineering in vivo: formation and characterization of contractile, vascularized three-dimensional cardiac tissue. *Tissue Eng* **11**, 803-813.

Black, A. F., Berthod, F., L'Heureux, N., Germain, L. and Auger, F. A. (1998). In vitro reconstruction of a human capillary-like network in a tissue-engineered skin equivalent. *FASEB J* **12**, 1331-1340.

Blancas, A. A., Lauer, N. E. and McCloskey, K. E. (2008). Endothelial differentiation of embryonic stem cells. *Current protocols in stem cell biology* **Chapter 1**, Unit 1F 5.

Blancas, A. A., Shih, A. J., Lauer, N. E. and McCloskey, K. E. (2011). Endothelial cells from embryonic stem cells in a chemically defined medium. *Stem Cells Dev* **20**, 2153-2161.

Blanco, M. J., Barrallo-Gimeno, A., Acloque, H., Reyes, A. E., Tada, M., Allende, M. L., Mayor, R. and Nieto, M. A. (2007). Snail1a and Snail1b cooperate in the anterior migration of the axial mesendoderm in the zebrafish embryo. *Development* **134**, 4073-4081.

Bone, H., Nelson, A., Goldring, C., Tosh, D. and Welham, M. (2011a). A novel chemically directed route for the generation of definitive endoderm from human embryonic stem cells based on inhibition of GSK-3. *Journal of cell science* **124**, 1992-2000.

Bone, H. K., Nelson, A. S., Goldring, C. E., Tosh, D. and Welham, M. J. (2011b). A novel chemically directed route for the generation of definitive endoderm from human embryonic stem cells based on inhibition of GSK-3. *J Cell Sci* **124**, 1992-2000.

Borges, J., Torio-Padron, N., Momeni, A., Mueller, M. C., Tegtmeier, F. T. and Stark, B. G. (2006). Adipose precursor cells (preadipocytes) induce formation of new vessels in fibrin glue on the newly developed cylinder chorioallantoic membrane model (CAM). *Minimally invasive therapy & allied technologies : MITAT : official journal of the Society for Minimally Invasive Therapy* **15**, 246-252.

Bottcher, R. T. and Niehrs, C. (2005). Fibroblast growth factor signaling during early vertebrate development. *Endocrine reviews* **26**, 63-77.

Brennan, J., Lu, C. C., Norris, D. P., Rodriguez, T. A., Beddington, R. S. and Robertson, E. J. (2001). Nodal signalling in the epiblast patterns the early mouse embryo. *Nature* **411**, 965-969.

Bu, L., Jiang, X., Martin-Puig, S., Caron, L., Zhu, S., Shao, Y., Roberts, D. J., Huang, P. L., Domian, I. J. and Chien, K. R. (2009). Human ISL1 heart progenitors generate diverse multipotent cardiovascular cell lineages. *Nature* **460**, 113-117.

Burridge, P. W., Anderson, D., Priddle, H., Barbadillo Munoz, M. D., Chamberlain, S., Allegrucci, C., Young, L. E. and Denning, C. (2007). Improved human embryonic stem cell embryoid body homogeneity and cardiomyocyte differentiation from a novel V-96 plate aggregation system highlights interline variability. *Stem Cells* **25**, 929-938.

Cai, L., Ye, Z., Zhou, B. Y., Mali, P., Zhou, C. and Cheng, L. (2007). Promoting human embryonic stem cell renewal or differentiation by modulating Wnt signal and culture conditions. *Cell Res* **17**, 62-72.

Capla, J. M., Ceradini, D. J., Tepper, O. M., Callaghan, M. J., Bhatt, K. A., Galiano, R. D., Levine, J. P. and Gurtner, G. C. (2006). Skin graft vascularization involves precisely regulated regression and replacement of endothelial cells through both angiogenesis and vasculogenesis. *Plastic and reconstructive surgery* **117**, 836-844.

Carmeliet, P. (2000). Mechanisms of angiogenesis and arteriogenesis. *Nature medicine* **6**, 389-395.

---- (2003). Angiogenesis in health and disease. *Nature medicine* **9**, 653-660.

---- (2005). Angiogenesis in life, disease and medicine. *Nature* **438**, 932-936.

Carmeliet, P. and Conway, E. M. (2001). Growing better blood vessels. *Nat Biotechnol* **19**, 1019-1020.

Carmeliet, P., Ferreira, V., Breier, G., Pollefeyt, S., Kieckens, L., Gertsenstein, M., Fahrig, M., Vandenhoeck, A., Harpal, K., Eberhardt, C., et al. (1996). Abnormal blood vessel development and lethality in embryos lacking a single VEGF allele. *Nature* **380**, 435-439.

Carmeliet, P. and Jain, R. K. (2000). Angiogenesis in cancer and other diseases. *Nature* **407**, 249-257.

Cerdan, C., McIntyre, B., Mechael, R., Levadoux-Martin, M., Yang, J., Lee, J. and Bhatia, M. (2012). Activin A promotes hematopoietic fated mesoderm development through upregulation of brachyury in human embryonic stem cells. *Stem cells and development* **13**, Epub ahead of print.

Chadwick, K., Wang, L., Li, L., Menendez, P., Murdoch, B., Rouleau, A. and Bhatia, M. (2003). Cytokines and BMP-4 promote hematopoietic differentiation of human embryonic stem cells. *Blood* **102**, 906-915.

Chen, S. S., Fitzgerald, W., Zimmerberg, J., Kleinman, H. K. and Margolis, L. (2007a). Cell-cell and cell-extracellular matrix interactions regulate embryonic stem cell differentiation. *Stem cells* **25**, 553-561.

Chen, T., Bai, H., Shao, Y., Arzigian, M., Janzen, V., Attar, E., Xie, Y., Scadden, D. T. and Wang, Z. Z. (2007b). Stromal cell-derived factor-1/CXCR4 signaling modifies the capillary-like organization of human embryonic stem cell-derived endothelium in vitro. *Stem Cells* **25**, 392-401.

Chen, X., Aledia, A. S., Ghajar, C. M., Griffith, C. K., Putnam, A. J., Hughes, C. C. and George, S. C. (2009). Prevascularization of a fibrin-based tissue construct accelerates the formation of functional anastomosis with host vasculature. *Tissue engineering. Part A* **15**, 1363-1371.

Chen, X., Aledia, A. S., Popson, S. A., Him, L., Hughes, C. C. and George, S. C. (2010). Rapid anastomosis of endothelial progenitor cell-derived vessels with host vasculature is promoted by a high density of cotransplanted fibroblasts. *Tissue engineering. Part A* **16**, 585-594.

Cheung, C., Bernardo, A. S., Trotter, M. W., Pedersen, R. A. and Sinha, S. (2012). Generation of human vascular smooth muscle subtypes provides insight into embryological origin-dependent disease susceptibility. *Nat Biotechnol* **30**, 165-173.

Cheung, C. and Sinha, S. (2011). Human embryonic stem cell-derived vascular smooth muscle cells in therapeutic neovascularisation. *J Mol Cell Cardiol* **51**, 651-664.

Cho, S. W., Moon, S. H., Lee, S. H., Kang, S. W., Kim, J., Lim, J. M., Kim, H. S., Kim, B. S. and Chung, H. M. (2007). Improvement of postnatal neovascularization by human embryonic stem cell derived endothelial-like cell transplantation in a mouse model of hindlimb ischemia. *Circulation* **116**, 2409-2419.

Choi, J. H., Ryu, Y. S., Kim, K. H., Lee, Y. R., Cha, K. W., Han, I. S. and Kwon, B. S. (2009a). In vitro development of a hemangioblast from a human embryonic stem cell, SNUhES#3. *Life sciences* **85**, 39-45.

Choi, K. D., Yu, J., Smuga-Otto, K., Salvagiotto, G., Rehrauer, W., Vodyanik, M., Thomson, J. and Slukvin, I. (2009b). Hematopoietic and endothelial differentiation of human induced pluripotent stem cells. *Stem Cells* **27**, 559-567.

Christoforou, N., Miller, R. A., Hill, C. M., Jie, C. C., McCallion, A. S. and Gearhart, J. D. (2008). Mouse ES cell-derived cardiac precursor cells are multipotent and facilitate identification of novel cardiac genes. *The Journal of clinical investigation* **118**, 894-903.

Cimato, T., Beers, J., Ding, S., Ma, M., McCoy, J. P., Boehm, M. and Nabel, E. G. (2009). Neuropilin-1 identifies endothelial precursors in human and murine embryonic stem cells before CD34 expression. *Circulation* **119**, 2170-2178.

Ciruna, B. and Rossant, J. (2001). FGF signaling regulates mesoderm cell fate specification and morphogenetic movement at the primitive streak. *Developmental cell* **1**, 37-49.

Cleaver, O. and Melton, D. A. (2003). Endothelial signaling during development. *Nature medicine* **9**, 661-668.

Colleoni, S., Galli, C., Giannelli, S. G., Armentero, M. T., Blandini, F., Broccoli, V. and Lazzari, G. (2010). Long-term culture and differentiation of CNS precursors derived from anterior human neural rosettes following exposure to ventralizing factors. *Exp Cell Res* **316**, 1148-1158.

Conlon, F. L., Lyons, K. M., Takaesu, N., Barth, K. S., Kispert, A., Herrmann, B. and Robertson, E. J. (1994). A primary requirement for nodal in the formation and maintenance of the primitive streak in the mouse. *Development* **120**, 1919-1928.

Costa, M., Sourris, K., Lim, S. M., Yu, Q. C., Hirst, C. E., Parkington, H. C., Jokubaitis, V. J., Dear, A. E., Liu, H. B., Micallef, S. J., et al. (2013). Derivation of endothelial cells from human embryonic stem cells in fully defined medium enables identification of lysophosphatidic acid and platelet activating factor as regulators of eNOS localization. *Stem Cell Res* **10**, 103-117.

Coultas, L., Chawengsaksophak, K. and Rossant, J. (2005). Endothelial cells and VEGF in vascular development. *Nature* **438**, 937-945.

Cross, M. J. and Claesson-Welsh, L. (2001). FGF and VEGF function in angiogenesis: signalling pathways, biological responses and therapeutic inhibition. *Trends in pharmacological sciences* **22**, 201-207.

D'Amour, K. A., Agulnick, A. D., Eliazer, S., Kelly, O. G., Kroon, E. and Baetge, E. E. (2005). Efficient differentiation of human embryonic stem cells to definitive endoderm. *Nat Biotechnol* **23**, 1534-1541.

D'Amour, K. A., Bang, A. G., Eliazer, S., Kelly, O. G., Agulnick, A. D., Smart, N. G., Moorman, M. A., Kroon, E., Carpenter, M. K. and Baetge, E. E. (2006). Production of pancreatic hormone-expressing endocrine cells from human embryonic stem cells. *Nat Biotechnol* **24**, 1392-1401.

Daley, G. Q. and Scadden, D. T. (2008). Prospects for stem cell-based therapy. *Cell* **132**, 544-548.

Dar, A., Domev, H., Ben-Yosef, O., Tzukerman, M., Zeevi-Levin, N., Novak, A., Germanguz, I., Amit, M. and Itskovitz-Eldor, J. (2012). Multipotent vasculogenic pericytes from human pluripotent stem cells promote recovery of murine ischemic limb. *Circulation* **125**, 87-99.

Davidson, K. C., Adams, A. M., Goodson, J. M., McDonald, C. E., Potter, J. C., Berndt, J. D., Biechele, T. L., Taylor, R. J. and Moon, R. T. (2012). Wnt/beta-catenin signaling promotes differentiation, not self-renewal, of human embryonic stem cells and is repressed by Oct4. *Proc Natl Acad Sci U S A* **109**, 4485-4490.

Davis, R. P., Ng, E. S., Costa, M., Mossman, A. K., Sourris, K., Elefanty, A. G. and Stanley, E. G. (2008). Targeting a GFP reporter gene to the MIXL1 locus of human embryonic stem cells identifies human primitive streak-like cells and enables isolation of primitive hematopoietic precursors. *Blood* **111**, 1876-1884.

Deng, C. X., Wynshaw-Boris, A., Shen, M. M., Daugherty, C., Ornitz, D. M. and Leder, P. (1994). Murine FGFR-1 is required for early postimplantation growth and axial organization. *Genes & development* **8**, 3045-3057.

Descamps, B. and Emanueli, C. (2012). Vascular differentiation from embryonic stem cells: novel technologies and therapeutic promises. *Vascular pharmacology* **56**, 267-279.

Dikovsky, D., Bianco-Peled, H. and Seliktar, D. (2006). The effect of structural alterations of PEG-fibrinogen hydrogel scaffolds on 3-D cellular morphology and cellular migration. *Biomaterials* **27**, 1496-1506.

Ding, B. S., Nolan, D. J., Butler, J. M., James, D., Babazadeh, A. O., Rosenwaks, Z., Mittal, V., Kobayashi, H., Shido, K., Lyden, D., et al. (2010a). Inductive angiocrine signals from sinusoidal endothelium are required for liver regeneration. *Nature* **468**, 310-315.

Ding, V., Ling, L., Natarajan, S., Yap, M., Cool, S. and Choo, A. (2010b). FGF-2 modulates Wnt signaling in undifferentiated hESC and iPS cells through activated PI3-K/GSK3beta signaling. *Journal of cellular physiology* **225**, 417-428.

Dravid, G., Ye, Z., Hammond, H., Chen, G., Pyle, A., Donovan, P., Yu, X. and Cheng, L. (2005). Defining the role of Wnt/beta-catenin signaling in the survival, proliferation, and self-renewal of human embryonic stem cells. *Stem cells* **23**, 1489-1501.

Drukker, M., Tang, C., Ardehali, R., Rinkevich, Y., Seita, J., Lee, A., Mosley, A., Weissman, I. and Soen, Y. (2012). Isolation of primitive endoderm, mesoderm, vascular endothelial and trophoblast progenitors from human pluripotent stem cells. *Nature Biotechnology* **30**, 531-542.

Duarte, A., Hirashima, M., Benedito, R., Trindade, A., Diniz, P., Bekman, E., Costa, L., Henrique, D. and Rossant, J. (2004). Dosage-sensitive requirement for mouse Dll4 in artery development. *Genes & development* **18**, 2474-2478.

Dumont, D. J., Jussila, L., Taipale, J., Lymboussaki, A., Mustonen, T., Pajusola, K., Breitman, M. and Alitalo, K. (1998). Cardiovascular failure in mouse embryos deficient in VEGF receptor-3. *Science* **282**, 946-949.

Dunn, N. R., Vincent, S. D., Oxburgh, L., Robertson, E. J. and Bikoff, E. K. (2004). Combinatorial activities of Smad2 and Smad3 regulate mesoderm formation and patterning in the mouse embryo. *Development* **131**, 1717-1728.

Dush, M. K. and Martin, G. R. (1992). Analysis of mouse Evx genes: Evx-1 displays graded expression in the primitive streak. *Developmental biology* **151**, 273-287.

Dyer, L. A. and Patterson, C. (2010). Development of the endothelium: an emphasis on heterogeneity. *Seminars in thrombosis and hemostasis* **36**, 227-235.

Eichmann, A., Corbel, C. and Le Douarin, N. M. (1998). Segregation of the embryonic vascular and hemopoietic systems. *Biochemistry and cell biology = Biochimie et biologie cellulaire* **76**, 939-946.

Ema, M., Yokomizo, T., Wakamatsu, A., Terunuma, T., Yamamoto, M. and Takahashi, S. (2006). Primitive erythropoiesis from mesodermal precursors expressing VE-cadherin, PECAM-1, Tie2, endoglin, and CD34 in the mouse embryo. *Blood* **108**, 4018-4024.

Evensen, L., Micklem, D. R., Blois, A., Berge, S. V., Aarsaether, N., Littlewood-Evans, A., Wood, J. and Lorens, J. B. (2009). Mural cell associated VEGF is required for organotypic vessel formation. *PLoS One* **4**, e5798.

Evseenko, D., Zhu, Y., Schenke-Layland, K., Kuo, J., Latour, B., Ge, S., Scholes, J., Dravid, G., Li, X., MacLellan, W. R., et al. (2010). Mapping the first stages of mesoderm commitment during differentiation of human embryonic stem cells. *Proc Natl Acad Sci U S A* **107**, 13742-13747.

Fatigati, V. and Murphy, R. A. (1984). Actin and tropomyosin variants in smooth muscles. Dependence on tissue type. *The Journal of biological chemistry* **259**, 14383-14388.

Ferrara, N., Carver-Moore, K., Chen, H., Dowd, M., Lu, L., O'Shea, K. S., Powell-Braxton, L., Hillan, K. J. and Moore, M. W. (1996). Heterozygous embryonic lethality induced by targeted inactivation of the VEGF gene. *Nature* **380**, 439-442.

Ferreira, L. S., Gerecht, S., Shieh, H. F., Watson, N., Rupnick, M. A., Dallabrida, S. M., Vunjak-Novakovic, G. and Langer, R. (2007). Vascular progenitor cells isolated from human embryonic stem cells give rise to endothelial and smooth muscle like cells and form vascular networks in vivo. *Circ Res* **101**, 286-294.

Flamme, I., Frolich, T. and Risau, W. (1997). Molecular mechanisms of vasculogenesis and embryonic angiogenesis. *J Cell Physiol* **173**, 206-210.

Forlani, S., Lawson, K. A. and Deschamps, J. (2003). Acquisition of Hox codes during gastrulation and axial elongation in the mouse embryo. *Development* **130**, 3807-3819.

Frerich, B., Lindemann, N., Kurtz-Hoffmann, J. and Oertel, K. (2001). In vitro model of a vascular stroma for the engineering of vascularized tissues. *International journal of oral and maxillofacial surgery* **30**, 414-420.

Fuchs, S., Hofmann, A. and Kirkpatrick, C. (2007). Microvessel-like structures from outgrowth endothelial cells from human peripheral blood in 2-dimensional and 3-dimensional co-cultures with osteoblastic lineage cells. *Tissue Eng* **13**, 2577-2588.

Gadue, P., Huber, T. L., Paddison, P. J. and Keller, G. M. (2006). Wnt and TGF-beta signaling are required for the induction of an in vitro model of primitive streak formation using embryonic stem cells. *Proc Natl Acad Sci U S A* **103**, 16806-16811.

Geback, T., Schulz, M. M., Koumoutsakos, P. and Detmar, M. (2009). TScratch: a novel and simple software tool for automated analysis of monolayer wound healing assays. *BioTechniques* **46**, 265-274.

Geiger, F., Lorenz, H., Xu, W., Szalay, K., Kasten, P., Claes, L., Augat, P. and Richter, W. (2007). VEGF producing bone marrow stromal cells (BMSC) enhance vascularization and resorption of a natural coral bone substitute. *Bone* **41**, 516-522.

Gerecht-Nir, S., Ziskind, A., Cohen, S. and Itskovitz-Eldor, J. (2003). Human embryonic stem cells as an in vitro model for human vascular development and the induction of vascular differentiation. *Lab Invest* **83**, 1811-1820.

Ghanaati, S., Unger, R. E., Webber, M. J., Barbeck, M., Orth, C., Kirkpatrick, J. A., Booms, P., Motta, A., Migliaresi, C., Sader, R. A., et al. (2011). Scaffold vascularization in vivo driven by primary human osteoblasts in concert with host inflammatory cells. *Biomaterials* **32**, 8150-8160.

Glaser, D. E., Gower, R. M., Lauer, N. E., Tam, K., Blancas, A. A., Shih, A. J., Simon, S. I. and McCloskey, K. E. (2011). Functional characterization of embryonic stem cell-derived endothelial cells. *J Vasc Res* **48**, 415-428.

Goldman, O., Feraud, O., Boyer-Di Ponio, J., Driancourt, C., Clay, D., Le Bousse-Kerdiles, M. C., Bennaceur-Griscelli, A. and Uzan, G. (2009). A boost of BMP4 accelerates the commitment of human embryonic stem cells to the endothelial lineage. *Stem Cells* **27**, 1750-1759.

Gomez, D. E. and Thorgeirsson, U. P. (1998). Lectins as tools for the purification of liver endothelial cells. *Methods in molecular medicine* **9**, 319-328.

Gonen-Wadmany, M., Goldshmid, R. and Seliktar, D. (2011). Biological and mechanical implications of PEGylating proteins into hydrogel biomaterials. *Biomaterials* **32**, 6025-6033.

Grainger, S. J. and Putnam, A. J. (2011). Assessing the permeability of engineered capillary networks in a 3D culture. *PLoS One* **6**, e22086.

Grapin-Botton, A. (2008). Endoderm specification. In *StemBook*. Cambridge (MA).

Guo, X., Stice, S. L., Boyd, N. L. and Chen, S. Y. (2013). A novel in vitro model system for smooth muscle differentiation from human embryonic stem cell-derived mesenchymal cells. *American journal of physiology. Cell physiology* **304**, C289-298.

Hall, H. (2007). Modified fibrin hydrogel matrices: both, 3D-scaffolds and local and controlled release systems to stimulate angiogenesis. *Curr Pharm Des* **13**, 3597-3607.

Hanjaya-Putra, D., Bose, V., Shen, Y. I., Yee, J., Khetan, S., Fox-Talbot, K., Steenbergen, C., Burdick, J. A. and Gerecht, S. (2011). Controlled activation of morphogenesis to generate a functional human microvasculature in a synthetic matrix. *Blood* **118**, 804-815.

Hanjaya-Putra, D. and Gerecht, S. (2009). Vascular engineering using human embryonic stem cells. *Biotechnology progress* **25**, 2-9.

Hao, H., Gabbiani, G. and Bochaton-Piallat, M. L. (2003). Arterial smooth muscle cell heterogeneity: implications for atherosclerosis and restenosis development. *Arterioscler Thromb Vasc Biol* **23**, 1510-1520.

Hao, J., Li, T. G., Qi, X., Zhao, D. F. and Zhao, G. Q. (2006). WNT/beta-catenin pathway up-regulates Stat3 and converges on LIF to prevent differentiation of mouse embryonic stem cells. *Developmental biology* **290**, 81-91.

Hart, A. H., Hartley, L., Sourris, K., Stadler, E. S., Li, R., Stanley, E. G., Tam, P. P., Elefanty, A. G. and Robb, L. (2002). Mixl1 is required for axial mesendoderm morphogenesis and patterning in the murine embryo. *Development* **129**, 3597-3608.

Hatano, R., Mercurio, K., Luna, J. I., Glaser, D. E., Leppert, V. J. and McCloskey, K. E. (2013). Endothelial cells derived from embryonic stem cells respond to cues from topographical surface patterns. *Journal of biological engineering* **7**, 18.

Hellstrom, M., Kalen, M., Lindahl, P., Abramsson, A. and Betsholtz, C. (1999). Role of PDGF-B and PDGFR-beta in recruitment of vascular smooth muscle cells and pericytes during embryonic blood vessel formation in the mouse. *Development* **126**, 3047-3055.

Herzog, Y., Kalcheim, C., Kahane, N., Reshef, R. and Neufeld, G. (2001). Differential expression of neuropilin-1 and neuropilin-2 in arteries and veins. *Mech Dev* **109**, 115-119.

Hill, K. L., Obrtlikova, P., Alvarez, D. F., King, J. A., Keirstead, S. A., Allred, J. R. and Kaufman, D. S. (2010). Human embryonic stem cell-derived vascular progenitor cells capable of endothelial and smooth muscle cell function. *Exp Hematol* **38**, 246-257 e241.

Hirashima, M. (2009). Regulation of endothelial cell differentiation and arterial specification by VEGF and Notch signaling. *Anatomical science international* **84**, 95-101.

Howard, L., Mackenzie, R. M., Pchelintsev, N. A., McBryan, T., McClure, J. D., McBride, M. W., Kane, N. M., Adams, P. D., Milligan, G. and Baker, A. H. (2013). Profiling of transcriptional and epigenetic changes during directed endothelial differentiation of human embryonic stem cells identifies FOXA2 as a marker of early mesoderm commitment. *Stem cell research & therapy* **4**, 36.

Huang, H., Zhao, X., Chen, L., Xu, C., Yao, X., Lu, Y., Dai, L. and Zhang, M. (2006). Differentiation of human embryonic stem cells into smooth muscle cells in adherent monolayer culture. *Biochem Biophys Res Commun* **351**, 321-327.

Huang, N. F., Dewi, R. E., Okogbaa, J., Lee, J. C., Jalilrufaihah, A., Heilshorn, S. C. and Cooke, J. P. (2013). Chemotaxis of human induced pluripotent stem cell-derived endothelial cells. *American journal of translational research* **5**, 510-520.

Huang, N. F., Niiyama, H., De, A., Gambhir, S. S. and Cooke, J. P. (2009). Embryonic stem cell-derived endothelial cells for treatment of hindlimb ischemia. *Journal of visualized experiments : JoVE*.

Huber, T. L., Zhou, Y., Mead, P. E. and Zon, L. I. (1998). Cooperative effects of growth factors involved in the induction of hematopoietic mesoderm. *Blood* **92**, 4128-4137.

Huelsken, J., Vogel, R., Brinkmann, V., Erdmann, B., Birchmeier, C. and Birchmeier, W. (2000). Requirement for beta-catenin in anterior-posterior axis formation in mice. *J Cell Biol* **148**, 567-578.

Hwang, Y. S., Chung, B. G., Ortmann, D., Hattori, N., Moeller, H. C. and Khademhosseini, A. (2009). Microwell-mediated control of embryoid body size regulates embryonic stem cell fate via differential expression of WNT5a and WNT11. *Proc Natl Acad Sci U S A* **106**, 16978-16983.

Jaffredo, T., Gautier, R., Eichmann, A. and Dieterlen-Lievre, F. (1998). Intraaortic hemopoietic cells are derived from endothelial cells during ontogeny. *Development* **125**, 4575-4583.

Jain, R. K. (2003). Molecular regulation of vessel maturation. *Nature medicine* **9**, 685-693.

James, D., Nam, H. S., Seandel, M., Nolan, D., Janovitz, T., Tomishima, M., Studer, L., Lee, G., Lyden, D., Benezra, R., et al. (2010). Expansion and maintenance of human embryonic stem cell-derived endothelial cells by TGFbeta inhibition is Id1 dependent. *Nat Biotechnol* **28**, 161-166.

Jiang, X., Rowitch, D. H., Soriano, P., McMahon, A. P. and Sucov, H. M. (2000). Fate of the mammalian cardiac neural crest. *Development* **127**, 1607-1616.

Johansson, B. M. and Wiles, M. V. (1995). Evidence for involvement of activin A and bone morphogenetic protein 4 in mammalian mesoderm and hematopoietic development. *Molecular and cellular biology* **15**, 141-151.

Johnson, E. O., Troupis, T. and Soucacos, P. N. (2011). Tissue-engineered vascularized bone grafts: basic science and clinical relevance to trauma and reconstructive microsurgery. *Microsurgery* **31**, 176-182.

Kane, N. M., Meloni, M., Spencer, H. L., Craig, M. A., Strehl, R., Milligan, G., Houslay, M. D., Mountford, J. C., Emanueli, C. and Baker, A. H. (2010). Derivation of endothelial cells from human embryonic stem cells by directed differentiation: analysis of microRNA and angiogenesis in vitro and in vivo. *Arterioscler Thromb Vasc Biol* **30**, 1389-1397.

Kane, N. M., Xiao, Q., Baker, A. H., Luo, Z., Xu, Q. and Emanueli, C. (2011). Pluripotent stem cell differentiation into vascular cells: a novel technology with promises for vascular re(generation). *Pharmacol Ther* **129**, 29-49.

Kataoka, H., Takakura, N., Nishikawa, S., Tsuchida, K., Kodama, H., Kunisada, T., Risau, W., Kita, T. and Nishikawa, S. I. (1997). Expressions of PDGF receptor alpha, c-Kit and Flk1 genes clustering in mouse chromosome 5 define distinct subsets of nascent mesodermal cells. *Development, growth & differentiation* **39**, 729-740.

Kaufman, D. S., Hanson, E. T., Lewis, R. L., Auerbach, R. and Thomson, J. A. (2001). Hematopoietic colony-forming cells derived from human embryonic stem cells. *Proc Natl Acad Sci U S A* **98**, 10716-10721.

Kaully, T., Kaufman-Francis, K., Lesman, A. and Levenberg, S. (2009). Vascularization--the conduit to viable engineered tissues. *Tissue engineering. Part B, Reviews* **15**, 159-169.

Kaupisch, A., Kennedy, L., Stelmanis, V., Tye, B., Kane, N. M., Mountford, J. C., Courtney, A. and Baker, A. H. (2012). Derivation of vascular endothelial cells from human embryonic stem cells under GMP-compliant conditions: towards clinical studies in ischaemic disease. *Journal of cardiovascular translational research* **5**, 605-617.

Kelly, O. G., Pinson, K. I. and Skarnes, W. C. (2004). The Wnt co-receptors Lrp5 and Lrp6 are essential for gastrulation in mice. *Development* **131**, 2803-2815.

Kemler, R., Hierholzer, A., Kanzler, B., Kuppig, S., Hansen, K., Taketo, M. M., de Vries, W. N., Knowles, B. B. and Solter, D. (2004). Stabilization of beta-catenin in the mouse zygote leads to premature epithelial-mesenchymal transition in the epiblast. *Development* **131**, 5817-5824.

Kennedy, M., D'Souza, S. L., Lynch-Kattman, M., Schwantz, S. and Keller, G. (2007). Development of the hemangioblast defines the onset of hematopoiesis in human ES cell differentiation cultures. *Blood* **109**, 2679-2687.

Khademhosseini, A., Ferreira, L., Blumling, J., 3rd, Yeh, J., Karp, J. M., Fukuda, J. and Langer, R. (2006). Co-culture of human embryonic stem cells with murine embryonic fibroblasts on microwell-patterned substrates. *Biomaterials* **27**, 5968-5977.

Kim, J., Moon, S. H., Lee, S. H., Lee, D. R., Koh, G. Y. and Chung, H. M. (2007). Effective isolation and culture of endothelial cells in embryoid body differentiated from human embryonic stem cells. *Stem Cells Dev* **16**, 269-280.

Kim, K. L., Song, S. H., Choi, K. S. and Suh, W. (2013). Cooperation of endothelial and smooth muscle cells derived from human induced pluripotent stem cells enhances neovascularization in dermal wounds. *Tissue engineering. Part A* **19**, 2478-2485.

Kimelman, D. (2006). Mesoderm induction: from caps to chips. *Nature reviews. Genetics* **7**, 360-372.

Kinder, S. J., Loebel, D. A. and Tam, P. P. (2001a). Allocation and early differentiation of cardiovascular progenitors in the mouse embryo. *Trends in cardiovascular medicine* **11**, 177-184.

Kinder, S. J., Tsang, T. E., Wakamiya, M., Sasaki, H., Behringer, R. R., Nagy, A. and Tam, P. P. (2001b). The organizer of the mouse gastrula is composed of a dynamic population of progenitor cells for the axial mesoderm. *Development* **128**, 3623-3634.

Kispert, A. and Herrmann, B. G. (1994). Immunohistochemical analysis of the Brachyury protein in wild-type and mutant mouse embryos. *Developmental biology* **161**, 179-193.

Kitagawa, M. and Era, T. (2010). Differentiation of mesodermal cells from pluripotent stem cells. *International journal of hematology* **91**, 373-383.

Koike, N., Fukumura, D., Gralla, O., Au, P., Schechner, J. S. and Jain, R. K. (2004). Tissue engineering: creation of long-lasting blood vessels. *Nature* **428**, 138-139.

Kokudo, T., Suzuki, Y., Yoshimatsu, Y., Yamazaki, T., Watabe, T. and Miyazono, K. (2008). Snail is required for TGFbeta-induced endothelial-mesenchymal transition of embryonic stem cell-derived endothelial cells. *J Cell Sci* **121**, 3317-3324.

Kolbe, M., Xiang, Z., Dohle, E., Tonak, M., Kirkpatrick, C. J. and Fuchs, S. (2011). Paracrine effects influenced by cell culture medium and consequences on microvessel-like structures in cocultures of mesenchymal stem cells and outgrowth endothelial cells. *Tissue engineering. Part A* **17**, 2199-2212.

Kraehenbuehl, T. P., Ferreira, L. S., Hayward, A. M., Nahrendorf, M., van der Vlies, A. J., Vasile, E., Weissleder, R., Langer, R. and Hubbell, J. A. (2011). Human embryonic stem cell-derived microvascular grafts for cardiac tissue preservation after myocardial infarction. *Biomaterials* **32**, 1102-1109.

Kraehenbuehl, T. P., Ferreira, L. S., Zammaretti, P., Hubbell, J. A. and Langer, R. (2009). Cell-responsive hydrogel for encapsulation of vascular cells. *Biomaterials* **30**, 4318-4324.

Krebs, L. T., Xue, Y., Norton, C. R., Shutter, J. R., Maguire, M., Sundberg, J. P., Gallahan, D., Closson, V., Kitajewski, J., Callahan, R., et al. (2000). Notch signaling is essential for vascular morphogenesis in mice. *Genes & development* **14**, 1343-1352.

Kubo, A., Shinozaki, K., Shannon, J. M., Kouskoff, V., Kennedy, M., Woo, S., Fehling, H. J. and Keller, G. (2004). Development of definitive endoderm from embryonic stem cells in culture. *Development* **131**, 1651-1662.

Kubota, Y., Kleinman, H. K., Martin, G. R. and Lawley, T. J. (1988). Role of laminin and basement membrane in the morphological differentiation of human endothelial cells into capillary-like structures. *J Cell Biol* **107**, 1589-1598.

Kume, T. (2010). Specification of arterial, venous, and lymphatic endothelial cells during embryonic development. *Histol Histopathol* **25**, 637-646.

Kurian, L., Sancho-Martinez, I., Nivet, E., Aguirre, A., Moon, K., Pendaries, C., Volle-Challier, C., Bono, F., Herbert, J. M., Pulecio, J., et al. (2013). Conversion of human fibroblasts to angioblast-like progenitor cells. *Nature methods* **10**, 77-83.

Kusuma, S., Shen, Y. I., Hanjaya-Putra, D., Mali, P., Cheng, L. and Gerecht, S. (2013). Self-organized vascular networks from human pluripotent stem cells in a synthetic matrix. *Proc Natl Acad Sci U S A* **110**, 12601-12606.

Kusuma, S., Zhao, S. and Gerecht, S. (2012). The extracellular matrix is a novel attribute of endothelial progenitors and of hypoxic mature endothelial cells. *FASEB J* **26**, 4925-4936.

Lagarkova, M. A., Volchkov, P. Y., Philonenko, E. S. and Kiselev, S. L. (2008). Efficient differentiation of hESCs into endothelial cells in vitro is secured by epigenetic changes. *Cell Cycle* **7**, 2929-2935.

Lanner, F., Sohl, M. and Farnebo, F. (2007). Functional arterial and venous fate is determined by graded VEGF signaling and notch status during embryonic stem cell differentiation. *Arterioscler Thromb Vasc Biol* **27**, 487-493.

Laschke, M. W., Rucker, M., Jensen, G., Carvalho, C., Mulhaupt, R., Gellrich, N. C. and Menger, M. D. (2008). Improvement of vascularization of PLGA scaffolds by inosculation of in situ-preformed functional blood vessels with the host microvasculature. *Annals of surgery* **248**, 939-948.

Laschke, M. W., Vollmar, B. and Menger, M. D. (2009). Inosculation: connecting the life-sustaining pipelines. *Tissue engineering. Part B, Reviews* **15**, 455-465.

Lawson, N. D., Scheer, N., Pham, V. N., Kim, C. H., Chitnis, A. B., Campos-Ortega, J. A. and Weinstein, B. M. (2001). Notch signaling is required for arterial-venous differentiation during embryonic vascular development. *Development* **128**, 3675-3683.

Lawson, N. D., Vogel, A. M. and Weinstein, B. M. (2002). sonic hedgehog and vascular endothelial growth factor act upstream of the Notch pathway during arterial endothelial differentiation. *Developmental cell* **3**, 127-136.

Lee, G., Chambers, S. M., Tomishima, M. J. and Studer, L. (2010). Derivation of neural crest cells from human pluripotent stem cells. *Nat Protoc* **5**, 688-701.

Lee, G., Kim, H., Elkabetz, Y., Al Shamy, G., Panagiotakos, G., Barberi, T., Tabar, V. and Studer, L. (2007). Isolation and directed differentiation of neural crest stem cells derived from human embryonic stem cells. *Nat Biotechnol* **25**, 1468-1475.

Lesman, A., Habib, M., Caspi, O., Gepstein, A., Arbel, G., Levenberg, S. and Gepstein, L. (2010). Transplantation of a tissue-engineered human vascularized cardiac muscle. *Tissue engineering. Part A* **16**, 115-125.

Lesman, A., Koffler, J., Atlas, R., Blinder, Y. J., Kam, Z. and Levenberg, S. (2011). Engineering vessel-like networks within multicellular fibrin-based constructs. *Biomaterials* **32**, 7856-7869.

Levenberg, S., Ferreira, L. S., Chen-Konak, L., Kraehenbuehl, T. P. and Langer, R. (2010). Isolation, differentiation and characterization of vascular cells derived from human embryonic stem cells. *Nat Protoc* **5**, 1115-1126.

Levenberg, S., Golub, J. S., Amit, M., Itskovitz-Eldor, J. and Langer, R. (2002). Endothelial cells derived from human embryonic stem cells. *Proc Natl Acad Sci U S A* **99**, 4391-4396.

Levenberg, S., Rouwkema, J., Macdonald, M., Garfein, E. S., Kohane, D. S., Darland, D. C., Marini, R., van Blitterswijk, C. A., Mulligan, R. C., D'Amore, P. A., et al. (2005). Engineering vascularized skeletal muscle tissue. *Nat Biotechnol* **23**, 879-884.

Li, Z., Hu, S., Ghosh, Z., Han, Z. and Wu, J. C. (2011). Functional characterization and expression profiling of human induced pluripotent stem cell- and embryonic stem cell-derived endothelial cells. *Stem Cells Dev* **20**, 1701-1710.

Li, Z., Suzuki, Y., Huang, M., Cao, F., Xie, X., Connolly, A. J., Yang, P. C. and Wu, J. C. (2008). Comparison of reporter gene and iron particle labeling for tracking fate of human embryonic stem cells and differentiated endothelial cells in living subjects. *Stem cells* **26**, 864-873.

Li, Z., Wilson, K. D., Smith, B., Kraft, D. L., Jia, F., Huang, M., Xie, X., Robbins, R. C., Gambhir, S. S., Weissman, I. L., et al. (2009). Functional and transcriptional characterization of human embryonic stem cell-derived endothelial cells for treatment of myocardial infarction. *PloS one* **4**, e8443.

Liang, C. C., Park, A. Y. and Guan, J. L. (2007). In vitro scratch assay: a convenient and inexpensive method for analysis of cell migration in vitro. *Nat Protoc* **2**, 329-333.

Linke, K., Schanz, J., Hansmann, J., Walles, T., Brunner, H. and Mertsching, H. (2007). Engineered liver-like tissue on a capillarized matrix for applied research. *Tissue Eng* **13**, 2699-2707.

Liu, P., Wakamiya, M., Shea, M. J., Albrecht, U., Behringer, R. R. and Bradley, A. (1999). Requirement for Wnt3 in vertebrate axis formation. *Nature genetics* **22**, 361-365.

Liu, Y., Festing, M., Thompson, J. C., Hester, M., Rankin, S., El-Hodiri, H. M., Zorn, A. M. and Weinstein, M. (2004). Smad2 and Smad3 coordinately regulate craniofacial and endodermal development. *Developmental biology* **270**, 411-426.

Lluis, F., Pedone, E., Pepe, S. and Cosma, M. P. (2008). Periodic activation of Wnt/beta-catenin signaling enhances somatic cell reprogramming mediated by cell fusion. *Cell Stem Cell* **3**, 493-507.

Loebel, D. A., Watson, C. M., De Young, R. A. and Tam, P. P. (2003). Lineage choice and differentiation in mouse embryos and embryonic stem cells. *Developmental biology* **264**, 1-14.

Lokmic, Z. and Mitchell, G. M. (2008). Engineering the microcirculation. *Tissue engineering. Part B, Reviews* **14**, 87-103.

Lu, S. J., Feng, Q., Caballero, S., Chen, Y., Moore, M. A., Grant, M. B. and Lanza, R. (2007). Generation of functional hemangioblasts from human embryonic stem cells. *Nature methods* **4**, 501-509.

Lu, S. J., Ivanova, Y., Feng, Q., Luo, C. and Lanza, R. (2009). Hemangioblasts from human embryonic stem cells generate multilayered blood vessels with functional smooth muscle cells. *Regen Med* **4**, 37-47.

Lugo, L. M., Lei, P. and Andreadis, S. T. (2011). Vascularization of the dermal support enhances wound re-epithelialization by in situ delivery of epidermal keratinocytes. *Tissue engineering. Part A* **17**, 665-675.

Majesky, M. W. (2003). Vascular smooth muscle diversity: insights from developmental biology. *Current atherosclerosis reports* **5**, 208-213.

---- (2007). Developmental basis of vascular smooth muscle diversity. *Arterioscler Thromb Vasc Biol* **27**, 1248-1258.

Marchand, M., Anderson, E. K., Phadnis, S. M., Longaker, M. T., Cooke, J. P., Chen, B. and Reijo Pera, R. A. (2013). Concurrent Generation of Functional Smooth Muscle and Endothelial Cells via a Vascular Progenitor. *Stem cells translational medicine*.

Marchetti, S., Gimond, C., Iljin, K., Bourcier, C., Alitalo, K., Pouyssegur, J. and Pages, G. (2002). Endothelial cells genetically selected from differentiating mouse embryonic stem cells incorporate at sites of neovascularization in vivo. *J Cell Sci* **115**, 2075-2085.

Margariti, A., Winkler, B., Karamariti, E., Zampetaki, A., Tsai, T. N., Baban, D., Ragoussis, J., Huang, Y., Han, J. D., Zeng, L., et al. (2012). Direct reprogramming of fibroblasts into endothelial cells capable of angiogenesis and reendothelialization in tissue-engineered vessels. *Proc Natl Acad Sci U S A* **109**, 13793-13798.

Marson, A., Foreman, R., Chevalier, B., Bilodeau, S., Kahn, M., Young, R. A. and Jaenisch, R. (2008). Wnt signaling promotes reprogramming of somatic cells to pluripotency. *Cell Stem Cell* **3**, 132-135.

McGonigle, S. and Shifrin, V. (2008). In vitro assay of angiogenesis: inhibition of capillary tube formation. *Current protocols in pharmacology / editorial board, S.J. Enna* **Chapter 12**, Unit12 12.

McGrath, K. E., Koniski, A. D., Maltby, K. M., McGann, J. K. and Palis, J. (1999). Embryonic expression and function of the chemokine SDF-1 and its receptor, CXCR4. *Developmental biology* **213**, 442-456.

Mikawa, T. and Gourdie, R. G. (1996). Pericardial mesoderm generates a population of coronary smooth muscle cells migrating into the heart along with ingrowth of the epicardial organ. *Developmental biology* **174**, 221-232.

Millauer, B., Wizigmann-Voos, S., Schnurch, H., Martinez, R., Moller, N. P., Risau, W. and Ullrich, A. (1993). High affinity VEGF binding and developmental expression suggest Flk-1 as a major regulator of vasculogenesis and angiogenesis. *Cell* **72**, 835-846.

Miquerol, L., Langille, B. L. and Nagy, A. (2000). Embryonic development is disrupted by modest increases in vascular endothelial growth factor gene expression. *Development* **127**, 3941-3946.

Mishina, Y., Suzuki, A., Ueno, N. and Behringer, R. R. (1995). Bmpr encodes a type I bone morphogenetic protein receptor that is essential for gastrulation during mouse embryogenesis. *Genes & development* **9**, 3027-3037.

Miyabayashi, T., Teo, J. L., Yamamoto, M., McMillan, M., Nguyen, C. and Kahn, M. (2007). Wnt/beta-catenin/CBP signaling maintains long-term murine embryonic stem cell pluripotency. *Proc Natl Acad Sci U S A* **104**, 5668-5673.

Mohr, J. C., de Pablo, J. J. and Palecek, S. P. (2006). 3-D microwell culture of human embryonic stem cells. *Biomaterials* **27**, 6032-6042.

Mohr, J. C., Zhang, J., Azarin, S. M., Soerens, A. G., de Pablo, J. J., Thomson, J. A., Lyons, G. E., Palecek, S. P. and Kamp, T. J. (2010). The microwell control of embryoid body size in order to regulate cardiac differentiation of human embryonic stem cells. *Biomaterials* **31**, 1885-1893.

Montano, I., Schiestl, C., Schneider, J., Pontiggia, L., Luginbuhl, J., Biedermann, T., Bottcher-Haberzeth, S., Braziulis, E., Meuli, M. and Reichmann, E. (2010). Formation of human capillaries in vitro: the engineering of prevascularized matrices. *Tissue engineering. Part A* **16**, 269-282.

Moon, S. H., Kim, J. S., Park, S. J., Lee, H. J., Do, J. T. and Chung, H. M. (2011). A system for treating ischemic disease using human embryonic stem cell-derived endothelial cells without direct incorporation. *Biomaterials* **32**, 6445-6455.

Moretti, A., Bellin, M., Jung, C. B., Thies, T. M., Takashima, Y., Bernshausen, A., Schiemann, M., Fischer, S., Moosmang, S., Smith, A. G., et al. (2010). Mouse and human induced pluripotent stem cells as a source for multipotent Isl1+ cardiovascular progenitors. *FASEB J* **24**, 700-711.

Moretti, A., Caron, L., Nakano, A., Lam, J. T., Bernshausen, A., Chen, Y., Qyang, Y., Bu, L., Sasaki, M., Martin-Puig, S., et al. (2006). Multipotent embryonic isl1+ progenitor cells lead to cardiac, smooth muscle, and endothelial cell diversification. *Cell* **127**, 1151-1165.

Mummery, C. L., Zhang, J., Ng, E. S., Elliott, D. A., Elefanty, A. G. and Kamp, T. J. (2012). Differentiation of human embryonic stem cells and induced pluripotent stem cells to cardiomyocytes: a methods overview. *Circ Res* **111**, 344-358.

Murry, C. E. and Keller, G. (2008). Differentiation of embryonic stem cells to clinically relevant populations: lessons from embryonic development. *Cell* **132**, 661-680.

Nakahara, M., Nakamura, N., Matsuyama, S., Yogiashi, Y., Yasuda, K., Kondo, Y., Yuo, A. and Saeki, K. (2009). High-efficiency production of subculturable vascular endothelial cells from feeder-free human embryonic stem cells without cell-sorting technique. *Cloning Stem Cells* **11**, 509-522.

Nakamura, T., Colbert, M. C. and Robbins, J. (2006). Neural crest cells retain multipotential characteristics in the developing valves and label the cardiac conduction system. *Circ Res* **98**, 1547-1554.

Nakanishi, M., Kurisaki, A., Hayashi, Y., Warashina, M., Ishiura, S., Kusuda-Furue, M. and Asashima, M. (2009a). Directed induction of anterior and posterior primitive streak by Wnt from embryonic stem cells cultured in a chemically defined serum-free medium. *FASEB J* **23**, 114-122.

Nakanishi, M., Kurisaki, A., Hayashi, Y., Warashina, M., Ishiura, S., Kusuda-Furue, M. and Asashima, M. (2009b). Directed induction of anterior and posterior primitive streak by Wnt from embryonic stem cells cultured in a chemically defined serum-free medium. *FASEB Journal* **23**, 114-122.

Narazaki, G., Uosaki, H., Teranishi, M., Okita, K., Kim, B., Matsuoka, S., Yamanaka, S. and Yamashita, J. K. (2008). Directed and systematic differentiation of cardiovascular cells from mouse induced pluripotent stem cells. *Circulation* **118**, 498-506.

Natesan, S., Zamora, D. O., Suggs, L. J. and Christy, R. J. (2012). Engineering a bilayered hydrogel to control ASC differentiation. *Journal of visualized experiments : JoVE*, e3953.

Natesan, S., Zhang, G., Baer, D. G., Walters, T. J., Christy, R. J. and Suggs, L. J. (2011). A bilayer construct controls adipose-derived stem cell differentiation into endothelial cells and pericytes without growth factor stimulation. *Tissue engineering. Part A* **17**, 941-953.

Ng, E. S., Azzola, L., Sourris, K., Robb, L., Stanley, E. G. and Elefanty, A. G. (2005a). The primitive streak gene Mixl1 is required for efficient haematopoiesis and BMP4-induced ventral mesoderm patterning in differentiating ES cells. *Development* **132**, 873-884.

Ng, E. S., Davis, R., Stanley, E. G. and Elefanty, A. G. (2008). A protocol describing the use of a recombinant protein-based, animal product-free medium (APEL) for human embryonic stem cell differentiation as spin embryoid bodies. *Nat Protoc* **3**, 768-776.

Ng, E. S., Davis, R. P., Azzola, L., Stanley, E. G. and Elefanty, A. G. (2005b). Forced aggregation of defined numbers of human embryonic stem cells into embryoid bodies fosters robust, reproducible hematopoietic differentiation. *Blood* **106**, 1601-1603.

Ng, Y. S., Rohan, R., Sunday, M. E., Demello, D. E. and D'Amore, P. A. (2001). Differential expression of VEGF isoforms in mouse during development and in the adult. *Developmental dynamics : an official publication of the American Association of Anatomists* **220**, 112-121.

Niiyama, H., Huang, N. F., Rollins, M. D. and Cooke, J. P. (2009). Murine model of hindlimb ischemia. *Journal of visualized experiments : JoVE*.

Nillesen, S. T., Geutjes, P. J., Wismans, R., Schalkwijk, J., Daamen, W. F. and van Kuppevelt, T. H. (2007). Increased angiogenesis and blood vessel maturation in acellular collagen-heparin scaffolds containing both FGF2 and VEGF. *Biomaterials* **28**, 1123-1131.

Nolan, D. J., Ginsberg, M., Israely, E., Palikuqi, B., Poulos, M. G., James, D., Ding, B. S., Schachterle, W., Liu, Y., Rosenwaks, Z., et al. (2013). Molecular signatures of tissue-specific microvascular endothelial cell heterogeneity in organ maintenance and regeneration. *Developmental cell* **26**, 204-219.

Nostro, M. C., Cheng, X., Keller, G. M. and Gadue, P. (2008). Wnt, activin, and BMP signaling regulate distinct stages in the developmental pathway from embryonic stem cells to blood. *Cell Stem Cell* **2**, 60-71.

Nourse, M. B., Halpin, D. E., Scatena, M., Mortisen, D. J., Tulloch, N. L., Hauch, K. D., Torok-Storb, B., Ratner, B. D., Pabon, L. and Murry, C. E. (2010). VEGF induces differentiation of functional endothelium from human embryonic stem cells: implications for tissue engineering. *Arterioscler Thromb Vasc Biol* **30**, 80-89.

Novosel, E. C., Kleinhans, C. and Kluger, P. J. (2011). Vascularization is the key challenge in tissue engineering. *Adv Drug Deliv Rev* **63**, 300-311.

Ogawa, K., Nishinakamura, R., Iwamatsu, Y., Shimosato, D. and Niwa, H. (2006). Synergistic action of Wnt and LIF in maintaining pluripotency of mouse ES cells. *Biochem Biophys Res Commun* **343**, 159-166.

Ott, H. C., Matthiesen, T. S., Goh, S. K., Black, L. D., Kren, S. M., Netoff, T. I. and Taylor, D. A. (2008). Perfusion-decellularized matrix: using nature's platform to engineer a bioartificial heart. *Nature medicine* **14**, 213-221.

Owens, G. K., Kumar, M. S. and Wamhoff, B. R. (2004). Molecular regulation of vascular smooth muscle cell differentiation in development and disease. *Physiological reviews* **84**, 767-801.

Oyamada, N., Itoh, H., Sone, M., Yamahara, K., Miyashita, K., Park, K., Taura, D., Inuzuka, M., Sonoyama, T., Tsujimoto, H., et al. (2008). Transplantation of vascular cells derived from human embryonic stem cells contributes to vascular regeneration after stroke in mice. *Journal of translational medicine* **6**, 54.

Paige, S., Osugi, T., Afanasiev, O., Pabon, L., Reinecke, H. and Murry, C. (2010). Endogenous Wnt/beta-catenin signaling is required for cardiac differentiation in human embryonic stem cells. *PLoS ONE* **5**, e11134.

Park, C., Afrikanova, I., Chung, Y. S., Zhang, W. J., Arentson, E., Fong Gh, G., Rosendahl, A. and Choi, K. (2004). A hierarchical order of factors in the generation of FLK1- and SCL-expressing hematopoietic and endothelial progenitors from embryonic stem cells. *Development* **131**, 2749-2762.

Park, I. H., Lerou, P. H., Zhao, R., Huo, H. and Daley, G. Q. (2008). Generation of human-induced pluripotent stem cells. *Nat Protoc* **3**, 1180-1186.

Park, S., Jun Koh, Y., Jeon, J., Cho, Y., Jang, M., Kang, Y., Kim, M., Choi, C., Sook Cho, Y., Chung, H., et al. (2010). Efficient differentiation of human pluripotent stem cells into functional CD34+ progenitor cells by combined modulation of the MEK/ERK and BMP4 signaling pathways. *Blood* **116**, 5762-5772.

Park, T. S., Zimmerlin, L. and Zambidis, E. T. (2013). Efficient and simultaneous generation of hematopoietic and vascular progenitors from human induced pluripotent stem cells. *Cytometry. Part A : the journal of the International Society for Analytical Cytology* **83**, 114-126.

Pearce, J. J. and Evans, M. J. (1999). Mml, a mouse Mix-like gene expressed in the primitive streak. *Mech Dev* **87**, 189-192.

Phelps, E. A. and Garcia, A. J. (2010). Engineering more than a cell: vascularization strategies in tissue engineering. *Current opinion in biotechnology* **21**, 704-709.

Pick, M., Azzola, L., Mossman, A., Stanley, E. G. and Elefanty, A. G. (2007). Differentiation of human embryonic stem cells in serum-free medium reveals distinct roles for bone morphogenetic protein 4, vascular endothelial growth factor, stem cell factor, and fibroblast growth factor 2 in hematopoiesis. *Stem cells* **25**, 2206-2214.

Plotkin, M., Vaibavi, S. R., Rufaihah, A. J., Nithya, V., Wang, J., Shachaf, Y., Kofidis, T. and Seliktar, D. (2014). The effect of matrix stiffness of injectable hydrogels on the preservation of cardiac function after a heart attack. *Biomaterials* **35**, 1429-1438.

Pola, R., Ling, L. E., Silver, M., Corbley, M. J., Kearney, M., Blake Pepinsky, R., Shapiro, R., Taylor, F. R., Baker, D. P., Asahara, T., et al. (2001). The morphogen Sonic hedgehog is an indirect angiogenic agent upregulating two families of angiogenic growth factors. *Nature medicine* **7**, 706-711.

Richardson, T. P., Peters, M. C., Ennett, A. B. and Mooney, D. J. (2001). Polymeric system for dual growth factor delivery. *Nat Biotechnol* **19**, 1029-1034.

Rivron, N. C., Liu, J. J., Rouwkema, J., de Boer, J. and van Blitterswijk, C. A. (2008). Engineering vascularised tissues in vitro. *European cells & materials* **15**, 27-40.

Robb, L., Hartley, L., Begley, C. G., Brodnicki, T. C., Copeland, N. G., Gilbert, D. J., Jenkins, N. A. and Elefanty, A. G. (2000). Cloning, expression analysis, and chromosomal localization of murine and human homologues of a Xenopus mix gene. *Developmental dynamics : an official publication of the American Association of Anatomists* **219**, 497-504.

Rubin, L. L. (2008). Stem cells and drug discovery: the beginning of a new era? *Cell* **132**, 549-552.

Rufaihah, A. J., Haider, H. K., Heng, B. C., Ye, L., Tan, R. S., Toh, W. S., Tian, X. F., Sim, E. K. and Cao, T. (2010). Therapeutic angiogenesis by transplantation of human embryonic stem cell-derived CD133+ endothelial progenitor cells for cardiac repair. *Regen Med* **5**, 231-244.

Rufaihah, A. J., Haider, H. K., Heng, B. C., Ye, L., Toh, W. S., Tian, X. F., Lu, K., Sim, E. K. and Cao, T. (2007). Directing endothelial differentiation of human embryonic stem cells via transduction with an adenoviral vector expressing the VEGF(165) gene. *J Gene Med* **9**, 452-461.

Rufaihah, A. J., Huang, N. F., Jame, S., Lee, J. C., Nguyen, H. N., Byers, B., De, A., Okogbaa, J., Rollins, M., Reijo-Pera, R., et al. (2011). Endothelial cells derived from human iPSCS increase capillary density and improve perfusion in a mouse model of peripheral arterial disease. *Arterioscler Thromb Vasc Biol* **31**, e72-79.

Rufaihah, A. J., Huang, N. F., Kim, J., Herold, J., Volz, K. S., Park, T. S., Lee, J. C., Zambidis, E. T., Reijo-Pera, R. and Cooke, J. P. (2013a). Human induced pluripotent stem cell-derived endothelial cells exhibit functional heterogeneity. *American journal of translational research* **5**, 21-35.

Rufaihah, A. J., Vaibavi, S. R., Plotkin, M., Shen, J., Nithya, V., Wang, J., Seliktar, D. and Kofidis, T. (2013b). Enhanced infarct stabilization and neovascularization mediated by VEGF-loaded PEGylated fibrinogen hydrogel in a rodent myocardial infarction model. *Biomaterials* **34**, 8195-8202.

Saeki, K., Yogiashi, Y., Nakahara, M., Nakamura, N., Matsuyama, S., Koyanagi, A., Yagita, H., Koyanagi, M., Kondo, Y. and Yuo, A. (2008). Highly efficient and feeder-free production of subculturable vascular endothelial cells from primate embryonic stem cells. *J Cell Physiol* **217**, 261-280.

Sahni, A., Baker, C. A., Sporn, L. A. and Francis, C. W. (2000). Fibrinogen and fibrin protect fibroblast growth factor-2 from proteolytic degradation. *Thrombosis and haemostasis* **83**, 736-741.

Sahni, A. and Francis, C. W. (2000). Vascular endothelial growth factor binds to fibrinogen and fibrin and stimulates endothelial cell proliferation. *Blood* **96**, 3772-3778.

Sahni, A., Khorana, A. A., Baggs, R. B., Peng, H. and Francis, C. W. (2006). FGF-2 binding to fibrin(ogen) is required for augmented angiogenesis. *Blood* **107**, 126-131.

Saif, J., Schwarz, T. M., Chau, D. Y., Henstock, J., Sami, P., Leicht, S. F., Hermann, P. C., Alcala, S., Mulero, F., Shakesheff, K. M., et al. (2010). Combination of injectable multiple growth factor-releasing scaffolds and cell therapy as an advanced modality to enhance tissue neovascularization. *Arterioscler Thromb Vasc Biol* **30**, 1897-1904.

Sakurai, H., Era, T., Jakt, L. M., Okada, M., Nakai, S. and Nishikawa, S. (2006). In vitro modeling of paraxial and lateral mesoderm differentiation reveals early reversibility. *Stem cells* **24**, 575-586.

Sakurai, H., Sakaguchi, Y., Shoji, E., Nishino, T., Maki, I., Sakai, H., Hanaoka, K., Kakizuka, A. and Sehara-Fujisawa, A. (2012). In vitro modeling of paraxial mesodermal progenitors derived from induced pluripotent stem cells. *PLoS One* **7**, e47078.

Samuel, R., Daheron, L., Liao, S., Vardam, T., Kamoun, W. S., Batista, A., Buecker, C., Schafer, R., Han, X., Au, P., et al. (2013). Generation of functionally competent and durable engineered blood vessels from human induced pluripotent stem cells. *Proc Natl Acad Sci U S A* **110**, 12774-12779.

Sato, N., Meijer, L., Skaltsounis, L., Greengard, P. and Brivanlou, A. H. (2004). Maintenance of pluripotency in human and mouse embryonic stem cells through activation of Wnt signaling by a pharmacological GSK-3-specific inhibitor. *Nature medicine* **10**, 55-63.

Sato, T. (2013). Mechanical and Chemical Regulation of Arterial and Venous Specification. In *Mechanical and Chemical Signaling in Angiogenesis* (ed. C. A. Reinhart-King), pp. 1-17: Springer Berlin Heidelberg.

Schatteman, G. C., Morrison-Graham, K., van Koppen, A., Weston, J. A. and Bowen-Pope, D. F. (1992). Regulation and role of PDGF receptor alpha-subunit expression during embryogenesis. *Development* **115**, 123-131.

Seetharaman, S., Natesan, S., Stowers, R. S., Mullens, C., Baer, D. G., Suggs, L. J. and Christy, R. J. (2011). A PEGylated fibrin-based wound dressing with antimicrobial and angiogenic activity. *Acta Biomater* **7**, 2787-2796.

Shaikh, F. M., Callanan, A., Kavanagh, E. G., Burke, P. E., Grace, P. A. and McGloughlin, T. M. (2008). Fibrin: a natural biodegradable scaffold in vascular tissue engineering. *Cells Tissues Organs* **188**, 333-346.

Shalaby, F., Ho, J., Stanford, W. L., Fischer, K. D., Schuh, A. C., Schwartz, L., Bernstein, A. and Rossant, J. (1997). A requirement for Flk1 in primitive and definitive hematopoiesis and vasculogenesis. *Cell* **89**, 981-990.

Shalaby, F., Rossant, J., Yamaguchi, T. P., Gertsenstein, M., Wu, X. F., Breitman, M. L. and Schuh, A. C. (1995). Failure of blood-island formation and vasculogenesis in Flk-1-deficient mice. *Nature* **376**, 62-66.

Shepherd, B. R., Chen, H. Y., Smith, C. M., Gruionu, G., Williams, S. K. and Hoying, J. B. (2004). Rapid perfusion and network remodeling in a microvascular construct after implantation. *Arterioscler Thromb Vasc Biol* **24**, 898-904.

Shepro, D. and Morel, N. M. (1993). Pericyte physiology. *FASEB J* **7**, 1031-1038.

Singh, R. K., Seliktar, D. and Putnam, A. J. (2013). Capillary morphogenesis in PEG-collagen hydrogels. *Biomaterials* **34**, 9331-9340.

Singla, D. K., Schneider, D. J., LeWinter, M. M. and Sobel, B. E. (2006). wnt3a but not wnt11 supports self-renewal of embryonic stem cells. *Biochem Biophys Res Commun* **345**, 789-795.

Slack, J. M., Darlington, B. G., Heath, J. K. and Godsave, S. F. (1987). Mesoderm induction in early Xenopus embryos by heparin-binding growth factors. *Nature* **326**, 197-200.

Sokol, S. (2011a). Maintaining embryonic stem cell pluripotency with Wnt signaling. *Development* **138**, 4341-4350.

Sokol, S. Y. (2011b). Maintaining embryonic stem cell pluripotency with Wnt signaling. *Development* **138**, 4341-4350.

Sone, M., Itoh, H., Yamahara, K., Yamashita, J. K., Yurugi-Kobayashi, T., Nonoguchi, A., Suzuki, Y., Chao, T. H., Sawada, N., Fukunaga, Y., et al. (2007). Pathway for differentiation of human embryonic stem cells to vascular cell components and their potential for vascular regeneration. *Arterioscler Thromb Vasc Biol* **27**, 2127-2134.

Song, S. H., Jung, W., Kim, K. L., Hong, W., Kim, H. O., Lee, K. A., Lee, K. Y. and Suh, W. (2013). Distinct transcriptional profiles of angioblasts derived from human embryonic stem cells. *Exp Cell Res* **319**, 1136-1145.

Steffens, L., Wenger, A., Stark, G. B. and Finkenzeller, G. (2009). In vivo engineering of a human vasculature for bone tissue engineering applications. *Journal of cellular and molecular medicine* **13**, 3380-3386.

Sumi, T., Tsuneyoshi, N., Nakatsuji, N. and Suemori, H. (2008). Defining early lineage specification of human embryonic stem cells by the orchestrated balance of canonical Wnt/beta-catenin, Activin/Nodal and BMP signaling. *Development* **135**, 2969-2979.

Sun, G., Shen, Y. I., Kusuma, S., Fox-Talbot, K., Steenbergen, C. J. and Gerecht, S. (2011). Functional neovascularization of biodegradable dextran hydrogels with multiple angiogenic growth factors. *Biomaterials* **32**, 95-106.

Sun, X., Cheng, L., Duan, H., Lin, G. and Lu, G. (2012). Characterization and comparison of embryonic stem cell-derived KDR+ cells with endothelial cells. *Microvascular research* **84**, 149-154.

Sun, X., Meyers, E. N., Lewandoski, M. and Martin, G. R. (1999). Targeted disruption of Fgf8 causes failure of cell migration in the gastrulating mouse embryo. *Genes & development* **13**, 1834-1846.

Swift, M. R. and Weinstein, B. M. (2009). Arterial-venous specification during development. *Circ Res* **104**, 576-588.

Takahashi, K., Tanabe, K., Ohnuki, M., Narita, M., Ichisaka, T., Tomoda, K. and Yamanaka, S. (2007). Induction of pluripotent stem cells from adult human fibroblasts by defined factors. *Cell* **131**, 861-872.

Takakura, N., Yoshida, H., Ogura, Y., Kataoka, H., Nishikawa, S. and Nishikawa, S. (1997). PDGFR alpha expression during mouse embryogenesis: immunolocalization analyzed by whole-mount immunohistostaining using the monoclonal anti-mouse PDGFR alpha antibody APA5. *The journal of histochemistry and cytochemistry : official journal of the Histochemistry Society* **45**, 883-893.

Takao, Y., Yokota, T. and Koide, H. (2007). Beta-catenin up-regulates Nanog expression through interaction with Oct-3/4 in embryonic stem cells. *Biochem Biophys Res Commun* **353**, 699-705.

Takashima, S., Kitakaze, M., Asakura, M., Asanuma, H., Sanada, S., Tashiro, F., Niwa, H., Miyazaki Ji, J., Hirota, S., Kitamura, Y., et al. (2002). Targeting of both mouse neuropilin-1 and neuropilin-2 genes severely impairs developmental yolk sac and embryonic angiogenesis. *Proc Natl Acad Sci U S A* **99**, 3657-3662.

Tam, P. P. and Beddington, R. S. (1987). The formation of mesodermal tissues in the mouse embryo during gastrulation and early organogenesis. *Development* **99**, 109-126.

Tam, P. P. and Behringer, R. R. (1997). Mouse gastrulation: the formation of a mammalian body plan. *Mech Dev* **68**, 3-25.

Tam, P. P. and Loebel, D. A. (2007). Gene function in mouse embryogenesis: get set for gastrulation. *Nature reviews. Genetics* **8**, 368-381.

Tan, J. Y., Sriram, G., Rufaihah, A. J., Neoh, K. G. and Cao, T. (2013a). Efficient Derivation of Lateral Plate and Paraxial Mesoderm Subtypes from Human Embryonic Stem Cells Through GSKi-Mediated Differentiation. *Stem Cells Dev* **22**, 1893-1906.

Tan, K. S., Tamura, K., Lai, M. I., Veerakumarasivam, A., Nakanishi, Y., Ogawa, M. and Sugiyama, D. (2013b). Molecular pathways governing development of vascular endothelial cells from ES/iPS cells. *Stem Cell Rev* **9**, 586-598.

Tatsumi, R., Suzuki, Y., Sumi, T., Sone, M., Suemori, H. and Nakatsuji, N. (2011). Simple and highly efficient method for production of endothelial cells from human embryonic stem cells. *Cell transplantation* **20**, 1423-1430.

Taura, D., Sone, M., Homma, K., Oyamada, N., Takahashi, K., Tamura, N., Yamanaka, S. and Nakao, K. (2009). Induction and isolation of vascular cells from human induced pluripotent stem cells--brief report. *Arterioscler Thromb Vasc Biol* **29**, 1100-1103.

ten Berge, D., Kurek, D., Blauwkamp, T., Koole, W., Maas, A., Eroglu, E., Siu, R. K. and Nusse, R. (2011). Embryonic stem cells require Wnt proteins to prevent differentiation to epiblast stem cells. *Nat Cell Biol* **13**, 1070-1075.

Thomson, J. A., Itskovitz-Eldor, J., Shapiro, S. S., Waknitz, M. A., Swiergiel, J. J., Marshall, V. S. and Jones, J. M. (1998). Embryonic stem cell lines derived from human blastocysts. *Science* **282**, 1145-1147.

Tian, L. and George, S. C. (2011). Biomaterials to prevascularize engineered tissues. *Journal of cardiovascular translational research* **4**, 685-698.

Topouzis, S. and Majesky, M. W. (1996). Smooth muscle lineage diversity in the chick embryo. Two types of aortic smooth muscle cell differ in growth and receptor-mediated transcriptional responses to transforming growth factor-beta. *Developmental biology* **178**, 430-445.

Torres-Vazquez, J., Kamei, M. and Weinstein, B. M. (2003). Molecular distinction between arteries and veins. *Cell and tissue research* **314**, 43-59.

Tremblay, P. L., Hudon, V., Berthod, F., Germain, L. and Auger, F. A. (2005). Inosculation of tissue-engineered capillaries with the host's vasculature in a reconstructed skin transplanted on mice. *American journal of transplantation : official journal of the American Society of Transplantation and the American Society of Transplant Surgeons* **5**, 1002-1010.

Trounson, A. (2006). The production and directed differentiation of human embryonic stem cells. *Endocrine reviews* **27**, 208-219.

Tsigkou, O., Pomerantseva, I., Spencer, J. A., Redondo, P. A., Hart, A. R., O'Doherty, E., Lin, Y., Friedrich, C. C., Daheron, L., Lin, C. P., et al. (2010). Engineered vascularized bone grafts. *Proc Natl Acad Sci U S A* **107**, 3311-3316.

Ueno, S., Weidinger, G., Osugi, T., Kohn, A. D., Golob, J. L., Pabon, L., Reinecke, H., Moon, R. T. and Murry, C. E. (2007). Biphasic role for Wnt/beta-catenin signaling in cardiac specification in zebrafish and embryonic stem cells. *Proc Natl Acad Sci U S A* **104**, 9685-9690.

Ungrin, M. D., Joshi, C., Nica, A., Bauwens, C. and Zandstra, P. W. (2008). Reproducible, ultra high-throughput formation of multicellular organization from single cell suspension-derived human embryonic stem cell aggregates. *PLoS One* **3**, e1565.

Vallier, L., Touboul, T., Chng, Z., Brimpari, M., Hannan, N., Millan, E., Smithers, L., Trotter, M., Rugg-Gunn, P., Weber, A., et al. (2009). Early cell fate decisions of human embryonic stem cells and mouse epiblast stem cells are controlled by the same signalling pathways. *PLoS ONE* **4**, e6082.

Vazao, H., das Neves, R. P., Graos, M. and Ferreira, L. (2011). Towards the maturation and characterization of smooth muscle cells derived from human embryonic stem cells. *PloS one* **6**, e17771.

Vittet, D., Prandini, M. H., Berthier, R., Schweitzer, A., Martin-Sisteron, H., Uzan, G. and Dejana, E. (1996). Embryonic stem cells differentiate in vitro to endothelial cells through successive maturation steps. *Blood* **88**, 3424-3431.

Vo, E., Hanjaya-Putra, D., Zha, Y., Kusuma, S. and Gerecht, S. (2010). Smooth-muscle-like cells derived from human embryonic stem cells support and augment cord-like structures in vitro. *Stem Cell Rev* **6**, 237-247.

Vodyanik, M. A., Bork, J. A., Thomson, J. A. and Slukvin, II (2005). Human embryonic stem cell-derived CD34+ cells: efficient production in the coculture with OP9 stromal cells and analysis of lymphohematopoietic potential. *Blood* **105**, 617-626.

Vodyanik, M. A. and Slukvin, II (2007). Hematoendothelial differentiation of human embryonic stem cells. *Current protocols in cell biology / editorial board, Juan S. Bonifacino ... [et al.]* **Chapter 23**, Unit 23 26.

Vodyanik, M. A., Yu, J., Zhang, X., Tian, S., Stewart, R., Thomson, J. A. and Slukvin, II (2010). A mesoderm-derived precursor for mesenchymal stem and endothelial cells. *Cell Stem Cell* **7**, 718-729.

Voyta, J. C., Via, D. P., Butterfield, C. E. and Zetter, B. R. (1984). Identification and isolation of endothelial cells based on their increased uptake of acetylated-low density lipoprotein. *J Cell Biol* **99**, 2034-2040.

Wagner, R. T., Xu, X., Yi, F., Merrill, B. J. and Cooney, A. J. (2010). Canonical Wnt/beta-catenin regulation of liver receptor homolog-1 mediates pluripotency gene expression. *Stem cells* **28**, 1794-1804.

Waldo, K. L., Hutson, M. R., Ward, C. C., Zdanowicz, M., Stadt, H. A., Kumiski, D., Abu-Issa, R. and Kirby, M. L. (2005). Secondary heart field contributes myocardium and smooth muscle to the arterial pole of the developing heart. *Developmental biology* **281**, 78-90.

Wang, A., Tang, Z., Li, X., Jiang, Y., Tsou, D. A. and Li, S. (2012a). Derivation of smooth muscle cells with neural crest origin from human induced pluripotent stem cells. *Cells Tissues Organs* **195**, 5-14.

Wang, C. H., Lee, Y. S., Lin, S. J., Mei, H. F., Lin, S. Y., Liu, M. H., Chen, J. R. and Cherng, W. J. (2012b). Surface markers of heterogeneous peripheral blood-derived smooth muscle progenitor cells. *Arterioscler Thromb Vasc Biol* **32**, 1875-1883.

Wang, H. U., Chen, Z. F. and Anderson, D. J. (1998). Molecular distinction and angiogenic interaction between embryonic arteries and veins revealed by ephrin-B2 and its receptor Eph-B4. *Cell* **93**, 741-753.

Wang, L., Fan, H., Zhang, Z. Y., Lou, A. J., Pei, G. X., Jiang, S., Mu, T. W., Qin, J. J., Chen, S. Y. and Jin, D. (2010). Osteogenesis and angiogenesis of tissue-engineered bone constructed by prevascularized beta-tricalcium phosphate scaffold and mesenchymal stem cells. *Biomaterials* **31**, 9452-9461.

Wang, L., Li, L., Shojaei, F., Levac, K., Cerdan, C., Menendez, P., Martin, T., Rouleau, A. and Bhatia, M. (2004). Endothelial and hematopoietic cell fate of human embryonic stem cells originates from primitive endothelium with hemangioblastic properties. *Immunity* **21**, 31-41.

Wang, Z. Z., Au, P., Chen, T., Shao, Y., Daheron, L. M., Bai, H., Arzigian, M., Fukumura, D., Jain, R. K. and Scadden, D. T. (2007). Endothelial cells derived from human embryonic stem cells form durable blood vessels in vivo. *Nat Biotechnol* **25**, 317-318.

Wanjare, M., Kuo, F. and Gerecht, S. (2013). Derivation and maturation of synthetic and contractile vascular smooth muscle cells from human pluripotent stem cells. *Cardiovascular research* **97**, 321-330.

Warnke, P. H., Springer, I. N., Wiltfang, J., Acil, Y., Eufinger, H., Wehmoller, M., Russo, P. A., Bolte, H., Sherry, E., Behrens, E., et al. (2004). Growth and transplantation of a custom vascularised bone graft in a man. *Lancet* **364**, 766-770.

White, M. P., Rufaihah, A. J., Liu, L., Ghebremariam, Y. T., Ivey, K. N., Cooke, J. P. and Srivastava, D. (2013). Limited gene expression variation in human embryonic stem cell and induced pluripotent stem cell-derived endothelial cells. *Stem cells* **31**, 92-103.

Wiles, M. V. and Johansson, B. M. (1999). Embryonic stem cell development in a chemically defined medium. *Exp Cell Res* **247**, 241-248.

Wilkinson, D. G., Bhatt, S. and Herrmann, B. G. (1990). Expression pattern of the mouse T gene and its role in mesoderm formation. *Nature* **343**, 657-659.

Winnier, G., Blessing, M., Labosky, P. A. and Hogan, B. L. (1995). Bone morphogenetic protein-4 is required for mesoderm formation and patterning in the mouse. *Genes & development* **9**, 2105-2116.

Woll, P. S., Morris, J. K., Painschab, M. S., Marcus, R. K., Kohn, A. D., Biechele, T. L., Moon, R. T. and Kaufman, D. S. (2008). Wnt signaling promotes hematoendothelial cell development from human embryonic stem cells. *Blood* **111**, 122-131.

Wozniak, G. (2003). Fibrin sealants in supporting surgical techniques: The importance of individual components. *Cardiovasc Surg* **11 Suppl 1**, 17-21.

Wu, S. M., Fujiwara, Y., Cibulsky, S. M., Clapham, D. E., Lien, C. L., Schultheiss, T. M. and Orkin, S. H. (2006). Developmental origin of a bipotential myocardial and smooth muscle cell precursor in the mammalian heart. *Cell* **127**, 1137-1150.

Xiao, Q., Zeng, L., Zhang, Z., Margariti, A., Ali, Z. A., Channon, K. M., Xu, Q. and Hu, Y. (2006). Sca-1+ progenitors derived from embryonic stem cells differentiate into endothelial cells capable of vascular repair after arterial injury. *Arterioscler Thromb Vasc Biol* **26**, 2244-2251.

Xie, C. Q., Zhang, J., Villacorta, L., Cui, T., Huang, H. and Chen, Y. E. (2007). A highly efficient method to differentiate smooth muscle cells from human embryonic stem cells. *Arterioscler Thromb Vasc Biol* **27**, e311-312.

Xiong, Q., Hill, K. L., Li, Q., Suntharalingam, P., Mansoor, A., Wang, X., Jameel, M. N., Zhang, P., Swingen, C., Kaufman, D. S., et al. (2011). A fibrin patch-based enhanced delivery of human embryonic stem cell-derived vascular cell transplantation in a porcine model of postinfarction left ventricular remodeling. *Stem Cells* **29**, 367-375.

Xu, R. H., Chen, X., Li, D. S., Li, R., Addicks, G. C., Glennon, C., Zwaka, T. P. and Thomson, J. A. (2002). BMP4 initiates human embryonic stem cell differentiation to trophoblast. *Nat Biotechnol* **20**, 1261-1264.

Yamaguchi, T., Takada, S., Yoshikawa, Y., Wu, N. and McMahon, A. (1999). T (Brachyury) is a direct target of Wnt3a during paraxial mesoderm specification. *Genes & development* **13**, 3185-3190.

Yamaguchi, T. P., Dumont, D. J., Conlon, R. A., Breitman, M. L. and Rossant, J. (1993). flk-1, an flt-related receptor tyrosine kinase is an early marker for endothelial cell precursors. *Development* **118**, 489-498.

Yamaguchi, T. P., Harpal, K., Henkemeyer, M. and Rossant, J. (1994). fgfr-1 is required for embryonic growth and mesodermal patterning during mouse gastrulation. *Genes & development* **8**, 3032-3044.

Yamahara, K., Sone, M., Itoh, H., Yamashita, J. K., Yurugi-Kobayashi, T., Homma, K., Chao, T. H., Miyashita, K., Park, K., Oyamada, N., et al. (2008). Augmentation of neovascularization [corrected] in hindlimb ischemia by combined transplantation of human embryonic stem cells-derived endothelial and mural cells. *PloS one* **3**, e1666.

Yamamizu, K., Matsunaga, T., Uosaki, H., Fukushima, H., Katayama, S., Hiraoka-Kanie, M., Mitani, K. and Yamashita, J. K. (2010). Convergence of Notch and beta-catenin signaling induces arterial fate in vascular progenitors. *J Cell Biol* **189**, 325-338.

Yamamizu, K. and Yamashita, J. K. (2011). Roles of cyclic adenosine monophosphate signaling in endothelial cell differentiation and arterial-venous specification during vascular development. *Circulation journal : official journal of the Japanese Circulation Society* **75**, 253-260.

Yamashita, J., Itoh, H., Hirashima, M., Ogawa, M., Nishikawa, S., Yurugi, T., Naito, M. and Nakao, K. (2000). Flk1-positive cells derived from embryonic stem cells serve as vascular progenitors. *Nature* **408**, 92-96.

Yanagisawa, K. O., Fujimoto, H. and Urushihara, H. (1981). Effects of the brachyury (T) mutation on morphogenetic movement in the mouse embryo. *Developmental biology* **87**, 242-248.

Yang, L., Soonpaa, M. H., Adler, E. D., Roepke, T. K., Kattman, S. J., Kennedy, M., Henckaerts, E., Bonham, K., Abbott, G. W., Linden, R. M., et al. (2008a). Human cardiovascular progenitor cells develop from a KDR+ embryonic-stem-cell-derived population. *Nature* **453**, 524-528.

Yang, X., Chrisman, H. and Weijer, C. J. (2008b). PDGF signalling controls the migration of mesoderm cells during chick gastrulation by regulating N-cadherin expression. *Development* **135**, 3521-3530.

Yee, D., Hanjaya-Putra, D., Bose, V., Luong, E. and Gerecht, S. (2011). Hyaluronic Acid hydrogels support cord-like structures from endothelial colony-forming cells. *Tissue engineering. Part A* **17**, 1351-1361.

You, L. R., Lin, F. J., Lee, C. T., DeMayo, F. J., Tsai, M. J. and Tsai, S. Y. (2005). Suppression of Notch signalling by the COUP-TFII transcription factor regulates vein identity. *Nature* **435**, 98-104.

Young, D. M., Greulich, K. M. and Weier, H. G. (1996). Species-specific in situ hybridization with fluorochrome-labeled DNA probes to study vascularization of human skin grafts on athymic mice. *The Journal of burn care & rehabilitation* **17**, 305-310.

Yu, J., Huang, N. F., Wilson, K. D., Velotta, J. B., Huang, M., Li, Z., Lee, A., Robbins, R. C., Cooke, J. P. and Wu, J. C. (2009). nAChRs mediate human embryonic stem cell-derived endothelial cells: proliferation, apoptosis, and angiogenesis. *PLoS One* **4**, e7040.

Yu, J., Vodyanik, M. A., Smuga-Otto, K., Antosiewicz-Bourget, J., Frane, J. L., Tian, S., Nie, J., Jonsdottir, G. A., Ruotti, V., Stewart, R., et al. (2007). Induced pluripotent stem cell lines derived from human somatic cells. *Science* **318**, 1917-1920.

Yu, P., Pan, G., Yu, J. and Thomson, J. (2011). FGF2 sustains NANOG and switches the outcome of BMP4-induced human embryonic stem cell differentiation. *Cell Stem Cell* **8**, 326-334.

Yurugi-Kobayashi, T., Itoh, H., Schroeder, T., Nakano, A., Narazaki, G., Kita, F., Yanagi, K., Hiraoka-Kanie, M., Inoue, E., Ara, T., et al. (2006). Adrenomedullin/cyclic AMP pathway induces Notch activation and differentiation of arterial endothelial cells from vascular progenitors. *Arterioscler Thromb Vasc Biol* **26**, 1977-1984.

Zambidis, E. T., Park, T. S., Yu, W., Tam, A., Levine, M., Yuan, X., Pryzhkova, M. and Peault, B. (2008). Expression of angiotensin-converting enzyme (CD143) identifies and regulates primitive hemangioblasts derived from human pluripotent stem cells. *Blood* **112**, 3601-3614.

Zeng, L., Xiao, Q., Margariti, A., Zhang, Z., Zampetaki, A., Patel, S., Capogrossi, M. C., Hu, Y. and Xu, Q. (2006). HDAC3 is crucial in shear- and VEGF-induced stem cell differentiation toward endothelial cells. *J Cell Biol* **174**, 1059-1069.

Zhang, G., Drinnan, C. T., Geuss, L. R. and Suggs, L. J. (2010). Vascular differentiation of bone marrow stem cells is directed by a tunable three-dimensional matrix. *Acta Biomater* **6**, 3395-3403.

Zhang, G., Hu, Q., Braunlin, E. A., Suggs, L. J. and Zhang, J. (2008a). Enhancing efficacy of stem cell transplantation to the heart with a PEGylated fibrin biomatrix. *Tissue engineering. Part A* **14**, 1025-1036.

Zhang, G., Wang, X., Wang, Z., Zhang, J. and Suggs, L. (2006). A PEGylated fibrin patch for mesenchymal stem cell delivery. *Tissue Eng* **12**, 9-19.

Zhang, G., Zhou, J., Fan, Q., Zheng, Z., Zhang, F., Liu, X. and Hu, S. (2008b). Arterial-venous endothelial cell fate is related to vascular endothelial growth factor and Notch status during human bone mesenchymal stem cell differentiation. *FEBS letters* **582**, 2957-2964.

Zhang, P., Li, J., Tan, Z., Wang, C., Liu, T., Chen, L., Yong, J., Jiang, W., Sun, X., Du, L., et al. (2008c). Short-term BMP-4 treatment initiates mesoderm induction in human embryonic stem cells. *Blood* **111**, 1933-1941.

Zhou, Y. and Snead, M. L. (2008). Derivation of cranial neural crest-like cells from human embryonic stem cells. *Biochem Biophys Res Commun* **376**, 542-547.

Zhu, J. (2010). Bioactive modification of poly(ethylene glycol) hydrogels for tissue engineering. *Biomaterials* **31**, 4639-4656.

Chapter 10

Appendix

Appendix I

Sequences of primers used for real time RT-PCR.

Gene [Gene bank ID]	Primer sequence	Product length	GenBank ID
BACTIN	F: 5'-CCAAGGCCAACCGCGAGAAGATGAC-3' R: 5'-AGGGTACATGGTGGTGCCGCCAGAC-3'	587 bp	*NM_001101.3*
BRACHYURY	F: 5'-GGGTGGCTTCTTCCTGGAAC-3' R: 5'-TTGGAGAATTGTTCCGATGAG-3'	172 bp	*NM_003181.2*
CD31	F: 5'-TCTATGACCTCGCCCTCCACAAA-3' R: 5'-GAACGGTGTCTTCAGGTTGGTATTTCA-3'	83 bp	*NM_000442.4*
CD34	F: 5- AAATCCTCTTCCTCTGAGGCTGGA-3' R: 5- AAGAGGCAGCTGGTGATAAGGGTT-3'	216 bp	*NM_001773.2*
CNN1	F: 5'-GTCCACCCTCCTGGCTTT-3' R: 5'-AAACTTGTTGGTGCCCATCT-3'	157 bp	*NM_001299.4*
COUP-TFII	F: 5'-CCATAGTCCTGTTCACCTCA-3' R: 5'-GGTACTGGCTCCTAACGTATTC-3'	111 bp	*NM_021005.3*
CXCR4	F: 5'-CGCCTGTTGGCTGCCTTA-3' R: 5'-ACCCTTGCTTGATGATTTCCA-3'	74 bp	*NM_003467.2*
DLL4	F: 5'-TGCTGCTGGTGGCACTTT-3' R: 5'-CTTGTGAGGGTGCTGGTT-3'	457 bp	*NM_019074.3*
eNOS	F: 5'-GGCTGCTCAGCACCTTGGCA-3' R:5'-GAGGGCCTCCAGCTCCTGCT-3'	56 bp	*NM_000603.4*
EPH-B4	F: 5'-AGAGGCCGTACTGGGACATGAG-3' R: 5'-TCCAGCATGAGCTGGTGGAG-3'	112 bp	*NM_004444.4*
EPHRIN-B2	F: 5'-CCCAGTGACATTATCATCCC-3' R: 5'-CATCTCCTGGACGATGTACACC-3'	108 bp	*NM_004093.3*
FOXA2	F: 5'-CCATTGCTGTTGTTGCAGGGAAGT-3' R: 5'-CACCGTGTCAAGATTGGGAATGCT-3'	196 bp	*NM_021784*
GATA2	F: 5'-AGCCGGCACCTGTTGTGCAA-3' R: 5'-TGACTTCTCCTGCATGCACT-3'	244 bp	*NM_032638.4*
GATA4	F: 5'-CCTCCTCTGCCTGGTAATGACT-3' R: 5'-CGCTTCCCCTAACCAGATTG-3'	76 bp	*NM_002052.3*
GSC	F: 5'-GATGCTGCCCTACATGAACGT-3' R: 5'-GACAGTGCAGCTGGTTGAGAAG-3'	71 bp	*NM_173849.2*
MIXL1	F: 5'-AAGCCCCAGCTGCCTGTT-3' R: 5'-CCCTCCAACCCCGTTTG-3'	63 bp	*NM_031944.1*
MYH11	F:5'-AGATGGTTCTGAGGAGGAAACG-3' R: 5'-AAAACTGTAGAAAGTTGCTTATTCACT-3'	85 bp	*NM_002474.2*
NANOG	F: 5'-TGATTTGTGGGCCTGAAGAAAA-3' R: 5'-GAGGCATCTCAGCAGAAGACA-3'	493 bp	*NM_024865.2*
NOTCH1	F: 5'-CACGCGGATTAATTTGCATCTG-3' R: 5'-TCTTGGCATACACACTCCGAGAAC-3'	129 bp	*NM_017617.3*
NRP1	F: 5'-CATCTCCTGGTTATCCTCATTC-3' R: 5'-GTCATACTTGCAGTCTCTGTCC-3'	137 bp	*NM_003873.5*

Gene [Gene bank ID]	Primer sequence	Product length	GenBank ID
NRP2	F: 5'-GCATGGCAAAAACCACAAGGTAT-3' R: 5'-TGGAGCGTGGAGCTTGTTCA-3'	76 bp	*NM_201266.1*
OCT4	F: 5'-CGTGAAGCTGGAGAAGGAGAAGCTG-3' R: 5'-AAGGGCCGCAGCTTACACATGTTC-3'	247 bp	*NM_002701.4*
PAX6	F: 5'-CTGGCTAGCGAAAAGCAACAG-3' R: 5'-CCCGTTCAACATCCTTAGTTTATCA-3'	66 bp	*NM_001604*
PDFGRβ	F: 5'-TGGCAGAAGAAGCCACGTT-3' R: 5'-GGCCGTCAGAGCTCACAGA-3'	63 bp	*NM_002609*
PDGFRα	F: 5'-GATTAAGCCGGTCCCAACCT-3' R: 5'-GGATCTGGCCGTGGGTTT-3'	65 bp	*NM_006206*
SMTN	F:5'-CGGCCTGCGCGTGTCTAATCC-3' R: 5'-CTGTGACCTCCAGCAGCTTCCGAA-3'	227 bp	*NM_134270.2*
SNAI1	F: 5'-CCCACATCCTTCTCACTGC-3' R: 5'-GTCAGCCTTTGTCCTGTAGC-3'	265 bp	*NM_005985*
SOX1	F: 5'-GCGGTAACAACTACAAAAAACTTGTAA-3' R: 5'-GCGGAGCTCGTCGCATT-3'	76 bp	*NM_005986*
SOX2	F: 5'-CCGCATGTACAACATGATGG-3' R: 5'-CTTCTTCATGAGCGTCTTGG-3'	370 bp	*NM_003106.2*
TAGLN	F: 5'-GGCAGCTTGGCAGTGACC-3' R: 5'-TGGCTCTCTGTGAATTCCCTCT-3'	101 bp	*NM_003186.3*
TIE2	F:5'-TGCCCAGATATTGGTGTCCT-3' R:5'-CTCATAAAGCGTGGTATTCACGTA-3'	73 bp	*NM_000459.3*
VE-CAD	F: 5'-AGCCCAAAGTGTGTGAGAACGC-3 R: 5'-CTGAGATGACCACGGGTAGGAA-3	225 bp	*NM_001795.3*
VEGFR2	F: 5-CGGCTCTTTCGCTTACTGTT-3' R: 5-TCCTGTATGGAGGAGGAGGA-3'	537 bp	*NM_002253.2*
VWF	F: 5'-TTCCAGAATGGCAAGAGAGTG-3' R: 5'-TGAGTTGGCAAAGTCATAAGG-3'	345 bp	*NM_000552.3*
αSMA	F: 5'-CACTGTCAGGAATCCTGTGA-3' R: 5'-CAAAGCCGGCCTTACAGA-3'	103 bp	*NM_001613.2*

Appendix II

List of antibodies used for flow cytometry.

Protein	Antibody details	Dilution	Clone	Catalogue	Supplier
CD31-APC	Anti-Human; Mouse monoclonal IgG1	1:10	AC128	130-092-652	Miltenyi Biotec
CD34-PE	Anti-Human; Mouse monoclonal IgG1	1:50	4H11	12-0349	eBioscience
PDGFRβ-FITC	Anti-Human; Mouse monoclonal IgG1	1:10	PR7212	MAB1263	R&D Systems
CD90-FITC	Anti-Human; Mouse monoclonal IgG1	1:10	5E10	555595	BD Biosciences
CD73-APC	Anti-Human; Mouse monoclonal IgG1	1:25	AD2	17-0739	eBioscience
CD105-PE	Anti-Human; Mouse monoclonal IgG1	1:25	266	560839	BD Biosciences
NG2-PE	Anti-Human; Mouse monoclonal IgG1	1:10	LHM-2	FAB2585P	R&D Systems
CD34-APC	Anti-Human; Mono monoclonal IgG2a	1:10	AC136	130-090-954	Miltenyi Biotec
CXCR4-PE	Chemokine (C-X-C) Receptor 4 Anti-Human; Mouse monoclonal IgG2a	1:25	12G5	561733	BD Pharmingen
DLL4-PE	Delta-like protein-4 Anti-Human; Mouse monoclonal IgG1	1:20	MHD4-46	346505	Biolegend
EphB4-FITC	Ephrin Receptor B4 Anti-Human; Rat monoclonal IgG1	1:10	395810	FAB3038F	R&D Systems
NRP1-APC	Neuropilin-1 (CD304) Anti-Human; Mouse monoclonal IgG2a	1:20	12C2	354505	Biolegend
NRP2-APC	Neuropilin-2 Anti-Human/mouse; Mouse monoclonal IgG2A	1:10	257103	FAB22151A	R&D Systems
VE-Cadherin-APC	Vascular Endothelial Cadherin Anti-Human; Mouse monoclonal IgG2B	1:10	123413	FAB9381A	R&D Systems
VEGFR2-APC	Anti-Human; Mouse monoclonal IgG1	1:10	ES8-20E6	130-093-601	Miltenyi Biotec
FcR Blocking Reagent	Human FcγR blocking reagent	1:10	-	130-059-901	Miltenyi Biotec
Isotype control-AF488	Alexa Flour 488 isotype control Anti-Human; mouse monoclonal IgG2A	1:25	G155-178	557703	BD Pharmingen
Isotype control-PE	Phycoerythrin isotype control Anti-Human; mouse monoclonal IgG1	1:25	MOPC-21	559320	BD Pharmingen
Isotype control-APC	Allophycocyanin isotype control Anti-Human; mouse monoclonal IgG1	1:25	X40	340442	BD Pharmingen

Appendix III

List of antibodies used for immunocytochemistry

Protein	Antibody details	Dilution	Clone	Catalogue	Supplier
Alkaline Phosphatase	Anti-Human; Rabbit polyclonal IgG	1:200	H-300	SC-30203	Santa Cruz Biotechnology
Brachyury	Anti-Human; Rabbit polyclonal IgG	1:200	Polyclonal	AB20680	Abcam
Brachyury	Anti-Human; Mouse monoclonal IgG2B	1:200	605502	MAB2085	R&D Systems
Calponin	Anti-Human; Mouse monoclonal IgG1	1:200	CALP	AB700	Abcam
CD31	Anti-Human; Mouse monoclonal IgG1	1:200	9G11	BBA7	R&D Systems
Collagen-IV	Anti-Human; Mouse monoclonal IgG	1:300	COL-94	C1926	Sigma-Aldrich
Fibronectin	Anti-Human; Rabbit polyclonal IgG	1:300	Polyclonal	F3648	Sigma-Aldrich
Laminin	Anti-Human; Rabbit polyclonal IgG	1:300	Polyclonal	AB19012	Millipore (Chemicon)
OCT-3/4	Anti-Human; Mouse monoclonal IgG	1:100	C-10	SC-5279	Santa Cruz Biotechnology
OCT-3/4	Anti-Human; Rabbit polyclonal IgG	1:200	Polyclonal	AB19857	Abcam
SSEA-4	Anti-Human; Mouse monoclonal IgG3	1:100	MC-813-70	MAB4304	Millipore (Chemicon)
TRA-1-60	Anti-Human; Mouse monoclonal	1:100	TRA-1-60	MAB4360	Millipore (Chemicon)
TRA-1-81	Anti-Human; Mouse monoclonal	1:100	TRA-1-81	MAB4381	Millipore (Chemicon)
VE-Cadherin	Anti-Human; Mouse monoclonal IgG2B	1:200	123413	MAB9381	R&D Systems
vWF	Anti-Human; Rabbit polyclonal IgG	1:800	Polyclonal	GTX26994	GeneTex
αSMA	Anti-Human; Mouse monoclonal IgG2A	1:100	1A4	MAB1420	R&D Systems
β-Catenin	Anti-Human; Rabbit polyclonal IgG	1:200	Polyclonal	AB16051	Abcam
Secondary antibody	Alexa Fluor 488 Goat anti-rabbit IgG (H+L)	1:200	-	A-11008	Molecular Probes
Secondary antibody	Alexa Fluor 488 Goat anti-mouse IgG (H+L)	1:200	-	A-11001	Molecular Probes

Protein	Antibody details	Dilution	Clone	Catalogue	Supplier
Secondary antibody	Alexa Fluor 594 Goat anti-rabbit IgG (H+L)	1:200	-	A-11037	Molecular Probes
Secondary antibody	Alexa Fluor 594 Goat anti-mouse IgG (H+L)	1:200	-	A-11005	Molecular Probes

Appendix IV

The location of controls and captured antibodies in the Human Angiogenesis Array is listed below. The picture shows the coordinates of each control/ captured antibody in the array.

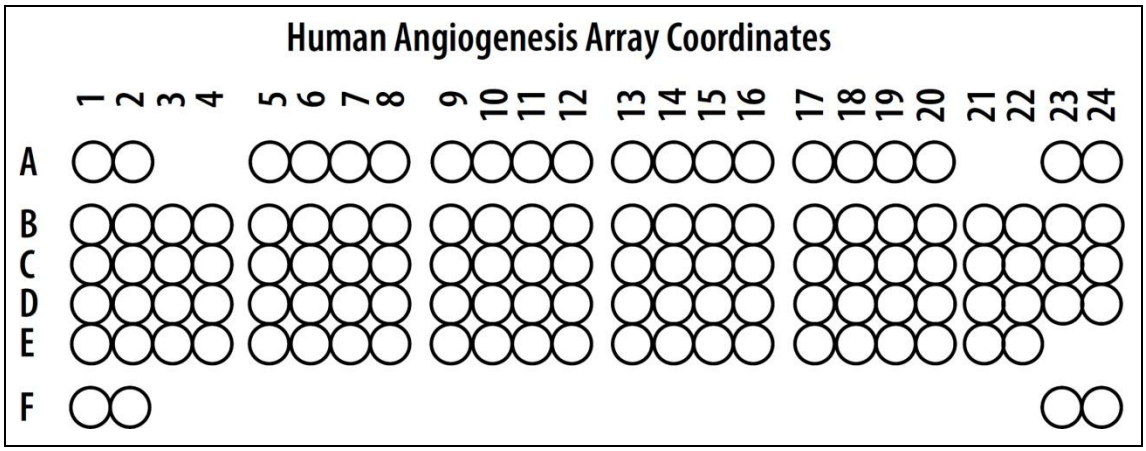

Coordinates	Target/ Control	Alternative Name/ Abbreviation	Description
A1, A2	Reference Spots		
A5, A6	Activin-A		
A7, A8	ADAMTS-1		A Disintegrin-like and Metalloproteinase Domain with Thrombospondin Motifs 1
A9, A10	Angiogenin	ANG	
A11, A12	Angiopoietin-1	Ang-1	
A13, A14	Angiopoietin-2	Ang-2	
A15, A16	Angiostatin/Plasminogen		
A17, A18	Amphiregulin	AR	
A19, A20	Artemin		
A23, A24	Reference Spots		
B1, B2	Coagulation Factor-III	TF	
B3, B4	CXCL16		
B5, B6	DPPIV	CD26	Dipeptidyl peptidase IV
B7, B8	EGF		Epidermal Growth Factor
B9, B10	EG-VEGF	PK1	Endocrine Gland-derived Vascular Endothelial Growth Factor
B11, B12	Endoglin	CD105	
B13, B14	Endostatin/Collagen	XVIII	
B15, B16	Endothelin-1	ET-1	
B17, B18	FGF acidic	FGF-1; aFGF	
B19, B20	FGF basic	FGF-2; bFGF	
B21, B22	FGF-4		
B23, B24	FGF-7	KGF	
C1, C2	GDNF		Glial Cell line-derived Growth Factor

Coordinates	Target/ Control	Alternative Name/ Abbreviation	Description
C3, C4	GM-CSF		Granulocyte Macrophage Growth Factor
C5, C5	HB-EGF		Heparin Binding EGF-like Growth Factor
C7, C8	HGF		Hepatocyte Growth Factor
C9, C10	IGFBP-1		Insulin-like Growth Factor Binding Protein 1
C11, C12	IGFBP-2		Insulin-like Growth Factor Binding Protein 2
C13, C14	IGFBP-3		Insulin-like Growth Factor Binding Protein 3
C15, C16	IL-1β	IL-1F2	Interleukin-1β
C17, C18	IL-8	CXCL8	Interleukin-8
C19, C20	LAP	TGF-β1	
C21, C22	Leptin		
C23, C24	MCP-1	CCL2	monocyte chemotactic and activating factor (MCAF)
D1, D2	MIP-1α	CCL3	Macrophage Inflammatory Protein-1α
D3, D4	MMP-8		Matrix Metalloproteinase-8
D5, D6	MMP-9		Matrix Metalloproteinase-9
D7, D8	NRG1-β1	HRG1-β1	Neuregulin
D9, D10	Pentraxin-3	PTX3; TSG-14	TNF-stimulated gene 14
D11, D12	PD-ECGF		Platelet-derived Endothelial Cell Growth Factor
D13, D14	PDGF-AA		Platlet-derived Growth Factor-AA
D15, D16	PDGF-AB/PDGF-BB		Platlet-derived Growth Factor-AB/BB
D17, D18	Persephin		
D19, D20	Platelet Factor-4	PF4; CXCL4	
D21, D22	PlGF		Placenta-derived Growth Factor
D23,D24	Prolactin		
E1, E2	Serpin-B5	Maspin	
E3, E4	Serpin-E1	PAI-1	
E5, E6	Serpin-F1	PEDF	
E7, E8	TIMP-1		Tissue Inhibitor of MetalloProteinases-1
E9, E10	TIMP-4		Tissue Inhibitor of MetalloProteinases-2
E11, E12	Thrombospondin-1	TSP-1	
E13, E14	Thrombospondin-2	TSP-2	
E15, E16	uPA		Uraokinase-type Plasminogen Activator
E17, E18	Vasohibin		
E19, E20	VEGF		Vascular Endothelial Growth Factor
E21, E22	VEGF-C		Vascular Endothelial Growth Factor-C
F1, F2	Reference Spots		
F23, F24	Negative Control		

Appendix V

Fibrinogen from Bovine Plasma [Cat. No. 154165; MP Biomedicals]

- Stock Concentration: 80mg/ml
- 400mg of fibrinogen is dissolved in 5ml of 0.1M NaHCO3 (pH8.3) at room temperature with gentle shaking for 2 hours. Then the stock solution is stored at -80 ^{0}C as 200/500µl aliquots.

Human Plasma Fibronectin [Cat No. 33016015; GIBCO]

- Stock Concentration: 5mg/ml
- 5mg of fibrinogen is dissolved in 5ml of sterile distilled water at room temperature with gentle shaking for 15 minutes. Then the stock solution is stored at -80 ^{0}C as 200/500µl aliquots.

Polyethylene glycol-4-arm, succinimidyl glutarate terminated [Cat No. 565768; Sigma; PEG-$(GS)_4$]

- 10,000 Da
- Stock Concentration: 8mg/ml
- 250mg of PEG-$(GS)_4$ is dissolved in 3.042ml of sterile PBS and allowed to dissolve for 10mins at room temperature. Then sterile PBS is added to a total volume of 30.042ml. Then the stock solution is stored at -20 ^{0}C as 50µl aliquots.

Recombinant Human bFGF [Cat No. 233-FB-025; R&D Systems]

- Stock Concentration: 10ng/µl
- 25µg of bFGF is dissolved in 2.5ml of sterile 0.1% BSA/PBS. Then the stock solution is stored at -20 ^{0}C as 100/200µl aliquots.

Recombinant Human BMP4 [Cat No. 314-BP-010/CF; R&D Systems]

- Stock Concentration: 100ng/µl
- 10µg of BMP4 is dissolved in 100µl of sterile PBS. Then the stock solution is stored at -20 ^{0}C as 10/20µl aliquots.

Recombinant Human EGF [Cat No. 236-EG-200; R&D Systems]

- Stock Concentration: 10ng/µl
- 200µg of EGF is dissolved in 20ml of sterile 0.1% BSA/PBS. Then the stock solution is stored at -20 ^{0}C as 100/200µl aliquots.

Recombinant Human PDGF$_{bb}$ [Cat No. PHG0045; GIBCO]

- Stock Concentration: 10ng/µl
- 100mM acetic acid is prepared by adding 5.75 µl of Acetic acid to 1ml of sterile 0.1% BSA/PBS
- 10µg of PDGF$_{bb}$ is dissolved in in 100µl of 100mM acetic acid in 0.1% BSA/PBS and allowed to dissolve for 10 minutes. Then 900µl of sterile 0.1% BSA/PBS is added to bring the final concentration to 10ng//µl. Then the stock solution is stored at -20 ^{0}C as 50µl aliquots.

Recombinant Human VEGF [Cat No. PHC9394; GIBCO]

- Stock Concentration: 10ng/µl
- 10µg of VEGF is dissolved in 1ml of sterile 0.1% BSA/PBS. Then the stock solution is stored at -20 ^{0}C as 100/200µl aliquots.

Thrombin from Human Plasma [Cat No. T6884-100UN; Sigma]

- Stock Concentration: 100U/ml
- 100U of thrombin is dissolved in 1ml of sterile distilled water. Then the stock solution is stored at -20 ^{0}C as 100µl aliquots.

Appendix VI

Fabrication of PEG-Fibrin gel

Appropriate volumes of individual components for fabrication of 100µl PEG-Fibrin gel

- **Solution A** (PEG-Fibrinogen Solution)
  - Fibrinogen (80mg/ml) : 12.50 µl
  - PEG-$(GS)_4$ (8mg/ml) : 3.13 µl
- **Solution B** (Cell suspension)
  - Cells suspended in ESFM : 34.37 µl
- **Solution C** (Thrombin-$CaCl_2$ Solution)
  - Thrombin (100U/ml) : 25.00 µl
  - Calcium chloride solution (40mM) : 75.00 µl

Protocol

- Solution A is made by mixing fibrinogen (80mg/ml) and PEG (8mg/ml) in a ratio of 40:1 such that the final concentrations of fibrinogen and PEG in the gel would be 10mg/ml and 0.25 mg/ml respectively. The resultant PEG-fibrinogen solution is incubated at 37^0C for 20 minutes.
- In the meantime, the cells to be encapsulated are suspended in appropriate volumes of media (Solution B)
- Solution C is prepared by mixing thrombin (100U/ml) with calcium chloride (40mM) in a ratio of 1:3 to yield a final concentration of 12.5U/ml in the gel.
- After 20 minutes of incubation, Solution A is mixed with Solution B to form PEG-Fibrinogen-Cell suspension.
- Then the PEG-fibrinogen-cell suspension is allowed to undergo gelation by addition of equal volume of Solution C. Immediately, the cell-gel mixture is pipetted into appropriate culture wells and incubated at 37^0C for 10 minutes for complete gelation. [Note: the gel undergoes initial gelation within 10-15 seconds]
- After the incubation, the gels are incubated in ESFM supplemented with bFGF (20ng/ml), EGF (10ng/ml) and VEGF (10ng/ml).